



A University of Sussex PhD thesis

Available online via Sussex Research Online:

<http://sro.sussex.ac.uk/>

This thesis is protected by copyright which belongs to the author.

This thesis cannot be reproduced or quoted extensively from without first obtaining permission in writing from the Author

The content must not be changed in any way or sold commercially in any format or medium without the formal permission of the Author

When referring to this work, full bibliographic details including the author, title, awarding institution and date of the thesis must be given

Please visit Sussex Research Online for more information and further details

Targeting β -catenin interactions in acute myeloid leukaemia

Megan Payne
University of Sussex



Thesis submitted for the degree of
PhD in Biochemistry
March 2022

Abstract

Acute myeloid leukaemia (AML) is a clonal disorder of haematopoietic stem cells (HSCs), characterised by the expansion of abnormal myeloblasts. AML arises from leukaemia stem cells (LSCs) which clonally evolve to evade chemotherapy and mediate relapse. Survival rates have improved over 50 years; however, the prognosis remains dismal for the elderly or those harbouring adverse cytogenetic events. There's an urgent unmet clinical need for targeted efficacious drugs in AML which reduce side-effects and induce robust remissions. One potential molecular drug target is β -catenin, the central mediator of Wnt signalling which is frequently dysregulated in myeloid leukaemia. β -Catenin is overexpressed, mislocalised, and overactive in AML, where it confers inferior patient survival and drives the emergence, maintenance, and drug resistance of LSC. The level, localisation and activity of β -catenin is governed heavily through protein interactions, and we recently characterised the first β -catenin interactome study in myeloid leukaemia cells. One putative novel interactor of β -catenin identified was Wilms Tumour 1 (WT1) protein which is frequently mutated and overexpressed in AML. This study explored the physical and functional interaction between β -catenin and WT1 in myeloid leukaemia cells. This thesis identified a non-direct, RNA independent association between β -catenin and WT1 in a variety of myeloid cell lines, and primary AML blasts. Functionally, WT1 knockdown significantly decreased β -catenin nuclear expression and Wnt signalling in the KG-1 cell line. Furthermore, induction of WT1 mutations (exons 8 and 9) increased β -catenin expression and augmented Wnt signalling output. Reciprocally, we showed that β -catenin knockdown repressed WT1 expression and signalling which was at least partly transcriptionally driven. Following on from interactome analyses we validated β -catenin interaction with two RNA binding proteins (RBP; MSI2 and LIN28B), and isolated β -catenin from initiation complexes in polysome profiling suggesting β -catenin might influence post-transcriptional gene expression. To assess which RNAs are associated with β -catenin we performed RBP immunoprecipitation (RIP) for β -catenin coupled to RNA sequencing (RIP-seq) and transcripts related to critical processes such as myeloid differentiation, IL-18 signalling and the canonical Wnt signalling pathway itself. Overall, this study reports the first physical and functional interaction between β -catenin and WT1 in AML and reveals a potential novel role for β -catenin in the regulation of post-transcriptional gene control, both of which could inform novel β -catenin targeting strategies in AML.

Declaration

I hereby declare that this thesis has not been and will not be, submitted in whole or in part to another University for the award of any other degree

Signature:

Contents

Abstract	2
Declaration	3
Acknowledgements	8
Abbreviations	9
List of Figures	14
List of tables	15
Chapter 1 Introduction	16
1.1 Normal Haematopoiesis	16
1.2 Acute myeloid leukaemia (AML)	19
1.2.1 AML statistics and diagnosis	19
1.2.2 AML classification and cytogenetics	19
1.2.3 AML treatment and survival	23
1.3 Canonical Wnt signalling	24
1.4 β-Catenin	27
1.5 β-Catenin in normal haematopoiesis	28
1.6 β-catenin in AML	29
1.6.1 Cell intrinsic roles	29
1.6.2 Cell extrinsic roles	30
1.6.3 Mouse models of β -catenin	30
1.6.4 β -catenin targeting approaches	31
1.7 The β-catenin interactome	33
1.8 Wilms tumour protein (WT1)	38
1.8.1 WT1 structure and function	38
1.8.2 WT1 in normal haematopoiesis	39
1.8.3 WT1 in AML	40
1.9 RNA binding partners (RBPs) of β-catenin	41
1.10 Aims and objectives	43
Chapter 2. Methods	44
2.1 Cell Culture	44
2.1.1 Suspension cell culture	44
2.1.2 Adherent cell line culture	44
2.1.3 Cell counting	44
2.1.4 Cell freezing/thawing	45
2.1.5 Treatment of cell lines	45
2.2 Primary AML cells and CD34⁺ HSC isolation	45

2.2.1 Collection of primary AML patient cells.....	45
2.2.2 Cord blood collection and CD34 ⁺ HSC isolation	46
2.2.3 Estimation of T-cell, B-cell, and HSC populations	47
2.3 Protein lysate and quantitation.....	47
2.3.1 Whole cell lysis.....	47
2.3.2 Nuclear/cytoplasmic lysis.....	48
2.3.3 Protein quantitation.....	48
2.4 Immunoblotting	49
2.5 Immunofluorescence	51
2.6 Co-Immunoprecipitation.....	52
2.6.1 Antibody to bead binding	52
2.6.2 Pre-clearing of protein lysate and co-immunoprecipitation	53
2.6.3 RNase A treatment of protein lysates	54
2.7 Preparation of plasmid DNA and cloning	54
2.7.1 Bacterial transformations	54
2.7.2 Plasmid DNA preparation (mini-prep)	56
2.7.3 Extraction of WT1 and ligation with pET49b/GST.....	56
2.7.4 PCR and Gibson assembly of β -catenin and pET47b/HIS.....	57
2.8 Protein expression.....	58
2.9 Protein purification	59
2.9.1 Protein lysis	59
2.9.2 HIS/GST affinity column	59
2.9.3 Size exclusion chromatography (SEC)	60
2.10 HIS/GST pull-downs.....	60
2.10.1 Removal of HIS/GST from purified WT1	61
2.10.2 HIS/GST pull-down with purified protein.....	61
2.10.3 HIS/GST pull down with cell lysate	61
2.11 Lentivirus preparation and transduction of cells	62
2.11.1 Preparation of plasmid DNA	62
2.11.2 Lentivirus preparation.....	65
2.11.3 Lentivirus transduction of leukaemia cell lines.....	65
2.12 Flow cytometry.....	66
2.12.1 Assessment of Wnt signalling	66
2.13 Polysome profiling	67
2.13.1 Preparation of cells and sucrose gradient	67
2.13.2 Ultracentrifugation and fractionation.....	68

2.13.3 Precipitation.....	68
2.14 RNA binding immunoprecipitation.....	69
2.14.1 Cell lysis.....	69
2.14.2 Preparation of magnetic beads for immunoprecipitation.....	69
2.14.3 Immunoprecipitation of RNA-binding protein-RNA complexes	70
2.14.4 RNA purification	70
2.15 RNA extraction of cells containing β-catenin shRNA and CRISPR/Cas9 knockdown	71
2.15.1 RNA extraction and clean up	71
2.16 Quantitative reverse transcription polymerase chain reaction (qRT-PCR)	71
2.16.1 cDNA generation and PCR.....	72
2.16.2 qPCR analysis	74
2.17 Statistics.....	75
Chapter 3. Validation of novel β-catenin interacting proteins in myeloid cells	76
3.1Introduction.....	76
3.2 Aims	76
3.3 Results.....	77
3.3.1 Validation of β -catenin interaction with LIN28B, MSI2 and WT1.....	77
3.3.2 Preparation of bacterial expression constructs pET49b-WT1 and pET47b- β -catenin.....	81
3.3.3 Optimisation of expression conditions for β -catenin and WT1	83
3.3.4 HIS affinity purification of WT1 and β -catenin	85
3.3.5 Size exclusion chromatography (SEC) and isolation of WT1 and β -catenin.....	86
3.3.6 GST pull down with WT1 bound detecting for β -catenin binding	90
3.3.7 HIS pull-down of bound β -catenin detecting for WT1.....	91
3.3.8 Assessment of purified β -catenin binding capacity for WT1 in cell lysate	92
3.3.9 Myeloid leukaemia cell lines co-express β -catenin and WT1 protein	94
3.3.10 AML patients express variable levels of β -catenin and WT1 protein	95
3.3.11 WT1 location and subcellular localisation is unaffected by β -catenin stabilisation.....	97
3.3.12 β -Catenin and WT1 are co-localised in myeloid leukaemia cell lines	98
3.4 Discussion	104
3.4.1 Validation of novel β -catenin interactors	104
3.4.2 Exploring if β -catenin and WT1 bind directly.....	104
3.4.3 Characterising co-expression of β -catenin and WT1	107
Chapter 4. Investigating crosstalk between WT1 and β-catenin signalling	109
4.1 Introduction.....	109
4.2 Aims	109
4.3 Results.....	110

4.3.1 Generation of myeloid cells exhibiting WT1 knockdown or overexpression	110
4.3.2 Integration of the β -catenin activated reporter (BAR) system in Wnt responsive myeloid cell lines.....	111
4.3.3 Assessing the Wnt responsiveness of myeloid cell lines	115
4.3.4 Assessment of WT1 knockdown efficiency and effect on β -catenin stability and nuclear localisation	117
4.3.5 Assessing the effect of WT1 knockdown on β -catenin activity	120
4.3.6 Assessing the effect of WT1 overexpression on β -catenin activity	122
4.3.7 Evaluating the impact of WT1 mutation on β -catenin expression	125
4.3.8 β -catenin knockdown affects WT1 expression levels in various myeloid cell lines.....	129
4.3.9 β -Catenin mediated regulation of WT1 is not by the proteasome.....	130
4.3.10 Identifying WT1 target genes in KG1 cells	131
4.3.10 β -catenin knockdowns reduce WT1 target gene expression.....	132
4.4 Discussion	134
4.4.1 WT1 modulation on β -catenin expression and Wnt signalling.....	134
4.4.2 β -Catenin modulation on WT1 expression and activity.....	136
Chapter 5. Characterising β-catenin roles in RNA biology	139
5.1 Introduction.....	139
5.2 Aims	140
5.3 Results.....	140
5.3.1 The β -catenin:WT1, :MSI2, or :LIN28B interactions are not mediated through RNA	140
5.3.2 β -Catenin and HuR (ELAVL1) are not co-complexed with one another in K562 and HEL cells	144
5.3.3 Understanding the role of β -catenin in protein translation	146
5.3.4 Identifying β -catenin associated RNAs through RNA binding protein immunoprecipitation and RNA sequencing (RIP-seq).....	150
5.4 Discussion	156
5.4.1 Association between β -catenin and RBPs.....	156
5.4.2 Understanding β -catenin's involvement at a polysome level	158
5.4.3 Establishing β -catenin associated RNA from RIP-seq	159
Chapter 6. Final Discussion	163
6.1 Summary.....	163
6.2 Future work	164
Bibliography.....	166
Appendix.....	182
Appendix Table 1: Clinical characteristics of AML/MDS patient diagnostic/relapse samples used in this study.....	182

Acknowledgements

Firstly, I would like to express my sincere gratitude to my supervisor Dr Rhys Morgan for his invaluable advice, continuous support, and patience over the last three and a half years. His keen attention to detail, organisation and knowledge have shaped me into the scientist I am today.

I would like to thank everyone at the school of Life science department, for making a very nice work environment. I would particularly like to thank Alessandro Agnarelli, Leanne Milton-Harris, and Sarah Connery that with their conversations have made the laboratory a lovely place to work.

Many thanks to Dr Erika Mancini for the huge help with protein purification experiments and use of reagents within the laboratory. Also, to the other members of my thesis committee team, Dr Georgios Giamas and Dr Timothy Chevassut for providing support and recommendations of experiments.

I would like to thank Dr Lorraine Smith for the continued support in giving me opportunities to teach alongside my PhD.

Finally, I would like to thank my parents and my partner Chris for their continued support as without them this would have not been possible.

Abbreviations

AML	Acute myeloid leukaemia
APC dye	Allophycocyanin
APC	adenomatous polyposis coli
APS	Ammonium persulfate
ARM	Armadillo repeat
BSA	Bovine serum albumin
β -TRCP	β -transducin repeat containing protein
CB	Cord blood
CBP	CREB binding protein
CBP	Common binding partner
CBF	Core binding factor
cDNA	Complementary deoxyribose nucleic acid
CEBPA	CCAAT/enhancer-binding protein alpha
CK1	casein kinase 1
CLP	Common lymphoid progenitor
CLSM	Confocal laser scanning microscope
CMP	Common myeloid progenitor
CN-AML	Cytogenetically normal acute myeloid leukaemia
Co-IP	Co-immunoprecipitation
CT	Cycle threshold
DAPI	4',6-diamidino-2-phenylindole
DC	Destruction complex
DDS	Denys-Drash syndrome
DKK1	Dickkopf WNT signalling pathway inhibitor 1
DMEM	Dulbecco's modified eagle medium
DMP	Dimethyl pimelimidate
DMSO	Dimethyl sulfoxide
DNA	Deoxyribose nucleic acid
DNMT3A	DNA (cytosine-5)-methyltransferase 3A
DOX	Doxycycline

DTT	Dithiothreitol
Dvl	Dishevelled
EDTA	Ethylenediaminetetraacetic acid
ELAV	embryonic lethal abnormal vision
ELF4a	eukaryotic initiation factor 4E
EMT	epithelial-mesenchymal transition
ESCs	Embryonic stem cells
EYFP	enhance yellow fluorescent protein
FAB	French–American–British
FACS	fluorescence activated cell sorting
FBS/FCS	Foetal bovine serum or calf serum
FITC	Fluorescein isothiocyanate
FLT3	Fms Related Receptor Tyrosine Kinase 3
FMRP	fragile X mental retardation protein
fuBAR	B-catenin ‘found unresponsive’ mutated reporter system
FZD7	Frizzled-7
GMP	Granulocyte-macrophage progenitor
GMLP	Granulocyte-macrophage-lymphocyte progenitor
GSK3 β	Glycogen synthase kinase 3 β
GST	Glutathione S-transferase
HDAC1	histone deacetylase 1
HRP	Horseradish peroxidase
HSCs	Hematopoietic stem cells
HSPC	Hematopoietic stem/progenitor cell
HIS	Histidine
IDH1/2	Isocitrate dehydrogenases
IF	Immunofluorescence
IMDM	Immunofluorescence Iscove’s modified dulbeccos medium
IPTG	Isopropyl β -D-1-thiogalactopyranoside
IRF4	Interferon regulatory factor 4
KTS	Lysine threonine and serine domain

LB	Luria Broth
LEF-1	Lymphoid enhancer-binding factor-1
LGR5	Leucine-rich repeat-containing G-protein coupled receptor 5
LRP5/6	lipoprotein receptor-related protein 5/6
LSCs	Leukemic stem cells
LT-HSC	Long-term hematopoietic stem cell
MDS	Myelodysplastic syndrome
MEP	Megakaryocyte-erythrocyte progenitor
MLL	Mixed lineage leukaemia
MNCs	Mononuclear cells
MPP	Multipotent progenitor cells
mRNAs	Micro ribonucleic acid
MRD	minimal residual disease
MSI2	Mushashi-2
NES	Nuclear export signal
NLS	Nuclear localisation signal
NK	Natural killer cell
NOVA	Neuro-oncological ventral antigen
NPM1	Nucleophosmin
NRAS	Neuroblastoma ras viral oncogene homolog
OD	Optical density
ORF	Open reading frame
Ori	Origin of replication
PAZ	Piwi/Argonaute/Zwille
pBAR	B-catenin activated reporter system
PBS	Phosphate buffered saline
PCAF	p300/CBP associated factor
PCR	Polymerase chain reaction
PE	Phycoerythrin
PIC	Protease inhibitor cocktail
PML-RARA	Promyelocytic leukaemia/retinoic acid receptor alpha

PROTAC	PROteolysis-TARgeting Chimaeras
P/S	Penicillin/streptomycin
PTM	post translational modifications
PUF	pumillio/FBF
PUM2	Pumilio-2
PVDF	Polyvinylidene fluoride
RBD	RNA-binding domains
RBM15	RNA binding motif protein-15
RBP	RNA binding protein
RIP	RNA immunoprecipitation
RNA	Ribonucleic acid
RNP	ribonucleoprotein
Rpm	Revolutions per minute
RPMI	Roswell park memorial institute
RRM	RNA recognition motif
RT	Room temperature
RT	Reverse transcription
RUNX1	Runt-related transcription factor 1
SB	Staining buffer
SBNO2	Strawberry Notch Homolog 2
SEC	Size exclusion chromatography
SDS-PAGE	sodium dodecyl sulphate polyacrylamide gel electrophoresis
shRNA	Short hairpin RNA
sFRP	secreted FZD-related proteins
SOC	Super optimal broth with catabolite repression
TBE	Tris-borate-EDTA
TBL1	Transducin β -like protein 1
TBLR1	TBL1-related protein
TBS	Tris-buffered saline
TBST	Tris-buffered saline with tween
TCEP	Tris(2-carboxyethyl)phosphine

TCF/LEF	T-cell/lymphoid enhancer
TE	Tris-EDTA
TET2	Tet methyl cytosine dioxygenase 2
UC	Universal container
UTR	3' untranslated region
VEGFA	Vascular endothelial growth factor A
WID	WT1-induced inhibitor of Dishevelled
WIF	Wnt inhibitory factor
WT1	Wilms tumor 1 protein

List of Figures

Figure 1: Normal haematopoiesis and the leukemic stem cell model.	18
Figure 2: Mutations associated with AML.	21
Figure 3: Driver mutation events in AML patients.	22
Figure 4: A schematic representation of the canonical Wnt signal transduction cascade.	27
Figure 5: Experimental strategy for analysis of β -catenin interaction partners.	34
Figure 6: Proteomics analysis of Wnt responsive cell lines K562 and HEL.	35
Figure 7: Proteomics analysis reveals β -catenin interaction with WT1.	37
Figure 8: A schematic representation of the WT1 protein.	39
Figure 9: Co-IPs to detect β -catenin association in K562 whole cell lysate.	78
Figure 10: Co-IPs to detect β -catenin association in HEL whole cell lysate.	80
Figure 11: Co-IP to detect β -catenin association in KG1 whole cell lysate.	81
Figure 12: Snapgene file of pET49b-WT1.	82
Figure 13: Snapgene file of pET47b- β -catenin vector.	82
Figure 14: Expression of recombinant WT1 and β -catenin constructs in Rosetta pLysS and BL21 competent cells.	84
Figure 15: Optimised HIS tag purification of WT1 and β -catenin.	86
Figure 16: Size exclusion chromatography of WT1 and β -catenin.	88
Figure 17: Analysing SEC fractions of WT1 and β -catenin.	89
Figure 18: GST pull-down with bound purified GST or WT1 protein and addition of β -catenin.	91
Figure 19: Assessment of cleaved WT1 binding with β -catenin/IRF4.	92
Figure 20: β -catenin-HIS pull-down with K562 and HEL lysate detecting for WT1.	93
Figure 21: β -catenin-HIS or IRF4-HIS pull down with addition of K562 lysate detecting for WT1.	94
Figure 22: Protein expression of β -catenin and WT1 in myeloid leukaemia cell lines.	95
Figure 23: Protein expression of β -catenin and WT1 in AML patients.	96
Figure 24: WT1 Co-IP to detect β -catenin association in AML patients.	97
Figure 25: Subcellular localisation of WT1 and β -catenin under basal and Wnt stimulated conditions.	98
Figure 26: WT1 and β -catenin co-localisation in K562 cells.	99
Figure 27: WT1 and β -catenin co-localisation in HEL cells.	100
Figure 28: WT1 and β -catenin co-localisation in NB4 cells.	101
Figure 29: WT1 and β -catenin co-localisation in KG1 cells.	102
Figure 30: WT1 and β -catenin co-localisation in HL60 cells.	103
Figure 31: Assessment of WT1 knockdown/overexpression in K562 cells.	111
Figure 32: Assessment of lentiviral transduction efficiency of KG1 cell BAR integration.	113
Figure 33: Assessment of DsRed+ in BARV-transduced A) NB4, B) HL60 and C) MV4-11 cells.	114
Figure 34: Representative flow cytometric analysis of four myeloid cell lines.	116
Figure 35: Effect of WT1 knockdown on β -catenin level in KG1 and NB4 cells.	117
Figure 36: Expression levels of β -catenin in transduced fuBAR myeloid cells with WT1 shRNA	119
Figure 37: Effect of WT1 knockdown on Wnt signalling output in myeloid cells.	121
Figure 38: Assessment of WT1 overexpression.	122
Figure 39: Effect of WT1 overexpression on Wnt signalling output.	124
Figure 40: Assessment of WT1 mutant expression.	126
Figure 41: Effect of mutant WT1 on Wnt signalling output.	128
Figure 42: Assessment of β -catenin knockdown in myeloid cells.	130
Figure 43: β -Catenin mediated regulation of WT1 is not via the proteasome.	131
Figure 44: Assessment of WT1 target genes in KG1 cells.	132

Figure 45: Assessment of WT1 targets with β -catenin knockdown.	133
Figure 46: RNaseA treatment of K562, HEL and KG1 fractions.	141
Figure 47: Assessment of β -catenin:WT1 association in absence of RNA.	142
Figure 48: Assessment of β -catenin:MSI2 or β -catenin:LIN28B associations in absence of RNA. ..	143
Figure 49: Assessment of HuR and β -catenin association by Co-IP.	145
Figure 50: Polysome profile of basal or Wnt signalling stimulated K562 and HEL cells.	148
Figure 51: Assessment of β -catenin abundance in polysome fractions.	149
Figure 52: RNA binding protein immunoprecipitation (RIP) optimisation.	151
Figure 53: Analysis of selected mRNAs from β -catenin RIP.	152
Figure 54: β -catenin associated RNA identified from RIP-seq.	154
Figure 55: Schematic representation of possible β -catenin and WT1 interactions.	155

List of tables

Table 1: The French-American-British (FAB) classification of Acute Myeloid Leukemia (AML).	20
Table 2: Ongoing clinical trials in AML.	24
Table 3: Current therapeutic targets of β -catenin.	32
Table 4: Current WT1 targeted therapies.	40
Table 5: Contents and essential information of antibodies.	50
Table 6: β -catenin and WT1 full length sequences.	55
Table 7: Primers designed for PCR reaction.	57
Table 8: PCR conditions for β -catenin and pET47b-HIS.	58
Table 9: WT1 and β -catenin plasmids.	63
Table 10: Reverse transcriptase (RT) PCR reaction steps.	72
Table 11: Forward and reverse primers for each target gene.	73

Chapter 1 Introduction

1.1 Normal Haematopoiesis

Haematopoiesis is the generation of all terminally differentiated blood cells within the body from embryonic development to adulthood (Rieger & Schroeder, 2012). This process originates in the bone marrow with a rare pool of tissue-specific stem cells known as hematopoietic stem cells (HSCs), that reside in a niche to promote stem cell maintenance and regulation. Analysis of the localisation of these cells in tissue sections showed that most HSCs reside adjacent to sinusoidal blood vessels in the bone marrow and spleen. Essential growth factors including CXCL12, and stem cell factor (SCF) were found to be expressed mainly by perivascular stromal cells and endothelial cells that are associated with sinusoids. When these growth factors are deleted, HSCs are substantially depleted from adult bone marrow and there is a loss of all quiescence and serially transplantable HSCs (Crane et al., 2017). However several other bone marrow cell types including megakaryocytes, monocytes and macrophages can directly or indirectly regulate HSC niche to provide a dormant HSC reservoir (Blank & Karlsson, 2015).

As shown in Figure 1, these HSCs have the capacity to both self-renew and give rise to multipotent progenitors (MPPs) that progressively lose self-renewal capacity as they form differentiating progeny that proliferate extensively. Blood formation is believed to develop through MPPs differentiating into the common lymphoid progenitor (CLP) or common myeloid progenitor (CMP) in a step-wise manner (Blank and Karlsson, 2015). However, this model is based on pre-defined flow sorted populations and more recently early haematopoiesis is believed to be formed of a cellular continuum of low prime undifferentiated (CLOUD)-HSCs. This subpopulation contains MPPs which do not differentiate into discrete progenitor types but instead represent transitory states (Velten et al., 2017). In some cell state transitions, lineage combinations will be more favoured than others, and therefore implies haematopoiesis is not as rigid as once thought. This is further supported by platelet bias of HSCs which has identified platelet-restricted lineage output as a key feature of HSC aging and directly contributes to the age-associated imbalance between myeloid and lymphoid leucocyte output (Grover et al., 2016). Furthermore platelet-primed HSCs have long-term myeloid lineage bias and can self-renew to lymphoid-biased HSCs and therefore

subtypes can be organised into a cellular hierarchy with platelet primed HSCs at the apex (Sanjuan-Pla et al., 2013).

The balanced production of haematopoietic cells is regulated by several cellular processes including quiescence, apoptosis, self-renewal, and differentiation to ensure the right cell is made at the right time. This is regulated by several genes including GATA1 a master regulator of erythrocyte development and suppressor of myeloid fate and PU.1 a regulator of myeloid development and suppressor of erythroid development. These two genes work in a molecular shift pattern so there is a constant balance between the production of erythroid and myeloid cells (Jagannathan-Bogdan & Zon, 2013). Cytokines also contribute to normal haematopoiesis for example transforming growth factor- β (TGF- β) regulates homeostasis of the immune system to quiescence by upregulating cyclin dependent kinases such as p15^{Ink4b} and regulation of SMAD proteins for self-renewal of HSCs (Blank & Karlsson, 2015). Also growth factors such as granulocyte-macrophage colony stimulating growth factor (GM-CSF) is an important immune regulator in haematopoiesis by recruiting circulating neutrophils, monocytes and lymphocytes to enhance their functions in defence (Shi et al., 2006). Signalling pathways are also involved in regulating haematopoiesis, including the notch pathway which has shown importance in regulating the cellular fate of HSCs in mice, the BMP pathway in regulating self-renewal in embryogenesis (Kim et al., 2014) and the Wnt/ β -catenin pathway which can regulate HSC stemness and differentiation (Han et al., 2016).

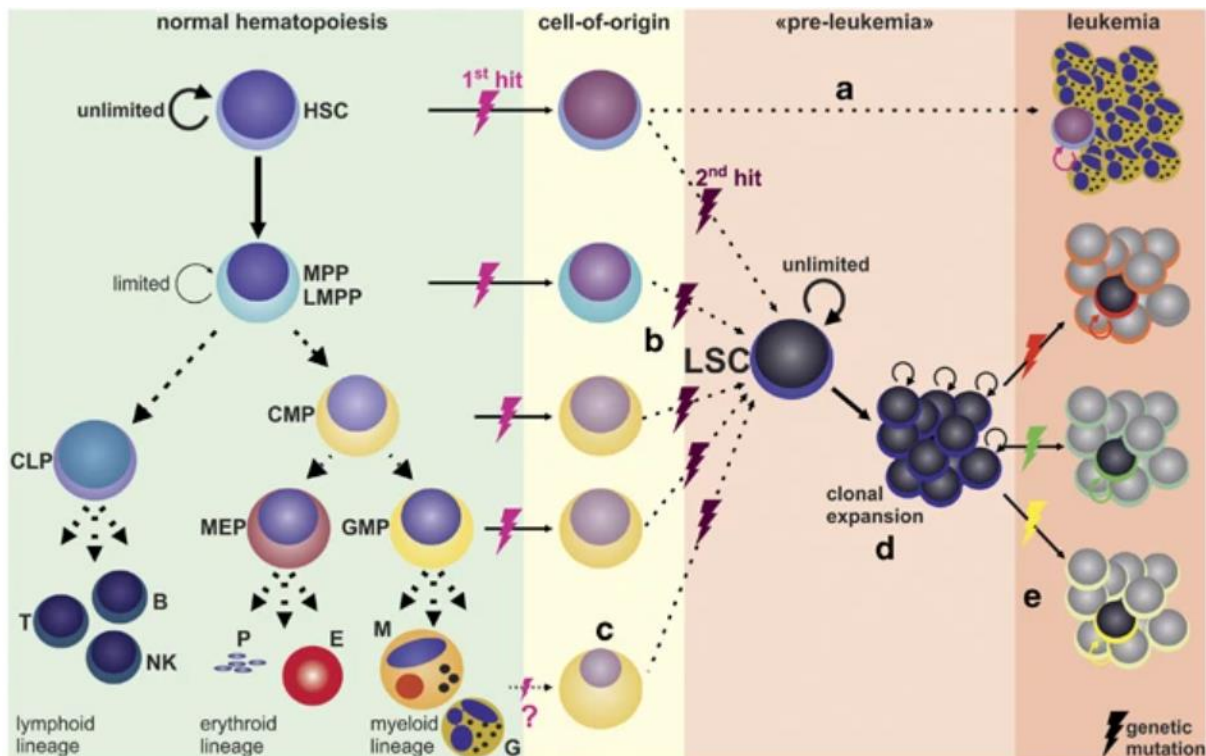


Figure 1: Normal haematopoiesis and the leukemic stem cell

In normal haematopoiesis, stem cells (HSCs) have the ability to self-renewal (circle arrow) and give rise to multipotent progenitors (MPPs) but these only have limited self-renewal abilities. The MPPs differentiate into common lymphoid and myeloid lineages (CLPs, CMPs). The formation of a leukemic stem cell (LSC) can arise from mutations in cells and form **a**) chronic myeloid leukaemia (CML), **b**) blast crisis of CML and acute myeloid patients (AML), **c**) AML LSCs arising from more differentiated HSCs, **d**) in a pre-leukemic phase, genetically unstable, self-renewing LSCs can clonally expand allowing for further mutations, **e**) the development of different leukemic clones (Riether et al., 2015).

Regulation of normal haematopoiesis occurs through the careful balance of cellular processes, activation/repression of genes and induction/suppression of signalling pathways essential for the development of functional blood cells. Disruptions in any of these factors contributes to dysregulated cell fate and function and consequently results in the development of haematological disorders, including acute myeloid leukaemia (AML).

1.2 Acute myeloid leukaemia (AML)

1.2.1 AML statistics and diagnosis

Acute myeloid leukaemia (AML) is a heterogeneous disorder of haematopoietic stem/progenitor cells (HSPC) characterised by the clonal expansion of immature myeloid committed blasts (Kumar, 2011). These cells accumulate in the bone marrow and can spill into the peripheral blood and can support leukemic cell progression by communicating with immune cells in reprogramming mesenchymal stromal cells in the bone marrow microenvironment (Aberger et al., 2017). AML predominates in adults aged 65 or over (De Kouchkovsky & Abdul-Hay, 2016), however does also present in 15-20% of acute leukaemia cases during infancy and adolescence (Lagunas-Rangel et al., 2017). In the UK alone around 3,200 people are diagnosed every year and survival rates are drastically low with 70% dying within the first year of diagnosis (Meyers et al., 2013) and patients older than 60 only having a 5-15% 5-year survival rate (Watts & Nimer, 2018). Patients typically experience a rapid onset of symptoms originating from impaired myelopoiesis including immunosuppression and severe anaemia, resulting in bone marrow failure (Kantarjian et al., 2021).

Diagnosis of AML is confirmed when 20% or more myeloid blasts (myeloblasts, monoblasts or megakaryoblasts) are present in the peripheral blood or bone marrow (Short et al., 2018) diagnosed through a variety of tests including immunophenotyping looking for common markers; CD13, CD33 and CD117 (Kaleem et al., 2003) and cytogenetic profiling. Overall outcome for AML patients is heavily dictated by their cytogenetic and molecular genetic profiles. Cytogenetically normal AML (CN-AML) is the largest subgroup of AML and represents 45% of adult patients with AML diagnosed younger than 60 years old. However, with further research this subgroup can be subdivided with mutations which heavily dictate prognosis and treatment options (Krauth et al., 2015).

1.2.2 AML classification and cytogenetics

AML is classified by two common systems known as the World Health Organisation (WHO) based on morphology, gene mutation and previous medical history whilst the French-American-British (FAB) system based solely on morphology of the disease and these eight categories are shown in Table 1.

Table 1: The French-American-British (FAB) classification of Acute Myeloid Leukemia

The FAB subtype is classified by the morphology and the % of cases for each class are displayed (Kumar, 2011).

FAB subtype	Morphological classification	% of all AML cases
AML-M0	Undifferentiated acute myeloblastic leukemia	5
AML-M1	Acute myeloblastic leukemia with minimal maturation	15
AML-M2	Acute myeloblastic leukemia with maturation	25
AML-M3	Acute promyelocytic leukemia	10
AML-M4	Acute myelomonocytic leukemia	20
AML-M4 eos	Acute myelomonocytic leukemia with eosinophilia	5
AML-M5	Acute monocytic leukemia	10
AML-M6	Acute erythroid leukemia	5
AML-M7	Acute megakaryoblastic leukemia	5

The WHO classification was developed to include molecular markers and chromosomal translocations. In 2016, AML was defined to six major disease entities, first AML with recurrent genetic abnormalities such as t(8;21) and t(15;17) and the production of chimeric proteins including RUNX1 and PML-RAR α . The second classification was AML with myelodysplasia related changes, the third was therapy-related myeloid neoplasms, then AML with myeloid sarcoma, AML with myeloid proliferation due to down syndrome. Finally, AML not otherwise specified (De Kouchkovsky & Abdul-Hay, 2016). Therefore, understanding the cytogenetic profile including AML mutations and chromosomal aberrations will help in designing treatment plans.

AML mutations can confer a proliferative and survival advantage and hence impair normal haematopoiesis resulting in leukemic blast cells as shown in Figure 1A-E (Lagunas-Rangel et al., 2017). These key oncogenic events are often classified according to the two-hit model of leukemogenesis (Figure 2). Class I mutations present in approximately two-thirds of AML cases and make up the most common mutational subset in AML and are characterised by

enhancing LSC proliferation (*FLT3*, *K/NRAS*, *c-KIT* and *TP53*) (Patel et al., 2012). Class II mutations have shown to block normal differentiation and apoptosis (*NPM1* and *CEBPA*) (DiNardo & Cortes, 2016). The final class without classification (*DNMT3A*, *TET2*, *IDH1/2* and *WT1*) have shown to heavily influence the epigenetic regulation of LSCs and can affect both cellular proliferation and differentiation (Patel et al., 2012).

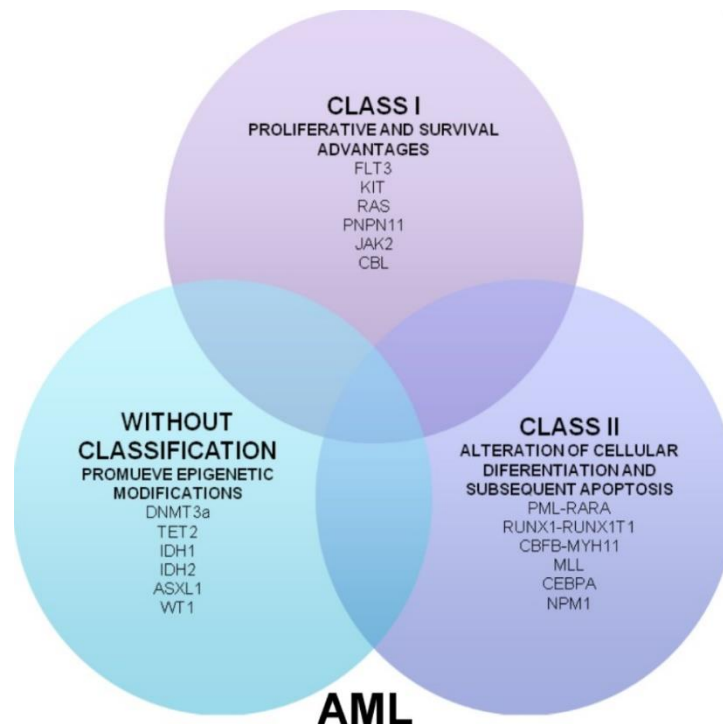


Figure 2: Mutations associated with AML.

Model of cooperation between mutations associated with AML (Lagunas-Rangel et al., 2017).

A study of AML mutations identified 5234 mutations involving 76 genes or regions in 1540 patients (Figure 3). Mutations in genes such as *DNMT3A* and *IDH1/2* were acquired earliest but were never found in isolation and were often linked with secondary mutations events occurring in *NPM1*. This data highlights development of AML occurs through evolutionary steps and patients could therefore be screened early for certain mutations to improve overall treatment plans (Papaemmanuil et al., 2016).

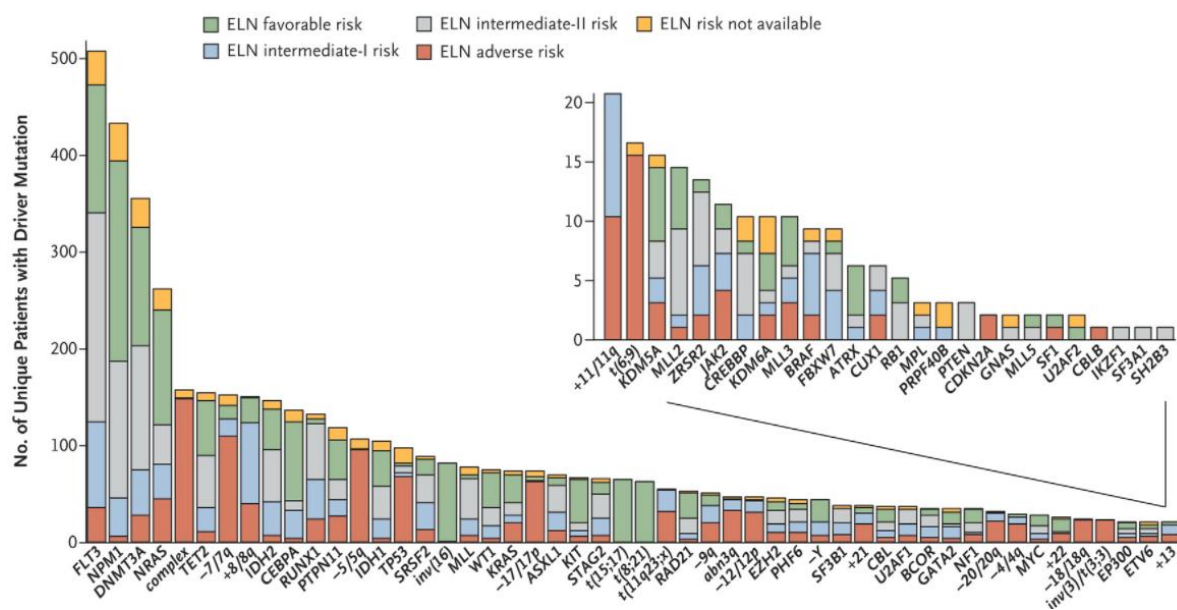


Figure 3: Driver mutation events in AML

Panel displaying mutations in 1540 patients with AML. Each bar presents a distinct driver lesion; the lesions include gene mutations, chromosomal aneuploidies, fusion genes, and complex karyotypes. The colours in each bar indicate the molecular risk according to the European Leukaemia Net (ELN) classification (Papaemmanuil et al., 2016).

AML mutations both independently and in conjunction with chromosomal translocations can contribute to the development of AML. Commonly one or more cytogenetic abnormalities are found in approximately 55% of patients with AML (Lagunas-Rangel et al., 2017). Currently patients can be classified into three classes for cytogenetics: favourable, intermediate, and unfavourable. Patients presenting with t(8;21)(q22;q22) with fusion product RUNX1/RUNX1T1 are favourable despite inhibiting the core binding factor (CBF) proteins, which are required as key regulators of haematopoietic development (Paschka & Döhner, 2013). Whereas patients with t(9;11)(q22;q23) have an intermediate prognosis and are associated with monocytic leukaemia and involve fusion of the MLL and MLLT3 genes. Finally, patients with t(6;9)(p23;q34) present with an unfavourable prognosis and are linked with basophilia and multilineage dysplasia (Lagunas-Rangel et al., 2017).

Overall cytogenetics in conjunction with fusion proteins act as a transcriptional repressor disrupting gene expression programmes including differentiation, apoptosis, and self-renewal, therefore allowing for LSCs to emerge, evolve and expand (Figure 1). Furthermore, both a mutation and chromosomal translocation can be present at the same time, for

example the class I mutation *c-KIT* has been associated with t(8;21) or inv(16) translocations (De Kouchkovsky & Abdul-Hay, 2016) and *WT1* mutations have been linked with t(15;17) (Yoon et al., 2017). Furthermore the t(15;17) translocation is often associated with the fusion protein PML-retinoic acid receptor alpha (PML-RAR α) fusion protein which contributes to leukomogenesis through interference with promyelolytic differentiation.

1.2.3 AML treatment and survival

Current treatment plans include chemotherapy with seven days of infusion with cytarabine and three days with anthracycline agents. However only eligible patients (patients <60 years old with good performance status, normal creatinine, albumin, and platelet count) would undergo induction therapy (initial chemotherapy) to achieve a blast count of <5% of total non-erythroid cells in the bone marrow (Estey, 2014). For patients aged over 65 this treatment method is unfavourable as they generally present with a more adverse cytogenetic risk profile and are more susceptible to treatment-related cytotoxicity and even in areas where patients received this chemotherapy only 20% patients were alive at 2 years (Estey, 2014). Instead treatments are now focusing on targeting molecular aberrations specific to the patient, these include midostaurin for *FLT3* mutant AML, venetoclax for raised BCL2 AML, ivosidenib/enasidenib for IDH mutant AML or gemtuzumab ozogamicin for CD33⁺ AML (Döhner et al., 2021; Kayser & Levis, 2021). There are also several clinical trials ongoing for further targeted therapies as shown in table 2 (AML clinical trials, cancer research UK, 2022). The first being an AML vaccine, which will involve putting 2 genes B7.1 and IL-2 into leukemia cells, followed by treatment with radiation to stop division, the cells are then injected into the body and the genes should stimulate the body to attack the leukaemia cells. Also the proteins p300 and CBP are required for LSC growth and the inhibitor CCS1477 blocks their activity as shown in the MOLM-16 (AML) model which demonstrated superior growth inhibition compared to cytarabine treatment (Ash conference, 2021).

Other treatments include combination chemotherapy treatments, with venetoclax and azacitidine which have previously shown to increase overall survival by 3.8 months versus commonly used AML treatments (Dombret et al., 2015). Furthermore improvements are being made for children with AML including the MyeChild01 trial which has shown to reduce blasts without imposing major side effects (Niktoreh et al., 2019).

Table 2: Ongoing clinical trials in AML

Clinical trial	Phase	Number of patients	Inclusion criteria
Vaccine (RFUSIN2-AML)	I	12	Recruiting those who have had a transplant
CCS1477	I/II	90	AML or MDS that has returned
Venetoclax with low dose cytarabine	II	156	NPM1 gene change and CD33 marker
Venetoclax with azacitidine	III	396	New diagnosis of AML and now in remission after chemotherapy
Gemtuzumab ozogamicin with chemotherapy for children	III	69	Between 12 weeks and 11 months old with either AML, MDS or isolate myeloid sarcoma

Therefore, emphasising the importance of novel agents is key in the ongoing development of targeted therapies. One molecule and pathway heavily dysregulated in AML but not completely understood is Wnt/ β -catenin signalling.

1.3 Canonical Wnt signalling

The Wnt/ β -catenin pathway is an evolutionary conserved signal transduction cascade important in the development and homeostasis of blood and immune cells and adult stem cells in several organ systems including the colon, skin, liver and mammary glands (Nusse & Clevers, 2017). Wnts, their receptors and active β -catenin are highly expressed in embryonic hematopoietic tissues indicating an essential role for this pathway in developmental haematopoiesis (Tarafdar et al., 2013).

In the absence of the Wnt ligand bound to the LRP/Frizzled receptors as shown in Figure 4, cytoplasmic levels of β -catenin are kept low as β -catenin is constantly degraded by the destruction complex (DC), made of the scaffolding protein axin, the tumour suppressor adenomatous polyposis coli (APC), casein kinase 1 (CK1) and glycogen synthase kinase 3 β (GSK3 β) (MacDonald et al., 2009). The latter two phosphorylate the amino terminal region of β -catenin, CK1 phosphorylates at the Ser45 residue which in turns activates GSK3 β phosphorylation at the N-terminal residues Thr41, Ser37 and Ser33 (Li et al., 2012). This creates a docking site for β -transducin repeat containing protein (β -TrCP) an E3 ubiquitin ligase to bind to β -catenin and initiate ubiquitination and proteasomal degradation (Staal et al., 2016). This elimination of β -catenin in the cytoplasm prevents β -catenin from reaching the nucleus and avoids its ability to serve as a co-factor for T-cell factor/lymphoid enhancer factor (TCF/LEF) mediated transcription, thereby leaving them Groucho-bound and Wnt targets repressed (MacDonald et al., 2009).

Upon binding of the Wnt ligand to the LRP/frizzled co-receptors, with the recruitment of scaffolding protein Dishevelled (Dvl), the LRP5/6 tail is phosphorylated and axin binds. Dvl becomes activated and inhibits GSK3 β , causing the proteasome and β TrCP to dissociate from the DC and hence lose its function. These events allow for newly synthesised β -catenin to accumulate in the cytosol and eventually translocate into the nucleus through a variety of context-dependent mechanisms (Morgan et al., 2014). β -Catenin can then bind TCF/LEF and activate several Wnt target genes such as *MYC* (He et al., 1998), *BIRC5* (Zhang et al., 2001) and *CCND1* (Shtutman et al., 1999).

There are also several context dependent mechanisms built in which ensure the appropriate dose and duration of Wnt signalling in specific cellular systems. These include the presence of transmembrane E3 ubiquitin ligases such as RNF43/ZNRF3 controlling Wnt receptor turnover (de Lau et al., 2014) and the secretion of Wnt antagonists such as dickkopf (DKK), Wnt inhibitory factor (WIF) or secreted FZD-related proteins (sFRP) which either block Wnt receptors or sequester Wnts away from targets (Pehlivan et al., 2018). The presence of dominant negative isoforms of TCF/LEF which may bind DNA but lack the β -catenin binding domains necessary to transduce a Wnt signal (Hovanes et al., 2001). The Wnt pathway can also mediate its own intensity through the activation of Wnt target genes that are either

positive (*LEF1*, *LGR5*, *FZD7*, *WNT3A*) (Santiago et al., 2017) (Chai et al., 2011) (Fernandez et al., 2014; He et al., 2015) or negative (*AXIN2*, *DKK1*, *SFRP2*, *RNF43/ZNRF3*) (Lustig et al., 2002) (Alfaro et al., 2008; Paluszczak et al., 2015) regulators of the pathway. Crosstalk between β -catenin and notch has also been highlighted between haematopoietic/leukaemia cells and stromal components. Using both co-culture and repopulation assays in mice, Kadekar et al. showed that mesenchymal stromal cells (MSCs) supported HSC expansion by preventing apoptosis of primitive MSCs through higher expression of β -catenin and Notch1 (Kadekar et al., 2015). The same phenomenon occurs in LSCs where studies showed higher levels of Notch signalling were required to maintain the leukemic role of the canonical Wnt, in which leukaemia cell proliferation, survival and chemoresistance increased (Takam Kanga et al., 2020) Therefore, all the above mechanisms could be targeted to create a tailored level of Wnt signalling and β -catenin appropriate for the biological demand.

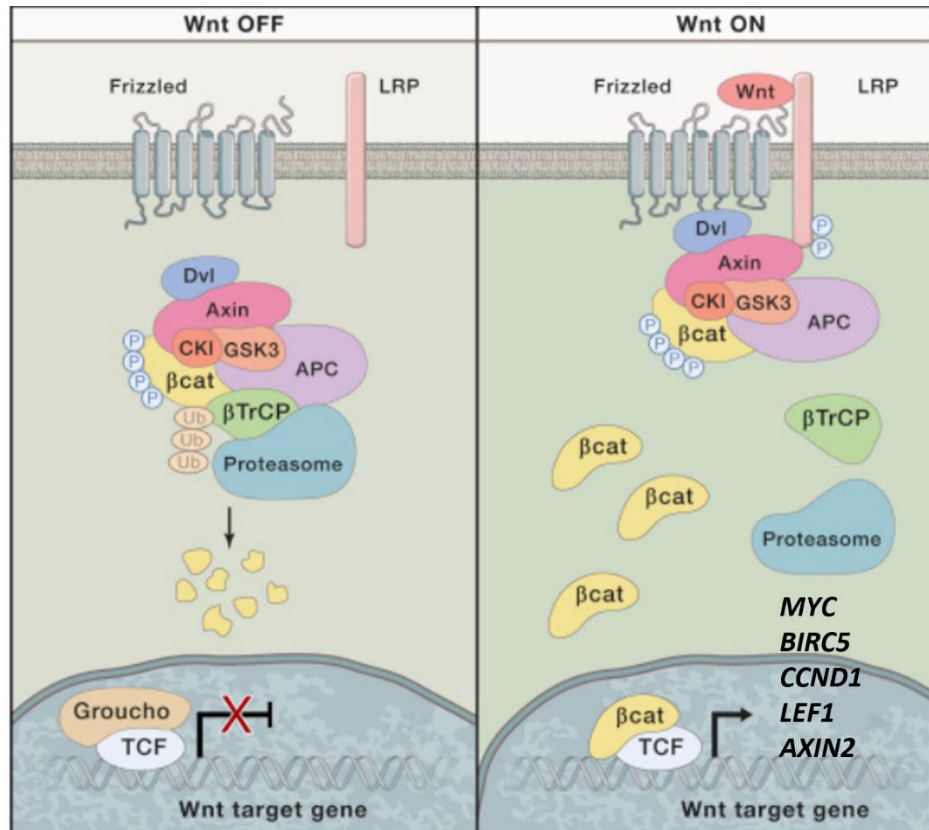


Figure 4: A schematic representation of the canonical Wnt signal transduction cascade.

On the left-hand side in the absence of the Wnt ligand, the destruction complex made of Axin, adenomatous polyposis coli (APC), casein kinase 1 (CK1) and glycogen synthase kinase 3 β (GSK3 β) targets β -catenin for degradation. On the right-hand side, the ligand Wnt binds to the Fz receptor and LRP5/6 co-receptor, the destruction complex falls apart and β -catenin is stabilised allowing for translocation of β -catenin to the nucleus. The TCF/LEF complex can then be activated to mediate transcriptional induction of target genes; *MYC*, *BIRC5*, *CCND1*, *LEF1* and *AXIN2* (Nusse and Clevers, 2017).

1.4 β -Catenin

β -Catenin is a multifunctional and evolutionary conserved molecule which exerts many roles in development and homeostatic processes (Valenta et al., 2012). It was originally identified in cell adherens junctions where it could bridge the cytoplasmic domain of cadherins to α -catenin and the actin cytoskeleton (Hülsken et al., 1994). The 781 amino acid protein contains a central structural core of 12 armadillo repeats (residues 138-664) and the positive charged

groove that spans this entire region constitutes the primary binding surface for β -catenin partners to participate in cellular functions including transcription (Xing et al., 2008). The amino terminus contains the phospho-degron site which mediates the molecules stability, whilst the carboxyl terminus provides specificity and harbours a transactivation domain (Huber et al., 1997). The β -catenin molecule lacks any canonical nuclear localisation signal (NLS) or nuclear export signal (NES), and instead nuclear entry/exit is facilitated by a host of NLS/NES containing chaperone proteins that act in a tissue-dependent manner (Morgan et al., 2014). The role of β -catenin in haematopoiesis remains unclear as strong adhesion junctions are typical role of epithelial, but not haematopoietic cells.

1.5 β -Catenin in normal haematopoiesis

From the late 1990's it was demonstrated that secreted Wnt ligands such as WNT1, WNT2B, WNT3A and WNT10B (which ultimately stabilise β -catenin expression) were expressed in bone marrow stroma and are capable of significantly expanding HSC number *in vitro*.

Wnt signalling is essential in normal haematopoiesis for self-renewal of HSCs and studies have shown Wnt proteins can be generated by the HSCs themselves and used in an autocrine/paracrine manner. Functional studies have shown that Wnt proteins can bind with steel factors to promote the growth and inhibit differentiation of murine HSCs and β -catenin and WNT3A can promote self-renewal and enhance the ability to reconstitute the haematopoietic system of lethally irradiated mice (Reya et al., 2003). Whilst loss of β -catenin led to reduced long-term growth and maintenance of HSC (Zhao et al., 2007). β -Catenin can also direct embryonic stem cells to form hematopoietic progenitors with erythrocyte potential and induces genes involved in maintaining stem cell pluripotency (Tarafdar et al., 2013). Overall β -catenin promotes stem cell maintenance and self-renewal across many tissues including the breast, stomach, gut and skin (Nusse & Clevers, 2017).

In contrast other studies have shown β -catenin is dispensable for haematopoiesis. Inducible Cre-loxP-mediated inactivation of the β -catenin gene in bone marrow progenitors does not impair the ability to self-renew and reconstitute lineages including myeloid, erythroid, or lymphoid (Cobas et al., 2004; Koch et al., 2008). However, in some of these models residual TCF activity remained or was not checked and therefore Wnt signalling may not have been

completely absent. Modulation of upstream Wnt signalling components known to increase β -catenin stability have introduced contradictory results for example inactivation of APC led to impaired HSC self-renewal potential (Famili et al., 2016; Lane et al., 2010). Whilst PORCN deletion (controlling Wnt ligand secretion) was dispensable altogether for HSC self-renewal, proliferation, and differentiation (Kabiri et al., 2015).

These results present a varied view of β -catenin's role in haematopoiesis; however one important study highlights the importance of Wnt signalling dose (Luis et al., 2012). This study proved that in the presence of a conditional deletion of APC, a gradient of five different Wnt signalling levels *in vivo* was determined. This model demonstrated that only very low levels of Wnt signalling (β -catenin) were required to sustain normal HSCs with elevated levels observed during myeloid and T-cell development. Very high levels of Wnt signalling impaired HSC self-renewal and differentiation potential, showing such low levels of Wnt/ β -catenin signalling is required for normal haematopoiesis, this makes β -catenin an attractive therapeutic target for AML since much of its overactivity could be safely eradicated with minimal myelotoxicity. Furthermore, LSCs have shown to hijack the Wnt pathway for efficient self-renewal and proliferation which caused dysregulated Wnt signalling leading to leukemogenesis and is therefore an ideal route for targeted therapy (Staal et al., 2016).

1.6 β -catenin in AML

Over the past twenty years a plethora of studies have demonstrated dysregulated Wnt/ β -catenin signalling in AML which can be split into intrinsic and extrinsic roles.

1.6.1 Cell intrinsic roles

Several studies have confirmed β -catenin to be overexpressed generally in AML blasts or cell lines versus normal HSC (Simon et al., 2005) which is commonly most associated with poor survival (Ysebaert et al., 2006). Studies examining specific AML subtypes have demonstrated dysregulated β -catenin (Griffiths et al., 2015) and/or the merit of targeting the molecule, such as the targeting *FLT3* mutant which resulted in reduced levels of the Wnt target gene *MYC* (Jiang et al., 2018). A further subtype associated with β -catenin is deletion of chromosome 5q [del(5q)], one of the most common cytogenetic abnormalities involved in therapy-related AML. Research has shown that β -catenin inhibition either by indomethacin or shRNA knockdown induced apoptosis and blocked *in vitro* proliferation and was detrimental to AML

cells with del(5q) (L. Li et al., 2017). The del(5q) abnormality is also present in 10-20% of primary myelodysplastic syndromes (MDS) which can transform to AML. β -Catenin expression was shown to be increased in patients harbouring the PML-retinoic acid receptor alpha (PML-RAR α) fusion protein, a result of t(15;17), hypothesised to be a direct result of overexpressed plakoglobin. Plakoglobin elevates β -catenin expression by helping it avoid degradation as it interacts with APC and therefore may contribute to the observed induction of Wnt target genes in hematopoietic cells (Müller-Tidow et al., 2004). Taken together these data highlight the importance of exploring β -catenin as a potential therapeutic target due to its presence and functional consequence for inferior patient survival in a variety of AML subtypes.

1.6.2 Cell extrinsic roles

In the normal bone marrow niche, targeted depletion of β -catenin in the stroma containing adherent haematopoietic and mesenchymal cells, resulted in diminished HSC maintenance and reconstituting capacity (Fleming et al., 2008; Nemeth et al., 2009). Whilst enforced β -catenin expression in the microenvironment within bone marrow stromal mesenchymal stem cells enhanced HSC self-renewal and maintenance in a contact-dependent fashion (Kim et al., 2009). Given the existence of this relationship in normal haematopoietic development, it perhaps unsurprising to see such an axis hijacked in leukaemia. Research has found that nuclear localisation of β -catenin indicative of Wnt signalling was reported in osteoblastic cells from 38% of patients with MDS or AML. Mouse models whereby targeted expression of a β -catenin active mutant (exon 3 encoding the phosphor-degron site) not reported in AML but in bone marrow osteoblasts led to AML with recurrent genetic abnormalities. Highlighting how altered β -catenin signalling in neighbouring cells can have impact on haematopoietic cells in close proximity. Furthermore, the rapid onset progression to AML may be due to the differences in β -catenin levels, activation of downstream pathways including notch or the targeted niche cell type (Stoddart et al., 2017) (Kode et al., 2014).

1.6.3 Mouse models of β -catenin

This functional concept of β -catenin in driving leukemogenesis has been explored in mouse models. *HOX* genes have been identified to regulate normal stem cell self-renewal and when co-expressed with *MEIS1A* oncogenes in mouse models, the Wnt/ β -catenin pathway is required for self-renewal of HSCs. More specifically β -catenin is required for *HOX*-gene

mediated transformation of HSC or *MLL-AF9* mediated transformation of committed progenitor cells. Lack of β -catenin in normal GMP limits the ability to transform committed progenitor cells (Wang et al., 2010) This is further supported by the link between a complete deletion of β -catenin in the MLL pre-LSC stage and a reduction of *in vitro* cloning ability. The level of β -catenin required for MLL pre-LSCs and LSCs development is unknown but the ablation of β -catenin at an early stage linked directly with impaired LSC function and reduced growth of human MLL leukemic cells (Yeung et al., 2010) (Dietrich et al., 2014). However, in many of these studies the activation of β -catenin alone was insufficient to induce leukaemia as a single event, but rather cooperated with well-known driver mutations. Akt-activated β -catenin (Perry et al., 2020), or presence of stem cell markers CD82, CD70 and CD27, both accelerated Wnt/ β -catenin pathway activation and overall leukomegenic potential (Riether et al., 2017). *In vivo* models of MLL-induced AML seem to have particular dependence on β -catenin, but other studies have found its dispensable for MLL leukemogenesis (Zhao et al., 2020) which could be explained by Wnt signalling dose as above, or may depend on the cell type from which the AML originated from (Siriboonpiputtana et al., 2017).

1.6.4 β -catenin targeting approaches

Despite knowledge of β -catenin's overexpression, overactivity, and mis localisation in AML for over 15 years, an effective β -catenin inhibitor is lacking in this setting. Given its transcriptional influence, it's hardly surprising that many of the small molecular inhibitors (SMI) designed for β -catenin to date have targeted its interaction with the TCF/LEF proteins or other transcriptional co-activators as summarised in Table 3. Most of these inhibitors of β -catenin's activity have shown to reduce LSC apoptosis and hence ability to self-renewal therefore stress the importance of exploring β -catenin as a therapeutic target in AML.

Table 3: Current therapeutic targets of β -catenin

Type of inhibitor	Mode of action	Effect	Reference
CGP049090 and PFK115-584	Prevent β -catenin:TCF/LEF complex	Extinguish Wnt signalling output and induce apoptosis	(Minke et al., 2009)
iCRT	Inhibitor of β -catenin responsive transcription by preventing β -catenin:TCF/LEF complex	Shown promise in normal karyotype AML	(Dandekar et al., 2014)
ICG-001	Disrupts β -catenin and p300	Positive response in cells overexpressing PRL-3 with success in CML	(Zhou et al., 2018)
BC2059	Abolished TBL1: β -catenin interaction	Degraded β -catenin and abrogated Wnt target gene expression in AML	(Fiskus et al., 2015)
BC2059 with JAK1/2 inhibitor ruxolitinib	Inhibit β -catenin:TCF4 signalling	Works against secondary AML from post-myeloproliferative neoplasms	(Saenz et al., 2019)
BC2059 with BET protein degrader ARV-771	Inhibit β -catenin:TCF4 signalling	Works against secondary AML from post-myeloproliferative neoplasms	(Saenz et al., 2019)
WNT974	PRCN inhibitor	Decreased β -catenin target gene expression in primary AML samples and limit LSC self-renewal without impacting apoptosis	(Pepe et al., 2022)
Idarubicin and 5-Aza-2'-deoxycytidine	Methylation inhibitor	Induce apoptosis and reduce growth in AML and reduced expression of β -catenin and its target genes	(K. Li et al., 2014)
Anti RSP03	Inhibit RSP03-LGR4 axis	Reduced LSC content of primary AML samples and suppressed nuclear β -catenin activity	(Salik et al., 2020)

For β -catenin's stability, localisation and transcriptional role in AML, several protein partners could be involved at any given time and a particular combination of these interactions will elicit β -catenin's activity. Therefore, identifying these novel partners could provide important molecular information for other methods of targeting β -catenin (Siapati et al., 2011).

1.7 The β -catenin interactome

The β -catenin interactome has been classified in solid tumours (Zhang & Wang, 2020), however in a myeloid context this is poorly understood and requires more exploration for designing therapeutic agents targeting β -catenin and its network. Recently we designed an interactome screen of cytosolic and nuclear β -catenin interacting partners (Figure 5) from representative Wnt responsive (K562 and HEL) and Wnt unresponsive (ML1) cell lines so that we could shortlist factors potentially involved in the nuclear localisation of β -catenin (Morgan et al., 2019).

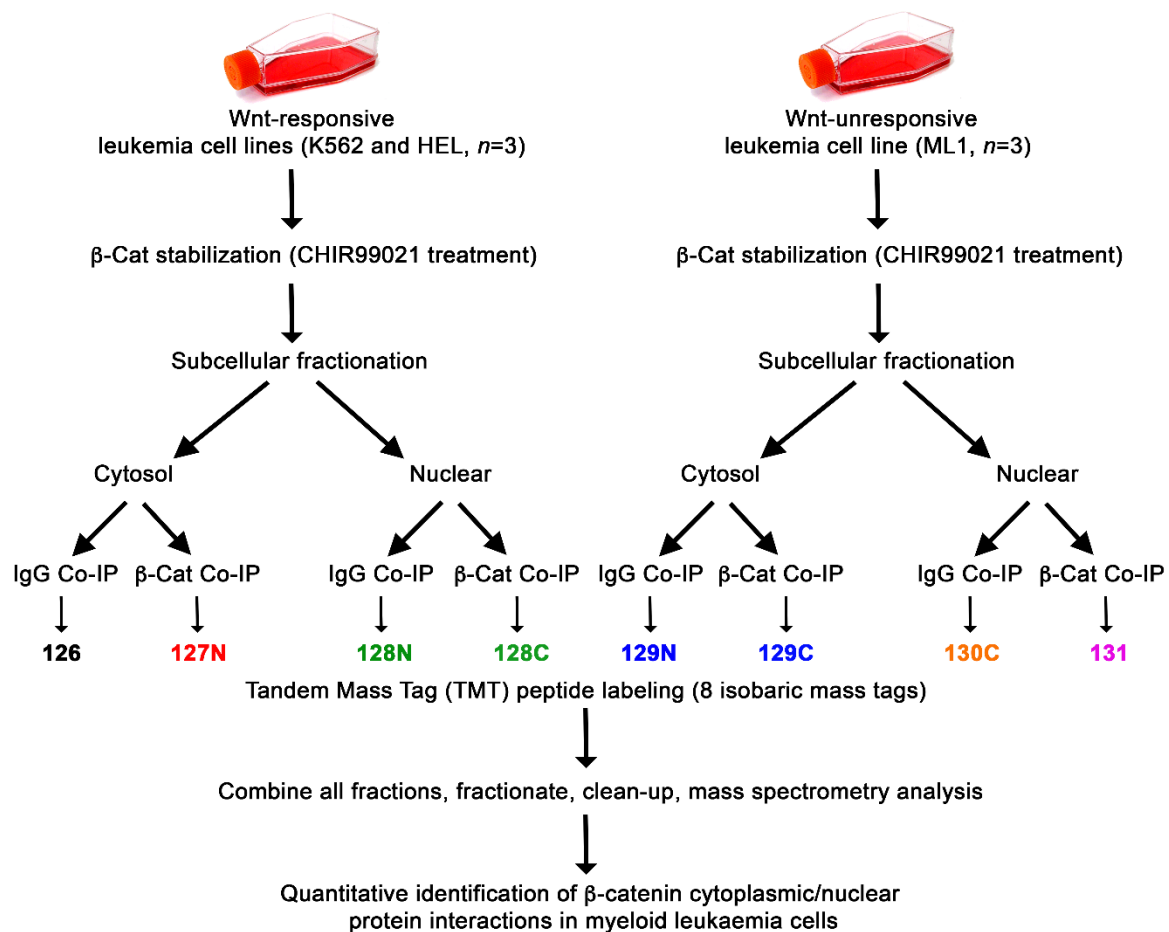


Figure 5: Experimental strategy for analysis of β -catenin interaction partners.

Wnt responsive K562/HEL cells and Wnt-unresponsive cells ML-1 were treated with CHIR99021 to stabilise β -catenin prior to cytosolic and nuclear fractionation. From these fractions either an IgG or β -catenin (β -cat) co-immunoprecipitation (co-IP) was performed generating eight samples which were each TMT labelled with a unique isobaric mass tag. All samples were pooled, fractionated, cleaned, and analysed by mass spectrometry. Mass intensities from each tag report the relative peptide abundance in each sample. Quantitative fold enrichment of β -catenin Co-IP was obtained by comparison with fraction-matched IgG co-IP control (Morgan et al., 2019).

Mass spectrometry analysis of the two Wnt responsive cell lines versus the Wnt unresponsive cell line highlighted an extensive plethora of 225 significantly enriched cytosolic interactions and 118 nuclear interactions for K562 and only 38 and 26 respectively for ML-1 (data not included). The two Wnt responsive cell lines were further analysed and several novel RNA

binding proteins Mushashi-2 (MSI2), LIN28B, Pumilio-2 (PUM2), RNA binding motif protein-15 (RBM15) and Wilms tumour protein (WT1) were identified in both cell lines (Figure 6). These are all RNA binding proteins and have all previously documented roles in HSC, AML or Wnt signalling biology.

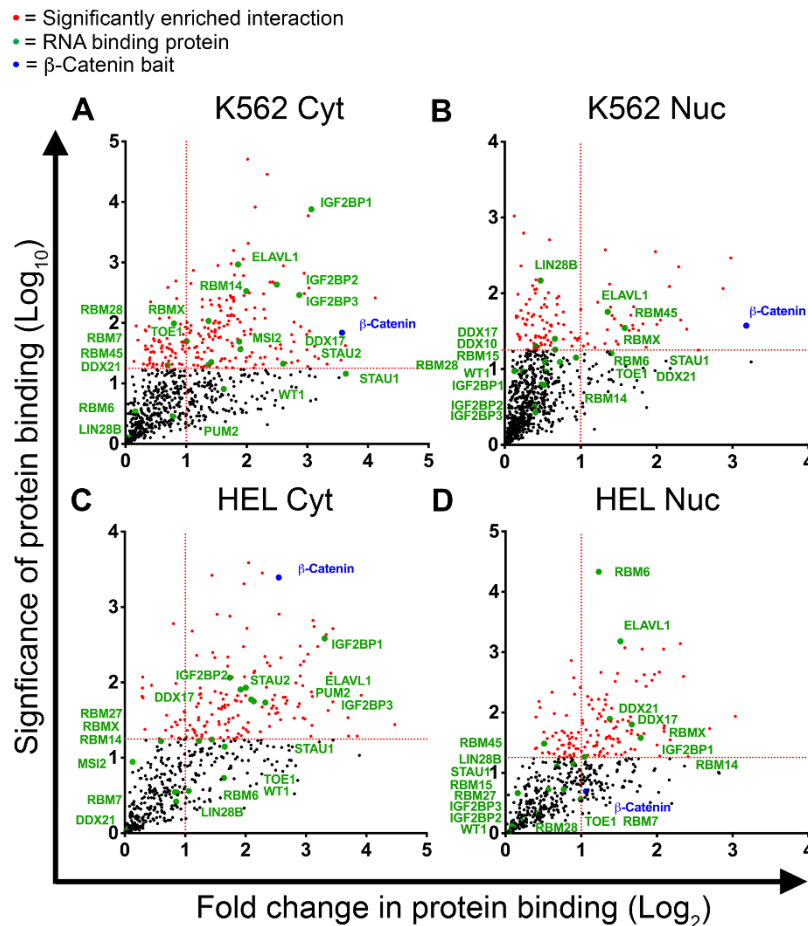


Figure 6: Proteomics analysis of Wnt responsive cell lines K562 and HEL.

RNA binding protein interactions detected in **(A)** K562 cytosolic, **(B)** K562 nuclear, **(C)** HEL cytosolic, and **(D)** HEL nuclear fractions. Vertical dashed red line indicates the threshold for 2-fold change in protein binding at $\text{log}_2 (=1)$ relative to IgG co-immunoprecipitation. Horizontal red line represents threshold for significant interactions at $P=0.05$ on log_{10} scale ($=1.3$). Highlighted red dots indicate statistically significant interactions and green highlighted events/labels indicate known interactions/associations for β -catenin (Morgan et al., 2019).

One protein of interest that arose was Wilms tumour 1 protein (WT1) due to its already established role in AML. Furthermore, the Morgan group have previously validated an association between WT1 and β -catenin in HEL cells but not SW620 cells which represent CRC cells (Morgan et al., 2019). This is important as highlights their interaction could be context dependent and hence interactions for β -catenin will vary between tissue types. As shown in Figure 7A/B, β -catenin was successfully Co-IP'd in both HEL cytoplasmic and nuclear fractions with WT1 (50 kDa) only detectable in the cytosol and nucleus of the AML cell line supporting a potential context-dependent interaction for β -catenin in myeloid cells.

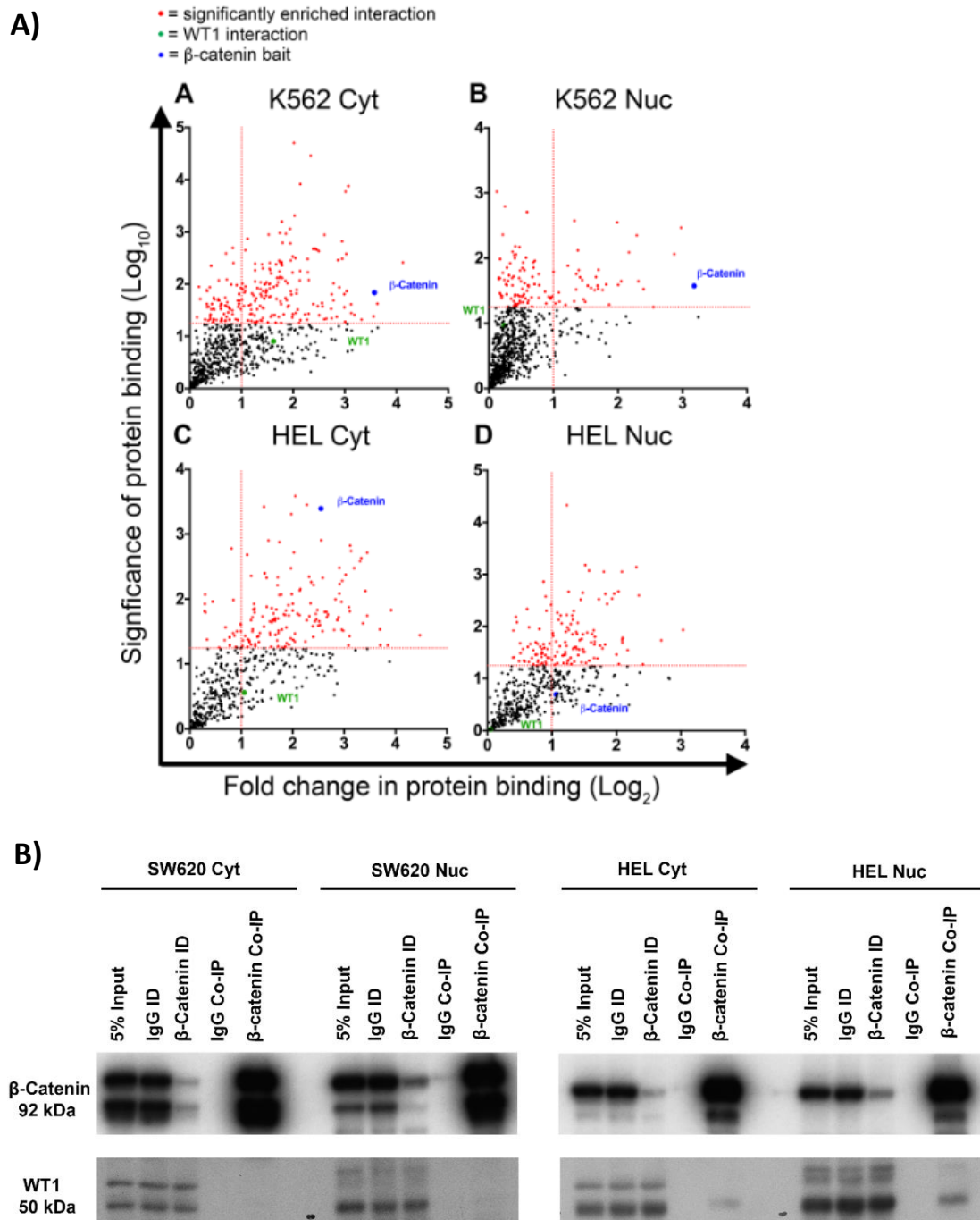


Figure 7: Proteomics analysis reveals β -catenin interaction with WT1.

A) Scatterplots showing summary of β -catenin protein interactions. Vertical dashed red line indicates the threshold for 2-fold change in protein binding at $\log_2(=1)$ relative to IgG co-IP. Horizontal red line represents threshold for significant interactions at $p=0.05$ on \log_{10} scale ($=1.3$). Highlighted red dots show all statistically significant interactions, blue dot shows β -catenin bait and green dot WT1, black dot represents all other proteins. **(B)** Representative immunoblots showing β -catenin and WT1 protein level from co-IPs pulled down from the cytosol or nucleus of SW620 or HEL cells (ID = immunodepleted) (Morgan et al., 2019).

1.8 Wilms tumour protein (WT1)

1.8.1 WT1 structure and function

The WT1 gene encodes a zinc finger transcription factor which plays essential roles in normal urogenital and cancer pathogenesis (Zhou et al., 2020). WT1 was first identified as a tumour suppressor gene responsible for the development of Wilms tumour (a paediatric kidney cancer) as well as Denys-Drash syndrome (DDS) (Ho et al., 2010). WT1 has been reported as overexpressed in the majority of AML cases and is frequently mutated which has led to extensive work to determine its mechanistic role in AML (Cilloni et al., 2006) (Zhou et al., 2020). The complex nature of WT1 being both overexpressed or mutated and the range of isoforms and tissue specific expression allows for WT1 to act as both a tumour suppressor and oncogene depending on the context (Rampal & Figueroa, 2016).

The nature and functional consequence of WT1 is related to its structure, WT1 is combined of four zinc finger domains located at exons 7-10 which are characteristic for transcription factors involved in regulation and differentiation (Morrison et al., 2008). As shown in Figure 8, the WT1 protein contains an N-terminal transactivation domain and a C-terminus with four zinc-fingers N-terminal domains that are involved in either repressing or activating several target genes, resulting in differentiation, apoptosis and cellular growth (Toska & Roberts, 2014). Different WT1 isoforms can arise from alternative splicing, first at exon 5 which causes a 17 amino acid insertion between the trans-regulatory domain and the zinc finger domain have been found more commonly in relapsed AML samples (Gu et al., 2010). The second splice event involves addition of three amino acids – lysine (K), threonine (T) and serine (S) between exons 9 and 10 resulting in significant reduction of DNA binding ability whilst enriching RNA binding (Bor et al., 2006; Morrison et al., 2006). This regulation of RNA processes could also be linked to the different isoforms of WT1 as could have different functional roles in different contexts.

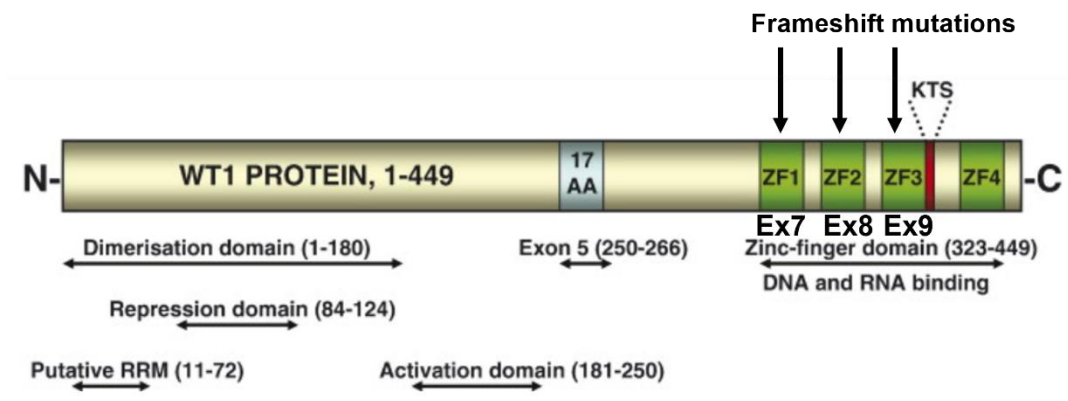


Figure 8: A schematic representation of the WT1 protein.

The N terminal domain consists of a dimerisation domain (1-180), a transcriptional activation (181-250) and repression domain (84-124) and a putative RNA recognition motif (RRM; 11-72). Alternative splicing results in four main WT1 isoforms: cassette exon 5 includes 17 amino acids in the middle of the protein. The second splicing factor arises at exon 9 with the addition of amino acids KTS at the C-terminal end of zinc finger 3. DNA and RNA binding motifs are mediated by the zinc-finger domains (Morrison et al., 2008).

1.8.2 WT1 in normal haematopoiesis

The specific role of WT1 in haematopoiesis is still unknown, studies have shown preferentially expressed in CD34⁺ haematopoietic progenitors and is down-regulated in more differentiated cells. More specifically WT1 has been implicated to regulate apoptosis, proliferation and differentiation and due to its absent expression in mature white blood cells suggests a role in normal haematopoiesis (Ariyaratana & Loeb, 2007). In human normal bone marrow cells only 1.2% of HSCs express WT1 representing a very quiescent population (Hosen et al., 2002). However this protein could still be a functional target as when WT1 was ectopically expressed, inhibited proliferation of CD34⁺ progenitors was observed (Svedberg et al., 2001) and in later studies when knocked out in mouse embryonic cells a reduced hematopoietic potential was caused by vascular endothelial growth factor (Vegf-a) (Cunningham et al., 2013) and therefore proves WT1 as a target in regulating haematopoiesis. Furthermore, the absence of WT1 in HSCs led to functional growth defects with a 75% reduction in erythroid blast-forming unit (BFU-E) and erythroid colony-forming unit (CFU-E) (Alberta et al., 2003). Overall implying WT1 has a role in HSC development and growth.

1.8.3 WT1 in AML

WT1 is overexpressed in the majority of AML patients and in MDS the expression of WT1 is associated with higher blast counts and increased progression to AML (Tamaki et al., 1999). Furthermore, the increased levels of WT1 are often linked with resistance to therapy, higher chance of relapse and poor survival rates (Barragán et al., 2004). To understand the role of WT1 expression, WT1 was downregulated in K562 cells and AML patients in chronic and blast crisis which resulted in inhibition of cell growth (Yamagami et al., 1996). Also, studies have identified that downregulation of the WT1 isoform 17+ induced apoptosis and normal levels of WT1 +17 resulted in a decrease of proapoptotic Bak (Ito et al., 2006).

To understand the role of WT1 overexpression in leukemogenesis, Nishida and colleagues established a transgenic murine model of overexpressed WT1 combined with the AML1-ETO fusion product, which by itself is unable to produce AML. However, when combined this led to rapid onset of leukaemia (Nishida et al., 2006). Furthermore, WT1 is highly expressed in LSCs and facilitates the maintenance of leukaemia in the murine MLL-AF9 induced mouse model of AML (Zhou et al., 2020) and therefore highlights the potential functional overlap of WT1 and β -catenin. Some inhibitors of WT1 have already been established in an AML context as shown in table 4 and have shown to inhibit proliferation and self-renewal of LSCs and are therefore a good, targeted therapy to explore.

Table 4: Current WT1 targeted therapies

Type of inhibitor	Mode of action	Effect	Reference
WP1130	Inhibits WT1-BCL ₂ L ₂ axis	Inhibits proliferation and self-renewal of LSCs	(Zhou et al., 2020)
galinpepimut-S	WT1 peptide vaccine	Overall survival rate of >34% at 3 years	(Maslak et al., 2018)
WT1 126 and 134	WT1 peptide vaccine	10 stable diseases with 50% blast reduction	(Keilholz et al., 2009)
WT1 235 and 243	WT1 peptide vaccine	One patient with morphological CR and one with molecular CR	(Yasukawa et al., 2009)

WT1 mutations are also associated with leukemogenesis and appear in approximately 6-15% of *de novo* AML (Hou et al., 2010). These mutations are often associated with younger age (Hou et al., 2010) and in the presence of *FLT3*-ITD mutations (Renneville et al., 2009) and *CEBPA* mutations (Gaidzik et al., 2009). *WT1* mutations occur primarily in exons 1, 7 and 9 resulting in the creation of a stop codon and expression of a truncated protein lacking the zinc finger domain (King-Underwood et al., 1996). Frameshift mutations at exons 7, 8 and 9 were explored by the Bonifer group as shown in Figure 8 which resulted in a truncated protein at different Zn²⁺ domains 1, 2 and 3 respectively. Most interestingly the presence of mutation 8 resulted in increased growth and clonogenicity (Potluri et al., 2021). Furthermore, *WT1* mutant transcripts with frameshift mutations are subject to mediated RNA decay without expression of the truncated protein (Abbas et al., 2010). This could result in a loss of DNA binding ability due to the formation of a truncated unfunctional protein, emphasising that mutations will have specific roles dependent on the context.

Overall due to the overlap of regulatory roles of β -catenin and *WT1* in normal HSC and the fact they are both linked with poor prognosis in AML and driving leukemogenesis emphasises the importance of exploring their association.

Furthermore, the functional overlap of *WT1* and Wnt signalling has been shown in hepatocellular carcinoma (Tan et al., 2018), epithelial to mesenchymal transition (von Gise et al., 2011) and *WT1* as a negative regulator of Wnt signalling in osteosarcoma (Kim et al., 2010). However, despite their considerable functional overlap, the relationship between these two highly dysregulated proteins has not yet been studied previously in a haematopoietic context and could aid understanding of their involvement in oncogenic roles in AML.

1.9 RNA binding partners (RBPs) of β -catenin

The functional overlap between *WT1* and β -catenin suggests a role for β -catenin in RNA biology. RNA binding proteins (RBPs) assemble with RNA to form ribonucleoprotein particles (RNPs) and can therefore regulate processes including transcription, splicing, modification, intracellular trafficking, translation, and decay (Gebauer et al., 2021). They are increasingly appreciated as being essential for normal haematopoiesis and they are understood to act as oncogenes or tumour suppressors in haematological malignancies. Alternative splicing has

shown to contribute to specific lineages, and mutations in RBPs can lead to dysregulated splicing. This emphasises the impact RBPs can have in haematological malignancies and hence the importance of using them to develop new therapeutic modalities (Hodson et al., 2019)

The interaction of β -catenin and RBPs has been established in colon cancer as this protein has shown to regulate mRNA splicing (Sato et al., 2005) and interact with the HuR protein (Kim et al., 2012). In normal haematopoiesis RBPs have shown to regulate self-renewal and differentiation by controlling protein abundance of isoforms or through the regulation of non-coding RNA. An emerging role of RBPs is their involvement in metabolism, thus genetic or posttranslational changes to an individual RBP could have consequences for RNA targets (Hodson et al., 2019) and understanding this network is vital for new therapeutic targets in AML. Some of the RBPs which arose (Figure 6) included MSI2 a protein that when knocked down induced apoptosis and overall AML chemosensitivity to daunorubicin is enhanced (Han et al., 2015). LIN28B is a stem cell reprogramming factor, downregulating let-7 microRNAs (mRNAs) and overexpression has been linked with AML (J. Zhou, C. Bi, et al., 2017). PUM2 contributes to the self-renewal of human embryonic stem cells (ESCs) (Naudin et al., 2017) and RBM15 is an RNA recognition motif-encoding gene and when fused with t(1;22)(p13;q13) increased AML progression (Ma et al., 2001).

Although little is known about β -catenin RBP or RNA association in a myeloid context, exploring this route is important to the various roles RBP can have in cellular processes and hence in driving the progression of AML.

1.10 Aims and objectives

Our previous β -catenin interactome revealed several RBPs of interest and this thesis aimed to validate and functionally assess these protein interactions with the overall aim of discovering novel therapeutic strategies for targeting Wnt signalling in AML. We mainly focused on the association with β -catenin and WT1 due to their previously documented roles in AML, therefore this thesis had the following aims;

1. Validation of novel β -catenin interactions; WT1, MSI2, LIN28B, RBM15 and PUM2 and more specifically understanding the expression, clinical relevance, and co-localisation of WT1 and β -catenin in a myeloid context
2. Understanding the functional relationship between β -catenin and WT1 in respect to signalling activity using knockdown, overexpression, and induced mutant expression.
3. Identifying what RNA complexes β -catenin associates with and the potential cellular processes and pathways this could implicate through RNA immunoprecipitation (RIP) coupled to RNA sequencing.

Chapter 2. Methods

2.1 Cell Culture

2.1.1 Suspension cell culture

The K562, HL60, HEL, U937, PLB-985, NOMO1 cell lines were obtained from European collection of authenticated cell culture (ECACC, Salisbury, UK). MV4-11, NB4 and MonoMac6 were purchased from DSMZ-German collection of microorganisms and cell culture (Braunschweig, Germany). OCI-AML3 cells were obtained from the Chevassut lab (Medical research building, BSMS, University of Sussex, Brighton) and MOLM-13, EOL1 cell lines from the Sussex drug discovery centre (SDDC; University of Sussex, Brighton). Cell lines ML-1 and THP-1 cells were obtained from the Darley Lab (University of Cardiff, Wales, UK). All cell lines were maintained at 37°C, 5% CO₂ in Roswell Park Memorial Institute media (RPMI; Merck-Millipore, Dorset, UK), supplemented with 2 mM L-glutamine (Merck Millipore), 100 mg/ml penicillin/streptomycin (P/S; Merck Millipore) and 10% foetal bovine serum (FBS; Merck Millipore) at a density of 1-3x10⁵/ml (cell line dependent). Cell lines KG-1 and KG-1a (ECACC) were maintained in the same culture conditions but supplemented with 20% FBS at a density of 2x10⁵/ml. Cells were cultured in 25-75cm³ suspension flasks depending on the experiment (Sarstedt, Numbrecht, Germany).

2.1.2 Adherent cell line culture

HEK293T cells were obtained from the Darley lab and cultured in Dulbecco's Modified Eagle Medium (DMEM; Merck Millipore), supplemented with 2mM L-glutamine, 100 mg/ml streptomycin and 10% FBS in 25cm² or 75cm² adherent flasks (Thermo Fisher Scientific, Oxford, UK).

2.1.3 Cell counting

The haemocytometer (Merk Millipore) and coverslip (Thermofisher Scientific) were cleaned with 70% ethanol (Thermofisher Scientific) and the coverslip was affixed to the haemocytometer. Flasks were swirled gently to ensure even distribution of cells and 7.5µl of cell culture was loaded into the haemocytometer. Using the Olympus CK2 microscope (Olympus, Southend on Sea, UK), the grid lines were focused using the 10X objective lens.

Using a hand tally counter, live cells only contained within a square were counted in each quadrant and an average was calculated. To calculate the number of cells/ml this average number was multiplied by 10,000 (10^4). If cells were too confluent under the microscope a 1:10 dilution of cells in respective media was used for the haemocytometer.

2.1.4 Cell freezing/thawing

The total number of cells was determined (2.1.3) and $\sim 3\text{--}6 \times 10^6/\text{ml}$ cells were collected into a universal container (UC; Thermofisher Scientific) and centrifuged at 1300rpm for 10 minutes. The supernatant was removed, and the pellet resuspended in 1ml of respective media (2.1.1-2) with 10% Dimethyl Sulfoxide (DMSO; Merck Millipore) and the cell suspension was added to a cryogenic vial (Thermofisher Scientific). Tubes were then loaded into a cool cell freezing container (Appleton Woods, Birmingham, UK) and frozen at -80°C , after > 3 hours tubes were moved to liquid nitrogen chamber for long term storage. Cells were thawed rapidly (< 1 minute) in a 37°C water bath. Cells were added to 10ml of pre-warmed culture media (2.1.1-2) and centrifuged at 1300rpm for 10 minutes. The pellet was resuspended in 1ml of fresh media and added into a 25cm^3 flask containing 4ml of respective media and incubated at 37°C , 5% CO_2 .

2.1.5 Treatment of cell lines

For Wnt signalling activation, cell lines were treated with $5\mu\text{M}$ of the GSK-3 β inhibitor CHIR99021 (Merck Millipore), or volume-matched DMSO control for 16hr (unless otherwise stated) at 37°C with 5% CO_2 . For proteasome inhibition, cell lines were treated with $1\mu\text{M}$ of MG-132 (Merck Millipore) or DMSO for either 24 or 48 hours at 37°C with 5% CO_2 .

2.2 Primary AML cells and CD34⁺ HSC isolation

2.2.1 Collection of primary AML patient cells

Primary cells collected from the University of Bristol (School of Cellular & Molecular Medicine, University of Bristol, Bristol, UK) were lysed (2.3) as whole, nuclear, or cytoplasmic cells lysates and transported back to the University of Sussex (Appendix Table 1).

2.2.2 Cord blood collection and CD34⁺ HSC isolation

Bone marrow, peripheral blood or leukapheresis samples from patients diagnosed with AML/MDS were collected in accordance with the Declaration of Helsinki and with approval of University Hospitals Bristol and Weston NHS Foundation Trust and London Brent Research Ethics Committee. Human cord blood was obtained following informed consent from healthy mothers at full-term undergoing elective caesarean sections at the Royal Sussex County Hospital, with approval from Brighton & Sussex University Hospitals NHS (BSUH) trust, the East of England – Essex Research Ethics Committee, Human Research Authority and Health and Care Research Wales (18/EE/0403). Cord blood (CB) was inspected for clots and diluted with an equal volume of Iscove's Modified Dulbecco's Medium (IMDM; Merck Millipore) containing P/S and 1:100 Heparin (Alfa Aesar by Thermofisher Scientific). After pipetting cord blood, pipettes were rinsed with 1% Virkon (Thermofisher Scientific) and placed in 5% Bioclense (Teknon; Thermofisher Scientific) overnight solution for de-contamination. Mononuclear cells (MNC) were isolated using a 1:2 ratio of Ficoll-Hypaque (1.077g/l; Merck Millipore) to cord blood (CB) in a UC. This was then centrifuged at 450 x g for 30 minutes with the brake off. Three layers formed, a clear upper layer (plasma), a fluffy white layer (MNC, monocytes, and platelets), and a white discrete layer on top of the red cell layer (granulocytes). Two thirds of the plasma layer was removed into virkon, making sure not to disturb the MNC layer. The MNC layer was then collected with a pipette and added into a fresh UC. The UC was topped up with IMDM and centrifuged at 1300rpm for 10 minutes. The supernatant was removed, and cells were resuspended using the vortex mixer, if they did not resuspend then 50µl of DNase (10mg/ml; Merck Millipore) was added to the cells. The UC was topped up with IMDM and centrifugation repeated. The supernatant was removed and 10ml of 1 x MACS red cell lysing solution was added (Miltenyi Biotec, Surrey, UK), incubated at room temperature for 10 minutes and then centrifuged at 1300rpm for 5 minutes. Supernatant was removed and cells were washed with 10ml of IMDM at 1300rpm for 5 minutes. Cells were resuspended in 1ml of IMDM, 50µl of cells were removed for immunophenotyping and the rest of the sample was used for a cell and viability count using 0.2% trypan blue (Merck Millipore) to generate a % viability of sample prior to cryopreservation. Approximately 5x10⁷/ml of cells were resuspended in an equal volume of cold 2X freezing medium containing 20% DMSO, 30% filtered foetal calf serum (FCS; Merck Millipore) and 50% IMDM alone and were frozen and stored at -80°C.

2.2.3 Estimation of T-cell, B-cell, and HSC populations

Cells were resuspended in 1ml of IMDM and $\sim 3 \times 10^5$ of isolated MNC's (2.2.2) were resuspended in 300 μ l of staining buffer (SB) containing 0.5% Bovine Serum Albumin (BSA; Thermofisher Scientific) in phosphate buffered saline (PBS; Merck Millipore) for immunophenotyping. This was then split between 3 wells of a flat 96 well plate (Thermofisher Scientific). To well one, 2 μ l of ISO-FITC (1:50 Biolegend; San Diego, US), ISO-PE (1:50, Biolegend), ISO-PerCPCy5.5 (1:50, Biolegend) and ISO-APC (1:50, Biolegend) was added (Isotype control). For well two, 2 μ l of ISO-FITC, ISO-PE, CD45-PerCPCy5.5 (1:50, Biolegend) and ISO-APC was added (CD45 only). To well three, 2 μ l of CD3-FITC (1:50, Biolegend), CD34-PE (1:50, Biolegend), CD45-PerCPCy5.5 and CD19-APC (1:50, Biolegend), was added (all antigens). The plate was incubated at room temperature for 30 minutes in the dark. Then 200 μ l of SB was added to each well and the plate centrifuged at 1300rpm for 5 minutes. The supernatant was removed and each well resuspended with 150 μ l of SB.

Analysis of 100,000 events per well was then completed using the Accuri C6 (BD, Biosciences, Berkshire, UK) in conjunction with C6 sample software (BD). Using FlowJo software Version 8.0 (BD) the quadrant tool was used to estimate T-cell (CD3⁺) Vs B-cell (CD19⁺) content to overall estimate HSC (CD34⁺) content.

2.3 Protein lysate and quantitation

2.3.1 Whole cell lysis

Cells were counted and $1-5 \times 10^6$ cells (cell line dependent) were extracted and washed with 10-25 ml of PBS and centrifuged at 1300rpm for 10 minutes. The pellet was resuspended in 100 μ l of cell lysis buffer (20mM Tris-HCl pH 7.5, 150mM NaCl, 1mM Na₂EDTA, 1mM EGTA, 1% Triton, 2.5mM sodium pyrophosphate, 1mM b-glycerophosphate, 1mM Na₃VO₄, 1 μ g/ml leupeptin; Cell signalling Technology, London, UK), containing complete™ Mini Protease-Inhibitor Cocktail (PIC; Merck Millipore) and incubated at 4°C for 30 minutes. Every 10 minutes samples were vortexed to promote homogenisation. After incubation, cell debris was removed by centrifugation at 17,000 x g for 10 minutes to pellet the debris. The supernatant was removed and either protein quantified or stored at -80°C.

2.3.2 Nuclear/cytoplasmic lysis

Cells were counted and $2-8 \times 10^6$ cells (cell line dependent) were washed in PBS and resuspended in 250µl of cytoplasmic lysis buffer (10mM Tris-HCl pH 8.0, 10mM NaCl, 1.5mM $MgCl_2$, 0.5% Igepal-CA630/NP40; Cell signalling technology), containing complete™ Mini PIC for 10 minutes at 4°C with a light vortex after 5 minutes. The supernatant (cytosolic fraction) was recovered by centrifugation at 800 x *g* at 4°C for 5 minutes and the nuclear pellet was washed with 500µl of PBS and centrifuged. Nuclear pellets were resuspended in 100µl of lysis buffer (2.2.1) with addition of 10% glycerol (Thermofisher Scientific) and 0.5mM Dithiothreitol (DTT; Merck Millipore) for Co-Immunoprecipitation (co-IP) only. Lysates were sonicated (5 x 30s with 30s rest periods, 4°C) and incubated at 4°C for 30 minutes to maximise nuclear lysis. Lysates were pelleted at 17,000 x *g* for 10 minutes at 4°C and collected supernatant (nuclear fraction) was either protein quantified or stored at -80°C.

2.3.3 Protein quantitation

To enable equal protein loading between samples for subsequent applications, the total amount of protein in each cell lysis was quantified by using the DC protein assay kit. (Detergent-Compatible Colourimetric Assay; Bio-Rad, Hertfordshire, UK). Protein standards (6.25-800µg/ml) of BSA diluted in water and lysis buffer (2.2.1) were made, with addition of a water control alone with lysis buffer to set the background absorbance. A flat 96-well plate was set up with two rows containing 31µl of each protein standard to overall generate the standard curve. For the sample wells, 1µl of cell lysate was added to 30µl of water. A working solution containing 20µl of protein assay solution S per 1ml of solution A was made and 30µl was added to each well. 100µl of Solution B was added and the plate was read immediately at 655nm using a spectrophotometer (Bio-Rad) in conjunction with Microplate Manager 6 software version 6.3. Sample concentrations were equalised accordingly for the subsequent experiment using water and 4X Laemmli sample buffer (NuPAGE; Thermofisher Scientific), heated at 95°C for 5 minutes and stored at -20°C.

2.4 Immunoblotting

To detect protein expression in cells immunoblotting is used to separate the proteins based on their molecular size and charge. Specific antibodies targeting these proteins are used to visualise the proteins.

Proteins were resolved on acrylamide gels of varying gradients (depending on size of protein being detected; Alfa Aesar by Thermofisher scientific). To make 2X resolving gel, 4.4ml of resolving buffer (1.5M Tris pH 8.8 and 0.4% SDS; Alfa Aesar by Thermofisher) was mixed with water (volume adjusted depending on % of acrylamide), 110µl of 0.5g/ml ammonium persulphate (APS; Thermofisher) and 7.2µl of TEMED (>99% Purity; Severn Biotech, Kidderminster, UK). After this had set, a 4.5% stacking gel was layered on top, containing 1.2ml of acrylamide, 2ml of stack buffer (0.5M Tris pH 6.8 and 0.4% SDS; Alfa Aesar by Thermofisher scientific), 4.4ml of water, 58µl of APS and 3.6µl of TEMED. The gels were added to the cassette chamber and running buffer (14.4g of glycine, 3g of Tris; Thermofisher Scientific and 10% SDS; Severn Biotech, made up to 1L with water) was added. 20µg of protein sample was loaded into the gel alongside one well containing 3µl of precision all blue protein standard ladder (Bio-Rad). Samples were electrophoresed (Bio-Rad) for 15 minutes at 100V to allow the samples to move through the stacking gel and then increased to 190V for 45 minutes, or until the dye front had run off.

Gels were removed and soaked in transfer buffer (14.4g of glycine, 3g of Tris and 200ml of methanol; Thermofisher scientific made up to 1L with water). To activate the Immobilon-P membranes (Merck Millipore; New Jersey, United states) they were soaked in methanol for 5 minutes, followed by 3 x 3-minute washes with water. Gels were combined with the membrane and transferred at 100V for 90 minutes (Bio-Rad). Following transfer, the membranes were blocked with 5% skimmed milk in Tris-buffered saline with tween (TBST; 100ml of 10X TBS; Severn Biotech, with 1g of Tween-20; Thermofisher Scientific, made up to 1L with water) for 1 hour at room temperature with rocking at 25rpm. Primary antibodies were added within 0.5% milk in TBST as shown in Table 5 and incubated overnight at 4°C with a gentle rock.

Table 5: Contents and essential information of antibodies.

All primary antibodies used with essential information including host and dilutions for immunoblotting.

Antibody	Host	Immuno-blotting dilution	Source
β -catenin	Mouse	1:10000	Becton Dickinson, Oxford, UK, Clone 14
WT1	Rabbit	1:2000	Abcam, Oxford, UK
LEF-1	Mouse	1:5000	Cell signalling technology
Lamin A/C	Mouse	1:50000	Merck Millipore
α -tubulin	Mouse	1:50000	Merck Millipore
β -actin	Mouse	1:2000000	Merck Millipore
Anti-Acetyl-Histone H3	Rabbit	1:20000	Cell signalling technology
His-tag	Rabbit	1:2000	Cell signalling technology
GST-tag	Rabbit	1:2000	Cell signalling technology
WT189	Rabbit	1:2000	Roberts Lab, University of Bristol
RBM15	Rabbit	1:2000	Cell signalling technology
Lin28b	Rabbit	1:2000	Cell signalling technology
MSI2	Rabbit	1:5000	Abcam
PUM2	Rabbit	1:2000	Bethyl, Montgomery, US

HuR	Mouse	1:5000	Thermofisher Scientific
TOE1	Rabbit	1:2000	Bethyl via Cambridge bioscience
Ribosomal Protein S6	Mouse	1:2000	Cell signalling technology
Ribosomal protein L7a	Mouse	1:2000	Cell signalling technology
Initiation factor ELF4a	Rabbit	1:2000	Abcam

Membranes were washed for 3 x 10 minutes in TBST, and secondary antibodies were added within 0.5% milk in TBST for Goat anti-Rabbit HRP (1:1000; Merck Millipore) and Goat anti-mouse HRP (1:1000, Merck Millipore) and incubated at room temperature for 1 hour on a rocking platform. A second set of 3 x 10 minute washes with TBST were completed and membranes developed using the LumiGLO Peroxidase chemiluminescence kit (Sera care, Milford, United States). Proteins were visualised on a Licor Odyssey with Image Studio software version 5.2, loading controls (β -actin, Lamin A/C, and α -tubulin) were exposed for 2 minutes and proteins of interest for 10 minutes on the chemiluminescence channel, the ladder was detected at 700nm over 2 minutes.

2.5 Immunofluorescence

Immunofluorescence allows for visualisation of the distribution of a target protein throughout a cell. By targeting proteins of interest using fluorescently labelled antibodies the subcellular level and localisation can be determined and the effect of different biological conditions analysed.

Cells were incubated overnight at 4×10^5 /ml with either 5 μ M of CHIR99021 or DMSO at 37°C, 5% CO₂. The next day 2×10^6 cells were extracted and washed with 20mls of PBS and centrifuged for 5 minutes at 1300rpm, a second wash was completed with 10mls of PBS. Cells were fixed in 1ml of fixative containing 2% paraformaldehyde (Merck Millipore) in PBS and

incubated at room temperature for 20 minutes with agitation. Cells were washed with 20mls of SB and centrifuged. The supernatant was removed, and cells were resuspended in 1ml of quenching buffer containing 100mM glycine (Merck Millipore) in PBS and incubated at room temperature for 5 minutes, followed by two washes and centrifugation. Cells were resuspended in 1ml of permeabilization buffer containing 0.1% Triton TX100 (Thermofisher Scientific) in 1 x PBS and incubated for 5 minutes at room temperature with occasional agitation, followed by two washes.

The pellet was then resuspended in 10 μ g/ml of WT1 and β -catenin primary antibodies (see table 2) and incubated at room temperature for 30 minutes. Cells were washed and resuspended in 1ml of staining buffer containing goat anti-mouse Alexa488 and goat anti-rabbit Alexa647 (1:500; Invitrogen, California, United states). Cells were incubated for 30 minutes at room temperature in the dark and washed. Cells were then resuspended in 2mls of DAPI (1:2000; Thermofisher Scientific) in staining buffer and incubated for 5 minutes at room temperature with agitation. Cells were washed and resuspended in 1ml of SB.

Confocal immunofluorescence was achieved using the resonant scanning head of a Zeiss LSM880 confocal microscope with a 40x oil immersion objective and assisted by ZEN software version 3.4. Images were collected for Alexa488 using the argon laser and for Alexa647 using the Hene63 laser, track one consisted of DAPI and Alexa647 together and track 2 consisted of Alexa488 alone. Wavelength 405nm was used to detect DAPI staining. Final editing of images and overlays were done using ImageJ software version 1.52.

2.6 Co-Immunoprecipitation

Co-Immunoprecipitation (Co-IP) is the process of precipitating a protein antigen out of complex cellular protein lysate using an antibody that specifically binds to that protein. This process can be used to isolate and concentrate a particular protein and identify any proteins associating with the target protein of interest which can be detected by immunoblotting.

2.6.1 Antibody to bead binding

Protein IgG dynabeads (Life technologies, California, United States) were vortexed until completely resuspended and 165 μ l of beads were applied to the magnet and the storage

ethanol was removed. The beads were resuspended in 165µl of PBS-0.02% Tween-20 (PBST) containing the respective antibodies; ~8µg of β -catenin, PUM2, MSI2, Mouse IgG (Becton Dickinson), 250µl of WT189 (concentration unknown, University of Bristol), ~ 5µg of Rabbit IgG (Merck Millipore), ~5µg of LIN28B, ~ 2µg of RBM15, or 50µl of HuR (concentration unknown). Beads were rotated at room temperature for 2 hours and applied to the magnet to remove any unbound antibody. Beads were washed 3 x 500µl with PBST and vortexed for 10 seconds. Beads were washed 3 x 1ml in coupling buffer consisting of 0.2M triethanolamine (Merck Millipore) in PBS with 0.01% Tween-20 and vortexed. Coupling buffer was removed and beads were crosslinked with 1ml of dimethyl pimelimidate (DMP; Merck Millipore) in coupling buffer and incubated at room temperature for 30 minutes. Beads were applied to a magnet, supernatant removed, and cross-linking repeated for a second time. Beads were then quenched with 1ml of quenching buffer containing 50mM ethanolamine (Merck Millipore) in PBS with 0.01% Tween-20 for 30 minutes rotating at room temperature and repeated. The beads were then washed in 500µl of elution buffer containing 0.2M glycine pH 2.5 in 0.01% Tween-20 with water, three times and finally resuspended in 165µl of PBST and stored at 4°C.

2.6.2 Pre-clearing of protein lysate and co-immunoprecipitation

To reduce background binding, protein lysates were first pre-cleared with isotype antibody complexes (2.5.1). Mouse/Rabbit IgG isotype control cross-linked beads were washed three times with 500µl of PBST (cell line dependent) and finally resuspended in 165µl of PBST. 33µl of beads were mixed per 2mg of total lysate protein and the final volume made to 1ml with lysis buffer (2.2.2). These were incubated for 6 hours at 4°C with rotation after which the supernatant was collected (following antibody:bead complex removal using magnet) and divided in half for respective co-IP reactions.

Individual co-IP reactions were made with 500µl of pre-cleared lysate, 33µl of antibody specific cross-linked beads and 467µl of lysis buffer and were incubated overnight at 4°C on a rotating platform. The following day, the supernatant was collected and stored as an immunodepleted fraction to check for antigen depletion. The bead complexes were washed 6 x 500µl in PBST (% cell line dependent) and resuspended in 30µl of lysis buffer after the final wash. 2 x laemmli buffer was added to the beads, 4 x laemmli buffer added to the 5% inputs

and immunodepleted samples and all were heated at 95°C for 5 minutes. Following denaturation, beads were placed on the magnet and the supernatant collected which contained the co-IP reaction. All samples were then either stored at -20°C or immunoblotted for target proteins of interest.

2.6.3 RNase A treatment of protein lysates

Prior to Co-IP 2mg of pre-cleared protein was incubated overnight with co-IP lysis buffer containing 20µg/ml of RNase A (Thermofisher Scientific) to digest RNA. This was then confirmed by agarose gel electrophoresis, reactions were run on a 1% agarose gel (Thermofisher Scientific) by dissolving the required amount of agarose powder in 1x Tris-Borate-EDTA (TBE) and heating until a homogenous solution was achieved. After the solution had cooled 2.5µl of gel red (Biotium, San Francisco, United States) was added, poured, and left to set at room temperature. Samples were prepared with 6X gel loading buffer (New England Biolabs) and run at 75V for 30 minutes.

2.7 Preparation of plasmid DNA and cloning

2.7.1 Bacterial transformations

To understand if β -catenin and WT1 proteins directly interact, the full peptide sequences as shown in table 6 were identified in UniProt and ordered (Eurofins Genomics, Germany) and integrated into pET47b-HIS and pET49b-GST/HIS bacterial expression vectors (Gift of Mancini group, University of Sussex, Brighton, UK) respectively.

Table 6: β -catenin and WT1 full length sequences.

Peptide sequences identified using UniProt and ordered from Eurofins.

Protein	Full Sequence
β -Catenin	MATQADLMELDMAMEPDRKAAVSHWQQQSYLDSGIHSGATTAPSLSGKGNPEEEDVDTS QVLYEWEQGFSSQFTQEQQVADIDGQYAMTRAQVRVRAAMFPETLDEGMQIPSTQFDAAHPT NVQRLAEPQMLKHAVVNLINYQDDAELATRAIPELTCLLNDEDQVVVNKAAVMVHQLSK KEASRHAIMRSPQMVSIVRTMQNTNDVETARCTAGTLHNLSSHREGLLAIFKSGGIPAL VKMLGSPVDSVLFYAITTLHNLLHHEGAKMAVRLAGGLQKQMVALLNKTNVKFLAITTDC LQILAYGNQESKLILASGGPQALVNIMRTYTYEKLWTTSRVLKVLVSVCSNKPATVEA GGMQALGLHLTDPSQRLVQNCWTLRNLSDAATKQEGMEGLLGLTLVQLLGSDDINVTCA AGILSNLTCNNYKNKMMVCQVGGIEALVRTVLRAGDREDITEPAICALRHLSRHHQEAEM AQNAVRLHYGLPVVVVLLHPPSHWPLIKATVGLIRNLALCPANHAPLREQGAIPRLVQLL VRAHQDTQRRTSMMGGTQQQFVEGVRMEEIVEGCTGALHILARDVHNIRIVIRGLNTIPLFV
WT1	MGSDVRDLNALLPAVPSLGGGGGCGALPVSGAAQWAPVLDFAAPPASAYGSLGGPAPPPAP PPPPPPPHSFQEPQSWGGAEPHEEQCLSFTVHFSGQFTGTAGACRYGPFPPPPPSQA SSGQARMFPNAPYLPSCLESQPAIRNQGYSTVTFDGTSPSYGHTPSHHAAQFPNHSFKHED PMGQQGSLGEQQYSVPPVYGCHTPTDSTGSAQLLRTPYSSDNLQMTSQLECMWTWNQ MNLGATLKGVAAGSSSVKWTEGQSNHSTGYESDNHTTPILCGAQYRIHTHGVRFGIQDV RRVPGVAPTLVRSASETSEKRPFCAYPGCNKRYFKLSHLQMHSRKHTGEKPYQCDFKDC

50 μ l aliquots of DH5 α *E.coli* competent cells (Mancini group, University of Sussex) were thawed on ice and incubated with 200ng/ μ l of pET47/pET49b vector DNA for 30 minutes on ice. First β -catenin/WT1 insert DNA was diluted in Tris-EDTA buffer containing 10mM Tris-HCl (ThermoFisher Scientific) and 1mM disodium EDTA pH 8.0 (Merck Millipore) to a final concentration of 220ng/ μ l and then incubated with 50 μ l of super competent DH5 α cells (University of Sussex) on ice for 30 minutes. Samples were then heat shocked at 42°C for 45 seconds in a pre-heated water bath and returned to ice for 2 minutes. 450 μ l of Luria Broth (LB; 10g of Bactotryptone, 5g of Bacto yeast extract; ThermoFisher Scientific, and 10 g of NaCl made up to 1L with water) was added for pET47/pET49b cultures. For β -catenin/WT1 cultures 950 μ l of super optimal broth with catabolite repression (SOC; New England Biolabs, Ipswich, UK) was added.

All cultures were shaken at 210rpm overnight at 37°C for 90 minutes, after 200 μ l of culture was spread onto an LB-agar plate containing appropriate antibiotics, kanamycin (1:1000 of 100mg/ml stock unless stated otherwise; Melford Laboratories, Ipswich, UK) for the vectors and ampicillin (1:1000 of 100mg/ml stock; ThermoFisher scientific) for the insert DNA. Plates were incubated at 37°C overnight to allow colony growth. Single colonies were picked from plates and grown in 10ml cultures containing LB broth supplemented with plasmid-specific antibiotics for selection overnight at 37°C with shaking at 210rpm (unless stated otherwise).

The next day glycerol stocks were taken for long term storage by adding 80% glycerol (Thermofisher Scientific) to culture mixture at a 1:1 ratio and stored at -80°C.

2.7.2 Plasmid DNA preparation (mini-prep)

To successfully isolate the plasmid DNA from the bacterial cultures, mini preps were completed, 10 ml of culture was set up by inoculating LB supplemented with plasmid-specific selection antibiotics with a glycerol stock scraping. Cultures were incubated overnight and centrifuged the next day at 4700 x *g* for 30 minutes to pellet cells. Plasmid DNA was extracted from the bacterial cell pellets using Gene JET plasmid miniprep kit (#K0502, Thermofisher Scientific) according to the manufacturer's protocol. Mini-prepped DNA was dissolved in 50µl of elution buffer (provided in the kit) and DNA concentration was determined using the Nanodrop 2000 spectrophotometer (Thermofisher Scientific) blanked against the elution buffer.

2.7.3 Extraction of WT1 and ligation with pET49b/GST

WT1 was inserted into the pET49b-glutathione S-transferase (GST) vector as this tag would help in solubility in expression and purification steps. 20µl of Fast digest (a digest is required to isolate the DNA required) reactions were made consisting of 10X fast digest buffer, 1µl of *HindIII* and *EcoRI* (Thermofisher scientific) and 1µg/ml of DNA. The reactions were heated at 37°C for 5 minutes and run on a 1% agarose gel as above (2.6.3). Bands were cut using a UV light source and DNA extracted by Monarch DNA gel extraction Kit (New England Biolabs) and mini-prepped as in section 2.6.2.

The restriction enzyme digest results in a single stranded overhang on the digested end of the DNA fragment, a ligation reaction is then required to combine these 'sticky ends' of the two pieces of DNA together as they will be complementary due to being cut by the same restriction enzymes. Using the cloneable ligation kit (Merck Millipore) 0.025pmol of pET49b was ligated with 0.1pmol of WT1 insert DNA and incubated for 15 minutes at room temperature. 400ng/µl of pET49b/WT1 DNA was then transformed in 50µl of DH5α cells, miniprep and sent for sequencing (Eurofins).

2.7.4 PCR and Gibson assembly of β -catenin and pET47b/HIS

The same method (2.6.3) was used for ligation of β -catenin and pET47b-Histidine (HIS), however due to them being of a similar size at ~ 5000 bp, a restriction digest could not discriminate between DNA bands via UV extraction. Instead, primers were designed and ordered from Eurofins, 50 μ l PCR reactions were made with 2X Phusion Mix (New England Biolabs), 2.5 μ l of forward and reverse primers (Eurofins) as shown in Table 7 and 10ng/ μ l of DNA.

The primer sequences are highlighted in blue, with the annealing temperatures determined by Snapgene and Phusion.

Table 7: Primers designed for PCR reaction.

The primer sequences are highlighted in blue, with the annealing temperatures determined by Snapgene and Phusion.

<u>Insert/Vector</u>	<u>Primer sequence</u>	<u>Snapgene anneal temp (°C)</u>	<u>Phusion anneal temp (°C)</u>
β -Catenin forward primer	TACCAGGATCCGAATTCAATGGCAACC	62	54
β -Catenin reverse primer	GCGGCCGCAAGCTTTACAGATCC	64	54
pET47b forward primer	ATCTGTAAAGCTTGCGGCCGCAGAG	66	71
pET47b reverse primer	GTTGCCATTGAATTCGGATCCTGGTACCCGGGT	69	71

PCR was then completed using the following conditions as shown in table 8 on the Proflex PCR system.

Table 8: PCR conditions for β -catenin and pET47b-HIS.

The PCR steps including initial denaturation, cycling, annealing and extension.

PCR step	Temperature and cycle time
Initial denaturation	98°C for 30 seconds
Cycling	98°C for 10 seconds
Annealing	B-catenin - 54°C for 3 steps pET47b - 71°C for 2 steps for a total of 10-20 seconds and a total of 30 cycles
Extension	72°C for 15-30 seconds per kb

After PCR was complete, 1 μ l of Dpn1 digest enzyme (New England Biolabs, Ipswich, UK) was added and reactions incubated at 37°C for 10 minutes, followed by PCR clean-up kit (Monarch, Ipswich, UK) following manufacturers guidelines. A 5X ISO buffer (1M Tris-HCl pH 7.5, 2M MgCl₂, 100mM dGTP, dATP, dTTP, dCTP, 1M DTT, 1.5g of PEG-8000 and 100mM NAD; New England Biolabs) was prepared. To make the assembly master mix, 350 μ l of 5X ISO buffer was added to 0.025pmol of pET47b DNA and 0.1pmol of β -catenin and assembled using Gibson assembly (New England Biolabs) and incubated at 50°C for 1 hour. To check successful sequencing 400ng/ μ l of β -catenin/pET47b was sent to Eurofins.

2.8 Protein expression

To identify the optimal protein expression conditions for pET49b-GST/HIS/WT1 and pET47b-HIS/ β -catenin, 200ng/ μ l of DNA was transformed in competent Rosetta pLySs cells (University of Sussex) or BL21 cells (University of Sussex) with appropriate antibiotics (kanamycin; 1:1000) and plated on appropriate agar plates.

Next day a 10ml LB culture with appropriate antibiotics was inoculated by picking a colony from the plates and incubated at 37°C with shaking at 210rpm overnight. These 10ml cultures were used to inoculate larger expression cultures (1L LB) containing 750 μ l of appropriate antibiotics and incubated until an optical density at 600nm (OD₆₀₀) of 0.6-0.7 was reached indicating cells were ready for induction. Protein expression was induced by addition of

0.5mM Isopropyl β -D-1-thiogalactopyranoside (IPTG, Merck Millipore), IPTG mimics allolactose, which removes a repressor from the lac operon to induce gene expression. To determine the optimal culturing condition, flasks were cultured in a shaking incubator at 37°C for 4 hours, 30°C for 6 hours or 18°C overnight. All samples were immunoblotted for target protein expression (2.4) to determine bands with optimal purified protein.

2.9 Protein purification

After identifying the optimal expression conditions for both constructs, protein needed to be purified and specific proteins of interest isolated by size exclusion chromatography (SEC).

2.9.1 Protein lysis

WT1 expression pellets were lysed in 10ml of protein purification lysis buffer; 20mM HEPES pH 7.5 (ThermoFisher Scientific), 0.5M NaCl, 0.1mM ZnCl₂ (Arcos Organics part of ThermoFisher Scientific, Oxford, UK), 12% glycerol and 2mM Tris(2-carboxyethyl)phosphine (TCEP; ThermoFisher Scientific). β -catenin expression pellets were lysed in 10ml of protein purification lysis buffer (PP2); 20mM HEPES pH 7.5, 250mM NaCl, 10% glycerol and 2mM TCEP. Both lysis buffers contained an EDTA-free containing complete™ Mini Protease-Inhibitor Cocktail (Merck Millipore). Lysates were incubated on ice for 30 minutes and 5 μ l of DNase (ThermoFisher Scientific) was added. Lysates were sonicated (35% amplitude, 2.5 minutes (5 seconds on, 10 seconds off) per 10ml culture) and then centrifuged at 20,000 x g at 4°C for 30 minutes. The supernatant was removed and kept on ice.

2.9.2 HIS/GST affinity column

Proteins were purified using an affinity Econo-column (Bio-Rad) specific to the GST or HIS tag expressed by the plasmid. Columns were pre-equilibrated by adding 2ml of Amintra CoHIS resin (Expedeon, Oxford, UK) or glutathione resin (Generon, Slough, UK) and the ethanol eluted through. The resin was then washed with 10ml of water and then 10ml of either WT1 or β -catenin purification buffer (same as lysis buffer, 2.8.1). The lysate (2.8.1) was added to the column and the column sealed; the column was placed on a rotator for 1 hour at room temperature. The unbound lysate was eluted through, and 3 initial 5ml washes with 5mM

imidazole (Arcos Organics, Oxford, UK) in WT1/ β -catenin buffer was completed. Bound proteins were then eluted with 10 x 5ml increasing imidazole concentrations (5-350mM) for HIS-tagged proteins and increasing glutathione (Arcos Organics, Oxford, UK) concentrations (5-500nM) for GST-tagged proteins. Following elution, the column was stripped with ethanol, washed with water, and recharged. Elution fractions were immunoblotted (2.4) for WT1, β -catenin, anti-HIS and anti-GST to determine optimal purification fractions.

2.9.3 Size exclusion chromatography (SEC)

Optimal affinity column fractions (2.8.2) were pooled and concentrated at 4000 x *g* for 20-minute intervals using Vivaspin concentrators (Sartorius, Germany) with an appropriate molecular weight cut off (20-100kDa depending on protein) to a final volume of 500 μ l. This concentrated volume was loaded onto a HiLoad 10/300 Superdex 200 gel filtration column (GE, Merck Millipore) pre-equilibrated with either WT1 SEC buffer containing 20mM HEPES pH 7.5, 200mM NaCl, 10% glycerol and 0.1mM ZnCl₂ made to 1L with water, or β -catenin SEC buffer containing 20mM Tris pH 8, 150mM NaCl and 2mM TCEP made to 1L with water connected to an AKTA purifier FPLC system (Cytiva, Marlborough, Massachusetts, USA). Fractions were eluted using the protein-specific SEC buffer at a flow of 0.45ml/min, monitoring protein elution by absorbance at 280nm and collecting 250 μ l fractions into a 48 deep well plate. SEC fractions were analysed by SDS-PAGE and Coomassie (Expedeon, Oxford, UK) stained to determine if method was successful and then immunoblotted (2.3) for WT1 and β -catenin. The SEC fractions with optimal protein were combined and concentrations determined by nanodrop. WT1 protein was used the same or following day for further experiments due to degradation but β -catenin protein was stored at -20°C.

2.10 HIS/GST pull-downs

After successful purification and isolation of WT1 and β -catenin, subsequent pull-down experiments were completed with one protein bound to HIS/GST resin and the second protein added to assess interaction capacity.

2.10.1 Removal of HIS/GST from purified WT1

For the HIS pull-down, β -catenin was bound to HIS resin and the HIS/GST tag from purified WT1 was removed to ensure it would also not bind to the HIS resin. This would indicate direct interaction between β -catenin and WT1 rather than WT1 with HIS resin. To remove the HIS/GST tag from the purified WT1-HIS/GST, protein was HIS affinity purified (2.9.2) and 3 x 200mM fractions of ~ 12ml were incubated overnight at 4°C with 30 μ l of protease 3CV inhibitor (University of Sussex). Protein was then SEC purified (2.9.3) and removal of the tag was confirmed by Coomassie stain with protein migrating to ~ 50kDa instead of ~ 76kDa indicating removal of the 26kDa HIS/GST tag.

2.10.2 HIS/GST pull-down with purified protein

200 μ l of coHIS resin or GST resin (50% slurry) was pre-equilibrated by washing three times with 500 μ l of pull-down buffer containing 20mM HEPES pH 7.5, 150mM NaCl and 2mM TCEP. 50 μ g/ml of β -catenin or 200 μ g/ml of WT1 lysate in pull-down buffer was incubated with tagged specific resin for 1 hour at 4°C on the roller to allow specific binding of the tagged over-expressed protein to the resin. The resin was pelleted by centrifugation at 800 x *g*, 4°C for 5 minutes and any unbound protein was removed, the resin was then washed three times with 1ml of pull-down buffer. Reciprocal protein to the one bound at a concentration matching the bound protein was then added and incubated for 1 hour at 4°C on the roller, the resin was pelleted and washed three times. 25% lysate inputs, unbound protein and resin samples were prepared in 4X SDS buffer and immunoblotted (2.4) to determine if a direct interaction was present.

2.10.3 HIS/GST pull down with cell lysate

The binding of WT1 and β -catenin was also explored in a cellular context as other common binding partners or cellular structures could influence the interaction of these two proteins. For β -catenin/HIS pull-downs 50 μ g/ml of purified β -catenin protein was used per 200 μ l of HIS resin and for WT1/GST pull downs, 400 μ g/ml of purified WT1 protein was used per 200 μ l of GST resin. After successful binding of the bait protein, 1mg/ml of either K562 or HEL total cell lysate was incubated with the resin at 4°C overnight for β -catenin pull-downs, however, was changed to 1 hour at 4°C for the WT1 pull-downs due to limited WT1 protein stability

overnight. The resin was pelleted and washed, inputs, unbound protein and resin samples were immunoblotted (2.4).

2.11 Lentivirus preparation and transduction of cells

To knock down/overexpress proteins of interest or induce mutated versions of a protein, lentiviral transduction was employed. Lentiviruses attach to its target cell via interactions between its viral envelope glycoprotein and a specific cell surface receptor which determines the cellular target for the virus. As lentiviruses express reverse transcriptase, they can convert viral RNA to double stranded DNA and integrase then inserts this viral DNA into host DNA and therefore divides along with host cell, so plasmid DNA is now incorporated into the host genome. Lentiviral particles were used to transduce various cell lines allowing the phenotypic assessment of protein knockdown/overexpression and mutations.

2.11.1 Preparation of plasmid DNA

The following lentiviral shRNA or CRISPR/Cas9 plasmids were ordered/obtained as shown in Table 9, shRNA knockdown and CRISPR/Cas9 constructs arrived as ready-transformed glycerol stocks that were spread onto appropriate LB agar plates with specific antibiotics and mini-prepped (2.6.2). WT1 shRNA over expression constructs plus respective non-targeted control were transformed in Stlb3 *E. coli* cells (2.6.1). The lentiviral envelope (pSL3 pMD.2G/VSV0G) and packaging plasmid (psPAX2) were supplied as a kind gift from the Darley lab (Cardiff University, Wales, UK).

Table 9: WT1 and β -catenin plasmids.

Plasmids used for lentivirus preparation including type of plasmid, host, and source.

Plasmid reference	Use of Plasmid	Host	Source
pBARVUbR / TCF reporter	BARV reporter system	Stbl3	Darley Lab, Cardiff
pfuBARVUbR / mutant TCF reporter	BARV mutant control reporter system	Stbl3	Darley Lab, Cardiff
MISSION® pLKO.1-puro shRNA Control	shRNA non-targeted control	Unknown	Merck Millipore
psPAX2 / HIV-1 Gag, Pol, Tat and Rev	Lentivirus packaging plasmid	DH5 α	Darley Lab, Cardiff
pSL3 (pMD.2G) / VSV-G	Lentivirus envelope plasmid	Stbl3	Darley Lab, Cardiff
MISSION plasmid WT1 shRNA pLKO_TRC0000040067	WT1 knockdown	Stbl3	Merck Millipore
MISSION plasmid WT1 shRNA pLKO_TRC0000040063	WT1 knockdown	Stbl3	Merck Millipore
MISSION plasmid WT1 shRNA pLKO_TRC0000010466	WT1 knockdown	Stbl3	Merck Millipore
MISSION plasmid WT1 shRNA pLKO_TRC0000009873	WT1 knockdown	Stbl3	Merck Millipore
MISSION plasmid WT1 shRNA pLKO_TRC0000288597	WT1 knockdown	Stbl3	Merck Millipore
pLV1-EF1A-hWT1-Puro	Over expressed WT1 isoform at ~ 60 kDa	Stbl3	Vector builder, Chicago, USA

pLV1-EF1A-Puro	Overexpressed WT1 non targeted control	Stbl3	Vector Builder
MISSION pLKO.1 beta-cat shRNA	β -catenin knockdown	Sbl3	Merck Millipore
MISSION pLKO.1 beta-cat shRNA 1248	β -catenin knockdown	Sbl3	Merck Millipore
CRISPR/Cas9 pLV Scramble_gRNA-hCas9- T2A-Puro	CRISPR/Cas9 non- targeted control	Stbl3	Vector Builder
pLV[CRISPR] CTNNB1[KO] 1120bsy	β -catenin knockdown	Stbl3	Vector builder
MISSION pLKO.1 beta-cat shRNA pLKO_TRCN0000314991	β -catenin knockdown	Stbl3	Merck Millipore
MISSION pLKO.1 beta-cat shRNA pLKO_TRCN0000314921	β -catenin knockdown	Stbl3	Merck Millipore
pCW57.1	Mutant control plasmid	ccdB survival	Addgene, Cambridge, UK
WT1 mutated exon 7	pCW57.1 Wt1 mut Ex7.1	Stbl3	Bonifer group, Birmingham University, Birmingham, UK
WT1 mutated exon 8	pCW57.1 Wt1 mut Ex8		Bonifer Group
WT1 mutated exon 9	pCW57.1 Wt1 mut Ex9		Bonifer Group

2.11.2 Lentivirus preparation

Mini preps (2.6.2) of respective DNA were completed. After preparing plasmid DNA, the next step was to generate lentiviral particles for each plasmid to use for the transduction of leukaemia cell lines, in which proteins would be either ectopically expressed, mutated, or silenced followed with functional assessment by immunoblot (2.4).

Prior to transfection, 25cm³ adherent flasks were treated with 2ml of poly-L-lysine (Merck Millipore) for 30 minutes at room temperature. The poly-L-lysine was removed, and flasks were washed with 5ml of DMEM (2.1.2), HEK293T cells were plated at 5x10⁶/5ml and incubated at 37°C overnight with the aim of reaching 80-90% confluence the following day.

Target plasmid DNA was transfected into HEK293 cells using the Lipofectamine 3000 kit (ThermoFisher Scientific) by forming a liposome with the cell membrane and consequently depositing the cargo (naked or purified nucleic acids) into the cell directly.

For each transfection, two tubes were prepared, Tube A contained 2.1µg of plasmid transfer DNA (table 5), 666µl of OptiMEM (ThermoFisher Scientific), 2.2µg of envelope plasmid (pSL3 pMD.2G/VSVG), 4µg of packaging plasmid (psPAX2) and 16µl of p3000 reagent. In a separate tube, tube B contained 675µl of OptiMEM and 19µl of p3000. Tube A was then added dropwise to tube B with gentle swirling to promote lipid-DNA complex binding and was incubated at room temperature for 20 minutes. The media in each 25cm³ flask was reduced to 2ml and the lipid-DNA complex was added and mixed, the flasks were incubated at 37°C, 5% CO₂ for 6 hours. After incubation, the transfection media was removed and replaced with 3ml of fresh DMEM and returned to the incubator overnight. The first harvest was collected and replaced with 2.5ml of DMEM overnight and the second harvest collected the following day, and the total volume was snap frozen in liquid nitrogen and stored at -80°C.

2.11.3 Lentivirus transduction of leukaemia cell lines

Lentivirus generated was introduced into various leukaemia cell lines by transduction. In each well of a non-treated tissue culture 24-well plate (Corning, New York, United States), 250µl of retronectin (Takara, Shiga, Japan) was added and incubated at room temperature for 2 hours or at 4°C overnight. Retronectin was aspirated and replaced with 250µl of 1% BSA in PBS solution and incubated at room temperature for 30 minutes to ensure the retronectin was

removed. Just before the incubation was finished, lentivirus was collected from the -80°C and defrosted in the water bath at 37°C and 1ml of appropriate lentivirus was added to each well. The plate was centrifuged at $2000 \times g$ for 90 minutes, lentivirus was safely discarded and replaced with $1-3 \times 10^5$ cells/ml of the appropriate cell line and incubated overnight at 37°C . For safety, when handling lentivirus, two pairs of gloves were always worn on each hand, lab coat fastened to cover all exposed skin, and anything that contained virus was washed with virkon and then isolated in a biohazard bin containing 5% Bioclense. At 24-48 hours post-transduction, cells were checked and if at a suitable density ($3-4 \times 10^5/\text{ml}$) were selected in $1\mu\text{g}/\text{ml}$ of puromycin. These cells were compared alongside an un-transduced parental control over a 96-hour period, once parental cells were dead, selection was complete. Cells passing through selection were checked for appropriate protein expression using western blotting (2.4) and if successful expanded for cryopreservation (2.1.4) and further culture as required (2.1.1).

2.12 Flow cytometry

To measure Wnt signalling output, cells were transduced (2.11.3) with the β -catenin activated reporter (BAR) system (Biechele & Moon, 2008). The pBARVUbR contains a concatemer of 12 T-cell factor (TCF; a readout for Wnt signalling as Wnt target genes are regulated by DNA-binding and context-dependent interactions with the TCF/lymphoid enhancer factor (LEF) domain) response elements upstream of β -globin minimal promoter linked to Venus (a variant of enhance yellow fluorescent protein ;EYFP) and constitutively expresses DsRed as a selectable marker. As a control, cell lines were transduced with the 'found unresponsive' BAR (pfuBARVUbR) reporter that contains mutated TCF response elements. This reporter system allows the assessment of Wnt signalling level through the detection of EYFP output using flow cytometry.

2.12.1 Assessment of Wnt signalling

The Wnt responsiveness of a variety of leukaemia cell lines; HL60, NB4, KG1 and MV-11 was explored. A 96 v-well plate (Thermofisher Scientific) was set up with $6 \times 10^5/\text{ml}$ of duplicate transduced pBARV/pfuBARV cells treated with either $5\mu\text{M}$ of CHIR99021 or DMSO overnight

at 37°C. The following day the plate was centrifuged at 1300 x *g* for 5 minutes and the media removed, cell pellets were resuspended in 150µl of SB (2.2.3). Cells were assessed for TCF reporter activity by flow cytometric (2.2.3) in which 1x10⁵ intact cells were analysed per sample.

Post-acquisition analysis was performed using FlowJo (2.2.3), untransduced parental cells not containing the BAR system were dsRED⁻ and therefore used to set the threshold for dsRED⁺ positive events. This gate was applied to all wells allowing the identification and assessment of pBARV/pfuBARV expressing cells. Following this a histogram of Venus YFP fluorescence intensity was used to measure Wnt signalling with the mutant pfuBARV serving as a negative control. pBARV/fuBARV expressing cells were then transduced with WT1 knockdown, overexpression, or mutation (2.11.3) and the impact of WT1 modulation assessed by flow cytometry.

2.13 Polysome profiling

Polysome profiling is a technique used to study the association of mRNAs with ribosomes. The experiment starts by collecting a lysate which will contain polysomes, monosomes (composing of one ribosome residing on an mRNA), the small (40S in eukaryotes) and large (60S in eukaryotes) ribosomal subunits, 'free' mRNA, and a host of other components. These components are separated by centrifugation in a sucrose gradient based on size e.g., larger subunits such as the 80S will travel further through the gradient. After centrifugation the contents of the tube are collected as fractions, these can then be immunoblotted (2.4) for certain proteins to identify the type of ribosomes they are associated with. In summary, this technique can be used to study the overall translation in cells, and more specifically to analyse individual proteins and their mRNAs.

2.13.1 Preparation of cells and sucrose gradient

K562 cells were cultured at 30x10⁶/75ml with CHIR99021 or DMSO (2.1.5). A sucrose gradient was prepared by weighing out 15% and 60% of agarose (Merck Millipore), 15ml of water was added to each and dissolved in the microwave on low. Once cooled, 50mM KCl (Merck Millipore) 20mM Tris HCl pH 8.0 (Merck Millipore) and 10mM MgCl₂ (Merck Millipore) was

added, and the final volume increased with water to 20ml. Following this 200µl of cycloheximide (100µg/ml; Merck Millipore), 40µl of DTT (1mM) and 66.6µl of protease inhibitor (1 tablet/ml; Roche by Merck) was added. The 15% sucrose was added into an ultracentrifuge tube (Beckman Coulter, High Wycombe, UK) and the 60% slowly pipetted on top, the ultracentrifuge tube was added to the fractionator and the 15-60% sucrose gradient programme selected. The gradients were then stored in the fridge at 4°C overnight.

2.13.2 Ultracentrifugation and fractionation

K562 cells were pelleted at 1300 x *g* for 10 minutes and resuspended in 20ml of PBS with centrifugation twice. Cell pellets were then resuspended in 500µl of lysis buffer containing 20mM Tris-HCl pH 8.0, 50mM KCl, 10mM MgCl₂, 1mM DTT, 1% NP40 (ThermoFisher Scientific), 100µg/ml cycloheximide, 24U/ml Turbo DNase (Invitrogen), RNasin plus 90U (Promega, Wisconsin, USA) and protease inhibitor. Lysates were incubated on ice for 30 minutes and after centrifuged at 17,000 x *g* for 10 minutes at 4°C. A second spin was completed if any debris was left over, the supernatant was collected and 450µl of lysate was loaded on to the top of the sucrose gradient. Sucrose gradients with lysates were centrifuged on the ultracentrifuge at 31,000 rpm for 3 hours and 30 minutes at 4°C.

The fractionator was washed and calibrated using water, the samples were loaded, and 12 fractions were collected into a separate 1.5ml eppendorf with a volume of ~ 1ml and stored at -80°C. The fractionator was then washed with water and 70% ethanol with components of the machine soaking in water until the next day.

2.13.3 Precipitation

For precipitation, 400µl of each fraction was added to 1.6ml of 100% ethanol (VWR Chemicals, Leicestershire, UK) and 5µl of glycoblue (Invitrogen) was added to aid in visualisation of pellet. These were incubated at -20°C overnight.

Fractions were centrifuged at 14,000 x *g* for 15 minutes at 4°C. The supernatant was removed, and pellets washed in 1ml of 70% ethanol and centrifuged. The supernatant was removed, and the pellet air-dried by the heat block at 95°C for 5 minutes. The pellets were resuspended in 4X laemmli buffer and heated at 95°C for 5 minutes. Samples were immunoblotted (2.4) to determine β-catenin protein content in polysomes.

2.14 RNA binding immunoprecipitation

RNA binding immunoprecipitation (RIP) is a technique used to map *in vivo* RNA-protein interactions, the RBP of interest is immunoprecipitated together with its associated RNA to identify bound transcripts (mRNAs, non-coding RNAs, or viral RNAs). Transcripts can then be detected by sequencing.

2.14.1 Cell lysis

Cells were treated at $25\text{-}50 \times 10^6$ with CHIR99021 or DMSO (2.1.5). The next day cells were collected and $\sim 4 \times 10^6$ cells were then centrifuged at 1500rpm for 10 minutes at 4°C. The supernatant was discarded, and the pellet was resuspended in 10ml of cold PBS and centrifuged and repeated once more. The cell pellet was resuspended in 100μl of lysis buffer (Magna RIP kit, Merck Millipore kit #17-700, + 0.5μl of protease inhibitor cocktail + 0.25μl of RNase inhibitor). Lysates were incubated on ice for 5 minutes and stored at -80°C overnight to complete lysis.

2.14.2 Preparation of magnetic beads for immunoprecipitation

Magnetic beads were completely dispersed by over end rotation. Microfuge tubes were set up, one per immunoprecipitation and 50μl of magnetic beads were added to each tube. Then 500μl of RIP wash buffer as provided in the kit was added and the tubes vortexed briefly. The tubes were placed on the magnetic separator and supernatant was removed. This wash step was repeated, and the beads were resuspended in 100μl of wash buffer containing 5μg of mouse IgG, β-catenin or HuR antibody (see table 2). The tubes were incubated for 30 minutes at room temperature with rotation. The tubes were placed on the magnetic separator and the supernatant containing any unbound antibody was discarded. 500μl of wash buffer was added, tubes vortexed and supernatant discarded, this was repeated for a second time. Finally, beads were resuspended in 500μl of wash buffer and tubes kept on ice.

2.14.3 Immunoprecipitation of RNA-binding protein-RNA complexes

The 500µl of wash buffer was removed by the magnet and the beads were resuspended in 900µl of RIP immunoprecipitation buffer (MagnaRIP kit; 860µl of RIP buffer, 35µl of 0.5M EDTA and 5µl of RNase inhibitor). The RIP lysates were thawed and centrifuged at 17,000 x *g* or 10 minutes at 4°C, 100µl of supernatant was removed and added to each bead-antibody complex in RIP immunoprecipitation buffer. The tubes were incubated with rotating at 4°C overnight. The tubes were placed on the magnetic separator and supernatant removed, 500µl of wash buffer was added vortexed briefly. The supernatant was discarded, and this wash step was completed another six times. Input (10-30%) and subsequent pull-down samples were immunoblotted (2.4) for β-catenin and HuR to check sufficient protein had bound to the beads prior to RNA purification.

2.14.4 RNA purification

Each immunoprecipitation, including the input sample was resuspended in 150µl of proteinase K buffer (1 x RIP wash buffer, 15µl of stock 10% SDS and 18µl of stock 10mg/ml proteinase K). This was added in this order to reduce risk of denaturation of proteinase K by addition of concentrated SDS. All tubes were incubated at 55°C for 30 minutes with shaking at 310rpm to digest the protein. The supernatant was collected by the magnetic stand and placed in a new eppendorf, 250µl of RIP wash buffer was added to each tube apart from the input. Then 400µl of phenol:chloroform:isoamyl alcohol (25:24:1; Thermofisher Scientific) was added to each tube, vortexed for 15 seconds and centrifuged at 14000rpm for 10 minutes to separate the phases. 350µl of the aqueous phase was removed into a new eppendorf and 400µl of chloroform (Thermofisher Scientific) was added and vortex and centrifugation repeated. 300µl of the aqueous phase was removed into a new eppendorf and 50µl of Salt solution I, 15µl of salt solution II and 5µl of precipitate enhancer (MagnaRIP Kit) was added to each tube with final addition of 850µl of absolute ethanol (Thermofisher Scientific). Tubes were mixed and kept at -80°C overnight to precipitate the RNA. The tubes were centrifuged at 14,000rpm for 30 minutes at 4°C and the supernatant discarded carefully. The pellet was washed with 500µl of 80% ethanol, centrifuged for 15 minutes and the supernatant discarded, and pellet air dried for 10 minutes at room temperature. The pellet was resuspended in 20µl of nuclease-free water and the tubes kept at -80°C. Quality of Input RNA was assessed by the

Nanodrop using nuclease-free water as the blank and acceptable samples for downstream applications met $\sim 300\text{ng}/\mu\text{l}$ of RNA per 10% input with $A_{260/280}$ and $A_{230/260}$ ratios close to 2.0. RNA samples were also validated by the mRNA bioanalyser Pico series II following manufacturer guidelines (Agilent RNA Pico; Santa Clara, California, USA).

2.15 RNA extraction of cells containing β -catenin shRNA and CRISPR/Cas9 knockdown

2.15.1 RNA extraction and clean up

Cell pellets of 5×10^6 cells were lysed in 1ml of Trizol (Life technologies by Thermofisher Scientific) and stored at -80°C . 200 μl of chloroform was added and samples vortexed. Samples were spun at $17,000 \times g$ for 15 minutes at 4°C to ensure separation, with RNA in the upper aqueous phase. This phase was removed to a separate eppendorf, containing 0.5ml isopropanol (Thermofisher scientific), vortexed briefly and left at room temperature for 5-10 minutes. Centrifugation was repeated to pellet the RNA, supernatant was discarded, and pellet washed in 80% ethanol, samples were centrifuged for 5 minutes. Supernatant discarded and pellets re-spun for 1 minute to remove dregs. The pellet was air dried for 5-10 minutes at room temperature and then resuspended in 100 μl of nuclease free water. Concentrations were then determined by the Nanodrop (2.14.4) 600 $\mu\text{g}/\text{ml}$ of RNA was then cleaned up using RNeasy MinElute Clean-up kit (Qiagen, Manchester, UK #74204) following manufacturer guidelines.

2.16 Quantitative reverse transcription polymerase chain reaction (qRT-PCR)

qRT-PCR is used when the starting material is RNA, this is first transcribed into complementary DNA (cDNA) by reverse transcriptase from total RNA or messenger RNA (mRNA). The cDNA is then used as the template for the qPCR reaction. A one step assay combines reverse transcription (RT) and PCR in a single tube and buffer using a reverse transcriptase alone with DNA polymerase. Often a mixture of oligo(dT)s and random primers are used, these primers anneal to the template mRNA strand and provide reverse transcriptase enzymes with a starting point for synthesis. Primers are designed to span an exon-exon junction with one of the amplification primers potentially spanning the actual exon-intron boundary, which reduces the risk of false positives from amplification of any contaminating genomic DNA, since

the intron genomic DNA sequence would not be amplified. For controls a minus RT should be included to test for contaminating DNA (genomic DNA) and ideally no amplification should occur.

2.16.1 cDNA generation and PCR

Purified RNA (2.14.4 and 2.15.1) was converted to cDNA by adding 9µl of pull-down RNA or 2µg total of purified total RNA with 2X reverse transcriptase (RT) buffer (volume adjusted accordingly depending on volume of RNA to make 19µl total) and 1µl of 20X enzyme mix (Thermofisher Scientific). The PCR tubes were then placed in the ProFlex PCR system (Thermofisher Scientific), and the following RT program was run (Table 10).

Table 10: Reverse transcriptase (RT) PCR reaction steps.

The temperature and time (minutes) for each step of the RT procedure.

Stage of cycle	Temperature (°C)	Time (minutes)
RT reaction	37	60
Stop the reaction	95	5
Hold	4	Hold

The tubes were removed from the cycler and the Input lysate cDNA was diluted with 180µl of nuclease free water, the pull-down samples were left undiluted, and all were kept at -20°C. Primers for target genes were ordered (Merck Millipore) as shown in table 11 and were reconstituted to 100µM in nuclease free water.

Table 11: Forward and reverse primers for each target gene.

Each primer set was reconstituted to 100µM in nuclease free water, each sequence and Tm° for optimum cycling stages are highlighted.

Oligo Name	Peptide name	Tm°	Length (bp)	5' -> 3' Sequence
1_ACTB_F	β-actin	66.1	22	TTGTTACAGGAAGTCCCTTGCC
2_ACTB_R	β-actin	67.2	22	ATGCTATCACCTCCCCTGTGTG
3_BIRC5_F	Survivin	64.7	21	AGGACCACCGCATCTCTACAT
4_BIRC5_R	Survivin	63.6	21	AAGTCTGGCTCGTTCTCAGTG
5_PTGS2_F	COX-2	67.1	19	CTGGCGCTCAGCCATACAG
6_PTGS2_R	COX-2	65.3	23	CGCACTTATACTGGTCAAATCCC
7_CCND1_F	Cyclin D1	66.9	20	GCTGCGAAGTGGAACCATC
8_CCND1_R	Cyclin D1	66.2	22	CCTCCTTCTGCACACATTTGAA
9_LEF1_F	LEF-1	68	19	AGAACACCCCGATGACGGA
9_LEF-1_R	LEF-1	65.4	22	GGCATCATTATGTACCCGGAAT
WT1_F1	WT1	60	20	CACAGCACAGGGTACGAGAG
WT1_R1	WT1	60	20	CAAGAGTCGGGGCTACTCCA
AREG_F1	AREG	50	20	TGGATTGGACCTCAATGACA
AREG_R1	AREG	50	20	ACTGTGGTCCCCAGAAAATG
AREG_F2	AREG	60	21	GTGGTGCTGTCGCTCTTGATA
AREG_R2	AREG	60	21	CCCCAGAAAATGGTTCACGCT
ETS1_F1	ETS1	60	23	AAACTTGCTACCATCCCGTACGT
ETS1_R2	ETS1	60	22	ATGGTGAGAGTCGGCTTGAGAT
JUNB_F1	JUNB	60	21	TGGTGGCCTCTCTACACGA
JUNB_R1	JUNB	60	17	GGGTCGGCCAGGTTGAC
VDR_F1	VDR	60	20	CTGACCCTGGAGACTTTGAC
VDR_R1	VDR	60	19	TTCCTCTGCACTTCCTCAT
BAK1_F1	BAK1	60	21	GTTTTCCGCAGCTACGTTTTT

BAK1_R1	BAK1	60	22	GCAGAGGTAAGGTGACCATCTC
DNMT3a_F1	DNMT3a	60	20	CCGATGCTGGGGACAAGAAT
DNMT3a_R1	DNMT3a	60	20	CCCGTCATCCACCAAGACAC
MYB_F1	MYB	60	21	GAAAGCGTCACTTGGGGAAAA
MYB_R1	MYB	60	23	TGTTTCGATTCGGGAGATAATTGG
GAPDH_F1	GAPDH	60	20	ACAGTCAGCCGCATCTTCTT
GAPDH_R1	GAPDH	60	20	ACGACCAAATCCGTTGACTC

After reconstitution, 7.5µl of primer (100µM stock) was diluted in 500µl of nuclease free water to make working stocks of primers for qPCR. Master mixes were made for each primer set containing 7.5µl of Go-Taq SYBR (Promega, Wisconsin, USA), 1.5µl of working stock forward and reverse primers and 1.5µl of nuclease free water. In each well of a MicroAmp 96 fast optical plate (ThermoFisher Scientific), 12µl of primer master mix was added to 3µl of cDNA and for a non-template control, 3µl of nuclease free water was used for each primer set, to ensure the primers were not amplifying and producing a cycle threshold (CT value). An optical film (ThermoFisher Scientific) was placed tightly over the top of the plate and the plate was centrifuged using the pulse setting up to the maximum speed of 4400 rpm to make sure all contents were concentrated to the bottom of the well. The plate was then loaded onto the StepOnePlus QPCR machine (ThermoFisher Scientific), quantitation standard curve, SYBR green reagents and standard curve (~2hr to complete run) settings were selected using StepOne software v2.3 (ThermoFisher Scientific). Targets and samples were assigned to corresponding wells, including the non-RT control wells and the run was started. Standard curves for each primer set and mRNA quantity of pull-down samples were then analysed.

2.16.2 qPCR analysis

All plates included samples with the housekeeping gene *ACTB* which should remain constant, control cells were used to generate a 1:4 standard curve (30-0.02ng) for the knockdown studies. For the RIP pull down analysis a 1:5 standard curve was generated (60-0.003) with the 10% input sample. Samples were added to the plate at 1:10 and 1:40 dilutions in triplicate, the standard curves were then used to work out the quantity of gene expression. All

subsequent target genes were normalised by dividing the target gene expression quantity determined from the standard curve of that target gene, by the *ACTB* quantity for that sample using StepOne as above.

2.17 Statistics

For correlation studies, ImageJ was used to quantify pixel intensity in from western blot images. The area for each respective protein was then divided by the corresponding β -actin density for that well. These numbers were then added into GraphPad Prism Version 8.0 and a scatter plot including linear regression was determined highlighting the Spearman R correlation value. A two-tailed t-test was conducted with a significance threshold set at $p = 0.05$.

Significance of difference was determined using paired students t tests with significance set at $P < 0.05$ or a one sample t-test with a theoretical mean of one. Bar graphs were plotted with error bars representative of one standard deviation and summarised from three independent biological replicates (unless otherwise stated) using GraphPad Prism.

Chapter 3. Validation of novel β -catenin interacting proteins in myeloid cells

3.1 Introduction

Wnt signalling is frequently dysregulated in AML and overexpression of the central mediator β -catenin is observed versus healthy CD34⁺ HSC (Simon et al., 2005). *In vivo* modelling has shown activation of this pathway is important in the self-renewal and drug resistance of leukemic stem cells (LSC), as the inhibition or deletion of β -catenin impaired LSC function and AML development induced by oncogenes such as HOXA9 and MEIS1 (Dietrich et al., 2014; Fong et al., 2015; Wang et al., 2010; Yeung et al., 2010). Furthermore, fusion genes commonly implicated in AML such as PML/RAR α and AML1/ETO regulate Wnt signalling genes and lead to overexpressed γ -catenin which enhances Wnt signalling through β -catenin stabilisation (Müller-Tidow et al., 2004). Therefore, Wnt signalling is important in the regulation of LSCs, however it does not entirely block the progression of LSCs, indicating additional cooperation partners may be involved. The stability, cellular localisation and transcriptional activity of β -catenin is heavily dictated by protein interactions which are poorly characterised in a haematopoietic context. Identifying these novel partners can provide important molecular information for targeting β -catenin. In 2019, the Morgan group performed the first β -catenin interactome in myeloid cell lines (HEL and K562) using quantitative mass spectrometry and identified a plethora of established and novel binding partners as shown in Figure 1 (Morgan et al., 2019). Following a stringent bioinformatics filtering process, the novel partners MSI2, LIN28B, PUM2, RBM15 and WT1 were selected for further study because of their previously documented roles in HSC, AML or Wnt signalling biology (see Introduction section 1.7). Interestingly, all these proteins are RNA-binding proteins (RBP) with various regulatory roles and could therefore identify a novel functional RNA role for β -catenin. However, such interactions first required validation through reciprocal co-immunoprecipitation (co-IPs) to confirm association.

3.2 Aims

Overall understanding the type and nature of β -catenin protein interactions could improve understanding of how this protein and Wnt signalling contributes to regulating normal and malignant haematopoiesis. To this end, this chapter has the following aims.

1. Validation of novel β -catenin protein interactions identified from mass spectrometry by reciprocal (Co-IP) in myeloid cells.
2. Characterising the WT1: β -catenin interaction using recombinant protein expression
3. Identification of appropriate models for further study of β -catenin protein interactions, and assessment of expression in primary AML patient samples.
4. Determination of effect of Wnt signalling activation (using the Wnt signalling agonist CHIR99021) on sub-cellular localisation and expression of interacting partners.

3.3 Results

3.3.1 Validation of β -catenin interaction with LIN28B, MSI2 and WT1

To validate the association between β -catenin and potential interactors of significance identified from the mass spectrometry, reciprocal Co-IP reactions were completed in cells used for MS studies. The principle of a Co-IP involves using an antibody against a specific target protein which forms an immune complex with that target in a sample, such as a cell lysate. The immune complex is then captured onto a beaded support to which an antibody-binding protein is immobilised (protein G) and any proteins not precipitated on the beads are washed away.

K562 and HEL cells were incubated overnight with either DMSO or the Wnt activator CHIR99021 (2.1.5). Whole cell inputs, immunodepleted (ID) and Co-IP samples were western blotted to examine protein abundance. As shown in Figure 9A, LIN28B protein (~32kDa) was successfully enriched in the Co-IP lane and interestingly β -catenin (92kDa) was detected in the LIN28B Co-IP lanes under both conditions, confirming an association between the two proteins. We next assessed MSI2 (35 kDa) as shown in Figure 9B and exhibited β -catenin association in CHIR99021 treated cells. As displayed in Figures 9C and 9D respectively, no β -catenin association with PUM2 (122kDa) or RBM15 (110kDa) was identified despite successful co-IPs for each (despite some high background signal in IgG Co-IP lanes). In Figure 9E, WT1 protein (50 kDa) exhibited association with β -catenin in Wnt stimulated conditions. These

data overall suggest interaction between β -catenin and LIN28B, MSI2 and WT1 in K562 cells, but validation was required for a second cell line from an AML background specifically.

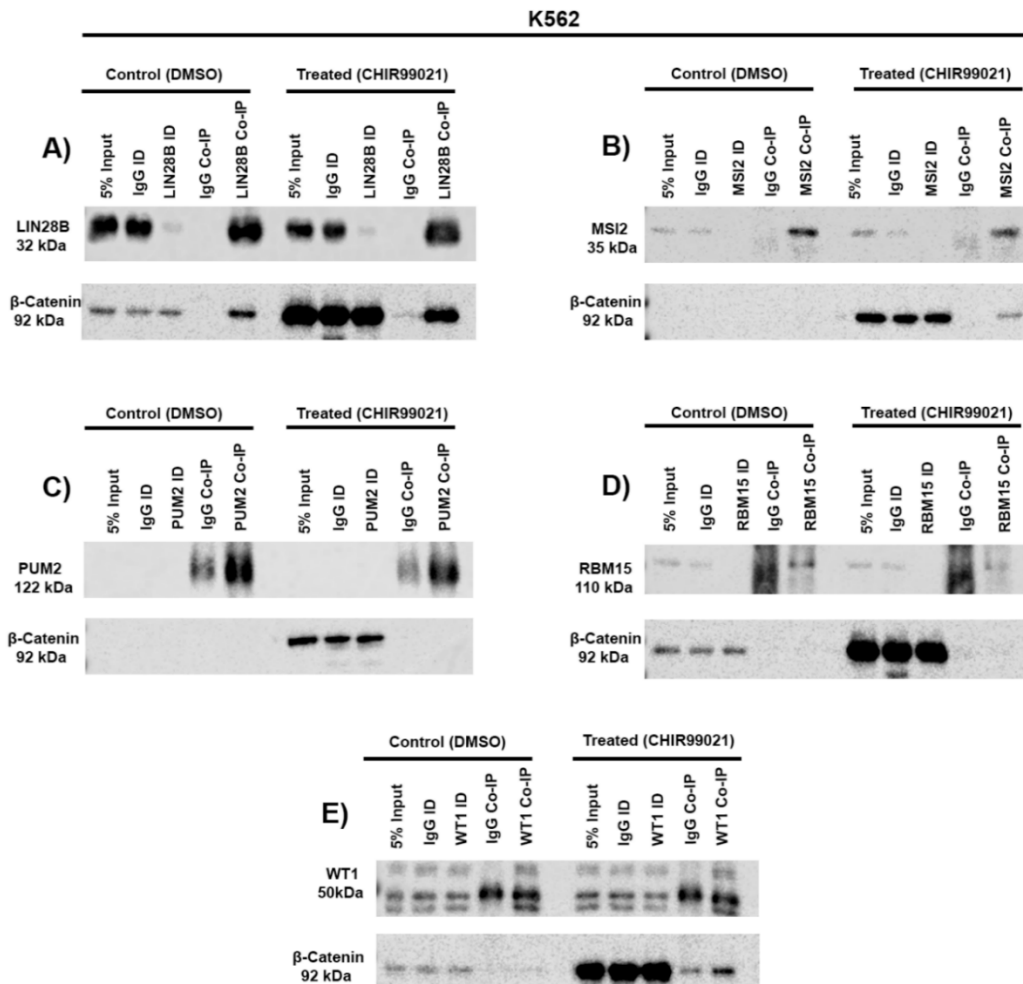


Figure 9: Co-IPs to detect β -catenin association in K562 whole cell

Immunoblots showing β -catenin abundance in **A) LIN28B B) MSI2 C) PUM2 D) RBM15 and E) WT1** Co-IPs derived from whole cell lysates of K562 cells +/-5 μ M CHIR99021. Total cell inputs (5%), immunodepleted (ID) and Co-IP lanes are shown.

To validate β -catenin partners in an AML cell line we repeated Co-IPs in the HEL cell line representing an erythroleukemia origin. As before, LIN28B Co-IP was successful and resulted in abundant β -catenin in both DMSO and CHIR99021 treated conditions (Figure 10A). As shown in Figure 10B, MSI2 Co-IPs were also efficient in this cell line and resulted in clear β -catenin enrichment in the Wnt signalling induced lysate (CHIR99021) and a feinter band in

the basal Wnt signalling lysate (DMSO). For PUM2 as shown in Figure 10C, Co-IPs were partly successful but contained high background in IgG Co-IP lanes. Unlike K562 cells, β -Catenin was detected in both DMSO and CHIR99021 treated PUM2 Co-IPs, but signal was also observed in the CHIR99021 IgG Co-IP lane indicative of non-specific binding. For RBM15 (Figure 10D) background signal was high in IgG lanes and failed to pull down β -catenin. Finally, as shown in Figure 10E, the WT1 Co-IP was successful and resulted in β -catenin pull down in both DMSO and CHIR99021 conditions.

In summary, reciprocal Co-IPs have validated an association between LIN28B, MSI2 and WT1 with β -catenin under both basal and Wnt stimulated conditions across two myeloid cell lines. Association with PUM2 or RBM15 could not be validated either through failure to detect β -catenin or presence of non-specific binding.

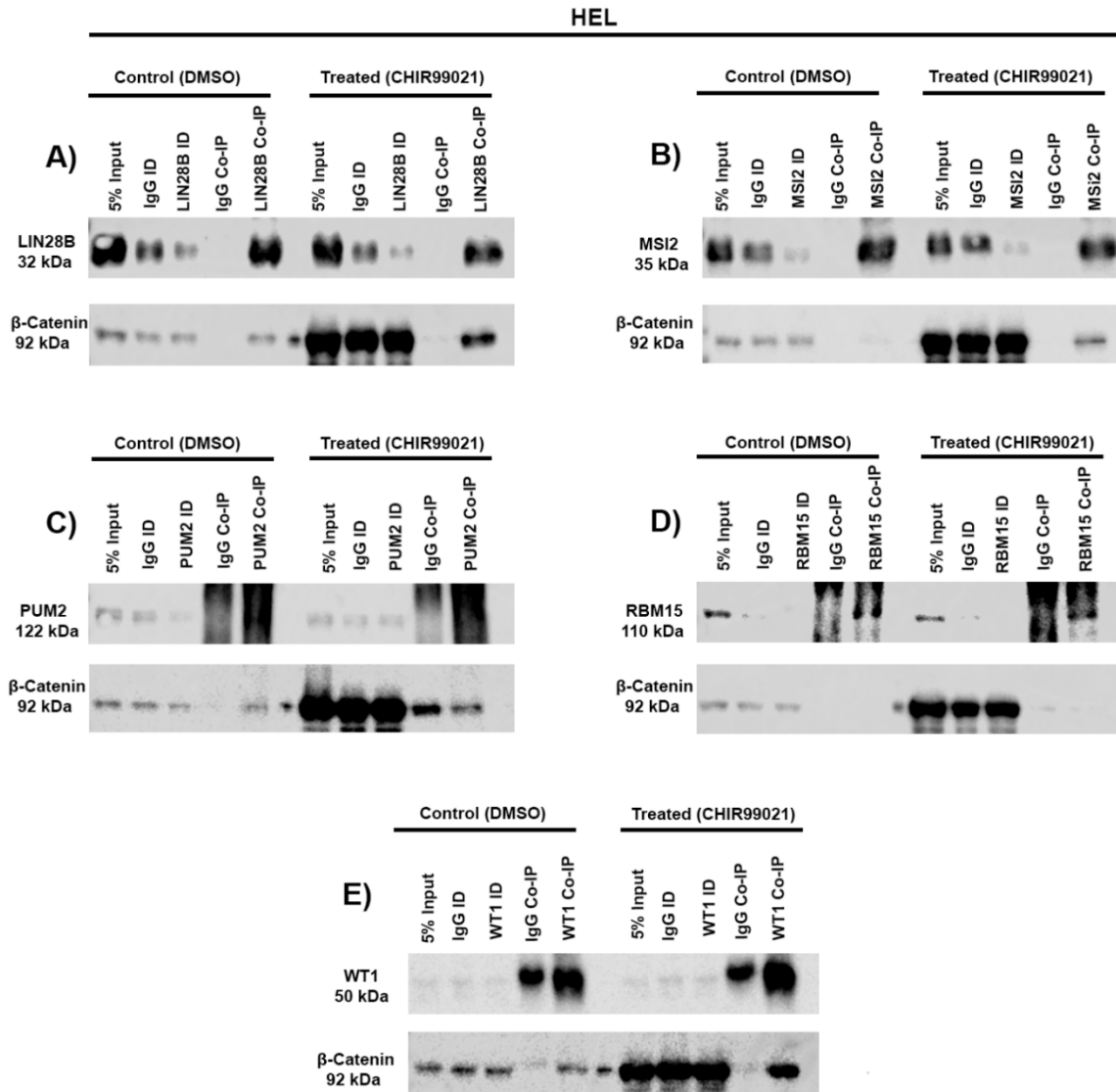


Figure 10: Co-IPs to detect β -catenin association in HEL whole cell

Immunoblots showing β -catenin abundance in **A) LIN28B B) MSI2 C) PUM2 D) RBM15 and E) WT1** Co-IPs derived from whole cell lysates of HEL cells +/-5 μ M CHIR99021. Total cell inputs (5%), immunodepleted (ID) and Co-IP lanes are shown.

Finally, given the importance of WT1 and its well documented role in AML (Potluri et al., 2021) we sought to validate the β -catenin:WT1 interaction in a second AML cell line; KG1. KG-1 cells are derived from a patient with erythroleukemia that evolved into AML with morphology resembling the AML1-ETO fusion gene subtype. As before, the WT1 Co-IP was successful and

resulted in abundant β -catenin pull down in CHIR99021 treated conditions and more modestly under basal Wnt signalling activation (Figure 11).

In summary, reciprocal Co-IPs have validated an association between WT1 and β -catenin under basal and Wnt stimulated conditions across three myeloid cell lines. However, to understand if their association was direct, pull-downs with purified recombinant WT1 and β -catenin was necessary.

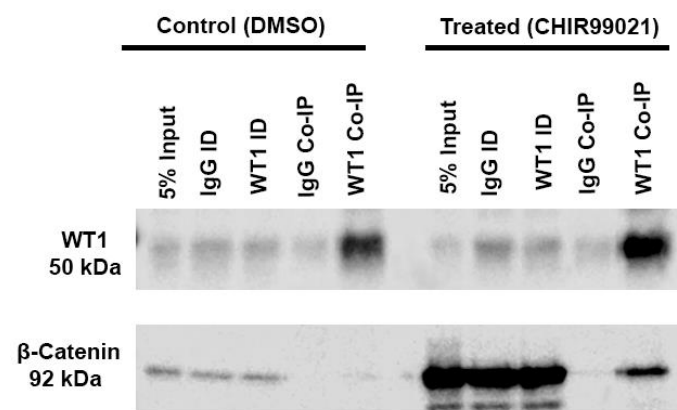


Figure 11: Co-IP to detect β -catenin association in KG1 whole cell lysate.

Immunoblots showing β -catenin abundance derived from whole cell lysates of KG1 cells +/- 5 μ M CHIR99021. Total cell inputs (5%), immunodepleted (ID) and Co-IP lanes are shown.

3.3.2 Preparation of bacterial expression constructs pET49b-WT1 and pET47b- β -catenin

To begin preparing recombinant proteins to test the direct binding capacity between β -catenin and WT1, full-length sequences of human WT1 and β -catenin proteins were identified from UniProt and ordered from Eurofins (Methods section 2). WT1 was inserted into the pET49b-GST/HIS vector to aid in WT1 expression and purification using previously characterised conditions (Fagerlund et al., 2012). β -catenin was inserted into the pET47b-HIS vector as was readily available in the lab and β -catenin purification is relatively stable as previously shown (Xing et al., 2008) (plasmid maps found on Snapgene).

These constructs were then checked by sequencing at Eurofins. As shown in Figure 12, full length WT1 was incorporated into the pET49b-GST vector successfully.

3.3.3 Optimisation of expression conditions for β -catenin and WT1

After successful preparation of the two constructs, the next aim was to express the proteins using competent Rosetta pLySs and BL21 cells over three different conditions: 37°C for 4 hours, 30°C for 6 hours and 18°C overnight. This was done to identify optimal protein expression conditions for both proteins as these three conditions covered a range of temperatures. Un-induced (without addition of IPTG; Methods section 2.8) and induced input samples were compared to induced lysate and pellet samples to check expression and solubility as shown in Figure 14. For WT1, a clear band is present in both cells in the pellet samples at ~76 kDa for condition tests at 37°C and 30°C (Figure 14A) matching size expected for WT1/pET49b. The optimal expression condition for WT1 was determined as 18°C in Rosetta PLyS due to the faintest band in the pellet which would suggest the most soluble variant. For β -catenin as shown in Figure 14B, both cells display a clear band at ~ 92 kDa for input, lysate, and pellet lanes. Usually β -catenin is ~ 92kDa on its own and with the addition of the 6 HIS residue tag this would not change the molecular weight as is only ~ 1 kDa. The condition at 18°C overnight in the BL21 displayed the most favourable clear pellet sample but also showed reduced β -catenin expression in the lysate. These data, in conjunction with previous reports indicate the optimal condition for recombinant β -catenin expression to be 37°C for 4 hours (Dar et al., 2016).

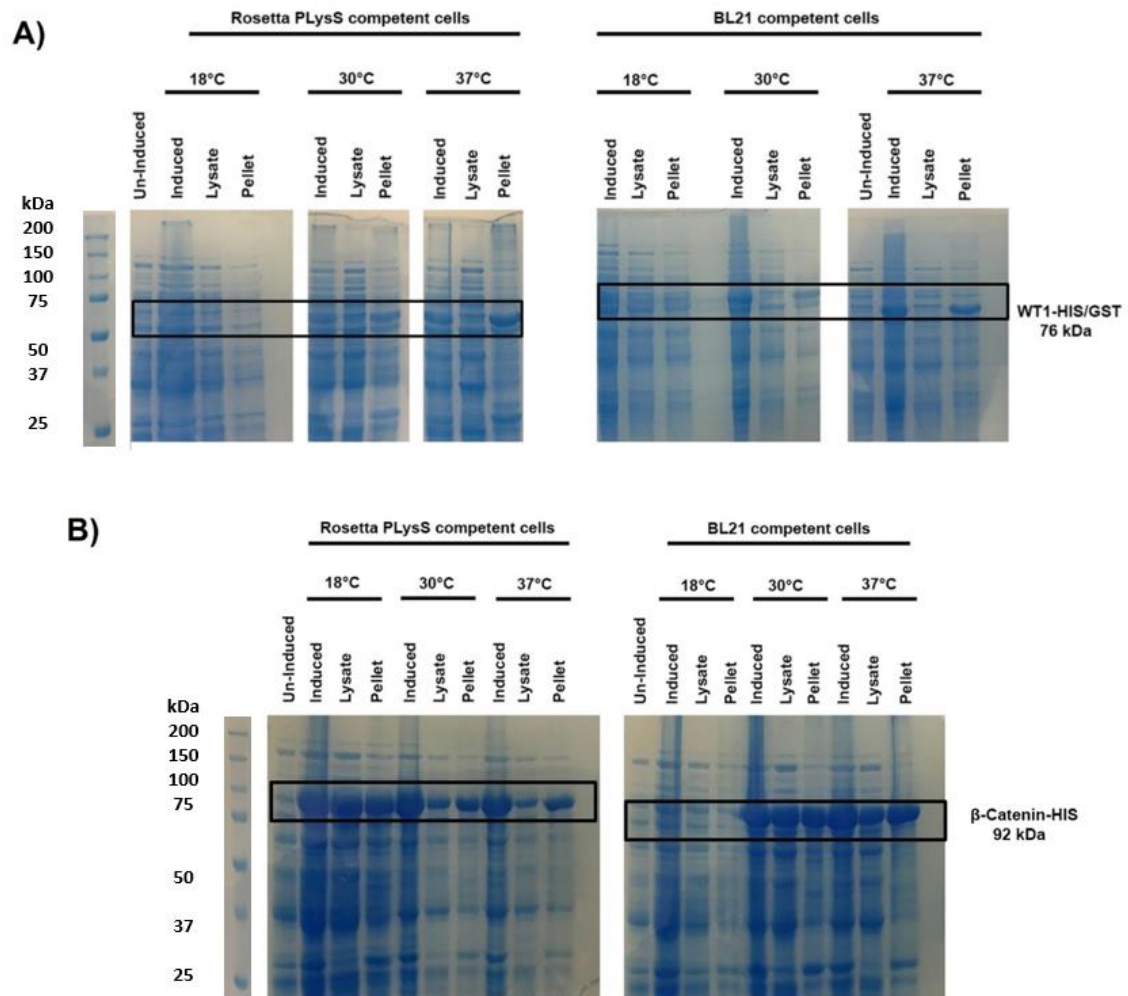


Figure 14: Expression of recombinant WT1 and β -catenin constructs in Rosetta pLysS and BL21 competent cells.

Coomassie blue stained 9% acrylamide gels showing **A)** WT1-HIS/GST and **B)** β -catenin-HIS protein expression under three different expression conditions: 37°C for 4 hours, 30°C for 6 hours and 18°C overnight. Un-induced and induced lysates and subsequent pellets are also shown.

3.3.4 HIS affinity purification of WT1 and β -catenin

Following successful expression, HIS affinity column purification of WT1 and β -catenin was completed to determine optimal fractions containing each construct, by elution with imidazole to act as a competitor for the resin and in turn displace the protein of interest.

As shown in Figure 15, the first lane contains the unbound material to the HIS resin, three washes with 5mM of imidazole were completed to remove as much background protein as possible, as this concentration of imidazole is too low to displace WT1 or β -catenin from the HIS resin. More washes over a range of 20-50mM of imidazole were tested to determine the optimal concentration for purifying protein. As shown in Figure 15A, at 20mM of imidazole the band for WT1-HIS/GST is still quite faint relative to background but becomes enriched in the 50mM and 200mM fractions, and as seen when above this concentration protein expression becomes fainter. For β -catenin (Figure 15B), a slightly different Imidazole range of 20-350mM was used as previous studies showed this to be a more suitable range (Fagerlund et al., 2012). Optimal fractions with enriched β -catenin were identified at 3 x 200mM Imidazole, and fractions for both proteins were pooled for size exclusion chromatography (SEC).

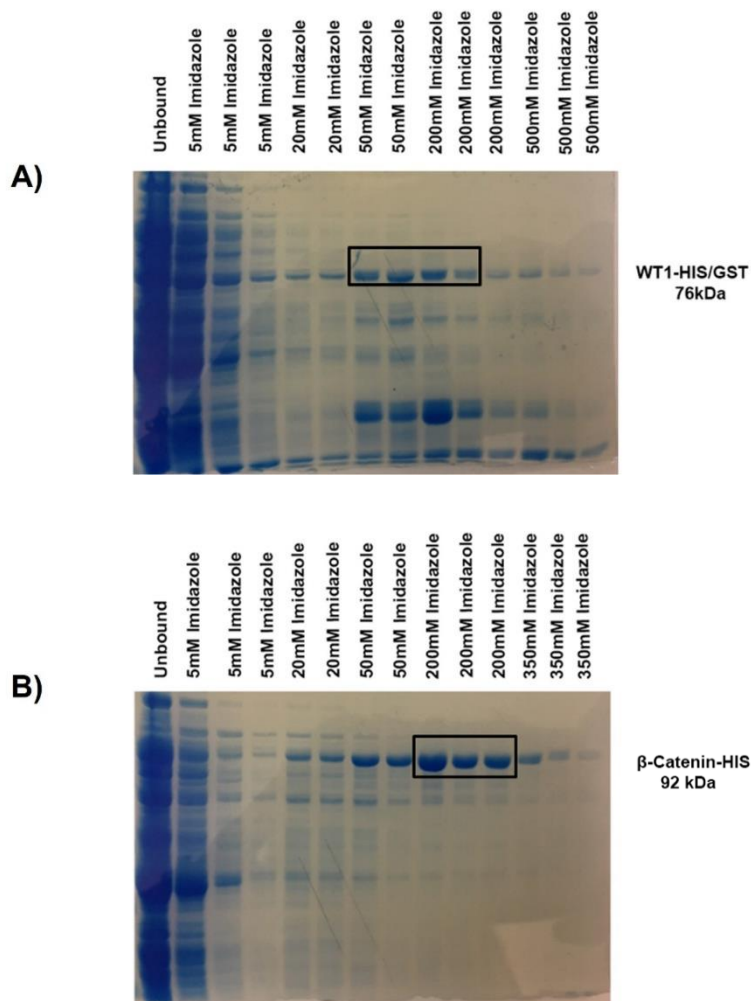


Figure 15: Optimised HIS tag purification of WT1 and β -catenin.

For **A)** WT1-HIS/GST and **B)** β -catenin-HIS expression lysates were mixed with HIS resin and eluted with increasing imidazole, all elution's were tested on a 9% SDS-PAGE gel and Coomassie stained.

3.3.5 Size exclusion chromatography (SEC) and isolation of WT1 and β -catenin

Following identification of optimal purification fractions for WT1 and β -catenin, fractions were loaded onto the pre-equilibrated HiLoad 10/300 Superdex 200 gel filtration column producing SEC traces. This procedure separates proteins based on size and therefore we can isolate our protein of interest as we know the expected molecular weight and can therefore obtain clean isolated WT1 or β -catenin protein. For WT1 as shown in Figure 16A, three peaks were found at 12.98, 15.07 and 21.07mL. The peak at 12.98mL corresponds to a protein size

of ~ 216 kDa which is a lot larger than expected. This could be due to the GST dimerising and therefore producing a larger size protein.

For β -catenin as identified in Figure 16B the three peak sizes were 13.45, 15.84 and 23.32mL. The first peak at first peak at 13.45mL corresponds to a size of ~ 163 kDa, which is also larger than the ~76 kDa expected. Therefore, these fractions required western blotting to determine the location of each both WT1 and β -catenin.

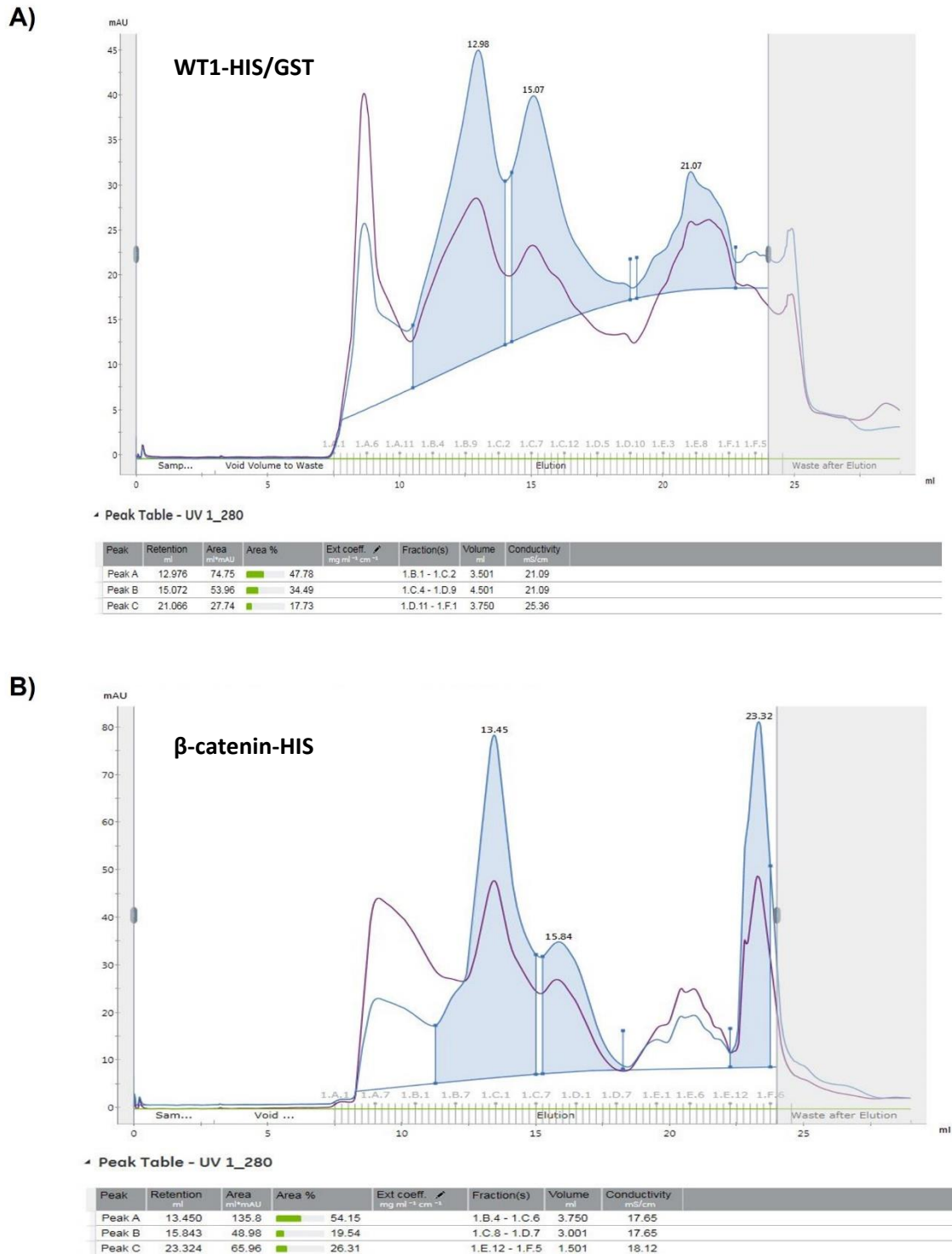


Figure 16: Size exclusion chromatography of WT1 and β -catenin.

For **A)** WT1-HIS/GST and **B)** β -catenin-HIS, pooled purification elutions were concentrated to 200ul and then loaded onto a HiLoad 10/300 Superdex 200 gel filtration column (GE) pre-equilibrated with specific protein buffer. The purple trace represents DNA, and the blue trace represents protein.

To determine if the bands identified were WT1 and β -catenin the fractions were immunoblotted. As shown in Figure 17A, a clear WT1 band at ~ 76 kDa is seen in fractions B12-C9 which were situated in peak ~ 12.98 mL. These fractions were western blotted using an Abcam WT1 antibody to ensure it was the WT1-HIS/GST construct since the size was larger than expected on the SEC trace. In addition to the ~ 76 kDa band, we also observed a smaller band around ~ 50 kDa indicative of WT1 degradation. For β -catenin a clear band is highlighted at ~ 92 kDa with greatest expression in fractions B11-C7 in both the coomassie and Western blot (Figure 17B). Overall showing the SEC peak at 13.45mL contained the β -catenin-HIS protein. Taken together, these data indicate that the optimal purification peaks for WT1 and β -catenin are 12.98mL and 13.45mL respectively.

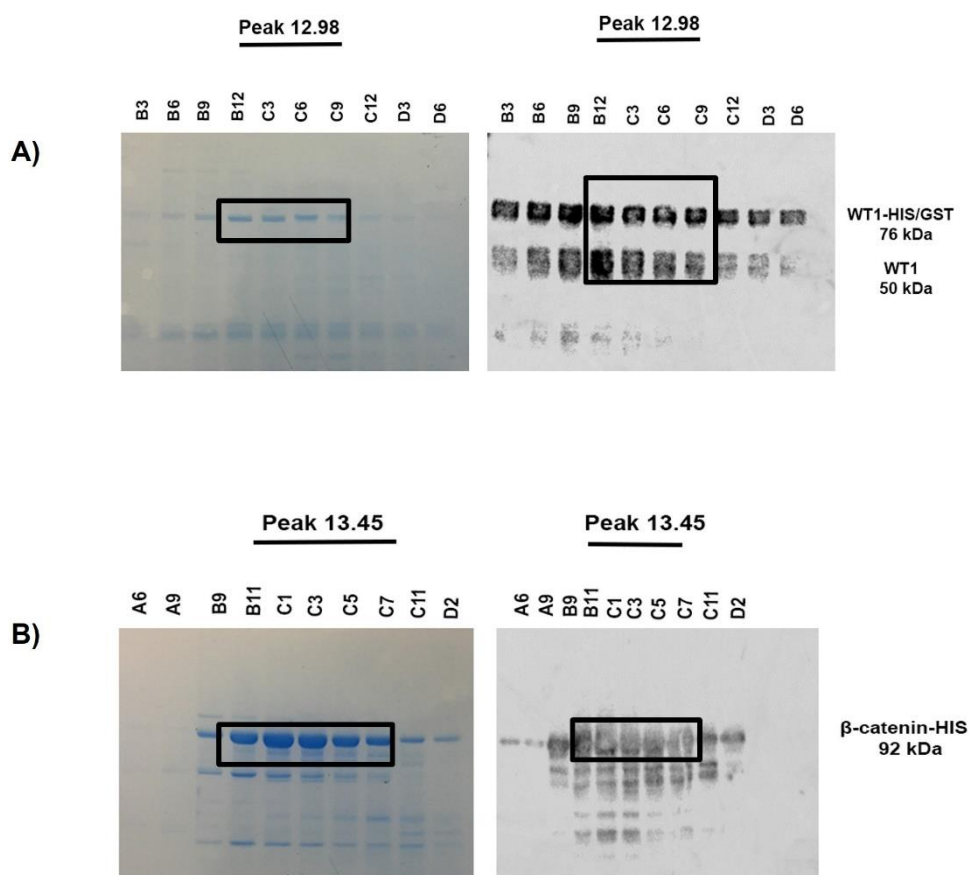


Figure 17: Analysing SEC fractions of WT1 and β -catenin.

Coomassie blue stained 9% acrylamide gels or immunoblots showing **A)** WT1-HIS/GST and **B)** β -catenin-HIS fractions western blotted for WT1 and β -catenin.

3.3.6 GST pull down with WT1 bound detecting for β -catenin binding

After isolating WT1 and β -catenin by HIS and SEC purification, the subsequent pull-down experiments were conducted to determine whether β -catenin could bind WT1 protein direct *in vitro*. WT1 was bound to GST resin and purified recombinant β -catenin protein applied to the column, followed by elution and detection of β -catenin. Purified GST protein (pET49b vector alone) was purified in the same manner as WT1 and used as a control for background binding. The optimal elution's determined were 20-200mM of imidazole, these were combined and concentrated. A pull-down was completed to test efficiency of β -catenin binding by comparing WT1-GST with addition of buffer and addition of purified β -catenin.

As shown in Figure 18A, clear bands for purified GST, WT1 and β -catenin are present, the GST resin alone lane has no bands as no purified protein was added so validates the resin was clean. The GST pull-down lane shows GST purified protein has bound to the resin with a band at ~ 26 kDa and upon the addition of purified β -catenin there is a faint band at ~ 92 kDa, suggesting β -catenin can bind non-specifically to GST resin.

The GST pull-down with bound WT1 and addition of β -catenin displayed a faint band for WT1 at ~ 76 kDa and β -catenin, however the β -catenin band was not more enriched than the band present with purified GST alone confirming β -catenin is interacting with the GST resin and not WT1 directly. It could also be suggested β -catenin is acting as a competitor for the GST resin and explains the reduced WT1 in the pull-down lanes versus input.

To explore background binding of β -catenin to GST resin, a pull-down was completed with GST-WT1 with addition of buffer compared to GST-WT1 with addition of β -catenin protein (Figure 18B). WT1 has bound successfully to GST resin highlighted by the band at ~ 76 kDa. A series of washes with buffer were completed and showed no removal of any significant WT1 protein. The first resin sample of WT1-GST with buffer indicated a band at ~ 76 kda for WT1 at a lower intensity than the resin sample tested prior to washing. This suggested some WT1 had been lost in the wash steps but there was still abundant WT1 bound to detect any interaction. However, the resin sample of WT1-GST with addition of β -catenin showed a reduction in the WT1 band intensity suggesting β -catenin could influence the binding affinity of WT1 to GST resin. In summary, β -catenin can impact WT1 binding to GST resin and suggests using bound WT1 as bait for recombinant β -catenin capture may not be suitable to assess direct binding capacity.

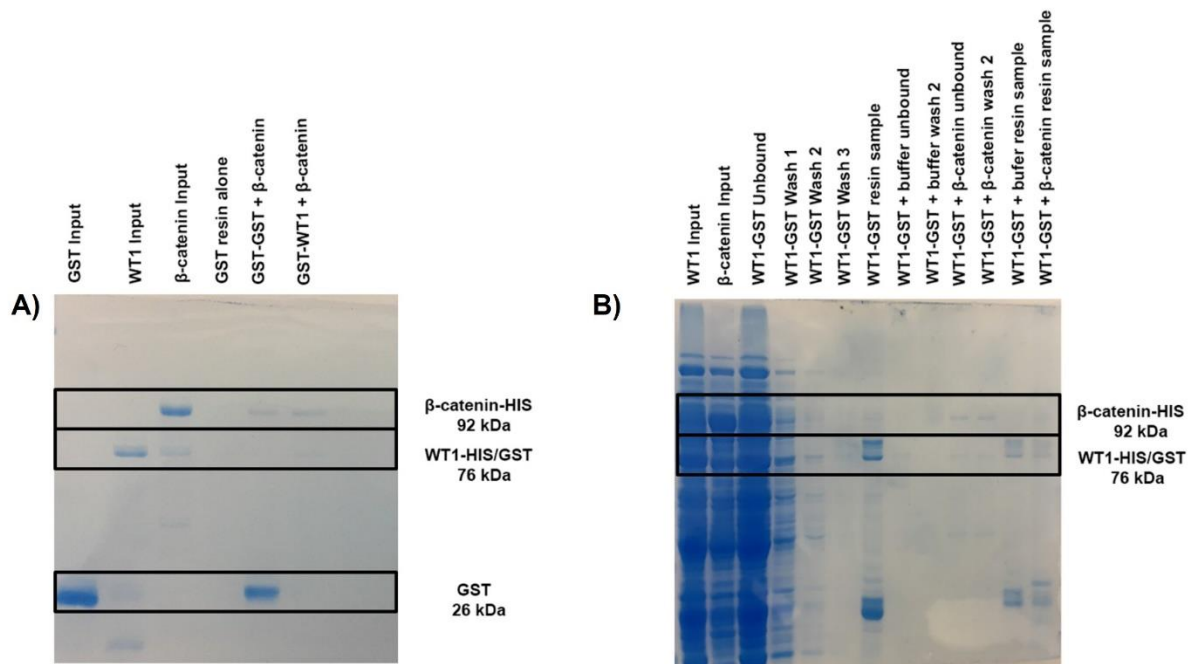


Figure 18: GST pull-down with bound purified GST or WT1 protein and addition of β -catenin. **A)** Input lanes (50ug/ml), resin alone and GST-GST, GST-WT1 pull-downs with addition of β -catenin were Coomassie stained **B)** WT1 bound to GST resin incubated with either buffer alone or β -catenin, inputs, washes, and resin samples were Coomassie stained.

3.3.7 HIS pull-down of bound β -catenin detecting for WT1

Given the failure to efficiently immobilise WT1 protein onto a resin column we attempted the reciprocal HIS pull-down using bound β -catenin for WT1 capture. A HIS pull-down was explored, but first involved cleaving the GST tag from WT1 using protease 3CV to prevent background binding of WT1 to the HIS resin. The optimal cleavage conditions for WT1 were determined as 37°C for 2 hours (data not shown). Cleaved WT1 was then added to HIS resin previously bound with β -catenin or IRF4 as shown in Figure 19. The purified WT1 input prior to cleavage shows bands at \sim 76kDa and \sim 50kDa and purified β -catenin at \sim 92kDa. IRF4 was used as a negative control again in this instance as is not a confirmed interactor of β -catenin and a clear band is seen at \sim 16kDa. It is clear both β -catenin and IRF4 have bound successfully to HIS resin. For the cleaved WT1 input, a clear band is at \sim 50kDa representing WT1 without the HIS/GST tag and a second band at \sim 26kDa for the HIS/GST tag. Finally, no WT1 band is detectable in either the β -catenin-HIS or IRF4-HIS pull-downs. In summary, cleaved WT1 does not interact with β -catenin-HIS, suggesting these two purified proteins do not directly

interact. This could mean the proteins associate through a common intermediate such as a shared protein partner or cellular structure. Therefore, this pull down was repeated but using K562 and HEL cell lysate, rather than purified protein.

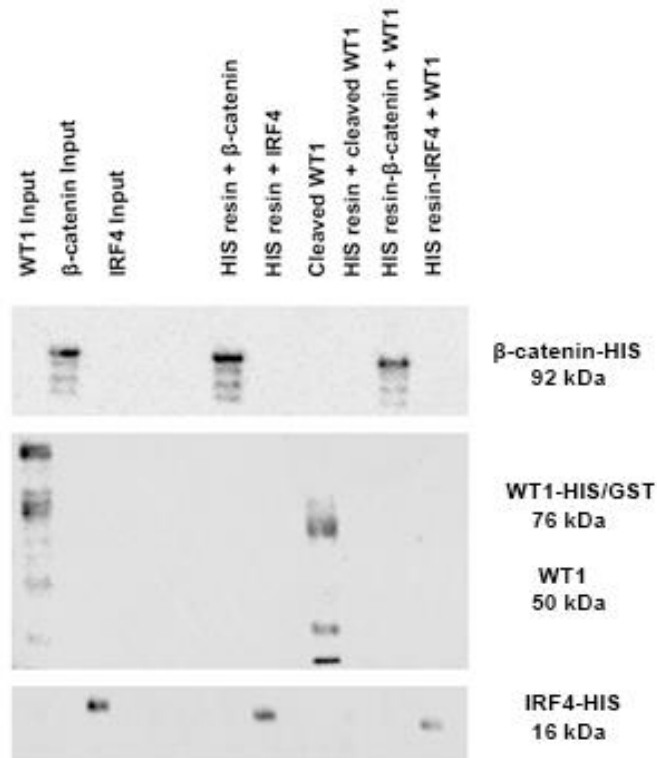


Figure 19: Assessment of cleaved WT1 binding with β -catenin/IRF4.

WT1 was cleaved with protease 3CV for 2 hours at 37°C. Western blot showing cleaved WT1 (~ 50 kDa) with either HIS resin bound β -catenin or IRF4. WT1 (200 μ g/ml), IRF4 (50 μ g/ml) and β -catenin (50 μ g/ml) were detected in inputs, resins, and pull-downs lanes.

3.3.8 Assessment of purified β -catenin binding capacity for WT1 in cell lysate

We next wanted to explore if β -catenin and WT1 interact in a different context, as other binding partners/structures could be facilitating association. To this end, we once again took HIS- β -catenin immobilised protein and applied cell lysate derived from cell lines harbouring high endogenous WT1 expression; K562 and HEL. Reassuringly, a clear band for purified β -catenin protein was observed in the input lane at ~ 92kDa as shown in Figure 20, but no band detected in K562/HEL lysate input (despite these cell lines expressing high endogenous β -catenin), probably a result of the very high purified β -catenin relative to levels in the cell

homogenate. K562 and HEL lysates exhibited only faint bands for WT1 perhaps surprising given we know cell lines express high levels of both proteins perhaps suggests protein yield in the lysate was low. Purified β -catenin has bound successfully to the HIS resin, but slight overspill of β -catenin signal was noted in the HIS resin only sample. In the two β -catenin-HIS pull-downs with K562 and HEL lysates, clear bands for β -catenin are detected but faint bands for WT1 are observed as expected due to the low amount present in the input sample. In summary, addition of cellular K562 and HEL lysate to β -catenin-HIS indicated only low abundance of WT1 making any β -catenin:WT1 association difficult to confirm.

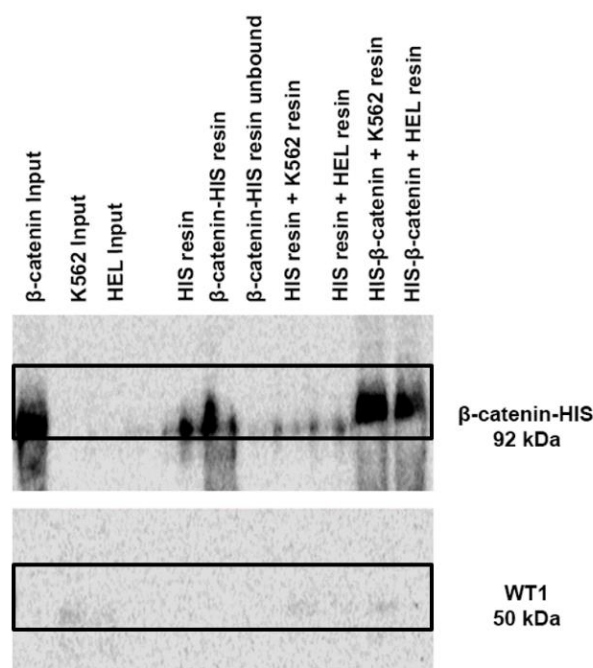


Figure 20: β -catenin-HIS pull-down with K562 and HEL lysate detecting for WT1.

Purified β -catenin input (50 μ g/ml) was bound to HIS resin and then incubated with K562 or HEL lysate (1mg/ml) at 4°C overnight. Inputs, resins, and pull-downs were western blotted for WT1 and β -catenin.

To confirm whether recombinant β -catenin was capable of binding known protein partners from cell lysate a positive control was required. LEF-1 was chosen as a positive control since it is a known interactor of β -catenin (Morgan et al., 2019). As shown in Figure 21 the K562 lysate input has clear bands at ~ 50kDa for both WT1 and LEF-1, reassuring since this cell line is known to abundantly express both proteins. Very faint β -catenin is observed endogenously

in the K562 lysate relative to the intense signal detected from purified β -catenin. The input for purified β -catenin is highlighted at ~ 92 kDa and has also bound to HIS resin successfully. No WT1 is detected in either β -catenin or IRF4 pull-downs, however LEF-1 is present in the last three lanes. This suggests LEF-1 is sticking to the HIS resin, but the band for LEF-1 in the β -catenin lane is modestly enriched. These data alleviate concerns that purified β -catenin protein lacks the structure/binding capacity to bind known partners *in vitro* such as LEF-1. This suggests β -catenin and WT1 protein only weakly associate in a specific cellular environment likely through a common intermediate.

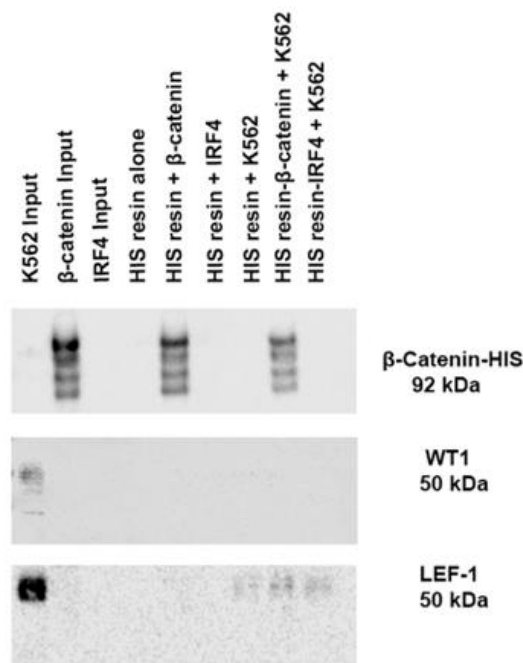


Figure 21: β -catenin-HIS or IRF4-HIS pull down with addition of K562 lysate detecting for WT1.

Purified β -catenin input ($50\mu\text{g/ml}$) or IRF4 ($50\mu\text{g/ml}$) was bound to HIS resin and then incubated with K562 lysate (1mg/ml) at 4°C overnight. Inputs, resins, and pull-downs were western blotted for WT1, β -catenin and LEF-1.

3.3.9 Myeloid leukaemia cell lines co-express β -catenin and WT1 protein

Once the nature of β -catenin:WT1 interaction had been characterised it was necessary to examine co-expression of the proteins across myeloid cell types to select suitable models for onward study. To this end we performed a western blot screen of 16 myeloid cell lines as shown in Figure 22A and assessed β -catenin and WT1 protein level. Overall, 50% (8/16) co-

express β -catenin and WT1 to varying degrees with K562, HEL, NOMO1 and NB4 exhibiting the strongest co-expression. HL60, MV411, KG-1 and EOL-1 have expression of both proteins but at various levels. THP-1, OCI-AML3 and KG1a only harboured expression of β -catenin, whilst U937, PLB-985, MonoMac6, MOLM-13 and ML-1 showed no expression of either protein. Through crude observations, there seemed to be a slight correlation between the levels of β -catenin and WT1 protein across cell lines. To formally assess this correlation, we performed a densitometric analysis of protein bands using ImageJ software in conjunction with a Spearman Rank test of correlation as shown in Figure 22B and identified a statistically significant correlation ($p < 0.01$) between β -catenin and WT1 protein level. In summary, these data show WT1 and β -catenin protein correlate in myeloid cells and that K562, HEL, NOMO1, NB4 and KG-1 maybe useful cells for studying the interaction further as they contain abundant levels of both proteins.

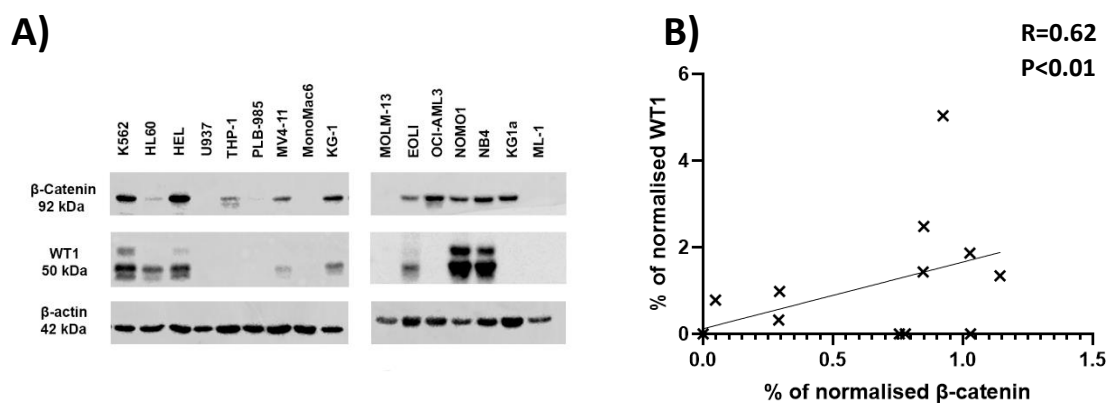


Figure 22: Protein expression of β -catenin and WT1 in myeloid leukaemia cell lines.

(A) Western blot showing screen of myeloid cells lines to determine the protein expression of β -catenin and WT1 with β -actin used as a loading control **(B)** Summary scatter plot showing the normalised level of quantified β -catenin and WT1 protein in each cell line. R and P values indicate the degree and significance of correlation as assessed by a Spearman Rank test of correlation.

3.3.10 AML patients express variable levels of β -catenin and WT1 protein

Previous data identified co-expression of β -catenin and WT1 to varying degrees in myeloid cell lines, however we also evaluated the clinical relevance of this relationship through co-expression analyses in primary AML patient blast samples. Whole cell lysates were generated

from mononuclear cell (MNC) fractions derived from the bone marrow of 37 AML patient blast samples and immunoblotted for WT1 and β -catenin versus normal cord blood (CB)-derived MNC and enriched CD34⁺ HSCs (Figure 23). Overall, we observed (9/30) (7 were omitted from total due to no actin present) co-overexpressed both proteins relative to normal CD34⁺ cord blood derived HSPC levels. We detected β -catenin expression in HSPC keeping with its self-renewal role in this context, but WT1 was undetectable given only 1.2% of the CD34⁺ HSPC pool are estimated to express this protein. Overall, we observed WT1 overexpression in around 47% (14/30) of our AML patient blast screen, consistent with previous estimates of high WT1 overexpression in this disease. This % was not too dissimilar from that of the myeloid screen in Figure 22 (~ 50%). This indicates a significant number of AML patient cases in which the β -catenin:WT1 association could be relevant.

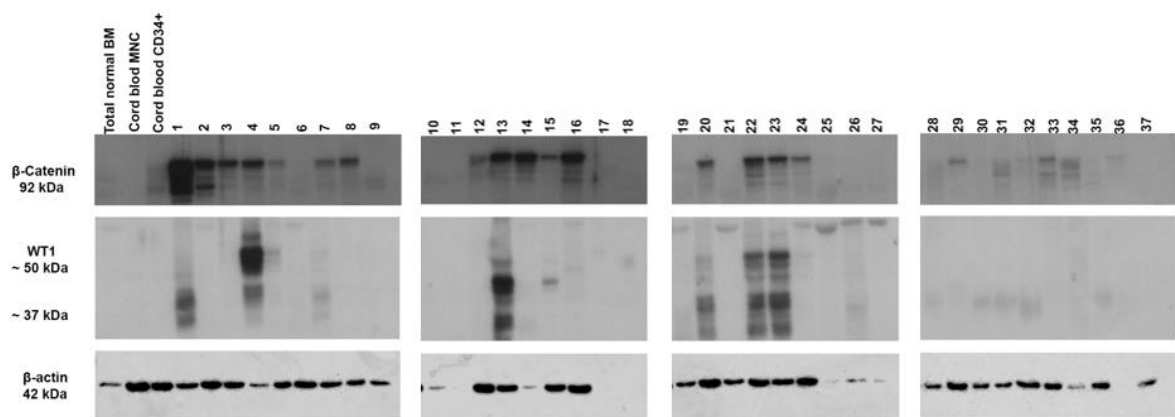


Figure 23: Protein expression of β -catenin and WT1 in AML patients. Western blot showing screen of AML patients to determine the protein expression of β -catenin and WT1 isoforms 50 kDa and 37 kDa with β -actin used as a loading control.

To assess the clinical relevance of this association we selected patients who displayed high levels of both proteins; patient 1, 4, 13, 20, 22 and 23 and performed WT1 Co-IPs from the BM MNC whole cell lysates extracted from these patients. As shown in Figure 24, all WT1 Co-IPs apart from patient 1 had good levels of WT1 in the Co-IP lane, however many also had considerable background signal present in the IgG lane. The absence of ample cellular

material means optimisation of patient Co-IPs was not possible, however patient 4 demonstrated good enrichment of WT1 in the Co-IP lane versus IgG background signal with a concomitant enrichment of β -catenin protein in the WT1 Co-IP lane. Taken together, these data suggest β -catenin:WT1 interaction is clinically relevant and worthy of onward functional study.

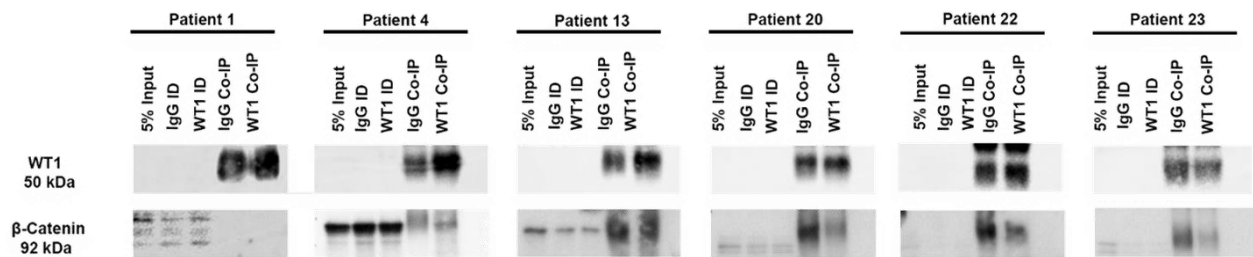


Figure 24: WT1 Co-IP to detect β -catenin association in AML patients.

Immunoblots showing β -catenin in WT1 Co-IPs derived from MNC fractions of five AML patient bone marrow blast samples expressing high level of both proteins. Total cell inputs (5%), immunodepleted (ID) and Co-IPs are shown.

3.3.11 WT1 location and subcellular localisation is unaffected by β -catenin stabilisation.

Given the correlation observed between β -catenin and WT1 expression in myeloid cells, we next wanted to examine WT1 level and subcellular localisation in response to Wnt signalling activation. To do this, cells were treated with CHIR99021 overnight and fractionated into cytoplasmic and nuclear homogenate followed by assessment of protein by western blotting. As shown in Figure 25, cytoplasmic and nuclear fractionation was efficient for all cell lines as indicated by the cytosolic marker α -tubulin and nuclear marker Lamin A/C. For NB4 the nuclear fraction expression was lightly low, but it was still clear that for K562, HEL, HL60, NB4 and KG1, CHIR99021 treatment induced β -catenin stability in both the nuclear and cytoplasmic fractions.

In all cell lines, WT1 was predominantly a nuclear protein in myeloid cells in keeping with its function as a transcription factor, and both proteins became enriched in the nucleus following Wnt signalling activation for all five cell myeloid cell lines tested. WT1 expression level and

localisation was unaffected by β -catenin stabilisation. Taken together, these data demonstrate that β -catenin stabilisation does not influence the level or localisation of WT1 protein but does show β -catenin and WT1 are localised in the same cellular compartments during Wnt stimulation.

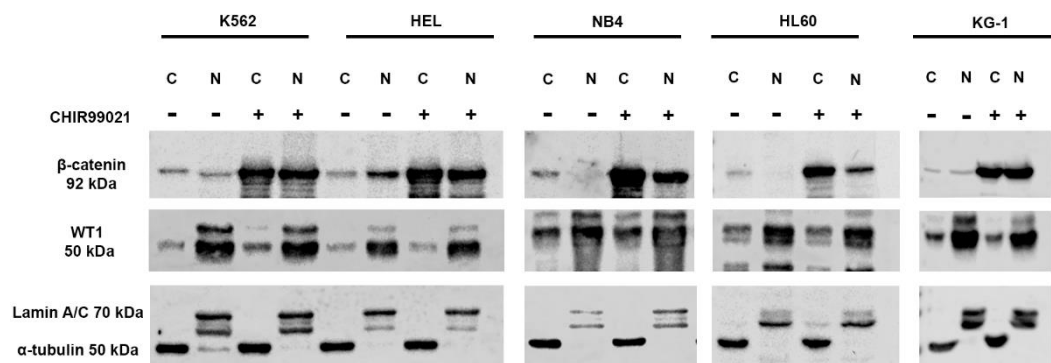


Figure 25: Subcellular localisation of WT1 and β -catenin under basal and Wnt stimulated conditions.

Representative western blots showing the level and subcellular localisation of β -catenin and WT1 protein in cytosolic and nuclear fractions of control or Wnt-stimulated myeloid cells. α -Tubulin indicates the purity of the cytosol (C) fraction and Lamin A/C indicates purity of the nuclear (N) fractions.

3.3.12 β -Catenin and WT1 are co-localised in myeloid leukaemia cell lines

Western blot studies above suggested that β -catenin and WT1 were localised to the same compartment (nucleus) during Wnt signalling activation. To confirm this and assess the degree of localisation within these compartments, β -catenin and WT1 protein expression was observed by confocal laser scanning microscopy (CLSM). As before, Wnt-responsive myeloid cell lines were treated either with control (DMSO) or Wnt agonist (CHIR99021) overnight, fixed, permeabilised and labelled with either anti-WT1 antibody or anti- β -catenin antibody.

As shown from Figures 26-30 for all five cell lines, WT1 is predominantly nuclear, and its level and localisation are unchanged following CHIR99021 treatment displayed in both the wide-view and zoomed images. Following Wnt activation, in all cases β -catenin becomes more enriched in the nucleus where WT1 is abundant, specifically seen in cell lines K562 (Figure 26B) and HEL (Figure 27B). Additionally, the overlapping signals of β -catenin and WT1 are ubiquitous across the nuclear region, rather than localised to discrete puncta. In summary,

these data confirm that WT1 level and localisation are unaffected by Wnt signalling activation and that β -catenin and WT1 are co-localised in the same region of the cells, especially following Wnt stimulation.

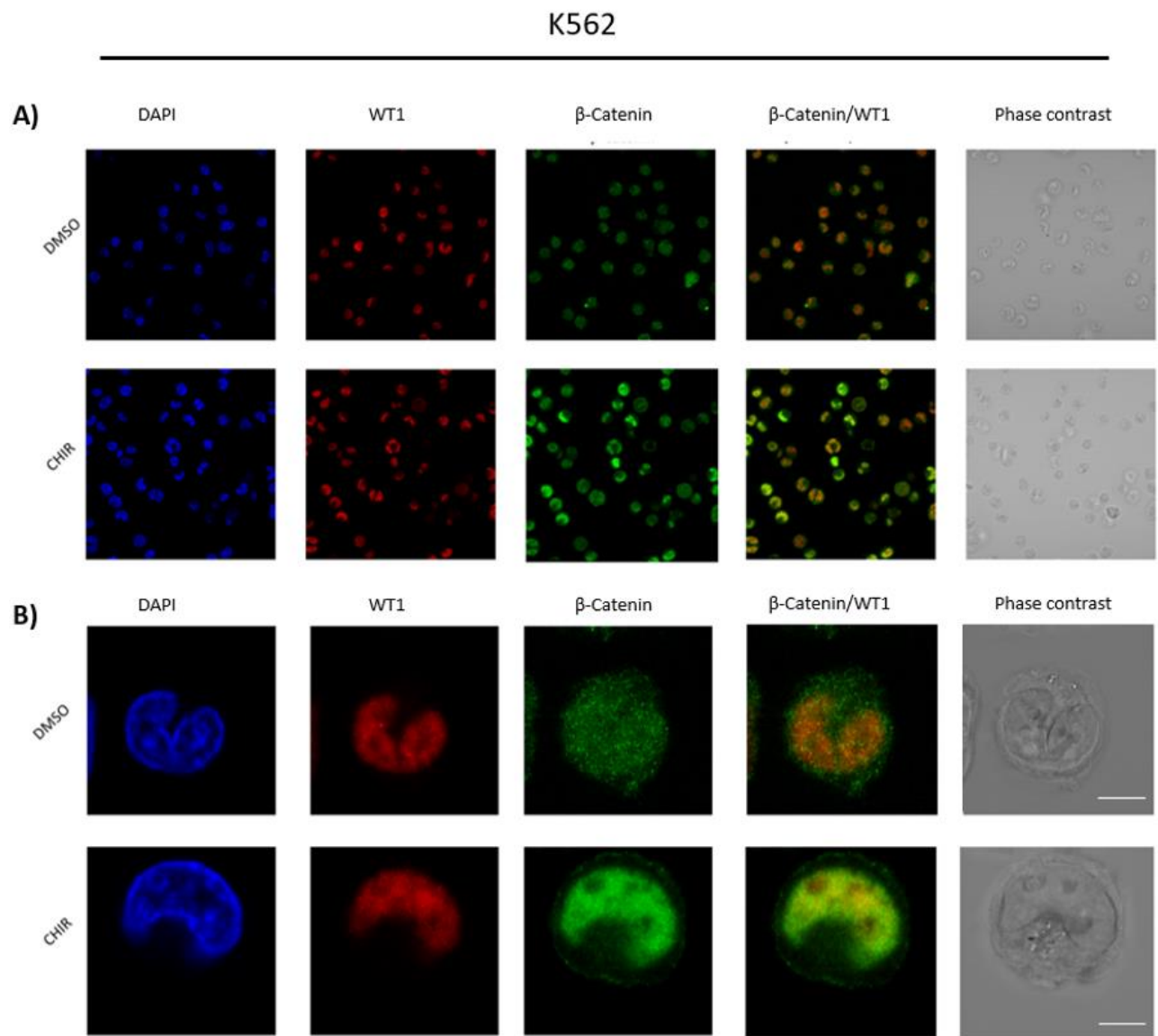


Figure 26: WT1 and β -catenin co-localisation in K562

CLSM images showing the localisation of WT1 and β -catenin protein in **A)** wide-view and **B)** zoomed. DAPI (blue), WT1 (red), β -catenin (green), merged and phase contrast (greyscale) images are shown. White scale bar indicates 5 μ m.

HEL

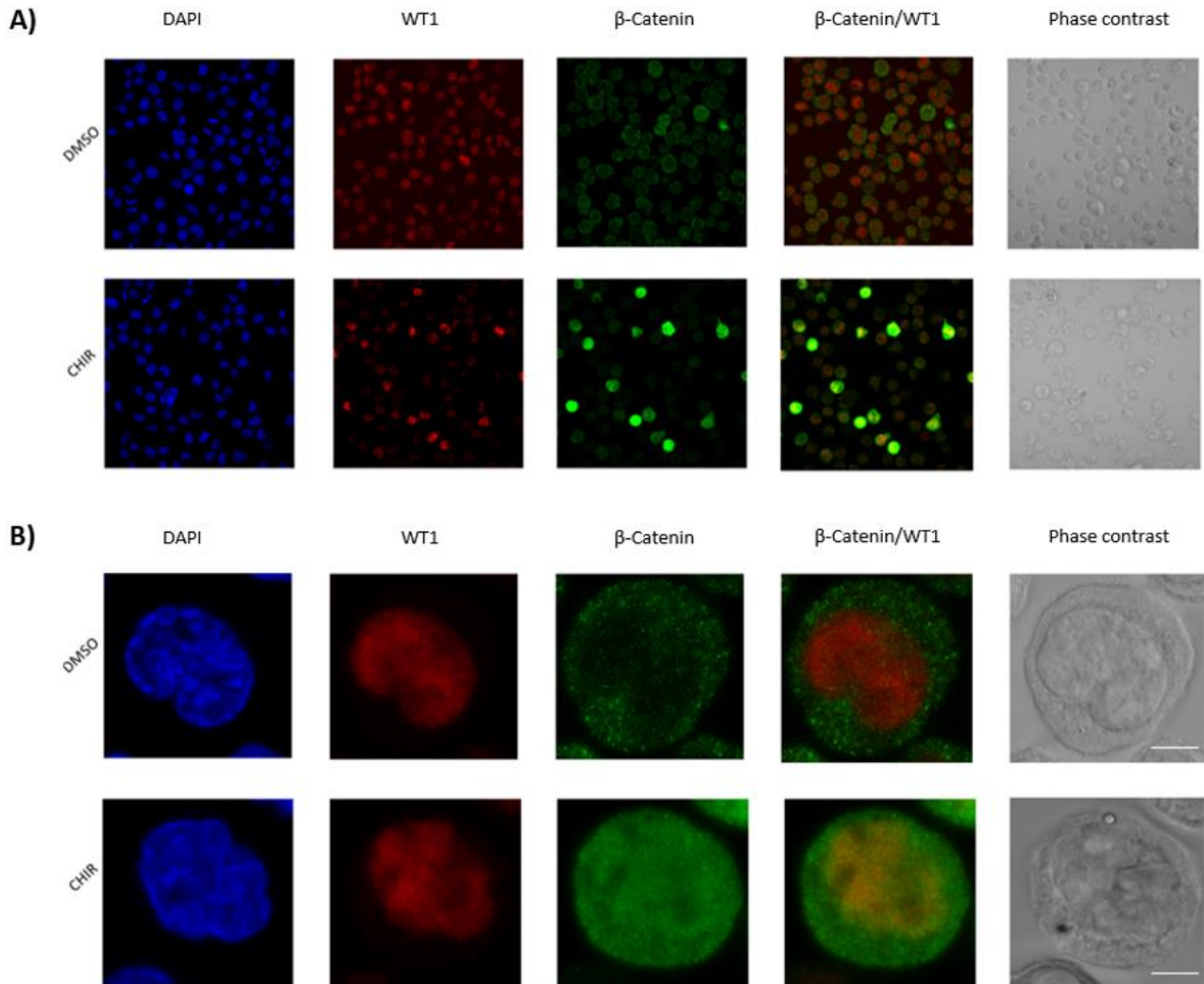


Figure 27: WT1 and β -catenin co-localisation in HEL cells.

CLSM images showing the localisation of WT1 and β -catenin protein in **A)** wide-view and **B)** zoomed. DAPI (blue), WT1 (red), β -catenin (green), merged and phase contrast (greyscale) images are shown, white scale bar indicates 5 μ M.

NB4

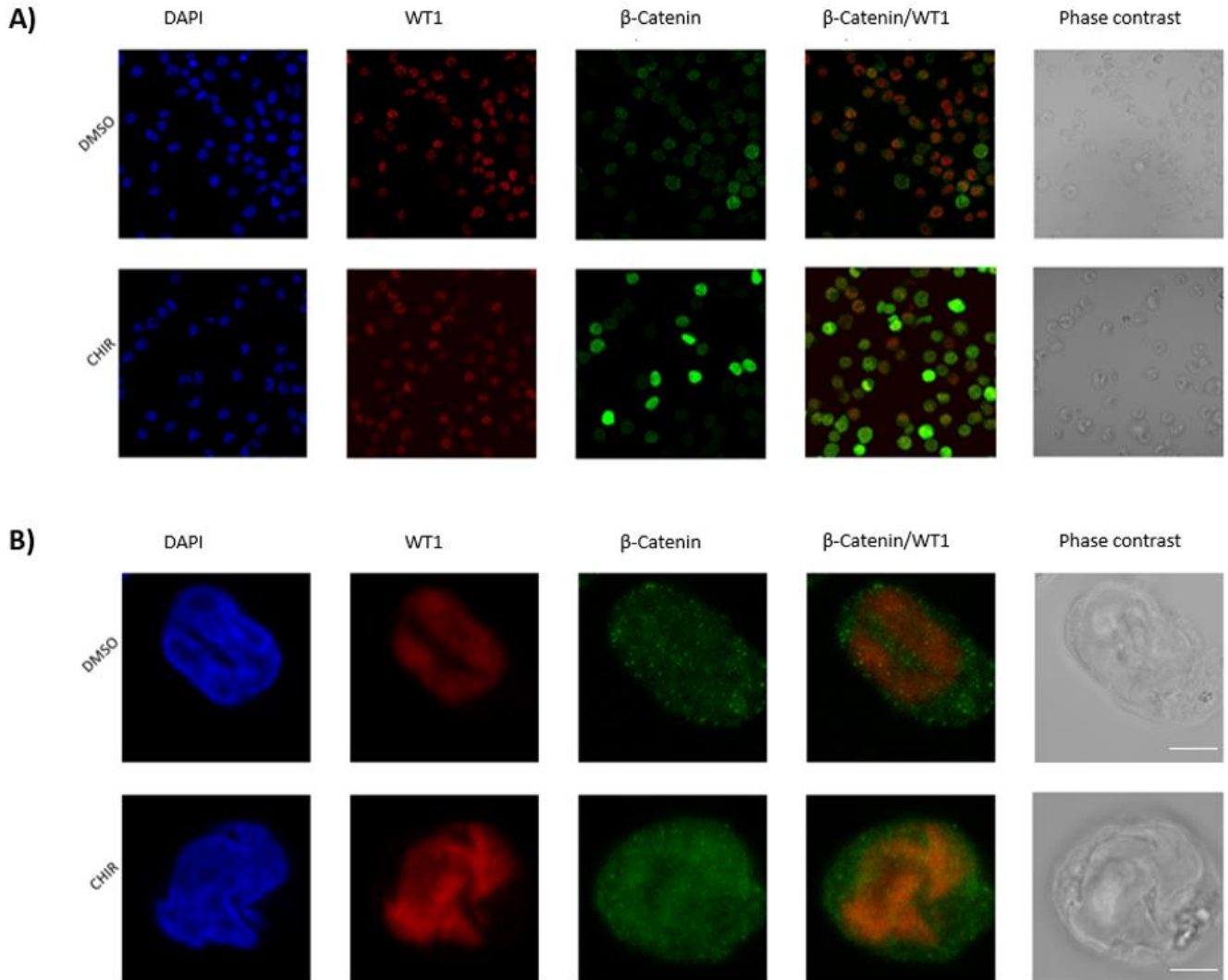


Figure 28: WT1 and β -catenin co-localisation in NB4

CLSM images showing the localisation of WT1 and β -catenin protein in **A)** wide-view and **B)** zoomed. DAPI (blue), WT1 (red), β -catenin (green), merged and phase contrast (greyscale) images are shown, white scale bar indicates 5 μ M.

KG1

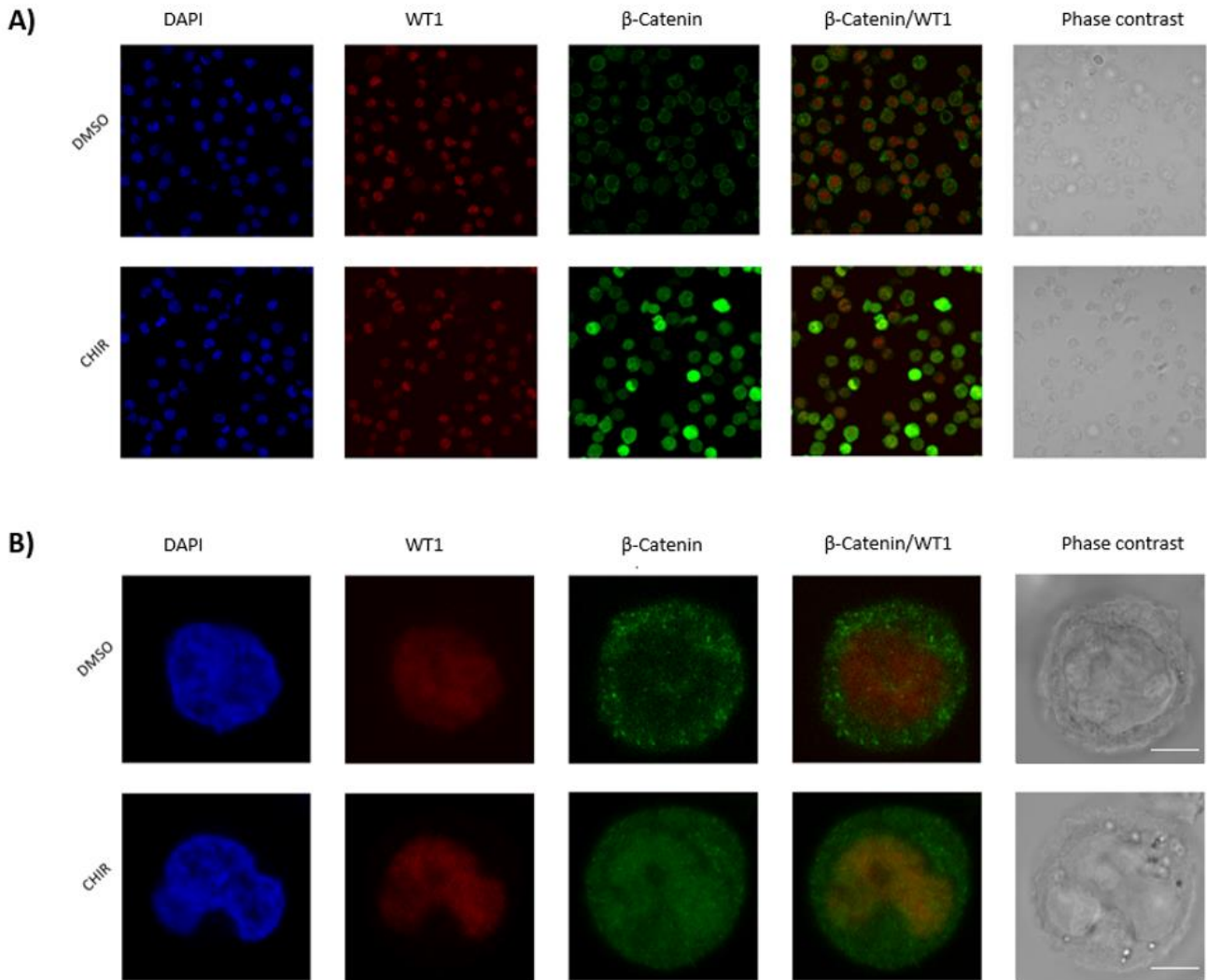


Figure 29: WT1 and β -catenin co-localisation in KG1 cells.

CLSM images showing the localisation of WT1 and β -catenin protein in **A)** wide-view and **B)** zoomed. DAPI (blue), WT1 (red), β -catenin (green), merged and phase contrast (greyscale) images are shown, white scale bar indicates 5 μ M.

HL60

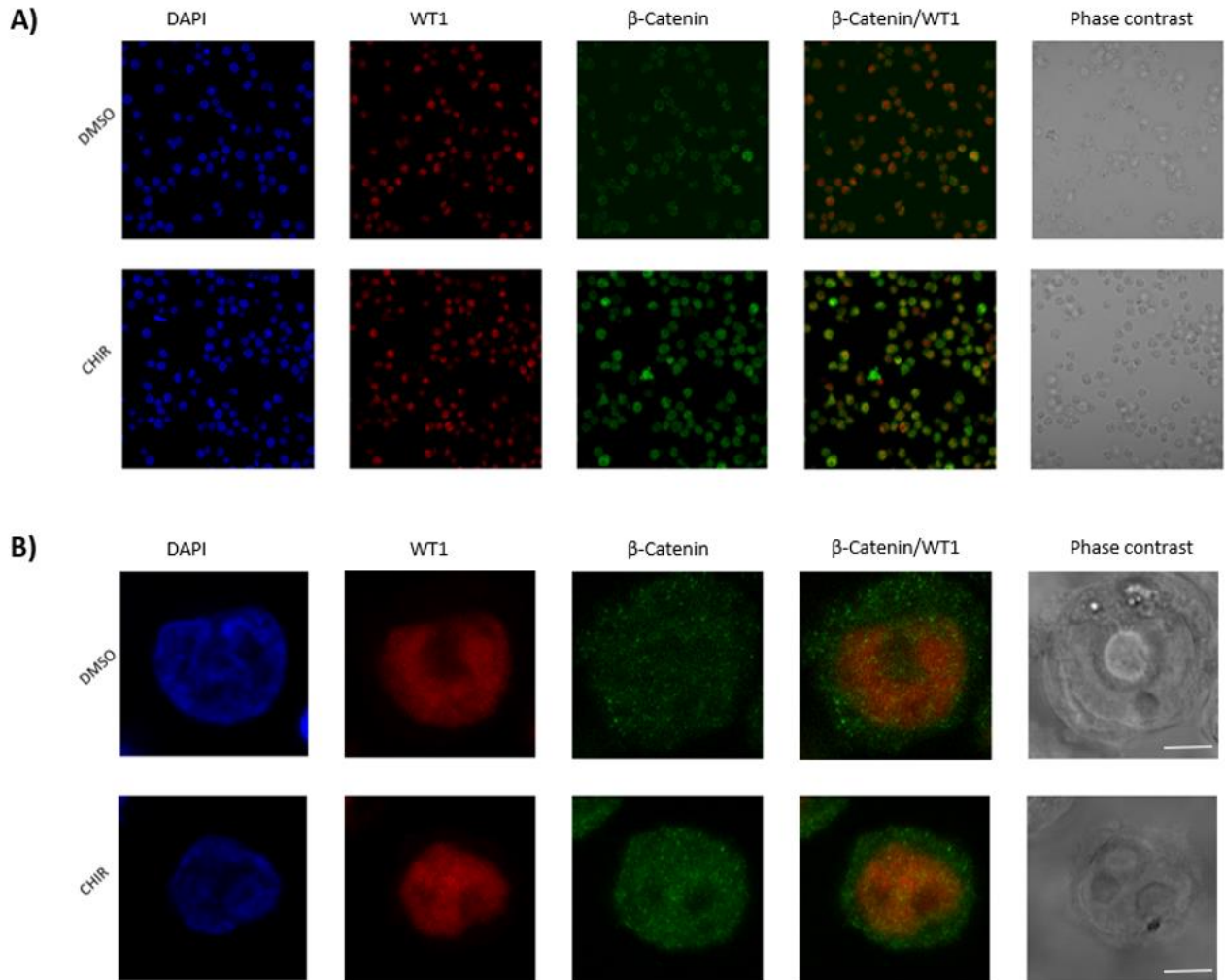


Figure 30: WT1 and β -catenin co-localisation in HL60

CLSM images showing the localisation of WT1 and β -catenin protein in **A)** wide-view and **B)** zoomed. DAPI (blue), WT1 (red), β -catenin (green), merged and phase contrast (greyscale) images are shown, white scale bar indicates 5 μ M.

3.4 Discussion

3.4.1 Validation of novel β -catenin interactors

In this current study we chose to follow up interactions with LIN28B as this protein is involved in post-transcriptional regulation of miRNA or mRNA expression and inhibition of LIN28B showed to impair leukaemia cell growth and metabolism in AML (J. Zhou, C. Bi, et al., 2017). Secondly MSI2, as high mRNA expression is associated with decreased survival in AML (Byers et al., 2011). Furthermore, members of the PUMILIO family (PUM2) are essential for haematopoietic stem/progenitor cell (HSPC) proliferation and survival and PUM1/2 can sustain myeloid leukemic cell growth (Naudin et al., 2017). RBM15 controls cell expansion and differentiation by regulating *MYC* levels and the notch signalling pathway, and in some forms of paediatric AML, RBM15 fuses to MLK1 and induces leukaemia through aberrant notch signalling (Ianniello et al., 2019). WT1 is highly expressed in leukemic stem cells and can drive leukemogenesis in a murine MLL-AF9 induced model of AML (Zhou et al., 2020).

An association between β -catenin and LIN28B, MSI2 and WT1 was validated in K562 and HEL cells, and the interaction with WT1 further confirmed in KG1 cells. The failure to detect β -catenin association with PUM2 and RBM15 highlight the importance of validating interactions identified through mass spectrometry. Given all of these proteins are RBP, we hypothesised that β -catenin could play a role in RNA biology in myeloid cells. This facet is explored further in Chapter 5. For this chapter we choose to focus our experiments on the interaction with WT1 given its importance in AML (Introduction 1.9). Given the considerable functional overlap between WT1 and β -catenin in both normal HSC (Hosen et al., 2007; Luis et al., 2012) and AML cells (Müller-Tidow et al., 2004; Nishida et al., 2006; Yeung et al., 2010) any context-dependent interaction between the two proteins, and subsequent functional crosstalk, could represent a novel oncogenic axis in AML.

3.4.2 Exploring if β -catenin and WT1 bind directly

After identifying β -catenin and WT1 were associated by Co-IP we next wanted to understand if this interaction was direct or indirect to understand the mechanistic basis for interaction. To do this we expressed both proteins recombinantly and purified each using tag specific columns and SEC. However, we were unable to detect either protein in reciprocal pull-downs using either purified protein or cell lysate. This implies the interaction is likely mediated

through a common binding partner in the cell, or a co-occupied cellular structure. In terms of common intermediates one such candidate could be the Wilms tumour suppressor WTX. WTX has shown to form a complex with β -catenin, AXIN1, beta-TrCP2, and APC, and analysis in zebrafish has identified that WTX promotes β -catenin ubiquitination and proteasomal degradation which therefore disrupts Wnt signalling (Major et al., 2007). Furthermore, WTX shuttles between the cytoplasm and the nucleus mediating binding of WT1 and hence modulating its activity (Cardoso et al., 2013; Rivera et al., 2009). A second example of a potential common partner is WID (WT1-induced inhibitor of Dishevelled), a novel WT1 transcriptional target that interacts with dishevelled via its c-terminal CXXC zinc finger and dishevelled binding domains. The interaction results in the potent inhibition of Wnt/ β -catenin signalling *in vitro* and *in vivo* (Kim et al., 2010). WT1 has shown to inhibit Wnt function during *Xenopus* development and interfered with Wnt-mediated transcription through the CREB binding protein (CBP) (Kim et al., 2009). A WT1 product lacking the first two zinc fingers failed to Co-IP with CBP, indicating that this portion of the DNA binding domain is essential for this protein interaction *in vitro* (Wang et al., 2001). CBP is a transcriptional coactivator and ChIP assays showed that WT1 and CBP were present together on WT1 targets *ETV5* and *NRP1* and CBP recruitment was more evident when cells were grown in the presence of Wnt3a (Kim et al., 2009). Furthermore β -catenin has also shown to bind to CBP, and inhibition of this interaction suppressed activation of pancreatic stellate cells (PSCs) as evidenced by decreased proliferation and downregulation of activation markers including *survivin* (Che et al., 2020). Overall showing the importance of CBP as a potential binding partner for WT1 and β -catenin.

A final potential binding partner is TCF4, as WT1 and TCF4 shared common target genes through distinct DNA binding elements as there was no overlap between WT1 binding sites and TCF4-GST clusters (Kim et al., 2009). TCF4 is an already established interactor of β -catenin and has previously been explored for small molecule inhibition with successful induction of apoptosis in which the survival was β -catenin dependent (Shin et al., 2017). Overall to assess if these potential interactors mediate β -catenin and WT1 association we could generate myeloid cell lines containing knockout of WTX, CBP and TCF4 and then repeat the above Co-IPs to see if we still obtain successful pull-down of the protein of interest. If a reduction or absence in expression compared to the original Co-IPs is observed, we can hypothesise the common binding partner absent is involved in the association between WT1 and β -catenin.

The other possibility is that β -catenin and WT1 could associate through their co-occupancy of shared cellular structures such as DNA or RNA. β -Catenin lacks a DNA binding domain and transcribes Wnt target genes by interacting with TCF/LEF family members and recruit activators such as BCL9/Pygo which bind via the c-terminus domain to initiate transcription activity in colon cancer (Bian et al., 2020). Moreover, Transducin β -like protein 1 (TBL1) and TBL1-related protein (TBLR1) have been identified as cofactors which aid in recruiting β -catenin to promoter regions of Wnt target genes (Perissi et al., 2004). This interaction has shown to promote migration to the promoters of these Wnt genes by removing repressors such as histone deacetylase 1 (HDAC1) to stimulate Wnt target gene expression (Li & Wang, 2008). Similarly, WT1 has shown to bind to promoters of 11 genes expressed in prostate cancer and engage transcriptional machinery (Kim et al., 2009), and more specifically WT1 lacking the KTS domain binds to known enhancer elements in leukemic stem cells (Ullmark et al., 2017). This overall implies WT1, and β -catenin could have common roles in transcription and further analysis should be completed to see if they occupy the same promoters, enhancer elements by chromatin accessibility assays to identify how open a region is, and co-activators in a myeloid context. To understand if DNA is involved you could treat with DNase and re-test the interaction but also measure the protein complexes formed with DNA by EMSA and identify RNA polymerase binding.

In addition, post translational modifications (PTM) of either protein could also mediate their association. β -Catenin has a number of PTM for example phosphorylation on the C-terminus e.g., Ser675 by protein kinase A appears to stabilise β -catenin and its nuclear accumulation. As a consequence of phosphorylation by CK1 and GSK3 β , β -catenin is ubiquitinated and sent to the proteasome for degradation and is inhibited by Wnt stimulation as no recruitment of β -TrCP is achieved. β -Catenin undergoes acetylation at lysine 19 and 49 by p300/CBP associated factor (PCAF) which induces nuclear translocation and increases its transcriptional activity, thereby upregulating Wnt signalling (Gao et al., 2014). Furthermore, for WT1 phosphorylation at Ser635 and 393 in the second and third zinc fingers can be phosphorylated by PKA or C which in turn blocks the ability of WT1 to bind to DNA and hence affect transcription. Also resulting in cytoplasmic retention and inefficient nuclear translocation (Yang et al., 2007). Furthermore, hypermethylation of WT1 in the promoter and first exon region was shown to be associated with silencing of WT1 mRNA expression in breast cancer

cell lines MCF-7 and MDA-MF-231, showing a significant association with increased risk for breast cancer (Ge et al., 2020). Overall showing PTM of β -catenin or WT1 could influence its direct protein interactions and hence its unsurprising that their direct interaction could not be demonstrated using recombinant proteins *in vitro* since the precise cellular conditions that mediate their association are likely absent. Regardless, identification of these common partners, structures or PTMs will be important for the design of disrupting mechanisms should the axis prove worthy of therapeutic targeting.

3.4.3 Characterising co-expression of β -catenin and WT1

To identify suitable models in which to study β -catenin:WT1 interplay, we examined co-expression of WT1 and β -catenin in myeloid cell lines and AML patients. In myeloid cell lines we detected a significant correlation of the two proteins, and this begged the question of whether the two proteins are capable of regulating each other's expression which will be examined in the proceeding chapter. Of these cell lines, a number including K562, HEL and KG1 were deemed appropriate models for functional study given their abundant expression levels of both proteins. In primary cell screens, we detected β -catenin level in HSPC in keeping with its self-renewal role in this context (Reya et al., 2003) but no WT1 as expected given only 1.2% of the CD34⁺ HSPC pool are estimated to express this protein (Hosen et al., 2002). In AML samples β -catenin and WT1 overexpression rates were comparable to previous estimates (Alanazi et al., 2020; Rampal & Figueroa, 2016) and numerous samples (~30%) co-overexpressed both proteins. We would have liked to have done further analysis of clinical features shared e.g., FAB type, morphology between the patient samples with high co-expression. However due to a limitation in clinical information and the small cohort tested we did not discover any associations.

In one of these patients; patient 4, association between β -catenin and WT1 was confirmed by WT1-CoIP highlighting the potential for this interaction to be clinically relevant. Patients 13, 20 and 22 also displayed an interaction but the respective IgG lane had too much background and therefore would require either a different rabbit antibody or further optimisation. WT1 expression remained nuclear under both basal and Wnt stimulated conditions across five different myeloid cell lines, and Wnt activation has no impact on WT1 expression or localisation. However previous research has identified Wnt signalling to be involved in Wilms

tumour and found similar WT1 and β -catenin protein expression levels (Corbin et al., 2009). Therefore, showing the two can still cooperatively work together in some diseases which could be the same in for an AML context.

To understand the subcellular localisation of WT1 and β -catenin further we performed co-localisation studies using CLSM. Using five myeloid cell lines we observed WT1 to be a nuclear protein as seen by the general staining of DNA (DAPI) which was not punctate showing general DNA association which was expected given its function as a transcription factor. This has been seen in embryonic and adult tissues previously (Mundlos et al., 1993) and more recently in the nucleus of kidney podocytes aiding in proliferation and migration of cells (Kaverina et al., 2017). Under Wnt stimulated conditions WT1 and β -catenin displayed co-localisation in the nucleus, therefore hypothesising their interaction could be likely due to co-occupancy by either DNA or RNA. This is further supported by the common promoters/genes regulated by both proteins. For example LEF-1 has shown to drive β -catenin nuclear localisation in myeloid cells (Morgan et al., 2019) and repression of WT1 mediated LEF-1 transcription by Mangiferin governed β -catenin Wnt signalling activation in hepatocellular carcinoma (Tan et al., 2018). Secondly *MYC* is deregulated by oncogenic Wnt/ β -catenin signalling which is critical in colorectal carcinogenesis (Rennoll & Yochum, 2015) and overexpression of WT1 induced an increase in *MYC* levels in breast cancer cells (Han et al., 2004). WT1 can promote cell proliferation in non-small lung cancer through upregulation of *CCND1* (Xu et al., 2013) as the increase in β -catenin in the nucleus resulted in activation of *CCND1* with influence of the G1 phase of the cell cycle and hence cell proliferation (Lecarpentier et al., 2019). To assess this chromatin immunoprecipitation (ChIP) could be used to assess shared promoter occupancy as can enrich DNA-binding proteins along with their specific targets. Overall WT1 and β -catenin show correlation of common target genes and hence a possible interaction, however, the nature of this interaction remains unknown and won't be worth exploring unless a functional relationship between WT1 and β -catenin can be demonstrated in AML cells thus justifying their therapeutic targeting.

Chapter 4. Investigating crosstalk between WT1 and β -catenin signalling

4.1 Introduction

Following confirmation that β -catenin and WT1 are associated (albeit not directly) we next wanted to understand the impact of WT1 modulation (knockdown, overexpression, and mutation) on β -catenin expression and Wnt signalling activity. WT1 is often overexpressed and mutated in AML where it confers inferior survival (Potluri et al., 2021) and elsewhere can negatively regulate Wnt/ β -catenin signalling (Kim et al., 2009). Previously WT1 knockdown has shown to decrease the frequency of LSCs, impair LSC self-renewal ability and prolong the survival in MLL-AF9 induced murine leukaemia models (Zhou et al., 2020). Furthermore WT1 can often be overexpressed and mutated in approximately 6-15% of *de novo* AML cases (Rampal & Figueroa, 2016). These mutations typically occur in exons 1,7 and 9 including base substitutions, deletions and insertions overall resulting in the creation of a stop codon and loss of function, forming a truncated protein (Abbas et al., 2010). However, the effect of WT1 mutations on Wnt signalling (also a known mediator of AML LSC activity) has not been previously investigated.

To our knowledge, there are also no reports of β -catenin regulating WT1 activity. It's surprising, given their individual contributions such as both cooperating with genetic aberrations in AML including t(8;21) *RUNX1-RUNX1T1* (Nishida et al., 2006) and t(9;11) *MLL-AF9* (Zhou et al., 2020) to promote leukemogenesis. The results of this study will help in understanding potential crosstalk between WT1 and β -catenin for novel treatment strategies in targeting these two oncoproteins in AML, which has proven challenging to this point.

4.2 Aims

The aim of this chapter is to investigate the effect of WT1 modulation on β -catenin and Wnt signalling in myeloid cells, and this will be achieved through interrogation of the following aims;

1. Optimisation of WT1 shRNA knockdown, overexpression and WT1 mutant expression.
2. Identification of suitable Wnt-responsive cell lines to examine WT1: β -catenin crosstalk

3. Determining the effect of WT1 modulation on β -catenin subcellular localisation and activity
4. Generation of β -catenin knockdown systems
5. Determination of the impact of β -catenin knockdown on WT1 expression and activity

4.3 Results

4.3.1 Generation of myeloid cells exhibiting WT1 knockdown or overexpression

To investigate the effect of WT1 modulation on Wnt signalling we first needed to overexpress or suppress WT1 expression using lentiviral transduction. For WT1 knockdown, 5 shRNA sequences each integrated within a lentiviral expression vector (pLKO.1) also containing a puromycin resistance gene were tested for most efficient knockdown of WT1 protein expression in K562 cells (known to express high endogenous WT1 protein; Chapter 3 Figure 22).

As shown in Figure 31A, shRNA#1 and shRNA#5 exhibited the most reduced WT1 expression versus the non-targeted shRNA control (prominent band at ~50kDa). WT1 knockdown was also observed in shRNA#2 and shRNA#4, albeit less efficient, and shRNA#3 exhibited the least effective WT1 reduction. We also assessed the effect of WT1 knockdown on β -catenin protein stability in the same Western blot and observed a small increase in β -catenin stability across WT1 shRNAs #2-#5 relative to control levels.

We also optimised ectopic expression of WT1 in K562 cells using the full length human WT1 DNA sequence (NM_024426.4) housed within the pLV1-EF1a-Puro lentiviral expression vector. K562 cells were transduced and WT1 protein levels examined as above. Figure 31A shows the empty vector control (O/E control) harbouring endogenous WT1 protein as expected, whilst K562 cells transduced with ectopic WT1 exhibited a single enriched band above 50kDa. We also assessed the impact of ectopic WT1 expression on β -catenin stability and noted a small increase in β -catenin stability.

Due to the cytotoxic effect of WT1 knockdown, shRNA #2 and #4 would be used as although they were not the most efficient at knocking down WT1 they remained the most viable following post-selection. Furthermore, we noted a dramatic red change in the cell colour

indicative of erythroid differentiation (Figure 31B). This is in keeping with a previous study demonstrating WT1 expression can suppress erythroid colony formation (Svedberg et al., 2001).

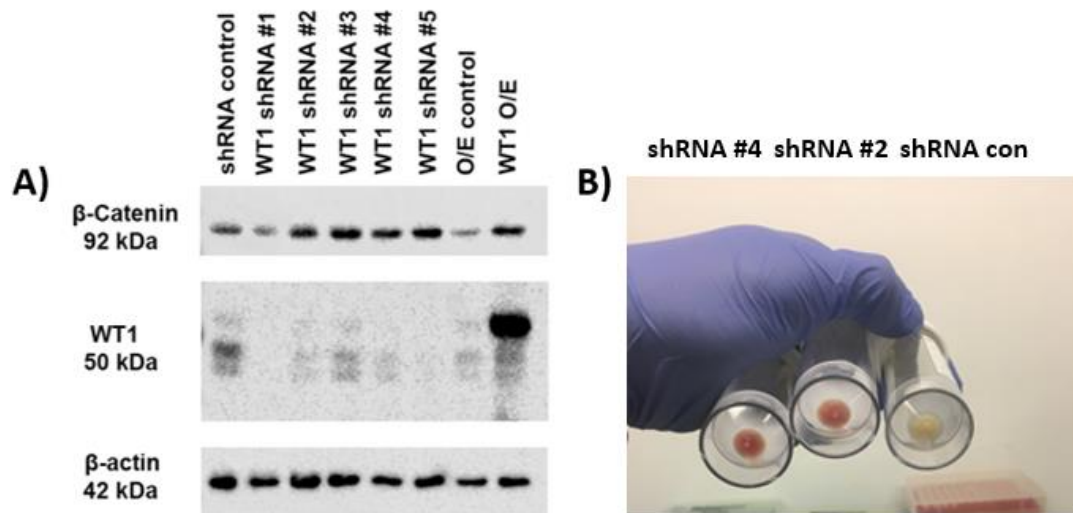


Figure 31: Assessment of WT1 knockdown/overexpression in K562 cells.

A) Western blot showing the level of WT1 and β -catenin protein in K562 cells following lentiviral transduction with either WT1 shRNA knockdown or overexpression (O/E). β -Actin was detected to indicate protein loading. **B)** Images showing K562 whole cell pellets derived from WT1 shRNA control versus WT1 knockdowns shRNA #2 and #4 cultures.

4.3.2 Integration of the β -catenin activated reporter (BAR) system in Wnt responsive myeloid cell lines

In anticipation of assessing the effect of WT1 modulation on Wnt signalling output, it was necessary to identify Wnt-responsive cell lines, expressing endogenous levels of both WT1 and β -catenin. For this we lentivirally transduced cells with the β -catenin activated reporter (BAR) system which measures TCF-mediated transcription through expression of Venus YFP alongside a negative control mutated 'found unresponsive' BAR (fuBAR) system (Biechele & Moon, 2008)

Previous work from this laboratory has already established this reporter system in two Wnt responsive cell lines; K562 and HEL (Morgan et al., 2019). However, despite the role of both WT1 and β -catenin in t(9;22) driven CML (Chang et al., 2013; Corrêa et al., 2012), K562 cells

are not AML, and HEL cells could not survive WT1 knockdown (data not shown). Therefore, further cell AML cell lines were required that could represent the heterogeneity of AML observed in the clinic. A previous cell line screen evaluating expression of WT1 and β -catenin in myeloid cell lines, determined KG-1, NB4, HL60 and MV4;11 to have detectable endogenous levels of both proteins (Figure 22). Our data has also shown that there is heterogeneity in the capacity of myeloid cell lines to transduce a Wnt signal, despite marked β -catenin stabilisation in the cytosol (Morgan et al., 2019). Therefore, it was necessary to identify myeloid cell lines capable of activating a Wnt signal in response to Wnt agonist treatment (CHIR99021).

To assess Wnt-responsiveness it was first necessary to lentivirally integrate the BAR reporter into cell lines and assess transduction efficiency by measuring fluorescence intensity of the dsRed⁺ selectable marker by flow cytometry. As seen in Figure 32, KG-1 cells exhibited very low transduction efficiency in BAR and fuBAR cells, respectively versus untransduced parental controls. This increased following 12 days post transduction, however we performed fluorescence activated cell sorting (FACS) to substantially enrich dsRed⁺ cells to >85% in each variant. Therefore, showing a good enrichment of dsRed⁺ positive cells suitable to use for future experiments.

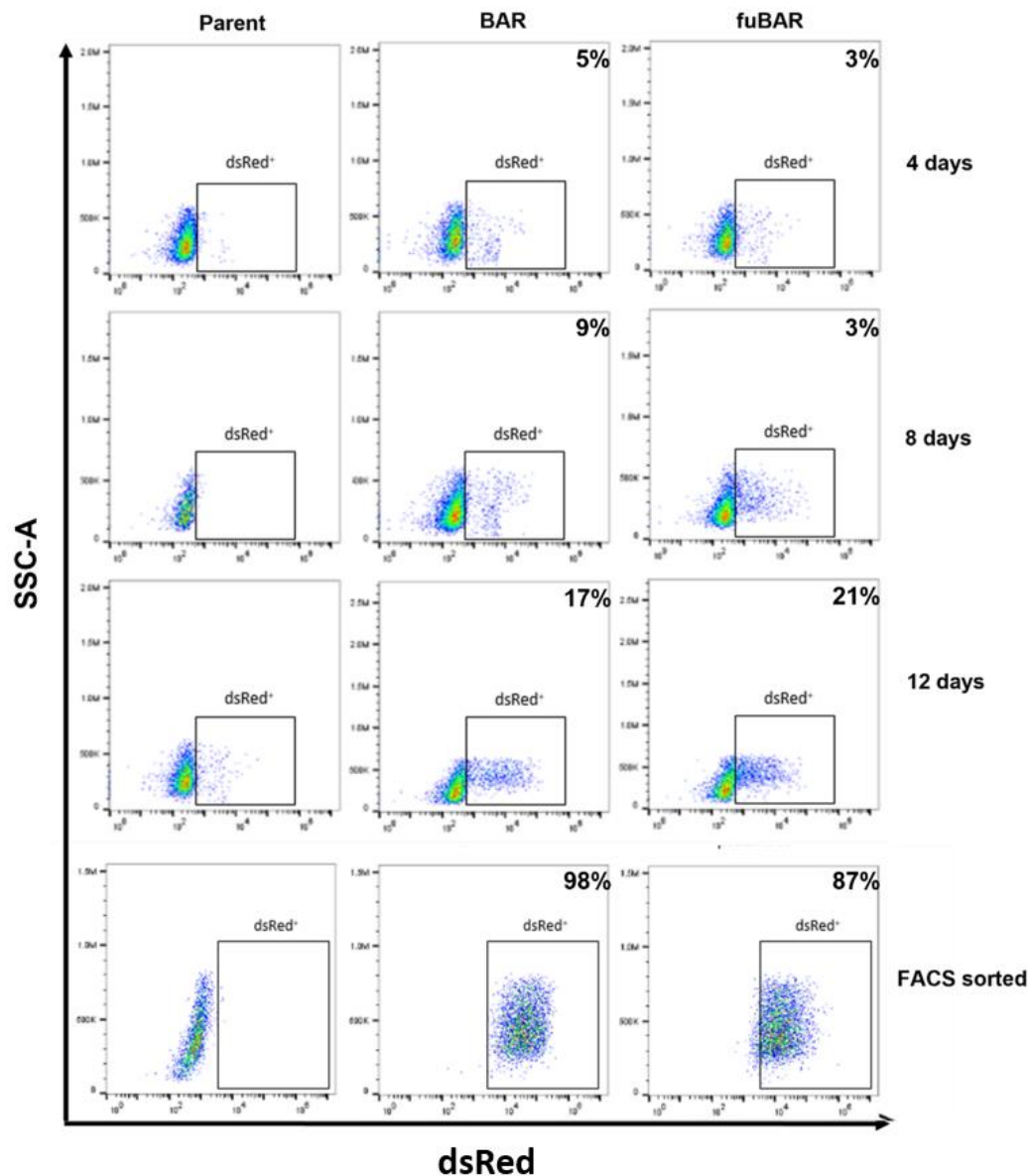


Figure 32: Assessment of lentiviral transduction efficiency of KG1 cell BAR integration.

Flow cytometric density plots demonstrating the intensity of dsRed fluorescence in 'β-catenin activated reporter' (BAR) or or negative control 'found unresponsive' (fuBAR) transduced KG-1 cells 4, 8, and 12 days post-transduction, or following FACS purification of dsRed. Untransduced KG-1 parental cells were used to set the dsRed negative threshold and % dsRed is given within individual plots.

The same procedure was repeated for NB4, HL60 and MV4;11 cells and as shown in Figure 33 all four cell lines demonstrated high transduction efficiency exhibiting >50% dsRed positivity in both BAR and fuBAR cultures by 8 days post-transduction, negating the need for FACS enrichment.

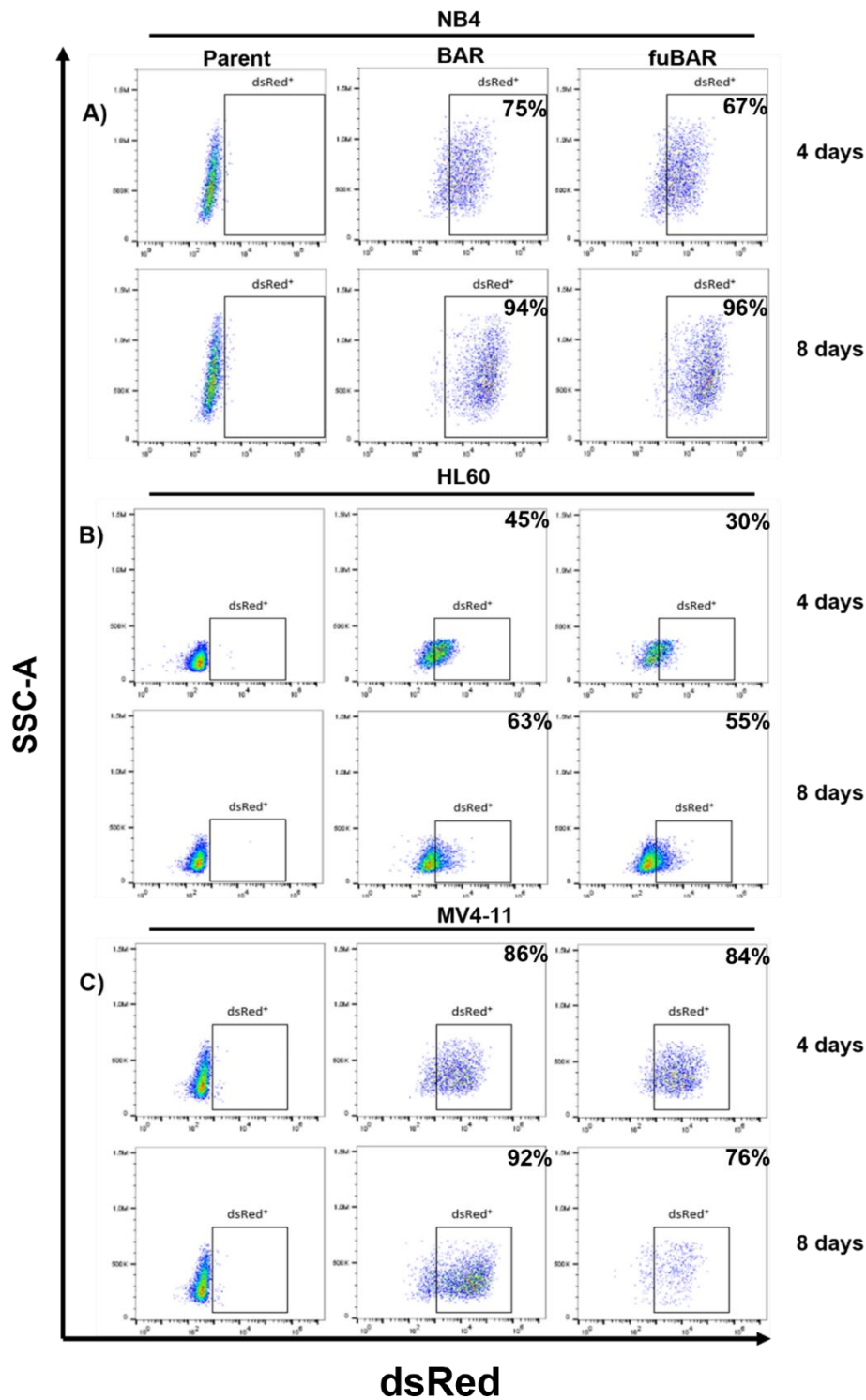


Figure 33: Assessment of DsRed+ in BARV-transduced A) NB4, B) HL60 and C) MV4-11 cells.

Flow cytometric density plots demonstrating the intensity of dsRed fluorescence in BAR or fuBAR transduced **A) NB4, B) HL60 and C) MV4;11** cells 4, 8, and 12 days post-transduction. Respective untransduced parental cells were used to set the dsRed negative threshold and % dsRed is given within individual plots.

In summary, we have four cell lines efficiently transduced with the BAR/fuBAR ready for assessment of Wnt-responsiveness.

4.3.3 Assessing the Wnt responsiveness of myeloid cell lines

After successful incorporation of the BAR reporter system into all required cell lines we next wanted to assess the Wnt-responsiveness each following treatment with the potent Wnt agonist and GSK3 β inhibitor; CHIR99021. All cell lines were treated overnight with CHIR99021 or DMSO and BAR output measured by flow cytometry.

As shown in Figure 34A and B, both KG1 and NB4 cells demonstrated large inductions of Venus YFP fluorescence in response to CHIR99021 treatment relative to DMSO control treated cells. This is indicative of raised TCF activity in these cells and a reliable marker of Wnt-responsiveness. In contrast, both HL60 and MV4;11 exhibited no observable increase in Venus YFP intensity following CHIR99021 treatment versus DMSO control level. Reassuringly, no increase in Venus YFP intensity was observed in any of the fuBAR cultures across all cell lines. In summary, KG1 and NB4 cells were identified as suitable Wnt responsive cell lines for assessing impact of WT1 modulation on Wnt signalling.

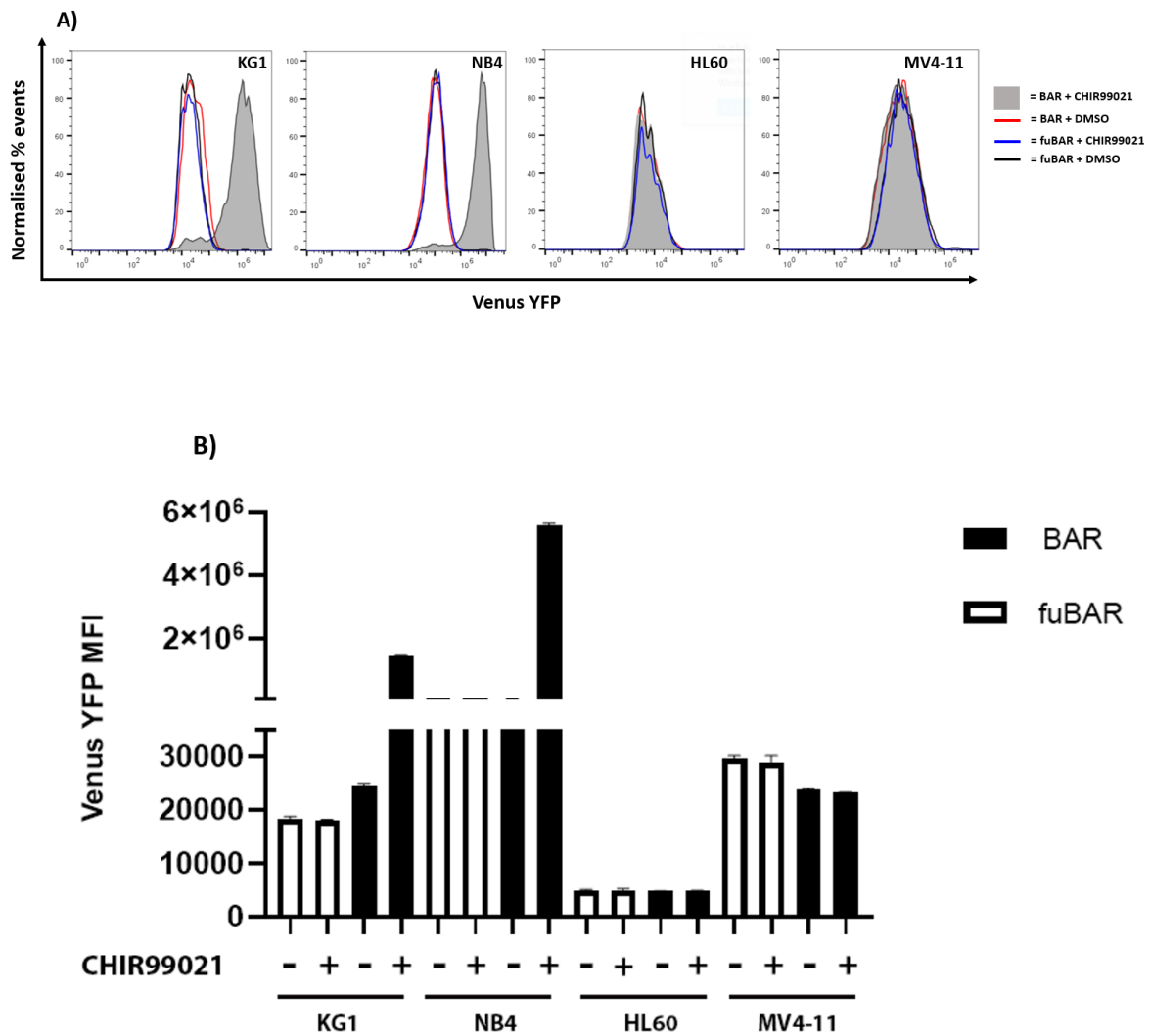


Figure 34: Representative flow cytometric analysis of four myeloid cell lines.

A) The intensity of the TCF-dependent expression of YFP from the 'β-catenin activated reporter' (BAR) reporter, or negative control 'found unresponsive β-catenin activated reporter' (fuBAR) control (containing mutated promoter binding sites) following treatment with CHIR99021/vehicle control (DMSO)]. **B)** Summary showing the median fluorescence intensity generated from the BAR/fuBAR reporters in myeloid cell lines treated ± CHIR99021. MFI: mean fluorescence intensity.

4.3.4 Assessment of WT1 knockdown efficiency and effect on β -catenin stability and nuclear localisation

After successful identification of NB4 and KG1 cells as Wnt-responsive cell lines expressing both WT1 and β -catenin, we next wanted to assess the effect of WT1 knockdown on β -catenin expression and TCF activity. Using lentiviral transduction of the optimal WT1 shRNA sequences #2 and #4 into KG1 and NB4 BAR/fuBAR cells we observed a significant reduction in WT1 expression in all transduced targets versus WT1 levels in the non-targeted shRNA controls (Figure 35). In NB4 cells, WT1 shRNA #2 was less effective than shRNA #4 in reducing WT1 expression. Following examination of subsequent β -catenin expression, we observed a single variant which exhibited reduced β -catenin level in response to WT1 knockdown (KG-1 fuBAR shRNA #2), however, this was not consistent across the rest of the cell lines. These data show that WT1 was efficiently reduced in KG1 and NB4 cells but had little impact on total β -catenin level.

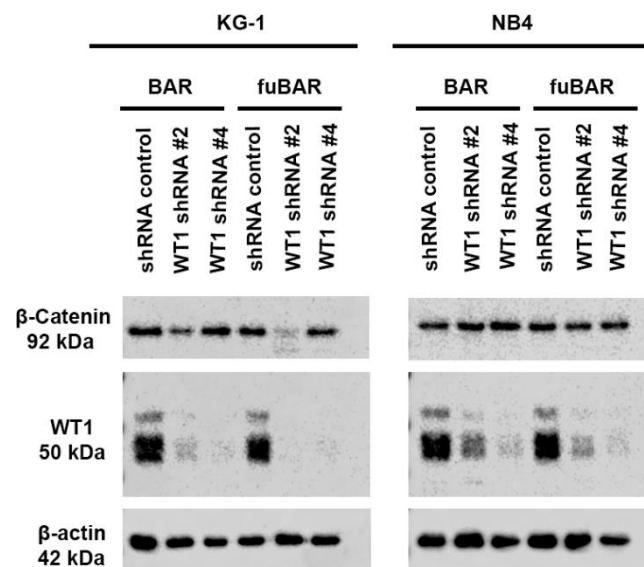


Figure 35: Effect of WT1 knockdown on β -catenin level in KG1 and NB4 cells.

Western blot showing the level of WT1 and β -catenin protein in KG-1 and NB4 cells following lentiviral transduction of BAR and fuBAR cells with WT1 knockdowns shRNA #2 and #4. β -Actin was detected to indicate protein loading.

We next wanted to explore the effect of WT1 knockdown on β -catenin nuclear localisation capacity. K562, KG1 and NB4 exhibiting WT1 knockdown were treated overnight with DMSO or CHIR99021 and then separated into cytosolic and nuclear fractions. As shown in Figure 36, WT1 was predominantly localised in the nuclear fractions of for all cultures, and the relative

distribution was unaltered following Wnt stimulation as observed in previous experiments (Chapter 3 Figure 25). Some residual WT1 expression remained in the nucleus of WT1 shRNA #2 for K562 and NB4 cultures but regardless, WT1 shRNA #4 still shows reduced WT1 expression and shows no impact on β -catenin nuclear localisation capacity in K562 and NB4 cells. However more interestingly for KG1 cells reduced β -catenin expression was seen in the nuclear fractions for both WT1 shRNAs under CHIR99021 conditions.

In summary, WT1 knockdown had no impact on β -catenin nuclear localisation capacity in K562 and NB4 cells but did appear to restrict nuclear β -catenin in KG1 cells suggesting context dependence across AML cell lines.

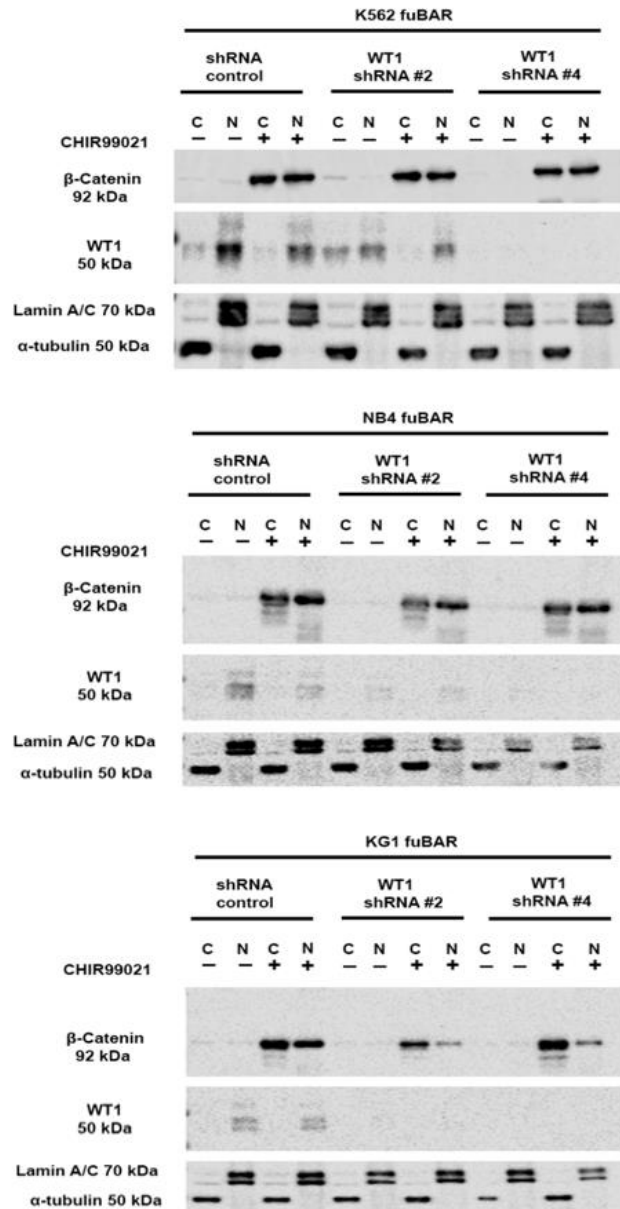


Figure 36: Expression levels of β -catenin in transduced fuBAR myeloid cells with WT1 shRNA

Representative immunoblots showing total β -catenin and WT1 in subcellular cytoplasmic (C) and nuclear (N) following CHIR99021 treatment (GSK3 β inhibitor). In **A**) K562, **B**) NB4 and **C**) KG1 cells with lentiviral transduction of WT1 shRNA #2 and #4 knockdowns. Lamin A/C and α -tubulin were used to indicate protein loading and fraction purity.

4.3.5 Assessing the effect of WT1 knockdown on β -catenin activity

Having shown that WT1 could potentially alter subcellular localisation of β -catenin in specific cell lines we next wanted to assess whether this translated into transcriptional activity of Wnt signalling. K562, NB4 and KG1 BAR/fuBAR cells were again treated overnight with either CHIR99021 or DMSO and cells assessed the following day for TCF reporter activity by flow cytometric analysis (as analysed previously in Figures 32 and 33). For K562 cells under basal conditions both WT1 shRNA's has no significant impact on Wnt signalling (Figure 37A/B). Under Wnt stimulated conditions WT1 shRNA #2 significantly reduced and WT1 shRNA #4 significantly increased Wnt signalling. For NB4 cells, under basal conditions WT1 shRNA #2 significantly increased Wnt signalling, whereas WT1 shRNA had no impact. Under Wnt stimulated conditions both WT1 shRNA reduced Wnt signalling but only WT1 shRNA #4 proved significant (Figure 37A/C). For KG-1 cells, a statistically significant reduction in both basal and induced Wnt signalling output was seen across both WT1 shRNAs versus the non-targeted control (Figure 37A/D). As expected, fuBAR cultures exhibited no induction of Wnt signalling output because of their mutated TCF sequences.

In summary, WT1 knockdown showed no consistent significant effect on Wnt signalling across the three cell lines. However, for KG-1 cells TCF activity was significantly reduced in the presence of both WT1 shRNAs under both basal and Wnt stimulated conditions. Therefore, in keeping with the reduced nuclear localisation of β -catenin previously observed in this cell line and how WT1 modulation is cell line dependent.

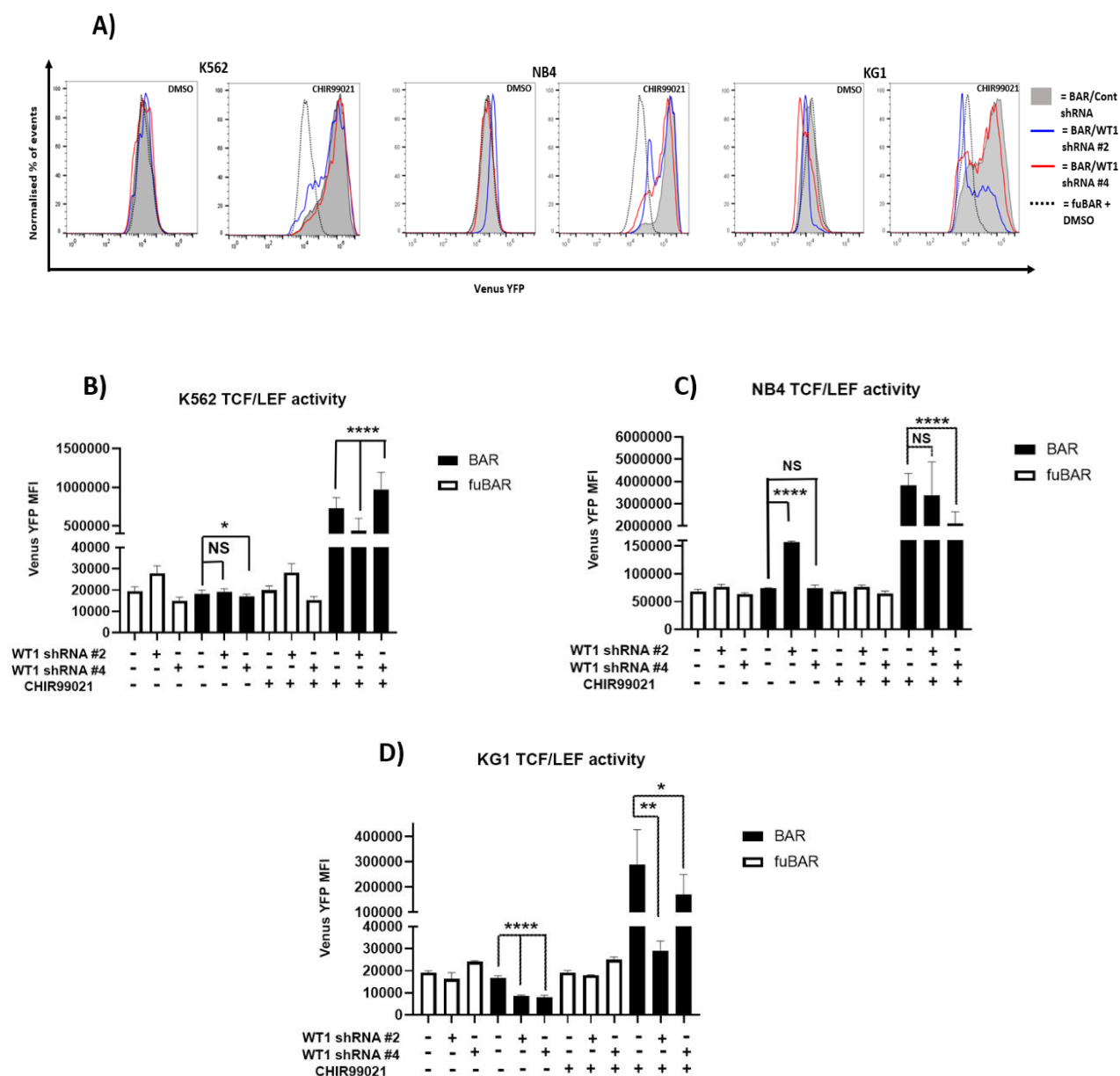


Figure 37: Effect of WT1 knockdown on Wnt signalling output in myeloid cells.

A) Representative flow cytometric histograms showing intensity of the TCF-dependent expression YFP from BAR, or fuBAR) in K562, NB4 and KG1 cells +/- WT1 shRNA +/- 5 μ M CHIR99021. Summary graph showing intensity of the TCF-dependent expression of YFP from BAR (black) and fuBAR (white) in **B)** K562, **C)** NB4 and **D)** KG1 cells transduced with non-targeted shRNA control, WT1 shRNA #1 or WT1 shRNA #2 and following overnight treatment with 5 μ M CHIR99021 or vehicle control (DMSO). All data represents mean \pm 1 s.d ($n = 3$). Statistical significance is denoted by * $P < 0.05$, ** $P < 0.01$, *** $P < 0.001$ and **** $P < 0.0001$.

4.3.6 Assessing the effect of WT1 overexpression on β -catenin activity

After determining WT1 knockdown could significantly impact Wnt signalling in KG-1 cells, it was necessary to examine the impact of WT1 overexpression in K562, NB4 and KG1 cells. Cells were lentivirally transduced with overexpressed WT1 (O/E) as previously (Figure 31) versus the respective empty vector control (O/E control) and Western blotted for WT1 as shown in Figure 38. Wild type endogenous WT1 was present at ~50kDa in all cell lines as expected, followed by the enrichment of a further higher molecular weight band at ~60kDa for cultures transduced with ectopic WT1. Interestingly in both K562 and NB4 cells, a modest but consistent increase in β -catenin was observed in O/E samples versus the non-targeted control lanes, which was not seen in KG1 cells.

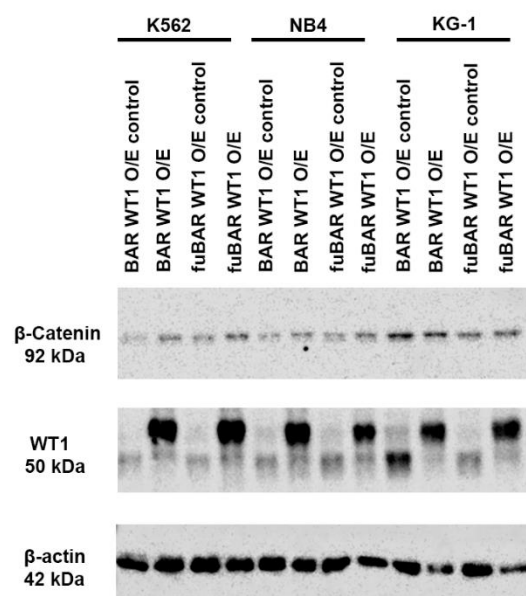


Figure 38: Assessment of WT1 overexpression.

Representative immunoblots of the level of WT1 and β -catenin protein in K562, NB4 and KG1 cells following lentiviral transduction of BAR and fuBAR cells with WT1 overexpression (O/E) and respective non-targeted control β -actin was detected to indicate protein loading.

We next assessed the effect of ectopic WT1 on Wnt signalling. As shown in Figure 39 for all three cell lines a small but statistically significant increase in TCF activity was determined for the WT1 O/E shRNA when compared to the non-targeted control under basal Wnt signalling

conditions. Under Wnt stimulated conditions, K562 showed a significant decrease in TCF activity in response to ectopic WT1, whilst NB4 showed no significant change. KG1 displayed a significant increase in Wnt signalling when treated with CHIR99021. It was noted that under basal conditions fuBAR cultures also displayed small but statistically significant increases in Venus YFP intensity in response to WT1 overexpression indicating that perhaps experimental conditions were raising the level of autofluorescence in this channel. Therefore, the changes observed in BAR cultures may not be real biological effects.

In summary, these data show no consistent effects of ectopic WT1 overexpression on β -catenin activity in myeloid cell lines.

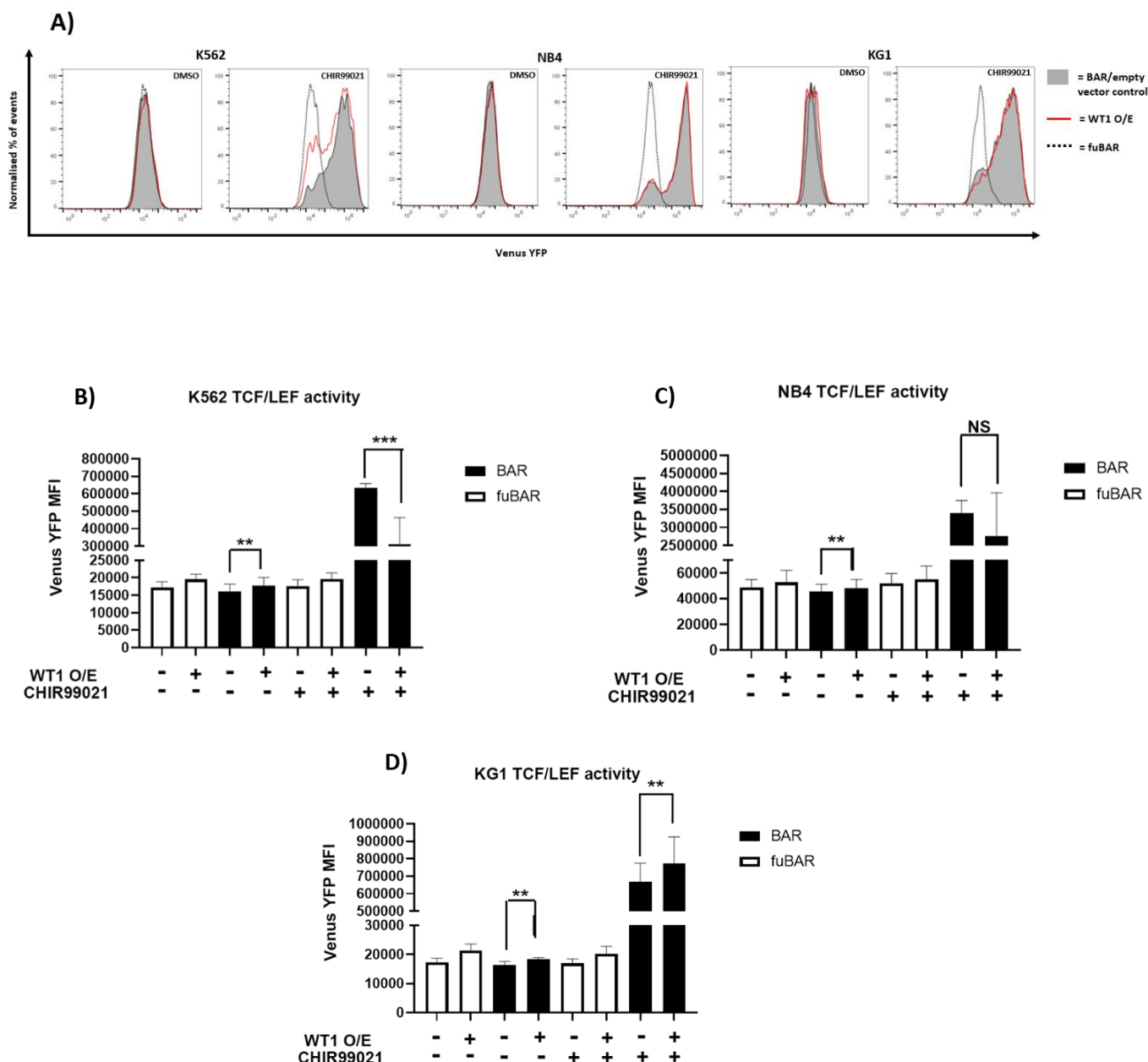


Figure 39: Effect of WT1 overexpression on Wnt signalling

A) Representative flow cytometric histograms showing intensity of the TCF-dependent expression YFP from BAR, or fuBAR in K562, NB4 and KG1 cells +/- WT1 shRNA +/- 5µM CHIR99021. Summary graph showing intensity of the TCF-dependent expression of YFP from BAR (black) and fuBAR (white) in **B)** K562, **C)** NB4 and **D)** KG1 transduced with non-targeted empty vector control or WT1 overexpression (O/E) and following overnight treatment with 5µM CHIR99021 or vehicle control (DMSO). All data represents mean \pm 1 s.d ($n = 3$). Statistical significance is denoted by * $P < 0.05$, ** $P < 0.005$, and *** $P < 0.0005$

4.3.7 Evaluating the impact of WT1 mutation on β -catenin expression

We next wanted to assess the functional impact of mutated WT1, as these mutations are frequent in AML presenting in 6-15% of cases (Rampal & Figueroa, 2016) and is therefore of clinical significance, however the impact on Wnt/ β -catenin signalling is not known. To explore the functional impact of mutated WT1 on β -catenin expression and subcellular localisation, KG1 and NB4 (BAR/fuBAR) cells were lentivirally transduced with a doxycycline (DOX) inducible expression plasmid encoding frameshift mutations to different exons of WT1 (Ex7, Ex8 or Ex9) or empty vector (pCW57.1). K562 cells were omitted since this represents CML and WT1 mutations are particularly relevant to AML. Once puromycin selection was complete, cells were treated for either 24 or 48 hours with DOX to check for the presence of the truncated WT1 mutant. As shown in Figure 40A, for NB4 cells endogenous wild type WT1 is present in both cell lines at ~50kDa, with the exon 8 and 9 mutants visible at lower molecular weight (~30 kDa), but no overall impact on β -catenin expression was determined. Furthermore, no WT1 mutant was present with exon 7 in keeping with a previous study who also couldn't detect this WT1 mutant in Kasumi-1 cells (Potluri et al., 2021). Therefore, only mutants at Ex8 and 9 were validated in KG1 cells (Figure 40B) with successful induction of the WT1 mutants at ~30 kDa and more interestingly this also led to an increase in endogenous WT1 at 50 kDa. Also, there is a clear abundance of exon 8 mutant versus exon 9 mutant, finally an increase in total β -catenin expression in the presence of both mutants, in keeping with ectopic WT1 which slightly raised β -catenin levels (Figure 38). Overall suggesting WT1 mutations could have an impact on regulating β -catenin expression.

After successful integration of the WT1 exon mutants into KG1 and NB4 cells we next wanted to explore the impact of WT1 mutants on β -catenin expression and localisation. As shown in Figure 40C, WT1 remains nuclear after Wnt stimulation as seen before (Chapter 3 Figure 25). β -Catenin expression is enriched after Wnt stimulation in both the cytoplasmic and nuclear fractions as expected for the control and the mutants Ex8 and Ex9 have no impact on β -catenin expression or localisation.

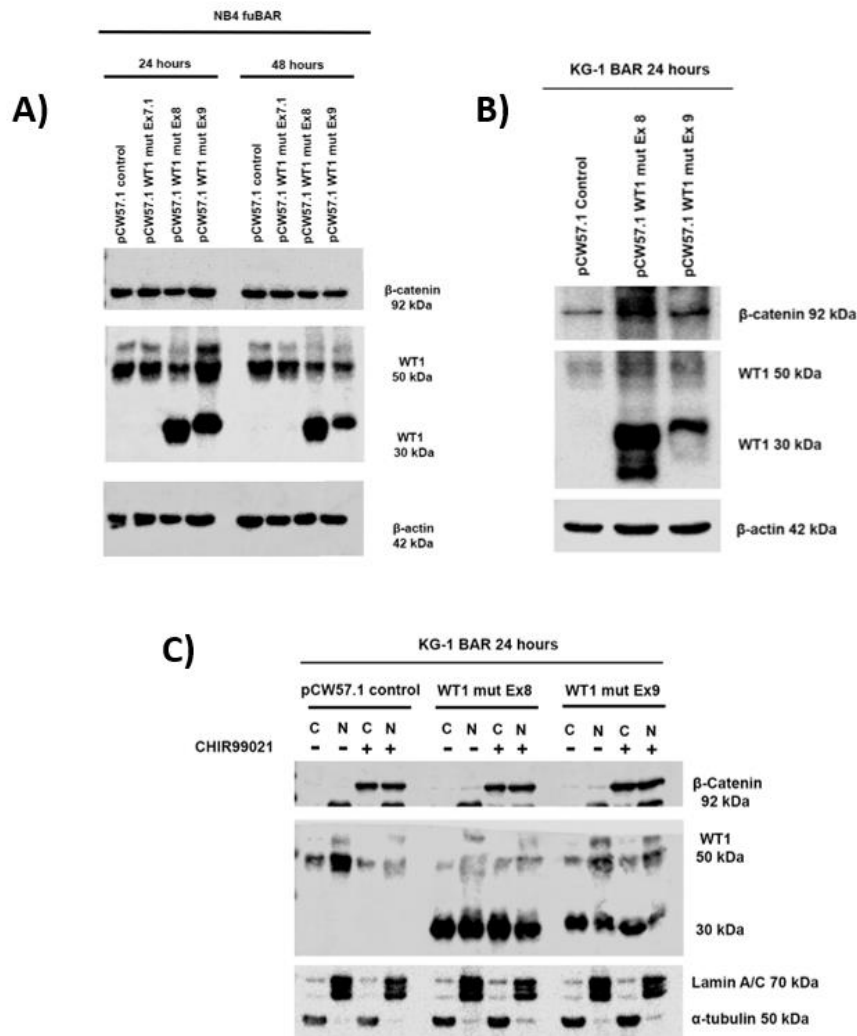


Figure 40: Assessment of WT1 mutant expression.

A) Representative immunoblots of the level of WT1 and β-catenin protein in NB4 'mutant responsive' β-catenin activated reporter (fuBAR) cells transduced with pCW57.1 control or respective WT1 mutant (Ex7, 8 and 9), following 24 or 48hours treatment with doxycycline (DOX. **B)** Representative immunoblots of the level of WT1 and β-catenin protein in KG1 β-catenin activated reporter (BAR) cells transduced with pCW57.1 control or respective WT1 mutant (Ex 8 and 9). Cells were treated for 24hrs with DOX to induce the plasmid. β-Actin was detected to indicate protein loading. **C)** Immunoblots showing the level of WT1 and β-catenin protein in KG1 BAR WT1 mutated cells in the cytoplasmic (C) and nuclear (N) fractions after 24hrs treatment +/- DOX and +/- CHIR99021 Lamin A/C and α-tubulin were used to assess protein loading and fraction purity.

Next, we looked at the effect of WT1 mutation on overall Wnt signalling activity. To do this KG1 and NB4 (BAR/fuBAR) cells were DOX treated for 48 hours total with addition of CHIR99021/DMSO after 24 hours. Cells were then analysed using flow cytometric analysis to assess BAR activity. As shown in Figure 41 for NB4 no significant difference was observed for either mutant versus control. However, for KG1 cells, both mutants showed a significant increase in induced TCF activity when compared to the mutant control, however more so for exon 8 which displayed highest levels of WT1 mutant protein expression and β -catenin stabilisation (Figure 41B). However, for NB4 no significant difference was observed for either mutant versus control. Therefore, showing the effect of WT1 mutation on TCF reporter activity could be cell line dependent as seen before with WT1 knockdown.

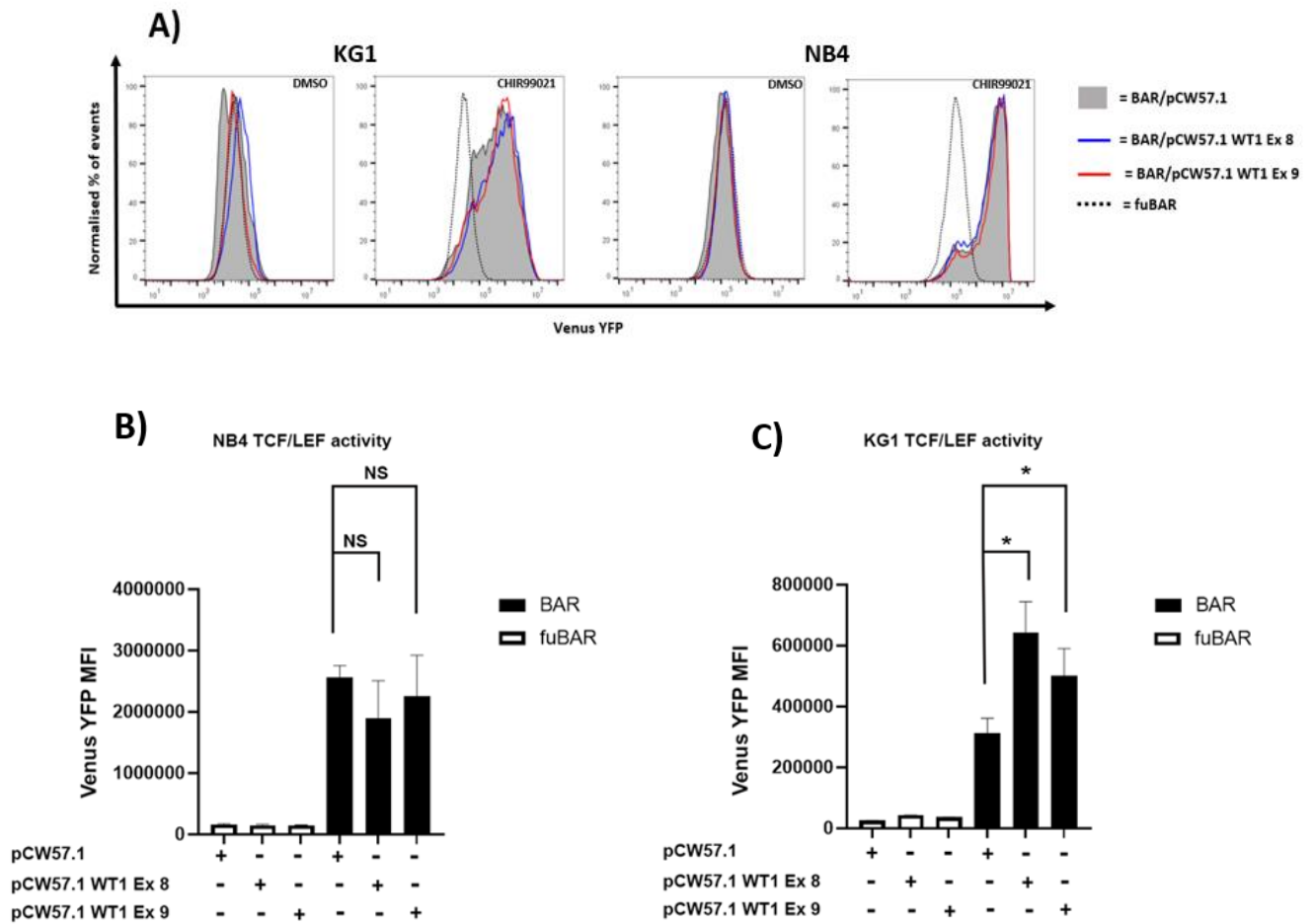


Figure 41: Effect of mutant WT1 on Wnt signalling

A) Representative flow cytometric histograms showing intensity of the TCF-dependent expression YFP from BAR, or fuBAR NB4 and KG1 cells +/- WT1 mutant +/- 5 μ M CHIR99021. Summary graph showing intensity of the TCF-dependent expression of YFP from BAR (black) and fuBAR (white) in **B)** KG1, **C)** NB4 transduced with mutant pCW57.1 control or WT1 mutants Ex 8 and Ex 9 and following overnight treatment with 5 μ M CHIR99021 or vehicle control (DMSO). All data represents mean \pm 1 s.d ($n = 3$). Statistical significance is denoted by * $P < 0.05$.

4.3.8 β -catenin knockdown affects WT1 expression levels in various myeloid cell lines

An examination of Wnt signalling impact on WT1 level/activity has not been reported previously. To investigate the effect of β -catenin modulation on WT1 signalling we first needed to suppress β -catenin expression using lentiviral transduction. Two shRNA sequences each integrated within a lentiviral expression vector (pLKO.1) and one CRISPR/Cas9 sequence (pLV), all containing a puromycin resistance gene were tested for most efficient knockdown of β -catenin in K562, NB4, KG1 and HEL cells (known to express high endogenous β -catenin protein; Chapter 3 Figure 22).

As shown in Figure 42A, shRNA #1 has successfully removed all or reduced β -catenin expression in K562, NB4 and KG1 cells when compared to the non-targeted shRNA control. However, shRNA #2 was unsuccessful in reducing β -catenin and was not used for further experimental work. K562 cells could not tolerate β -catenin knockdown for a prolonged length of time, so we explored HEL as an alternative cell line (Figure 42B), however only cells containing the β -catenin shRNA #1 remained viable post-selection. More interestingly WT1 expression is reduced in the presence of β -catenin shRNA #1 and β -catenin CRISPR/Cas9 for all cell lines suggesting β -catenin can impact WT1 expression level.

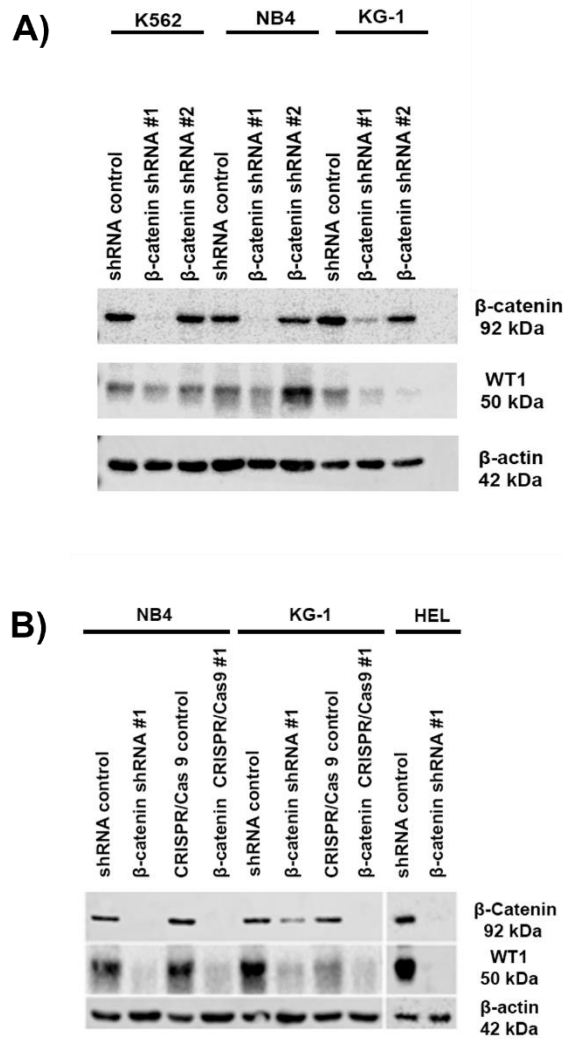


Figure 42: Assessment of β -catenin knockdown in myeloid cells.

Western blot showing the level of β -catenin and WT1 protein in **A)** K562, NB4 and KG1 cells following lentiviral transduction with two β -catenin shRNA knockdowns. **B)** NB4, and KG1 following lentiviral transduction with β -catenin shRNA #1 and CRISPR/Cas9 β -catenin knockdown and HEL with β -catenin shRNA #1. β -Actin was detected to indicate protein loading.

4.3.9 β -Catenin mediated regulation of WT1 is not by the proteasome

Like β -catenin (Chen et al., 2018) WT1 protein is known to be regulated by ubiquitination and proteasomal mediated degradation. We therefore hypothesised that the resultant WT1 loss upon β -catenin knockdown could be through β -catenin normally protecting WT1 from the proteasome. To investigate this, we treated β -catenin knockdown cells with the proteasome

inhibitor MG132 to assess whether WT1 expression could be recovered. β -Catenin stability is also regulated by the proteasome and MG132 increased β -catenin expression as expected. However, treatment of both NB4 and KG1 cells harbouring a β -catenin knockdown failed to restore WT1 protein level, and instead reduced stability further (Figure 43) implying β -catenin does not protect WT1 from proteasomal degradation. Instead, it is likely from these data that the MG132 stabilises a protein that negatively governs WT1 stability.

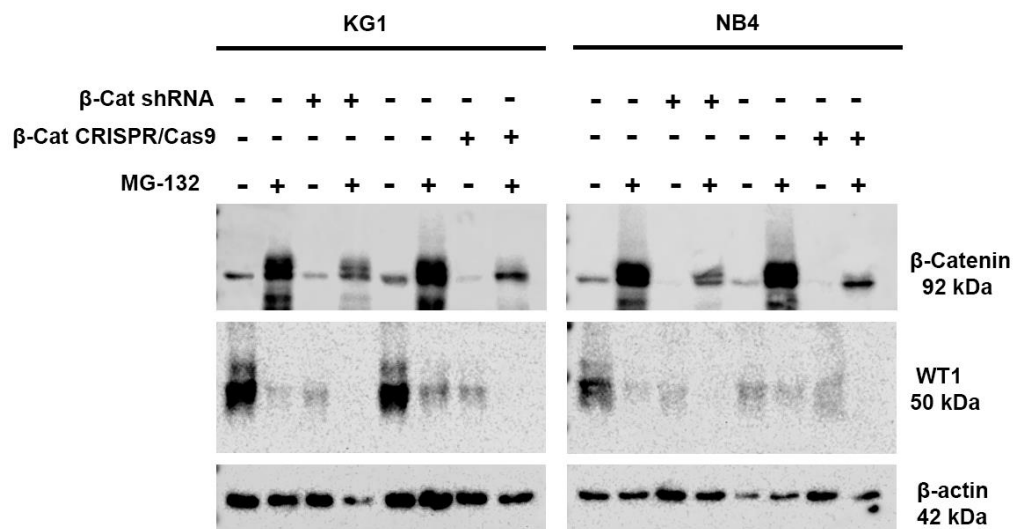


Figure 43: β -Catenin mediated regulation of WT1 is not via the proteasome.

Immunoblot showing protein level of β -catenin and WT1 in NB4 and KG1 cells +/- β -catenin shRNA, +/- β -catenin CRISPR/Cas9 following 16 hours incubation with 1 μ M proteasome inhibitor MG132. β -Actin detection indicates protein loading.

4.3.10 Identifying WT1 target genes in KG1 cells

To assess the impact of β -catenin knockdown on WT1 signalling we examined the mRNA expression of a panel of previously identified WT1 target genes using qRT-PCR. WT1 targets first required validation in myeloid cell lines since we needed to confirm WT1 targets in this specific tissue type. To ascertain this a panel of previously characterised WT1 target genes were assessed in cells harbouring WT1 knockdown to confirm them as WT1 targets in myeloid cells.

To this end, we analysed WT1 target genes validated in KG-1 cells and normalised to the house-keeping gene *ACTB* (Figure 44). *WT1* was significantly reduced as expected, with *AREG* and *ETS1* being significantly reduced in the presence of WT1 shRNA #4. Other confirmed target genes were *JUNB* and *BAK1* but *MYB*, *DNMT3A* and *VDR* were upregulated indicating WT1 might repress their expression in this context. In summary the WT1 target genes for further analysis were *AREG*, *JUNB*, *BAK1* and *ETS1* which are also not known targets of Wnt signalling.

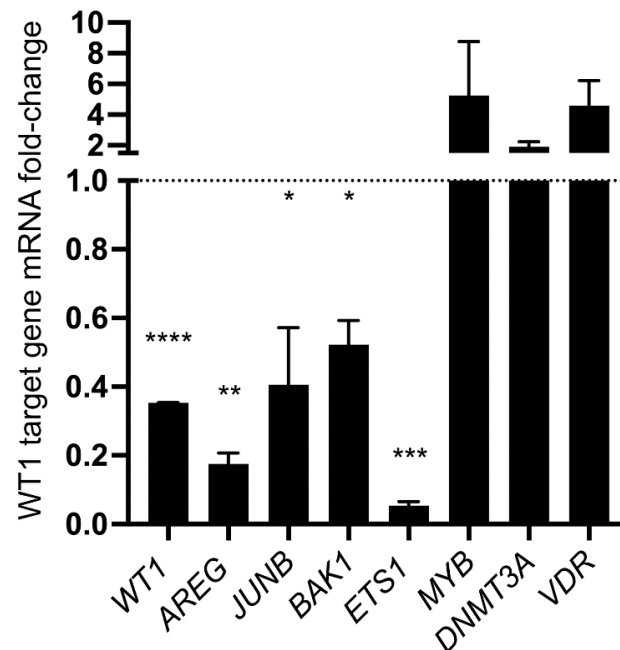


Figure 44: Assessment of WT1 target genes in KG1 cells.

Summary graph showing fold change in mRNA expression of genes previously identified as WT1 target genes, in KG-1 cells by qRT-PCR. Fold change is in response to knockdown of WT1 using WT1 shRNA relative to expression in non-targeted shRNA control (dashed line). Expression was normalized to the housekeeping gene β -actin (*ACTB*). All data represents mean \pm 1 s.d ($n = 3$). Statistical significance is denoted by * $P < 0.05$, ** $P < 0.005$, *** $P < 0.0005$ and **** $P < 0.0001$ as deduced by a one-sample t-test.

4.3.10 β -catenin knockdowns reduce WT1 target gene expression

After identifying *bona-fide* WT1 downstream targets, we next assessed how these target genes were impacted in the presence of β -catenin shRNA and CRISPR knockdowns by qRT-PCR. As shown in Figure 45 in both KG1 and NB4 cells we observed a significant reduction in all WT1 target genes assessed (except for ETS1 in NB4 cells), including WT1 mRNA itself, upon either shRNA or CRISPR/Cas9 mediated β -catenin knockdown. These data suggest for the first

time that β -catenin is capable of regulating WT1 mRNA and respective WT1 signalling at a transcriptional level.

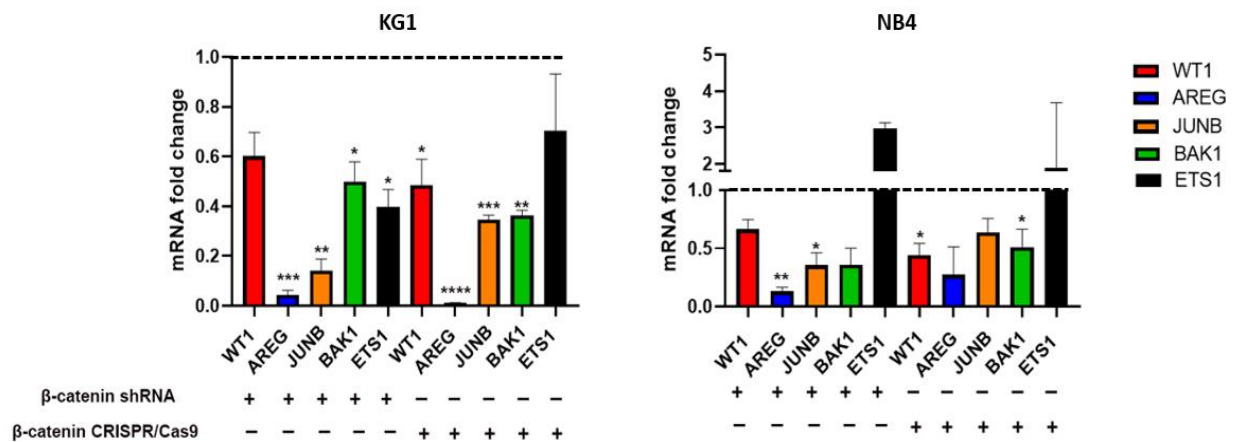


Figure 45: Assessment of WT1 targets with β -catenin knockdown.

Summary graph the fold change in WT1 target gene mRNA expressed as assessed by qRT-PCR in KG1 and NB4 cells expressing either β -catenin shRNA or CRISPR/Cas9 knockdown. Fold change is relative to relative matched respective controls (dashed line) and overall expression was normalized to the housekeeping gene β -actin (*ACTB*). All data represents mean \pm 1 s.d ($n = 3$). Statistical significance is denoted by * $P < 0.05$, ** $P < 0.01$, *** $P < 0.001$ and **** $P < 0.0001$ as deduced by a one-sample t-test.

4.4 Discussion

4.4.1 WT1 modulation on β -catenin expression and Wnt signalling

This research identified NB4 and KG1 as two further Wnt-responsive cell lines (Figure 33A) to use in this study alongside the already established K562 and HEL cell lines (Morgan et al., 2019). The first aim of this study was to modulate the expression of WT1 and investigate the subsequent effect on β -catenin stability and Wnt signalling. Using these three cell lines, we successfully incorporated two WT1 shRNA knockdowns (Figure 35) and determined a decrease in nuclear β -catenin expression and an overall significant decrease in Wnt signalling for KG1 cells containing the BAR system (Figure 36C/37C). This aligns with previous studies demonstrating cooperation between WT1 and Wnt signalling in which WT1 was found to stimulate epicardial expression of *Ctnnb1* and *Lef1*, essential components of the β -catenin signalling pathway (von Gise et al., 2011). WT1 also contributes to early organogenesis by regulating Wnt signalling during diaphragm development in mice (Paris et al., 2015). WT1 has shown to regulate Wnt4 and in turn the process of MET during early stages of metanephric kidney development (Sim et al., 2002). Studies have shown that downregulation of WT1 caused Wnt11 to decrease at the mRNA and protein levels, resulting in β -catenin translocating from the nucleus to the cytoplasm (Y. Li et al., 2014). Overall showing WT1 can act in a cooperative manner with Wnt signalling.

Furthermore, WT1 has displayed antagonistic behaviour with Wnt signalling in other contexts, for example WT1 induction inhibited Wnt-mediated transcription by preventing the recruitment of TCF onto a promoter (Kim et al., 2009). A recent study showed that deletion of WT1 led to up-regulation of β -catenin and Sertoli-specific WT1 deletion effected the stabilisation of β -catenin in the testis (Chang et al., 2008), further down-regulation of WT1 has shown to induce podocyte dysfunction and apoptosis through activating Wnt/ β -catenin signalling (Jing et al., 2015). A novel target of WT1, WID, functions to negatively regulate Wnt/ β -catenin signalling (Kim et al., 2010). Overall, WT1 and β -catenin are able to mutually antagonize each other and repress the expression of their respective target genes (Zhou et al., 2015). This shows the importance of context when assessing such relationships as even within the same tissue there were inconsistent effects (e.g., no decrease of β -catenin in NB4 and K562 cells).

KG1 cells are an erythroleukemia cell line, whereas NB4 are an acute promyelocytic leukaemia cell line with characteristic t(15;17) translocation and K562 a chronic myeloid leukaemia cell line (Svedberg et al., 1999). Therefore, implying targeting the WT1/ β -catenin association could only be significant for those patients derived from a similar morphology and genotype of KG1. KG1 cells have the presence of a large submetacentric chromosome (MAR-1), besides two normal copies of chromosome 1 (Pelliccia et al., 2012) and are a mutant p53-expressing human AML cell line (Weisberg et al., 2015). So, knowing this about KG-1 cells we tried to find another cell line with similar morphology, we attempted this with KG1a a subline of KG1 with lost myeloid features. However, we could not detect WT1 expression (Figure 22) and therefore could not carry out subsequent experiments. Furthermore, we could expand this work on KG-1 to try and identify what feature of this cell line is unique in causing the functional effects with β -catenin, by for example inhibiting p53 and repeating the experiments.

We also explored the impact of WT1 overexpression on β -catenin expression and Wnt signalling (Figure 38/39) as WT1 overexpression is found in a majority of AML patients and has been reported to play as a negative prognostic factor in this disease (Rampal & Figueroa, 2016) as it can enhance proliferation and inhibit apoptosis (Zhou et al., 2020). The size of the ectopic WT1 we overexpressed was ~ 60 kDa which represents a higher molecular weight than the endogenous WT1 ~ 50 kDa present in our cell lines. WT1 isoforms have shown to have distinct features in mammary epithelial cells, in which WT1 (-Ex5/-KTS) showed proliferation and caused cell cycle arrest in G2 (Burwell et al., 2007). More specifically in an AML context WT1 isoform (+Ex5/+KTS) was dominant although in a lower quantity than CD34⁺ cells (Luna et al., 2013). Furthermore, we identified a varied effect on Wnt signalling across our three cell lines under both basal and Wnt stimulated conditions, overall implying this ectopic isoform at 60 kDa alone does not regulate Wnt signalling in a hematopoietic context. However, identifying which WT1 isoform is causing functional impact is important for targeting this molecule as could then use this information in designing drug targets for example to inhibit the KTS domain.

We examined the impact of WT1 mutation on β -catenin expression and Wnt signalling output as these mutations are found in ~ 10% of AML cases (Rampal & Figueroa, 2016). This relationship has not been previously explored, using doxycycline (DOX)-inducible mutant WT1

expression constructs we expressed WT1 mutations (to exons 7, 8 and 9) in NB4 cells (Figure 38/39) which truncated the protein at different Zn²⁺- finger domains (Rampal & Figueroa, 2016). However, we could not successfully express the mutant at exon 7 which agrees with previous work (private communication with Bonifer group) (Potluri et al., 2021). Therefore, in KG1 cells we only expressed mutations to exons 8 and 9 (Figure 40B). Overall, in both NB4 and KG1 cells, exon 8 was expressed more abundantly than exon 9. The presence of both mutations led to increased expression of endogenous WT1 and an increase in total β -catenin expression. Research confirmed presence of exon 8 mutation but not the exon 9 mutation led to significantly increased growth and clonogenicity and a decrease in apoptosis, similar to β -catenin phenotypes implying the β -catenin increase is compatible with the WT1 mutation phenotype (Potluri et al., 2021). This links further to our research where we observed a significant increase in TCF activity with both mutants but more so in the presence of exon 8, therefore confirming WT1 mutation can impact β -catenin expression and overall Wnt signalling. This has been identified before in a Wilms tumor context specifically, where WT1 mutations specifically at exon 8 have been shown to activate the Wnt signalling pathway (Fukuzawa et al., 2009; Fukuzawa et al., 2004). This was achieved through WT1 interacting with *WTX* and *CTNNB1* (Cardoso et al., 2013) and therefore further studies are required to understand the exact mechanism in a haematological context, as we know deregulation of β -catenin is critical in the development of a number of malignancies (Maiti et al., 2000).

In summary we have identified functional cooperation between WT1 and β -catenin in an AML context. However due to WT1's complexity in expressing multiple isoforms resulting in varied effects on driving leukemogenesis, it would be hard to pinpoint where and how WT1 and β -catenin are cooperating. However, our study as mentioned above has pinpointed one particular cell line KG1 which shows the functional consequence of this relationship and is interesting as contains mutant p53 and therefore would be the ideal setting to explore further mechanistic roles.

4.4.2 β -Catenin modulation on WT1 expression and activity

To complement the WT1 modulation work, we performed reciprocal experiments to overall understand the impact of β -catenin knockdown on WT1 expression and signalling activity. We successfully reduced β -catenin expression in three myeloid cell lines (Figure 42) and more

interestingly observed a dramatic decrease in total WT1 expression. Studies have shown that loss of β -catenin can significantly impact long-term growth and maintenance of HSCs (Zhao et al., 2007) and we can now speculate this deficient growth could be due to other proteins such as WT1 being reduced in the presence of β -catenin knockdown.

We wanted to understand this WT1 loss further and hypothesised β -catenin could be protecting WT1 from proteasome-mediated degradation. As we know like β -catenin, WT1 is ubiquitinated and regulated by the proteasome (Makki et al., 2008) (Zhou et al., 2020). NB4 and KG1 cells were treated with the proteasome inhibitor MG132, however WT1 level failed to restore and instead reduced stability further (Figure 43). This loss of WT1 following proteasome inhibition has been reported before, after treatment with bortezomib which targeted WT1 transcript. Bortezomib reduced cell viability in MO7-e a megakaryoblast cell line and P39 cell line derived from an MDS-CMML patient in a dose and time dependent matter (Galimberti et al., 2008) (Alimena et al., 2011). Therefore, this could be a potential route for reducing WT expression in haematological malignancies, however this treatment is not specific at targeting WT1 alone and therefore could stabilise proteins such as β -catenin resulting in further establishment of LSCs (Ysebaert et al., 2006).

We then explored the impact of β -catenin knockdown on WT1 signalling and identified a significant reduction in genes with important roles in LSC proliferation and tumorigenicity; *AREG* (Baillio et al., 2011), *JUNB* (Gurzov et al., 2008), *BAK1* (Liu et al., 2016) and *ETS1* genes (Fry & Inoue, 2018) (except for *ETS1* in NB4 cells) (Figure 45). Therefore, suggesting β -catenin mediated regulation of WT1 expression is in part transcriptionally driven. WT1 or its targets have not been classified as Wnt target genes because very few studies have been performed in a haematological setting. Our original study suggested the β -catenin:WT1 interaction was not detectable in SW620 colorectal cancer cells (Morgan et al., 2019) suggesting this relationship may have been missed in a research community primarily focussed on epithelial tissues.

To our knowledge this is the first report of β -catenin mediated regulation of WT1 expression activity in AML, and has significance given previous functional overlap between these proteins. β -Catenin plays an important role in HSC self-renewal and overexpression expands the HSC pool by both phenotype and proliferation (Reya et al., 2003). In an AML context both

proteins are overexpressed with similar genetic aberrations in AML such as t(8;21), RUNX-RUNX1T1 (Nishida et al., 2006) and t(9;11) MLL-AF9 (Zhou et al., 2020) in promoting leukemogenesis. Therefore, this chapter highlights that these two frequently dysregulated proteins in AML could cooperate in specific subtypes of AML and could be worth exploring therapeutically in these contexts.

Chapter 5. Characterising β -catenin roles in RNA biology

5.1 Introduction

After determining WT1, MSI2 and LIN28B association with β -catenin we speculated β -catenin could have roles in RNA biology given these proteins are established RNA-binding proteins (RBP). For instance, WT1 has shown to bind preferentially to 3' untranslated (UTRs) of developmental mRNA targets which are downregulated upon WT1 knockout in developing kidney mesenchyme (Bharathavikru et al., 2017), but has not yet been explored in an AML context. LIN28B is involved in post transcriptional regulation of miRNA or mRNA expression, regulates microRNA (miRNA) biogenesis, and is overexpressed in multiple leukaemia's including AML (Helsmoortel et al., 2016) where it can promote proliferation (J. Zhou, C. Bi, et al., 2017) and self-renewal (J. Zhou, Z. L. Chan, et al., 2017). Lastly, MSI2 is a member of the Musashi RBPs and regulates the expression of target mRNAs involved in translation and can regulate proliferation, cell cycle, apoptosis and chemosensitivity (Han et al., 2015). Given the role of these RBPs individually in AML or tumorigenic processes, their interaction with β -catenin or β -catenin's wider role in RNA biology warrants further investigation in an AML context.

β -Catenin mediates most of its protein interactions such as those with TCF/LEF, APC or cadherins via its armadillo repeat domain (ARM)(Valenta et al., 2012). Whether β -catenin is capable of binding RNA directly through these domains is not so well established. β -Catenin does not possess the typical features of an RNA binding protein (RBP); RNA recognition motif (RRM), Piwi/Argonaute/Zwille (PAZ) domain, RGG (Arg-Gly-Gly) box, Sm domain and Zinc finger (Hur & Jeong, 2013). However more recently the structural core of the β -catenin Armadillo repeats have shown to structurally resemble the pumillio/FBF (PUF) repeat domains of the pumillio protein which were first identified in drosophila (Edwards et al., 2001), therefore, emphasising β -catenin could act as an RBP like Pumillio and is supportive evidence for β -catenin having an RNA binding role (Moore et al., 2018).

β -Catenin has already been shown to bind and stabilise certain oncogenic mRNAs in colon cancer through alternative RNA splicing and RNA stability of unstable transcripts such as COX-2 mRNA (Kim et al., 2012; Lee et al., 2007) (Lee & Jeong, 2006). Specifically, the C-terminal domain of β -catenin can interact with HuR, and ARM repeat associated with RNA to form the

RNA- β -catenin-HUR complex *in vitro* and in cells. Therefore, understanding how β -catenin can bind RNA and regulate RNA dependent processes in an AML context is vital to provide more background on how this protein could be used as a therapeutic target.

5.2 Aims

In AML, efforts to understand β -catenin's oncogenic influence have largely focused on its transcriptional activity. However, we believe β -catenin could be serving a role in post-transcriptional gene expression in AML. To investigate this hypothesis and develop new therapeutic strategies to disrupt aberrant β -catenin activity in AML we have the following aims:

1. Assessment of RNA dependence for the β -catenin:WT1, MSI2 or LIN28B interactions
2. Characterisation of β -catenin abundance in actively translating polysomes under both basal and Wnt stimulated conditions
3. Determination of RNAs associated with β -catenin through RBP immunoprecipitation (RIP) coupled to RNA sequencing (RIP-seq)

5.3 Results

5.3.1 The β -catenin:WT1, :MSI2, or :LIN28B interactions are not mediated through RNA
Since β -catenin, WT1, MSI2 and LIN28B are all documented to bind RNA, we wanted to ascertain whether these individual interactions were being observed merely because of β -catenin binding RNA. To confirm this, the Co-IPs from Chapter 3 (Figure 9-11) were repeated from cell lysates pre-treated with RNase prior to Co-IP to degrade any single-stranded RNA. Complete digestion of RNA was confirmed in K562, KG1 and HEL DMSO and CHIR99021 treated fractions (Figure 46). As observed in Figure 47, association between WT1 and β -catenin remained in the absence of RNA in K562, KG1 and HEL under both basal and Wnt stimulated conditions. Likewise, the β -catenin:MSI2 (Figure 48A/B) and β -catenin:LIN28B (Figure 48C/D) association remained intact despite RNA digestion in both basal and Wnt stimulated K562 and HEL cells. In summary, the association between β -catenin and these RBPs is not indirect via RNA, rather more likely through an RBP complex.

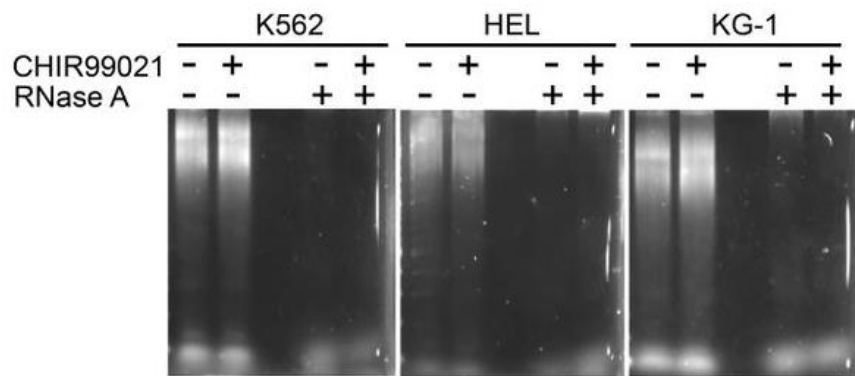


Figure 46: RNaseA treatment of K562, HEL and KG1 fractions.

Representative agarose gel electrophoresis images showing the stability of total RNA in K562, HEL and KG1 cell lysates +/- 5 μ M CHIR99021 treatment overnight with +/- 20 μ g/mL RNaseA prior to Co IP analyses.

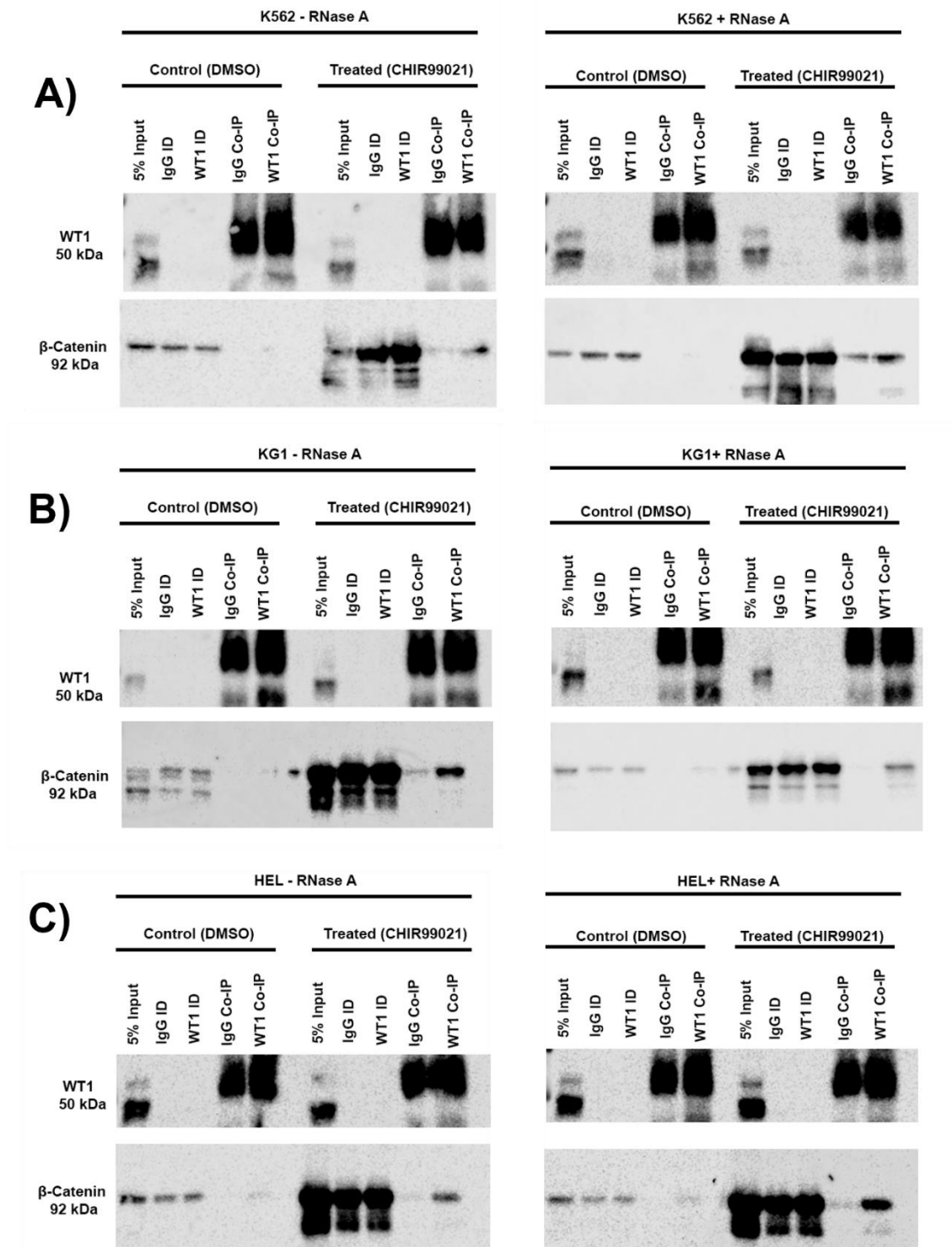


Figure 47: Assessment of β -catenin:WT1 association in absence of RNA.

Immunoblots showing WT1 Co-IPs performed from **A)** K562 **B)** KG-1 and **C)** HEL treated with +/- 5 μ M CHIR99021 treatment overnight and +/- 20 μ g/mL RNaseA prior to Co-IP Total cell inputs (5%), immunodepleted (ID) and Co-IP lanes are shown.

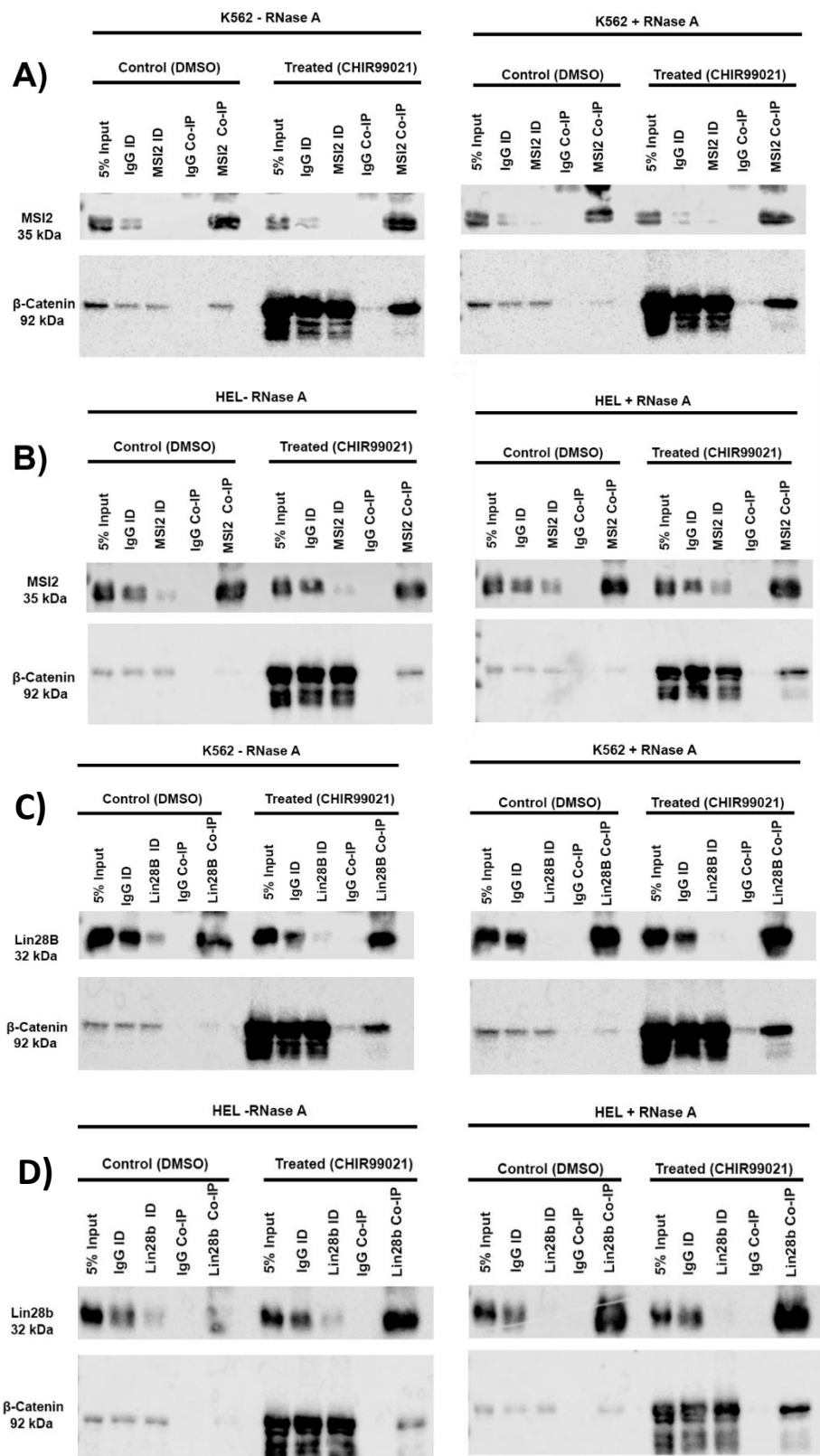


Figure 48: Assessment of β -catenin:MSI2 or β -catenin:LIN28B associations in absence of RNA. Immunoblots showing MSI2 Co-IPs performed in in **A)** K562 and **B)** HEL and Lin28b Co-IP in **C)** K562 and **D)** HEL treated with +/- 5 μ M CHIR99021 and +/- 20 μ g/mL RNaseA. Total cell inputs (5%), immunodepleted (ID) and Co-IP lanes are shown.

5.3.2 β -Catenin and HuR (ELAVL1) are not co-complexed with one another in K562 and HEL cells

Research has already identified HuR (ELAVL1) as a well-established RBP that interacts with β -catenin in colon cancer (Kim et al., 2012). This interaction is further supported by ELAVL1 being a significantly enriched interactor in our mass spectrometry analysis (Figure 6), albeit with a high CRAPome score (322/716) indicating that it could represent a background contaminant. Therefore, we wanted to establish if this association was real in an AML context.

As shown in Figure 49A and 49B the HuR Co-IP was efficient with increased enrichment of HuR in the Co-IP lanes and little HuR present in the IgG lanes. Except for a single β -catenin band detected in the RNaseA treated Co-IP of HEL cells, no other β -catenin was detected in any other HuR Co-IP generated from basal or activated K562/HEL cells. We then completed the reciprocal β -catenin Co-IP under the same conditions in the same cell lines as shown in Figure 49C (which was effective) and failed to detect HuR expression. This data would suggest that any role for β -catenin in RNA biology is not mediated through a HuR interaction.

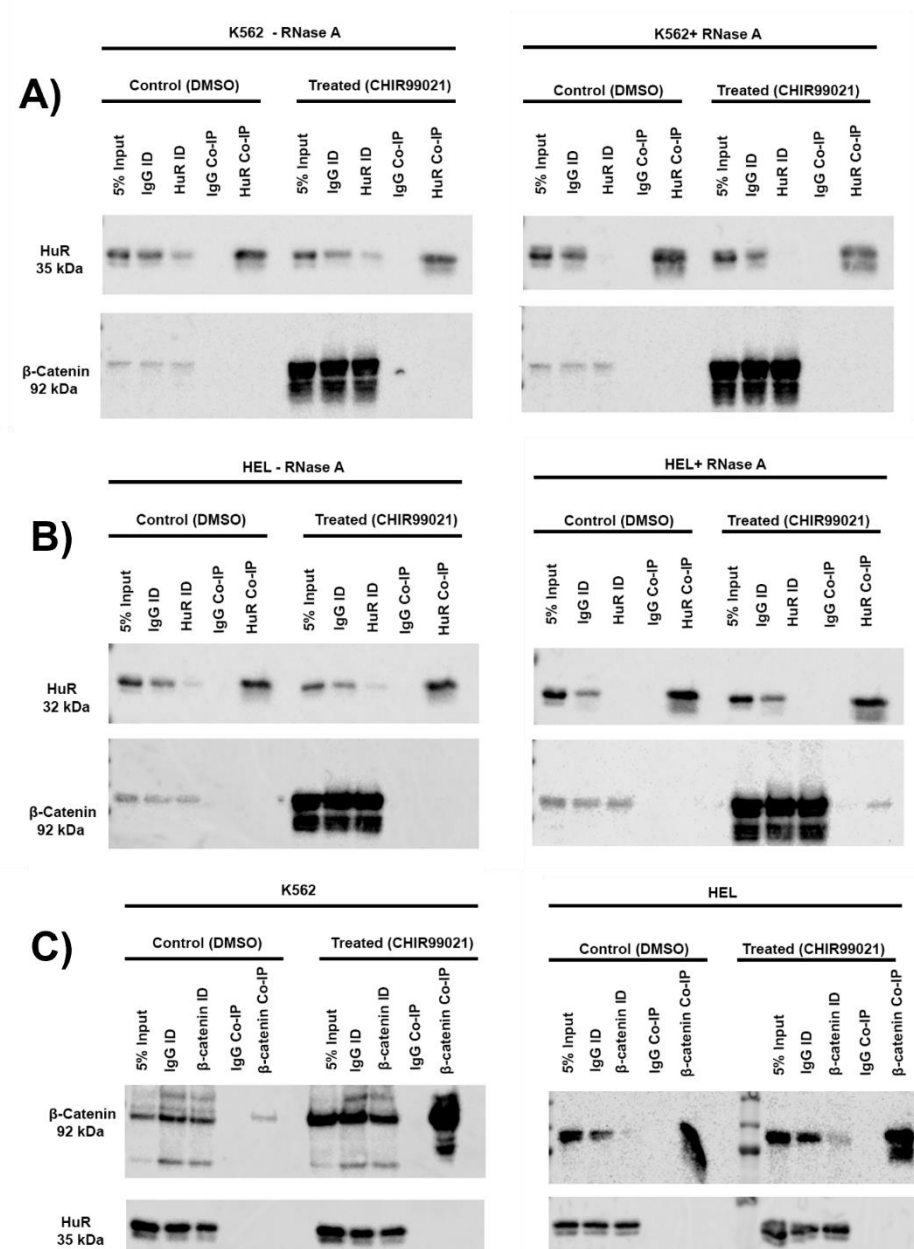


Figure 49: Assessment of HuR and β-catenin association by Co-IP.

Immunoblot showing HuR and β-catenin Co-IPs +/- RNase A treatment to determine if HuR and β-catenin are associated, and RNA bound. **A)** K562 **B)** HEL whole cell lysate treated with +/- 5μM CHIR99021 and +/- 20μg/mL RNaseA. **C)** β-catenin Co-IP to determine association with HuR in K562 and HEL cell lysate +/- 5μM CHIR99021. Total cell inputs (5%), immunodepleted (ID) and Co-IP lanes are shown.

5.3.3 Understanding the role of β -catenin in protein translation

RNA expression is regulated at multiple stages post-transcription, from initial splicing right through to eventual mRNA translation. In addition to reports of β -catenin regulating early stages of RNA biogenesis, previous reports suggest β -catenin could also be recruited to the messenger ribonucleoprotein and translational pre-initiation complex, fulfilling a translational repressor function (Ehyai et al., 2018). Since this has not been examined in a haematopoietic context previously and given that we have shown β -catenin interacts with MSI2, a regulator of mRNA translation, we wanted to explore a role for β -catenin in translational processes. To this end, we used polysome profiling; a method used for examining the translation status of specific RNAs by separating polysomes using sucrose-gradient separation (Chassé et al., 2017).

To assess β -catenin abundance in specific polysome fractions K562 and HEL cells +/- CHIR99021 were lysed and translated mRNA associated with polysomes were separated by sucrose gradients into fractions (Figure 50). The ribonucleoprotein (RNP) represents the untranslated components between F1-2, followed by the 40S, 60S and 80S ribosomal subunits in F3-5. The curve then resolves into low and heavy molecular weight polysomes in F5-9 until it reaches polysome run-off in F9-F12 (Pospíšek & Valásek, 2013). CHIR99021 treatment did not appear to substantially alter the trend of each polysome trace, however for K562 an increase in A260 was seen with 40s and 60s ribosomes and for HEL a greater absorbance with 80s. This matched previous studies which showed an increase in the 80s when β -catenin co-complexed with eukaryotic initiation factor 4E (eIF4E) versus control conditions (Ehyai et al., 2018)

Samples from each polysome trace were immunoblotted as shown in Figure 51. β -Actin was used as a negative control since this should only appear in the first few fractions where protein is most enriched from the input being loaded onto the sucrose gradient, as seen with HEL, apart from F8 (Figure 51B). However, for K562 the presence of β -actin in fractions 9, 10 and 11 for DMSO and fraction F9 for CHIR99021 are challenging to explain and could represent artefact (Figure 51A). The ribosomal marker L7a appeared in most fractions from the polysome profile in Figure 5 for both K562 and HEL cells indicating the 60s ribosomal subunit. Under both DMSO and CHIR treated conditions the initiation factor eIF4a is present in fractions F1-F6 due to its involvement in the pre-initiation complex and binding of mRNA

to the ribosome. β -Catenin was detected in the input and F1 for DMSO fractions and in F1-F4 under Wnt stimulated conditions. In summary, β -catenin is expressed in fractions F1-2 (Figure 51) under DMSO conditions and F1-F4 under Wnt stimulated conditions for both K562 and HEL cells. Both β -catenin and eIF4a are expressed within the early fractions. Taken together, these data imply β -catenin could also be recruited to the pre-initiation complex in a myeloid context; however, its direct role in this complex cannot be inferred from this data alone.

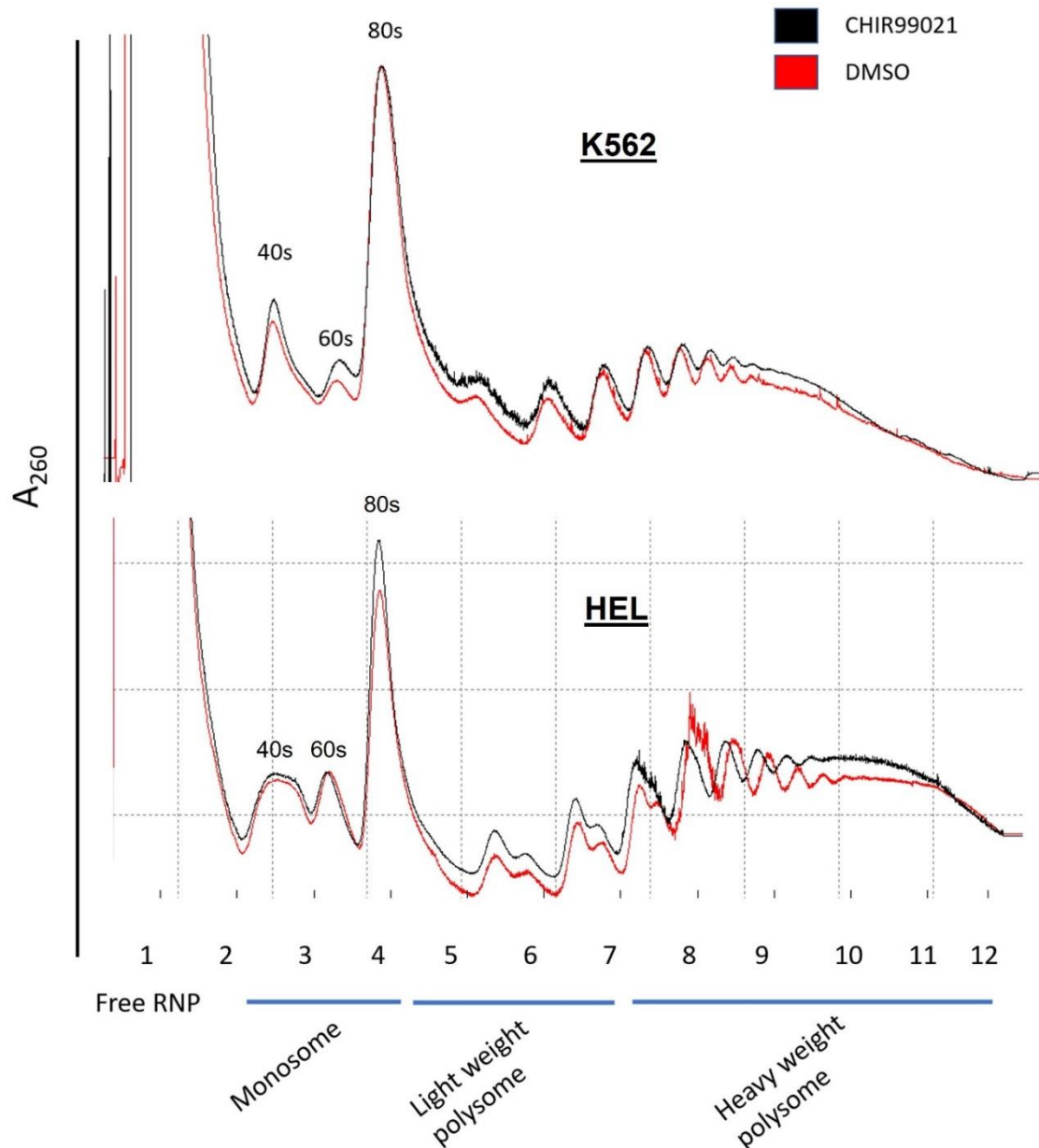


Figure 50: Polysome profile of basal or Wnt signalling stimulated K562 and HEL cells.

Polysome trace identifying the separation of ribosomes in K562 and HEL cells treated overnight +/- CHIR99021 and cytoplasmic lysates were separated by 15-60% sucrose and separated into respective fractions. Free ribonucleoprotein (RNP)(F1), monosome (F2-4), light weight polysome (F5-7) and heavy weight polysome (F8-12)) are highlighted for respective fractions.

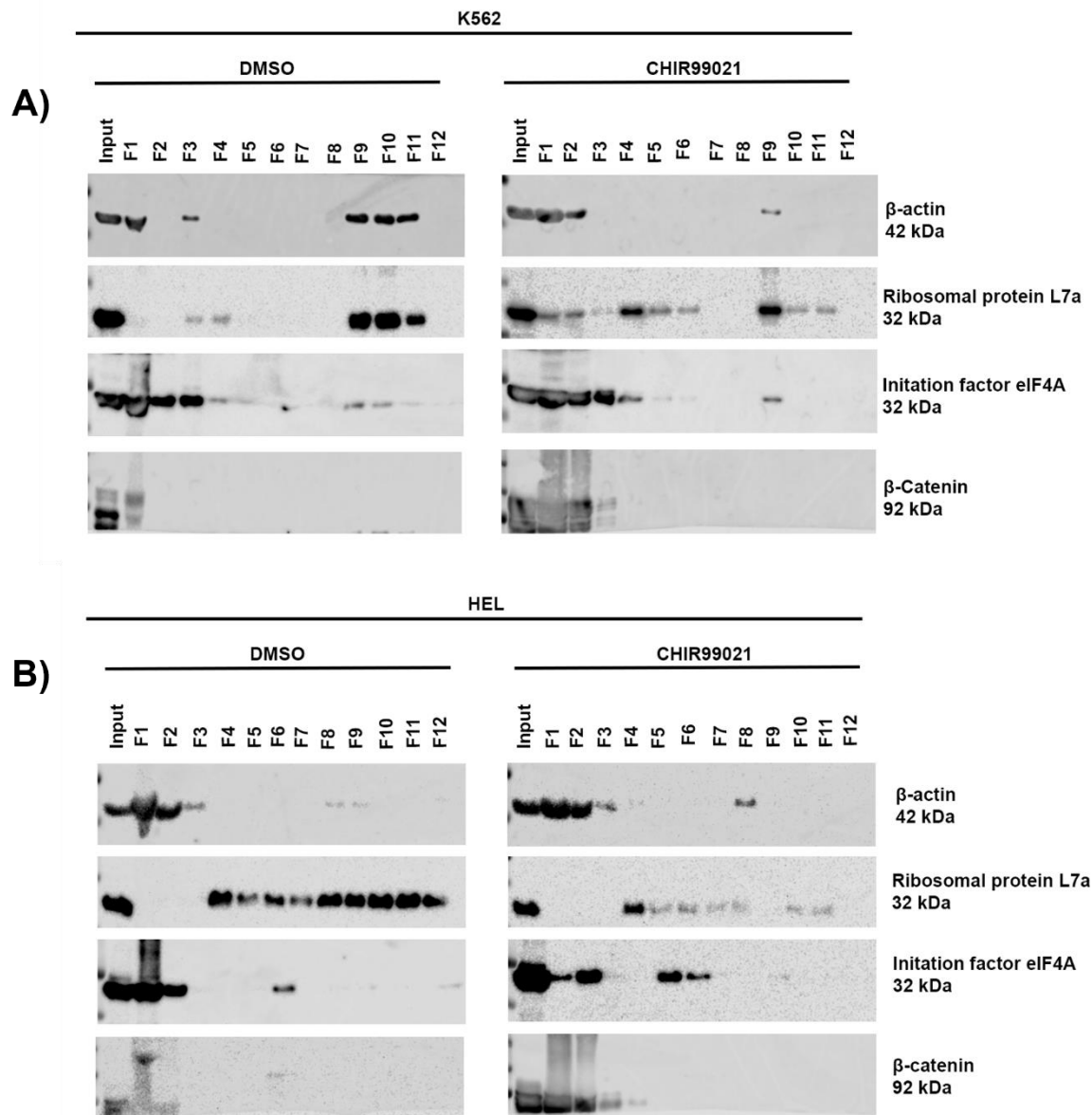


Figure 51: Assessment of β -catenin abundance in polysome fractions.

Immunoblots showing the association of various ribosome subunits with β -catenin in **A)** K562 and **B)** HEL. Input and polysome fractions (F1-F12) were boiled in 4X SDS-buffer and blotted for β -actin, ribosomal protein L7a, initiation factor protein eIF4a and β -catenin expression

5.3.4 Identifying β -catenin associated RNAs through RNA binding protein immunoprecipitation and RNA sequencing (RIP-seq)

Following the identification of β -catenin:RBP association (e.g., LIN28B, MSI2) and potential presence in translation initiation components from the polysome profiles it was necessary to identify the RNAs that could be regulated by β -catenin in myeloid cells (either directly or indirectly). To explore this, we performed β -catenin (or IgG) RNA-binding protein immunoprecipitation (RIPs). We opted to use the MagnaRIP™ kit since it is optimised to preserve protein:RNA interactions. Purification of these RIPs allows interrogation and identification of target RNAs via downstream applications such as RNA-sequencing (RIP-seq) or qRT-PCR (RIP-PCR).

Since the MagnaRIP kit was new to our laboratory, we first optimised RIP in myeloid cells using a well-established RBP; HuR alongside β -catenin RIP. As observed in Figure 5A HuR successfully RIP'd with minimal background binding in the IgG lane similar to β -catenin. To validate RNA association, we detected the expression of a known HuR RNA target *ACTB* (Joseph et al., 2014) by qRT-PCR and detected a marked ~1200-fold enrichment of *ACTB* relative to control IgG (Figure 52B) confirming experimental conditions were optimal for retaining protein:RNA interactions. We then performed β -catenin RIP in KG-1 cells using previously optimised antibody concentrations (Chapter 2 methods 2.6) (Figure 52C) and observed efficient β -catenin enrichment in the RIP lane. Therefore, following successful β -catenin RIP we isolated and purified any present RNA and measured the quantity and quality through Bioanalyzer analysis as shown in Figure 52D. These analyses showed enrichment of RNA bands with sizes ranging 25-4000 nt in lanes 3, and 5-7 representing the DMSO and CHIR99021 treated β -catenin RIP, relative to IgG RIPs (low RNA as expected as deduced from fainter bands). These data suggested that β -catenin could be associated with RNA of varying size and quantity.

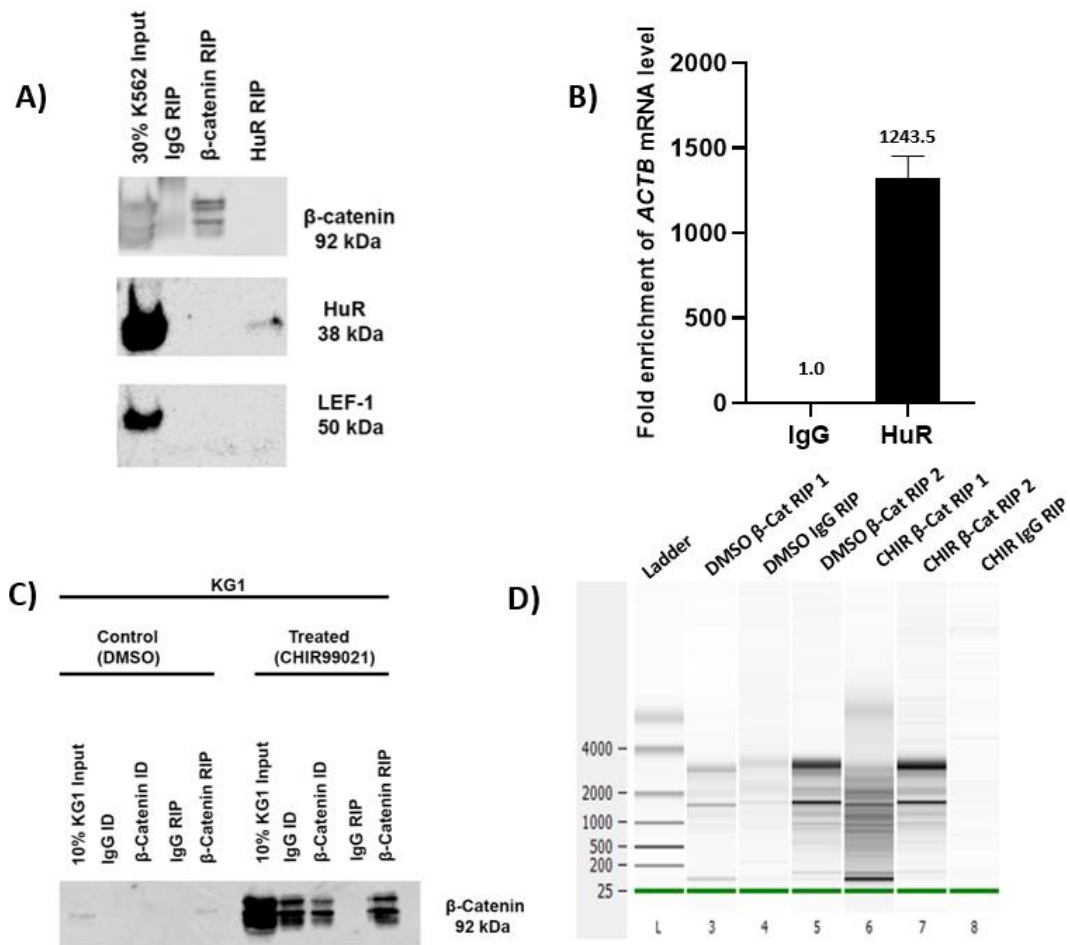


Figure 52: RNA binding protein immunoprecipitation (RIP) optimisation.

A) Immunoblot showing HuR (established RBP) and β-catenin RIP optimised in K562 cells using the MagnaRIP kit. **B)** qRT-PCR analysis of known HuR RNA target *ACTB* mRNA level in IgG or HUR RIPs performed in K562 cells using MagnaRIP kit. **C)** Immunoblot showing β-catenin RIPs from KG1 cells +/- CHIR99021 using the MagnaRIP kit. **D)** Gel analysis of RNA concentration and size isolated from IgG or β-catenin RIPs performed in KG1 cells +/- CHIR99021 using mRNA Pico Series II chip on an Agilent 2100 bioanalyser system.

Once β-catenin RIP was confirmed optimal using the MagnaRIP kit we next wanted to assess whether β-catenin was bound to RNAs of interest. *CCND1* was chosen as this is a Wnt target gene and already a reported target RNA of β-catenin (Lee et al., 2007), *LEF1* and *BIRC5* (*survivin*) are also Wnt target genes (Santiago et al., 2017) (Zhang et al., 2013), *WT1* was

selected given the finding in previous chapters that β -catenin could regulate *WT1* mRNA expression. Relative levels of these mRNA targets in β -catenin RIPs were compared to the IgG RIP (Figure 53). We observed no detectable fold change in *CCND1* (*cyclin D1*) or *LEF1* between β -catenin and IgG RIPs and *BIRC5* was completely undetectable (data not shown). We did however detect a small but non-significant enrichment (~6-fold) of *WT1* mRNA in β -catenin versus IgG RIP indicating that β -catenin could potentially associate with *WT1* mRNA.

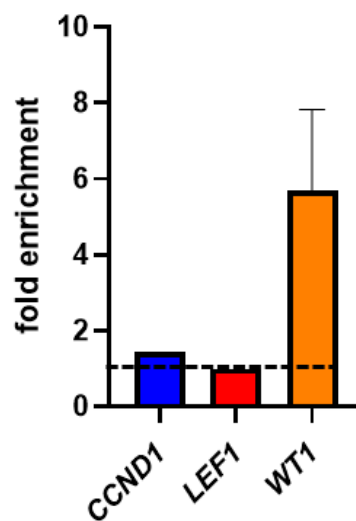


Figure 53: Analysis of selected mRNAs from β -catenin RIP.

qRT-PCR analysis of selected target genes *CCND1*, *LEF1* and *WT1* isolated from IgG or β -catenin RIPs generated from KG-1 cells using MagnaRIP. mRNA fold enrichment in β -catenin is given relative to level from matched IgG RIPs (dashed line) and overall expression was normalized to the housekeeping gene β -actin (*ACTB*).

Since we and others had demonstrated the capacity for β -catenin to bind either RBP or RNA, we finally wanted to perform a more cell-wide analysis of all the RNAs bound with β -catenin in AML cells for the first time. DMSO or CHIR99021 treated β -catenin RIPs were performed as previous and RNA quantity determined. β -Catenin/IgG RIPs were repeated where necessary to generate three replicate samples containing a minimum of 10ng total RNA and sent to Leeds Genomics for library preparation and subsequent RNA-seq analysis. RNA sequencing results were analysed by galaxy software using trimming tool trimmomatic to remove adapter contents. RNA star alignment was used to align the raw data to the reference

human genome. The most down and upregulated genes in CHIR99021 treated versus DMSO treated β -catenin RIPs were summarised in a volcano plot (Figure 54A). The most significantly enriched RNA was PRR9, and most significantly depleted was MTURN. We observed a notable number of mitochondrial encoded tRNAs were identified; MT-TI, MT-TW, MT-TQ and MT-TT suggesting novel function of β -catenin in mitochondrial RNA biology. Using gene ontology (GO) search terms for 'Biological Process' (Figure 54B) we observed significant enrichment of RNAs associated with the myeloid cell differentiation (*CEBPA*, *SBNO2*, *LEF-1* and *VEGFA*) and also Wnt signalling itself including (*LEF-1*, *JUN*, *DVL1*, *TCF7*) (Figures 54B). Using WikiPathway analysis (Figure 54C) we confirmed this association with Wnt signalling and also found significant enrichment of RNAs linked with IL-18 signalling (*IL10*, *JUN* and *VEGFA*) and intrinsic apoptotic signalling in response to DNA damage (*BCL3*, *ABL1* and *BAK1*). Although these results require validation, taken together they suggest an association of β -catenin with RNA linked to critical processes in AML and also the Wnt pathway itself.

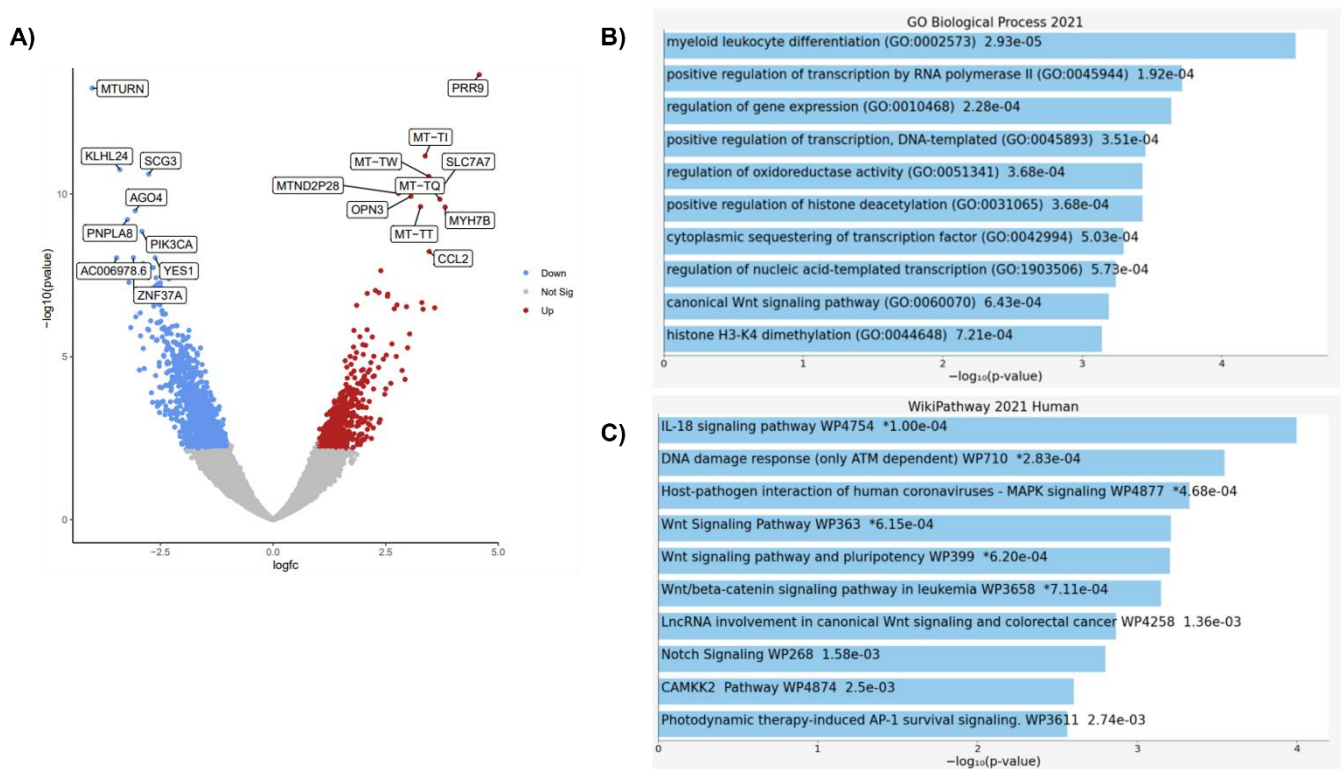


Figure 54: β -catenin associated RNA identified from RIP-seq.

A) Volcano plot showing most significantly down and upregulated genes from β -catenin CHIR99021 versus DMSO RIPs. Count outputs from feraturecounts were used to find the differentially expressed genes by DESeq2 and genes with significant adjusted p-value and $\log_2(FC) > 1$ or < -1 were selected to the creat the volacno plot. **B)** Graph showing most significantly enriched GO search terms associated with 'Biological Processes' in the DMSO β -catenin versus CHIR99021 β -catenin RIPs with p values given in right side of bars. **C)** Graph showing most significantly enriched signalling pathways from WikiPathway analysis in the DMSO β -catenin versus CHIR99021 β -catenin RIPs with p values given in right side of bars.

Overall the possible interactions between β -catenin and the RNA binding protein WT1 and possible target mRNAs are summarised in figure 55. Exploring these could form the basis of novel strategies to therapeutically target β -catenin in AML.

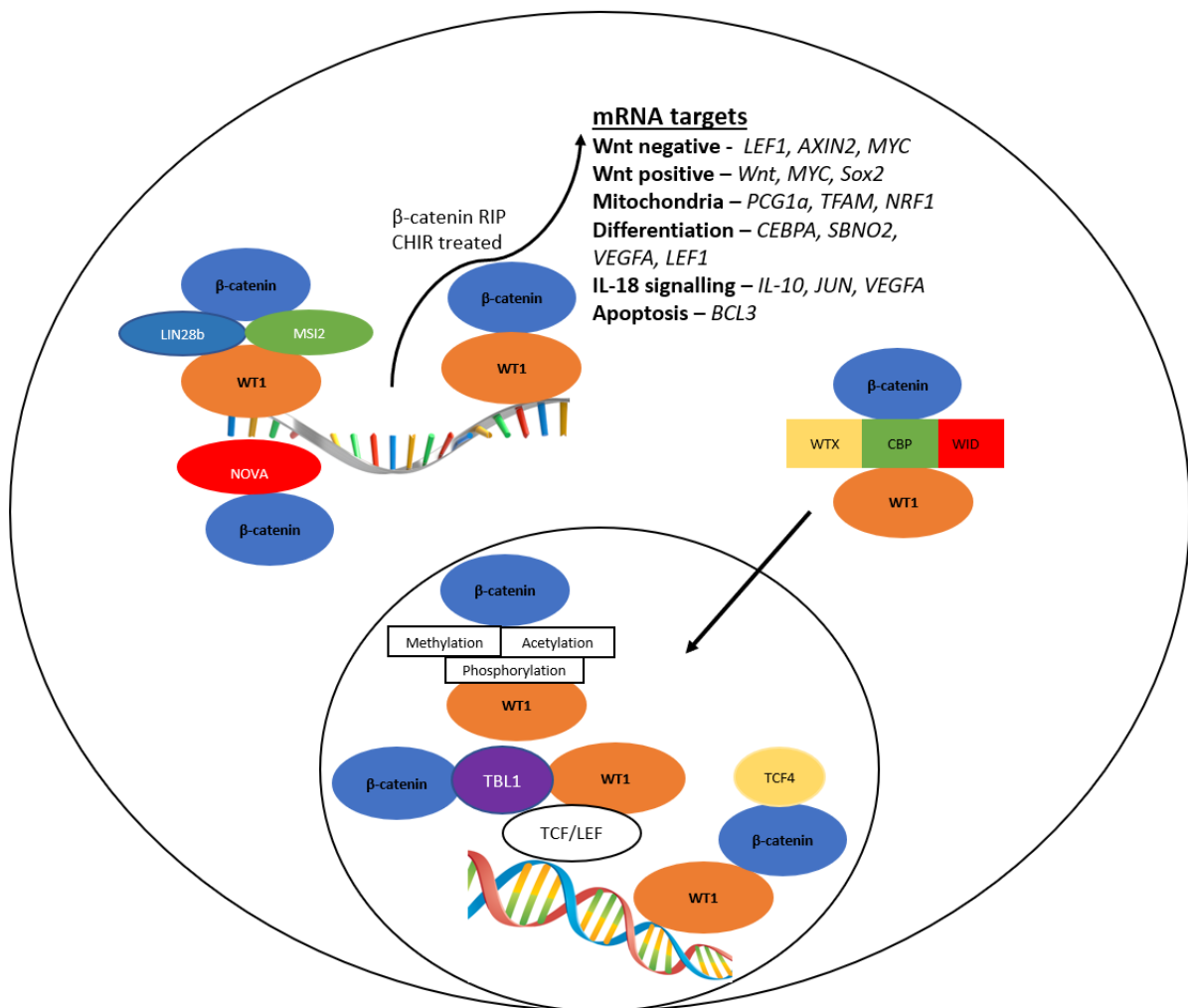


Figure 55: Schematic representation of possible β-catenin and WT1 interactions.

Summary of the hypothetical β-catenin and WT1 interactions with common binding proteins WTX, CBP and WID. Within the nucleus with TBL1 and TCF/LEF complex and interaction with TCF4, finally how the effect of post translational modifications such as methylation, acetylation and phosphorylation could affect binding. The possible interaction with RNA binding proteins and the key mRNA targets that arose from our RNA sequencing analysis following CHIR treatment.

5.4 Discussion

5.4.1 Association between β -catenin and RBPs

This chapter validated an association between β -catenin and three RBPs (LIN28B, MSI2 and WT1) in both K562 and HEL cells, which was not mediated by RNA. RBPs are vital for the splicing, processing, and translation of target mRNAs, thus increasing the diversity of transcriptomes and proteomes. Therefore, identifying any role for β -catenin in RNA biology will be important.

The first RBP associator LIN28B has been identified as a novel downstream target of Wnt/ β -catenin signalling, this pathway represses let-7 microRNA expression but not the primary transcripts, which shows a post-transcriptional regulation of repression. Loss of function of LIN28 impaired Wnt/ β -catenin mediated let-7 inhibition and breast cancer stem cell phenotype. Furthermore, β -catenin can induce Lin28 upregulation and let-7 downregulation in both cancer samples and mouse models (Cai et al., 2013). Therefore, highlighting the therapeutic importance of targeting the Wnt/ β -catenin pathway in association with LSCs (Cai et al., 2013). Furthermore, in an AML context overexpression of LIN28B renders AML cells growth independent of cytokines and enhances tumorigenicity through let-7 dependent mechanisms, suggesting the role of a more aggressive tumour phenotype. LIN28/let-7 inhibition led to LSC differentiation and ultimately leukemic cell death in TF-1a AML cells and therefore targeting both could be an effective therapeutic option for AML patients (J. Zhou, C. Bi, et al., 2017).

A second RBP, MSI2 has shown to promote ESCC (esophageal squamous cell carcinoma) cell proliferation via regulation of Wnt/ β -catenin (Z. Li et al., 2017) and is already established as a poor prognostic factor in AML by regulating translation through binding of HOXA9, MYC and IKZF2 mRNAs (Han et al., 2015) (Byers et al., 2011) and this could relate to our findings of β -catenin in the initiation complex (Lambert et al., 2019; Park et al., 2019; Thoma et al., 2008). Furthermore, depletion of MSI2 resulted in decreased proliferation and induced apoptosis, and high levels of MSI2 mRNA were associated with decreased survival in AML patients leading to its proposal as a prognostic marker (Byers et al., 2011).

β -Catenin has already been reported to regulate alternative splicing and stability of target RNAs in human colorectal cancer cell line LoVo (Kim et al., 2012), however this has not been examined in a haematological context. Most of the RBPs studied in the context of cancer are characterised by the presence of canonical RNA-binding domains (RBDs). However, studies have more recently shown that RBPs can harbour non-canonical RBDs. More specifically protein-protein interaction domains such as ARM arose as the most predominant common RNA binding motif amongst these unorthodox cancer-related RBPs (Moore et al., 2018). This is significant in our research as β -catenin contains no canonical RNA binding domain but does contain the 12 repeated ARM domains. This could overall be tested by isolating each part of the ARM binding domain of β -catenin and evaluate if binding of the established RBP or RNA still occurs.

Furthermore, previous research in colon cancer has already established β -Catenin can regulate the alternative splicing of the estrogenic receptor- β RNA, and also the stability of oncogenic transcripts such as *COX-2* in colon cancer by forming a ribonucleoprotein (RNP) complex with HuR through distinct and non-overlapping binding sites in 3'UTR (Lee et al., 2007). β -Catenin and HuR interacted with *COX-2* mRNA exclusively in the cytoplasm of LoVo cells when compared to normal HSCs and therefore could explain the significant impact of oncogenic β -catenin on cancer cell development (Kim et al., 2012). To explore this in a haematopoietic context we looked at the association between HuR and β -catenin in K562 and HEL cells, however, could not detect pull-down by either Co-IP (Figure 49). Therefore, suggesting any β -catenin association with RNA is not mediated by HuR as seen in a colon cancer context.

A second mechanism by which β -catenin has displayed RNA binding potential is through the Neuro-oncological ventral antigen (NOVA) proteins NOVA1 and NOVA2, which enhance the stability of β -catenin mRNA and in turn regulate epithelial-mesenchymal transition (EMT) in breast cancer cells. The interaction with NOVA is instrumental for β -catenin accumulation, which can enhance protein stability without degradation, therefore showing the significance of this RBP interaction (Moore, 2005). Moreover, Wnt stimulation suppresses NOVA protein expression, but they are not transcriptional targets of Wnt signalling because TCF was dispensable in this effect, suggesting β -catenin may function as an RBP (Tang et al., 2020). Overall, for an AML specific relevance, EMT is associated with metastasis formation, but is a

feature of solid tumours not blood cancers, however it can contribute to tumor invasion and chemoresistance and therefore by targeting β -catenin as an RBP in this instance could aid in inhibiting leukemogenesis (Pradella et al., 2017).

However, identifying how β -catenin binds to these RBPs and RNA is of significant interest as could aid in understanding how its involved in the regulation of several cellular processes including translation and driving proliferation by Wnt signalling. Previous research has shown β -catenin in pituitary cells enabled the stabilisation of Pitx2 mRNA by regulating AU-rich elements in the 3' UTR. This stabilisation was partly mediated by stabilising/destabilising the AU-rich binding proteins since the level of AU-stabilising protein (HuR) in the cytoplasm increased, resulting in the interaction with Pitx2 mRNA upon the pathway activation (Briata et al., 2003). This binding of 3'UTR and AU-rich elements has also been established with COX-2 at mentioned above, as COX-2 mRNA stabilisation in NIH323 and 293T cells was significantly induced in response to β -catenin activation which triggered the cytoplasmic location of HuR (Lee & Jeong, 2006). This relationship is not limited to colon cancer but has also been shown in breast cancer with β -catenin stabilising the mRNA transcripts CA9 and SNAI2 by regulating their AU rich elements in the 3' UTR (D'Uva et al., 2013). This could be applied in an AML context by observing the effect of mRNA transcripts in our myeloid cell lines.

5.4.2 Understanding β -catenin's involvement at a polysome level

We wanted to understand the potential role of β -catenin in translational processes to understand how it could be implicated in gene regulation in an AML context. To characterise where β -catenin could be involved we used polysome profiling and identified an association with β -catenin and the initiation factor complex in both K562 and HEL cells (Figure 50 and 51). β -catenin protein expression broadly correlated with eIF4a; an initiation factor protein which mediates binding of mRNA to the ribosome and unwinds the mRNA secondary structure in the 5'UTR to facilitate ribosome binding (Svitkin et al., 2001). A β -catenin interactome study identified a novel cytoplasmic β -catenin binding partner fragile X mental retardation protein (FMRP) and acknowledged a role for β -catenin at the pre-initiation complex as a translational repressor in vascular smooth muscle cells (VSMCs), this protein has also bound to eIF4E which supports our finding of β -catenin and association with multiple eIFs by mass spectrometry analysis (Morgan et al., 2019).

It was proposed in the absence of Wnt stimulation, β -catenin can function as a membrane protein with cadherins and also simultaneously with the translational machinery to repress translation. Upon Wnt activation, β -catenin is localised and accumulates in the nucleus to activate target gene transcription and in doing so dissociates from the pre-initiation complex to de-repress translation. The subcellular localisation of β -catenin is dictated by protein-protein interactions, and β -catenin has a structural role in the plasma membrane by linking adhesion proteins to the actin cytoskeleton in normal haematopoiesis (Logan & Nusse, 2004). However, blood cells lack these components, so β -catenin could have a more prominent role in the cytoplasm resulting in enhance RNA roles in a myeloid context. These are important factors for considering its direct impact on transcription and translation (Ehyai et al., 2018). Therefore, more knowledge in understanding RNA proteins associated with β -catenin broadens the avenues for this already established suitable target in AML.

5.4.3 Establishing β -catenin associated RNA from RIP-seq

Given the association with multiple RBPS, WT1, LIN28B and MSI2 we wanted to identify RNA targets associated with β -catenin. Following optimisation of the magnaRIP protocol for performing β -catenin RIP we showed via RIP-seq that many of the associated RNAs are linked with Wnt signalling, differentiation, and DNA damage response.

Optimised β -catenin RIPs identified WT1 as a potential mRNA target of β -catenin with a ~6-fold enrichment, suggesting β -catenin could bind WT1 mRNA which is further supported by qPCR analysis of β -catenin knockdown affecting WT1 mRNA (Chapter 4 Figure 45). Therefore β -catenin could regulate WT1 levels, but this has not been confirmed previously until this study. The direct binding of β -catenin to WT1 mRNA is unknown, however previous research has identified that TET2 can bind and modulate WT1 mRNA target gene expression by activating genes in the Wnt target pathway in a dose dependent manner which suppressed leukemia cell proliferation in HL60 cells (Wang et al., 2015). Furthermore, WT1 has also shown to bind to BCL2L2 transcript and facilitate the self-renewal of leukemia initiating cells in the MLL-AF9 mouse model and treatment with WP1130 disrupted this axis and decreased the progression of LSCs (Zhou et al., 2020). Overall showing a possible relevance for exploring WT1 mRNA and the effect of β -catenin knockdown in influencing WT1 in an AML context.

For a more global analysis of β -catenin associated RNAs in the cell we sent β -catenin RIPs for RNA-sequencing to identify what RNA binding proteins β -catenin could be associating with (Figure 52). The most significant finding was several Wnt components involved in leukaemia and pluripotency; *LEF-1*, *AXIN2*, and *MYC*. Research has previously identified a negative feedback loop of Wnt signalling through transcriptional upregulation of *AXIN2* and a close homologue conductance in colorectal cancer, by subsequently inducing degradation of β -catenin through an interaction with *APC* (Lustig et al., 2002). Furthermore, a positive feedback loop involving the Wnt/ β -catenin/*MYC*/Sox2 axis defined a highly tumorigenic cell population in ALK-positive large cell lymphoma. The regulatory role of *MYC* is related to its ability to influence DNA binding and transcriptional activity of Sox2. Also, a high level of Wnt/ β -catenin promotes a relatively high expression of *MYC*, which in turn exerts Sox2 (Wu et al., 2016). This demonstrates a positive feedback loop and emphasises exploring key mediators of the Wnt/ β -catenin pathway such as *FRZ5* and *LEF-1* is key in targeting β -catenin in this subset of patients. Identifying post-transcriptional feedback loops in an AML context using the Wnt/ β -catenin pathway is of significance as would aid in inhibiting LSC growth and development. However, we cannot confirm this yet as we don't know whether β -catenin is having positive or negative influences on these transcripts and also based on this evidence it will most likely be cell context dependent due to the specific Wnt target genes involved.

We also observed a considerable number of mitochondrial encoded tRNAs, and previous research has characterised a role for β -catenin regulating mitochondrial biogenesis as loss of mitochondrial mass is consistent with repressed expression of transcriptional genes *PCG1 α* , *TFAM*, and *NRF1* observed in shRNA β -catenin knockdown cells of breast cancer cells (Vergara et al., 2017). This needs further validation in an AML context but could be involved in mitochondrial biogenesis in a similar manner.

Significant enrichment of RNAs were associated with myeloid differentiation. The transition of self-renewing, pluripotent stem cells to myeloid differentiation is achieved by down regulation of Wnt signalling (Reya et al., 2003), however when re-introduced β -catenin has shown to give a growth advantage and differentiation potential (Baba et al., 2005). Furthermore data from the Qian group showed that activated β -catenin can inhibit monocyte/macrophage differentiation by disrupting PU.1-mediated transcription (Sheng et al., 2016), a key transcription factor controlling granulocyte/monocyte commitment also

known to be regulated by γ -catenin (Morgan et al., 2013). A further role for β -catenin in myelopoiesis has recently been reported in normal and emergency granulopoiesis. Disruption of the β -catenin:TCF4 interaction (through expression of a dominant negative TCF4 mutant), resulted in impaired granulocytic differentiation driven by repressed G-CSFR expression and disrupted G-CSF signalling (Danek et al., 2020). In our research under CHIR treated conditions we identified β -catenin could bind and regulate RNA transcripts that govern myeloid differentiation including; *CEBPA*, *SBNO2*, *VEGFA* and *LEF-1*. *CEBPA* is required for the coordination of enhancer activity during granulocytic-monocytic lineage differentiation (Pundhir et al., 2018), *SBNO2* regulates osteoclast differentiation (Maruyama et al., 2013), *VEGFA* features a autocrine and paracrine role in osteoblastic and endothelial differentiation (Mayer et al., 2005) and finally *LEF-1* orchestrates helper T cell differentiation in conjunction with *TCF-1* (Choi et al., 2015). The contribution of β -catenin to post-transcriptional regulation of these is not yet known but could be explored by inhibiting β -catenin and measuring the effect on mRNA levels (Friedman, 2007).

An association with IL-18 signalling was also identified, IL18 is secreted primarily by monocytes/macrophages and IL18 signalling is regularly involved in IFN γ production for innate immunity and has shown to directly activate T-bet expression in AML. Therefore IL-18 could be used to improve anticancer immunity in AML patients by induction of T-bet (Bachmann et al., 2007). Furthermore, IL18 has previously shown to stimulate GSK3 β degradation and therefore β -catenin nuclear localisation and stabilisation in smooth muscle cell proliferation (Reddy et al., 2011). Also, IL-18 in bone marrow stromal cells has shown to represent a pro-leukomegenic influence by acting as a tumor cell proliferative factor, however, does seem to depend greatly on the cell type (Uzan et al., 2014). From our RIP-seq analysis the transcripts for IL-18 signalling upregulated were *IL-10*, *JUN* and *VEGFA* this was interesting as *IL-10* has shown to play a dual role but more dominantly as a tumor suppressor as it reduces the expression of pro-inflammatory cytokines supporting AML cell proliferation (Pievani et al., 2020). The functional role of *JUN* is undefined, however knockdown has shown to decrease AML cell survival and propagation (C. Zhou et al., 2017) and *VEGFA* levels at a time of diagnosis are associated with poor survival due to acting as a stimulator of angiogenesis (Weidenaar et al., 2011). In summary exploring the consequence of β -catenin

regulating IL-18 and these subsequent transcripts could pose significant due to the roles they have displayed in driving leukaemia.

β -Catenin was associated with intrinsic apoptotic signalling in response to DNA damage. Research has identified *BCL3* (one of the identified RNA transcripts in our RIP-seq) to promote Wnt signalling by WNT3A increasing the level and nuclear translocation of *BCL3* which binds directly to β -catenin and enhances the acetylation at lysine 49 and transcriptional activity in colorectal cancer. *BCL3* is overexpressed in colorectal cancer and drives tumorigenesis and silencing *BCL3* suppresses the self-renewal capacity of LSCs and sensitizes cells to chemotherapeutic agents by decreasing the Wnt/ β -catenin pathway. Overall showing the significance of β -catenin in regulating *BCL3* mRNA (Chen et al., 2020) as it could influence apoptosis (a well-defined Wnt phenotype) in LSC development and therefore is a significant avenue to explore.

In summary, data from this chapter has identified β -catenin associated RNA targets which are involved in a number of key processes in an AML context. Should such targets pass through validation and functional assessment, they could inform novel strategies for therapeutic targeting of β -catenin in AML. This raises the intriguing possibility that in addition to β -catenin's well defined transcriptional role in AML it may also directly regulate post-transcriptional RNA processes including transport, translation, and stability. To assess this after confirmed validation of putative β -catenin RNA targets we could evaluate the role of β -catenin in RNA stability using 3'UTR reporters to understand how β -catenin positively or negatively influences binding of AU rich elements to the 3'UTR.

Furthermore, to explore the influence of β -catenin on target mRNA stability we could treat AML cell lines harbouring β -catenin knockdown with inhibitors of *de novo* transcription such as actinomycin D or triptolide, then perform a time-course assessment of target RNA stability by measuring transcript level by qRT-PCR.

Chapter 6. Final Discussion

6.1 Summary

There is considerable evidence to support targeting β -catenin as a treatment for AML given its central role in the canonical Wnt signalling pathway and its widely documented effect on leukemogenesis (Simon et al., 2005). β -Catenin's localisation, stability and transcriptional activity is heavily dictated by protein-protein interactions and therefore targeting components of this network may inform novel drug design.

The relationship between β -catenin and WT1 has not previously been documented in a haematopoietic context and was therefore the main basis of this thesis, to overall understand the biological and clinical relevance in AML. Our results summarised a functional relationship between the two proteins in one particular cell line KG1, this was one limitation in our study as discussed. However, this result is still significant since the vast heterogeneity of AML could mean the β -catenin:WT1 axis is particularly relevant to the pathogenesis of a specific AML subtype (e.g. erythroleukemia) and thus represent a targeted treatment. Targeting WT1 could be challenging given the range of isoform expression and variable functions and disrupting the β -catenin:WT1 interaction could be even more difficult given our failure to identify direct interaction (thus paving the way for SMI development). Instead, attempts to target just WT1 so far have focussed on harnessing the immune system. Studies have already highlighted one treatment to boost immunity towards tumour associated antigens by the means of peptide vaccine, this would allow the induction of humoral and cellular adaptive immune responses to specific antigens (Di Stasi et al., 2015). Treatment with WT1 peptides 126 and 235 which can induce WT1 specific cytotoxic T lymphocytes (CTLs) and reduce leukemic cell growth and in mice led to tumor rejection, showing WT1 is a potential target for cancer immunotherapy. Overall, this method of treatment is still to be optimised for dosage and should be tested with MDS patients to understand the maximal effect (Oka et al., 2017).

6.2 Future work

We have established WT1, a gene frequently overexpressed and mutated in AML, can regulate nuclear β -catenin level and Wnt transcriptional output in AML cells. To understand the binding nature of β -catenin and WT1 we could knock down expression of one of the common binding partners, WTX, CREB or TCF4 and repeat the WT1 and β -catenin Co-IPs and see if the reciprocal protein is still pulled down. To identify the specific regions of β -catenin through which the WT1 interaction (with CBP) is mediated we could create a series of deletional mutants through targeted deletion of the carboxy- or amino-termini, and/or several armadillo domains repeats, or indeed the zinc-finger domains for WT1. Pull down of WT1 mutants in this study was not possible because the WT1 antibody binds to the region missing and therefore would not bind to the beads successfully. Also, we could look at the effect of WT1 isoforms on specific binding and try to identify the expression pattern of these in AML patients, to overall link any common similarities identified within specific AML subtypes.

The second area of future work from this thesis would concentrate on understanding β -catenin's role in RNA biology. Firstly, we would look to explore the functional relationship between LIN28B and MSI2 with β -catenin by knocking down expression of both proteins to determine the effect on β -catenin expression and signalling. Furthermore, we could use qPCR to understand the effect of β -catenin knockdown on LIN28B and MSI2 target genes. To further understand β -catenin's role in RNA biology we would use qPCR to validate the targets pulled down from the RIP-seq. We would also look to investigate if β -catenin has post-transcriptional stabilising or destabilising influences on these RNAs, then look to distinguish between post-transcriptional and transcriptional roles.

Most efforts to target β -Catenin in AML have been related to its transcriptional activity, however this thesis suggest it could regulate gene expression (independent of Wnt activity) through post-transcriptional mechanisms. So, future therapeutic strategies should aim to shut down both its transcriptional and post-transcriptional roles, which will necessitate the full elucidation of its RNA binding network and mechanism in order to develop effective SMIs.

Overall given that overexpression of β -catenin protein is primarily driven through post-transcriptional influences in AML cells, approaches to target degradation of this protein could have success in leukaemia such as TBL1 as mentioned before and also PROteolysis-TArgeting Chimaeras (PROTAC). Studies have shown a β -catenin targeted PROTAC exploiting the axin domain was effective at degrading both endogenous and WNT3a induced β -catenin as well as reducing Wnt signalling output in HEK293T and various colorectal cancer cell lines (Sun et al., 2019). Provided PROTACs can permeate the membranes of myeloid cells with similar efficiency, the employment of PROTACs seems an entirely sensible strategy to reducing the excessive β -catenin protein levels observed in AML cells. Furthermore, the Lee group identified methyl 3-[[4-methylphenyl)sulfonyl]amino} benzoate (MSAB) as a potent inhibitor of TCF reporter activity in HCT116 cells (Hwang et al., 2016). Further interrogation of the mechanism revealed that MSAB could bind β -catenin in its armadillo region and target the molecule for direct proteasomal degradation thus limiting its nuclear presence and activity. This compound suppressed the growth of several Wnt-dependent cell lines that were almost exclusively of epithelial origin, but no haematological cells were tested. Targeted β -catenin:RNA interactions, possibly through disrupting its interaction with the 3'UTR regions of RNA, could represent a novel context-dependent strategy for suppressing its oncogenic activity in AML.

Bibliography

- Abbas, S., Erpelinck-Verschueren, C. A., Goudswaard, C. S., Löwenberg, B., & Valk, P. J. (2010). Mutant Wilms' tumor 1 (WT1) mRNA with premature termination codons in acute myeloid leukemia (AML) is sensitive to nonsense-mediated RNA decay (NMD). *Leukemia*, 24(3), 660-663. <https://doi.org/10.1038/leu.2009.265>
- Aberger, F., Hutterer, E., Sternberg, C., Del Burgo, P. J., & Hartmann, T. N. (2017). Acute myeloid leukemia - strategies and challenges for targeting oncogenic Hedgehog/GLI signaling. *Cell Commun Signal*, 15(1), 8. <https://doi.org/10.1186/s12964-017-0163-4>
- Alanazi, B., Munje, C. R., Rastogi, N., Williamson, A. J. K., Taylor, S., Hole, P. S., Hodges, M., Doyle, M., Baker, S., Gilkes, A. F., Knapper, S., Pierce, A., Whetton, A. D., Darley, R. L., & Tonks, A. (2020). Integrated nuclear proteomics and transcriptomics identifies S100A4 as a therapeutic target in acute myeloid leukemia. *Leukemia*, 34(2), 427-440. <https://doi.org/10.1038/s41375-019-0596-4>
- Alberta, J. A., Springett, G. M., Rayburn, H., Natoli, T. A., Loring, J., Kreidberg, J. A., & Housman, D. (2003). Role of the WT1 tumor suppressor in murine hematopoiesis. *Blood*, 101(7), 2570-2574. <https://doi.org/10.1182/blood-2002-06-1656>
- Alfaro, M. P., Pagni, M., Vincent, A., Atkinson, J., Hill, M. F., Cates, J., Davidson, J. M., Rottman, J., Lee, E., & Young, P. P. (2008). The Wnt modulator sFRP2 enhances mesenchymal stem cell engraftment, granulation tissue formation and myocardial repair. *Proc Natl Acad Sci U S A*, 105(47), 18366-18371. <https://doi.org/10.1073/pnas.0803437105>
- Alimena, G., Breccia, M., Musto, P., Cilloni, D., D'Auria, F., Latagliata, R., Sanpaolo, G., Gottardi, E., Saglio, G., & Mandelli, F. (2011). Erythroid response and decrease of WT1 expression after proteasome inhibition by bortezomib in myelodysplastic syndromes. *Leuk Res*, 35(4), 504-507. <https://doi.org/10.1016/j.leukres.2010.08.021>
- Ariyaratana, S., & Loeb, D. M. (2007). The role of the Wilms tumour gene (WT1) in normal and malignant haematopoiesis. *Expert Rev Mol Med*, 9(14), 1-17. <https://doi.org/10.1017/s1462399407000336>
- Baba, Y., Garrett, K. P., & Kincade, P. W. (2005). Constitutively active beta-catenin confers multilineage differentiation potential on lymphoid and myeloid progenitors. *Immunity*, 23(6), 599-609. <https://doi.org/10.1016/j.immuni.2005.10.009>
- Bachmann, M., Dragoi, C., Poleganov, M. A., Pfeilschifter, J., & Mühl, H. (2007). Interleukin-18 directly activates T-bet expression and function via p38 mitogen-activated protein kinase and nuclear factor-kappaB in acute myeloid leukemia-derived predendritic KG-1 cells. *Mol Cancer Ther*, 6(2), 723-731. <https://doi.org/10.1158/1535-7163.Mct-06-0505>
- Baillo, A., Giroux, C., & Ethier, S. P. (2011). Knock-down of amphiregulin inhibits cellular invasion in inflammatory breast cancer. *J Cell Physiol*, 226(10), 2691-2701. <https://doi.org/10.1002/jcp.22620>
- Barragán, E., Cervera, J., Bolufer, P., Ballester, S., Martín, G., Fernández, P., Collado, R., Sayas, M. J., & Sanz, M. A. (2004). Prognostic implications of Wilms' tumor gene (WT1) expression in patients with de novo acute myeloid leukemia. *Haematologica*, 89(8), 926-933.
- Bharathavikru, R., Dudnakova, T., Aitken, S., Slight, J., Artibani, M., Hohenstein, P., Tollervey, D., & Hastie, N. (2017). Transcription factor Wilms' tumor 1 regulates developmental RNAs through 3' UTR interaction. *Genes Dev*, 31(4), 347-352. <https://doi.org/10.1101/gad.291500.116>
- Bian, J., Dannappel, M., Wan, C., & Firestein, R. (2020). Transcriptional Regulation of Wnt/ β -Catenin Pathway in Colorectal Cancer. *Cells*, 9(9). <https://doi.org/10.3390/cells9092125>
- Biechele, T. L., & Moon, R. T. (2008). Assaying beta-catenin/TCF transcription with beta-catenin/TCF transcription-based reporter constructs. *Methods Mol Biol*, 468, 99-110. https://doi.org/10.1007/978-1-59745-249-6_8

- Blank, U., & Karlsson, S. (2015). TGF- β signaling in the control of hematopoietic stem cells. *Blood*, 125(23), 3542-3550. <https://doi.org/10.1182/blood-2014-12-618090>
- Bor, Y. C., Swartz, J., Morrison, A., Rekosh, D., Ladomery, M., & Hammarskjöld, M. L. (2006). The Wilms' tumor 1 (WT1) gene (+KTS isoform) functions with a CTE to enhance translation from an unspliced RNA with a retained intron. *Genes Dev*, 20(12), 1597-1608. <https://doi.org/10.1101/gad.1402306>
- Briata, P., Ilengo, C., Corte, G., Moroni, C., Rosenfeld, M. G., Chen, C. Y., & Gherzi, R. (2003). The Wnt/beta-catenin-->Pitx2 pathway controls the turnover of Pitx2 and other unstable mRNAs. *Mol Cell*, 12(5), 1201-1211. [https://doi.org/10.1016/s1097-2765\(03\)00407-6](https://doi.org/10.1016/s1097-2765(03)00407-6)
- Burwell, E. A., McCarty, G. P., Simpson, L. A., Thompson, K. A., & Loeb, D. M. (2007). Isoforms of Wilms' tumor suppressor gene (WT1) have distinct effects on mammary epithelial cells. *Oncogene*, 26(23), 3423-3430. <https://doi.org/10.1038/sj.onc.1210127>
- Byers, R. J., Currie, T., Tholouli, E., Rodig, S. J., & Kutok, J. L. (2011). MSI2 protein expression predicts unfavorable outcome in acute myeloid leukemia. *Blood*, 118(10), 2857-2867. <https://doi.org/10.1182/blood-2011-04-346767>
- Cai, W. Y., Wei, T. Z., Luo, Q. C., Wu, Q. W., Liu, Q. F., Yang, M., Ye, G. D., Wu, J. F., Chen, Y. Y., Sun, G. B., Liu, Y. J., Zhao, W. X., Zhang, Z. M., & Li, B. A. (2013). The Wnt- β -catenin pathway represses let-7 microRNA expression through transactivation of Lin28 to augment breast cancer stem cell expansion. *J Cell Sci*, 126(Pt 13), 2877-2889. <https://doi.org/10.1242/jcs.123810>
- Cardoso, L. C., De Souza, K. R., De, O. R. A. H., Andrade, R. C., Britto, A. C., Jr., De Lima, M. A., Dos Santos, A. C., De Faria, P. S., Ferman, S., Seuánez, H. N., & Vargas, F. R. (2013). WT1, WTX and CTNNB1 mutation analysis in 43 patients with sporadic Wilms' tumor. *Oncol Rep*, 29(1), 315-320. <https://doi.org/10.3892/or.2012.2096>
- Chai, R., Xia, A., Wang, T., Jan, T. A., Hayashi, T., Bermingham-McDonogh, O., & Cheng, A. G. (2011). Dynamic expression of Lgr5, a Wnt target gene, in the developing and mature mouse cochlea. *J Assoc Res Otolaryngol*, 12(4), 455-469. <https://doi.org/10.1007/s10162-011-0267-2>
- Chang, G., Zhang, H., Wang, J., Zhang, Y., Xu, H., Wang, C., Zhang, H., Ma, L., Li, Q., & Pang, T. (2013). CD44 targets Wnt/ β -catenin pathway to mediate the proliferation of K562 cells. *Cancer Cell Int*, 13(1), 117. <https://doi.org/10.1186/1475-2867-13-117>
- Chang, H., Gao, F., Guillou, F., Taketo, M. M., Huff, V., & Behringer, R. R. (2008). Wt1 negatively regulates beta-catenin signaling during testis development. *Development*, 135(10), 1875-1885. <https://doi.org/10.1242/dev.018572>
- Chassé, H., Boulben, S., Costache, V., Cormier, P., & Morales, J. (2017). Analysis of translation using polysome profiling. *Nucleic Acids Res*, 45(3), e15. <https://doi.org/10.1093/nar/gkw907>
- Che, M., Kweon, S. M., Teo, J. L., Yuan, Y. C., Melstrom, L. G., Waldron, R. T., Lugea, A., Urrutia, R. A., Pandol, S. J., & Lai, K. K. Y. (2020). Targeting the CBP/ β -Catenin Interaction to Suppress Activation of Cancer-Promoting Pancreatic Stellate Cells. *Cancers (Basel)*, 12(6). <https://doi.org/10.3390/cancers12061476>
- Chen, C., Zhu, D., Zhang, H., Han, C., Xue, G., Zhu, T., Luo, J., & Kong, L. (2018). YAP-dependent ubiquitination and degradation of β -catenin mediates inhibition of Wnt signalling induced by Physalin F in colorectal cancer. *Cell Death Dis*, 9(6), 591. <https://doi.org/10.1038/s41419-018-0645-3>
- Chen, X., Wang, C., Jiang, Y., Wang, Q., Tao, Y., Zhang, H., Zhao, Y., Hu, Y., Li, C., Ye, D., Liu, D., Jiang, W., Chin, E. Y., Chen, S., Liu, Y., Wang, M., Liu, S., & Zhang, X. (2020). Bcl-3 promotes Wnt signaling by maintaining the acetylation of β -catenin at lysine 49 in colorectal cancer. *Signal Transduct Target Ther*, 5(1), 52. <https://doi.org/10.1038/s41392-020-0138-6>
- Choi, Y. S., Gullicksrud, J. A., Xing, S., Zeng, Z., Shan, Q., Li, F., Love, P. E., Peng, W., Xue, H. H., & Crotty, S. (2015). LEF-1 and TCF-1 orchestrate T(FH) differentiation by regulating

- differentiation circuits upstream of the transcriptional repressor Bcl6. *Nat Immunol*, 16(9), 980-990. <https://doi.org/10.1038/ni.3226>
- Cilloni, D., Gottardi, E., & Saglio, G. (2006). WT1 overexpression in acute myeloid leukemia and myelodysplastic syndromes. *Methods Mol Med*, 125, 199-211. <https://doi.org/10.1385/1-59745-017-0:199>
- Cobas, M., Wilson, A., Ernst, B., Mancini, S. J., MacDonald, H. R., Kemler, R., & Radtke, F. (2004). Beta-catenin is dispensable for hematopoiesis and lymphopoiesis. *J Exp Med*, 199(2), 221-229. <https://doi.org/10.1084/jem.20031615>
- Corbin, M., de Reyniès, A., Rickman, D. S., Berrebi, D., Boccon-Gibod, L., Cohen-Gogo, S., Fabre, M., Jaubert, F., Faussillon, M., Yilmaz, F., Sarnacki, S., Landman-Parker, J., Patte, C., Schleiermacher, G., Antignac, C., & Jeanpierre, C. (2009). WNT/beta-catenin pathway activation in Wilms tumors: a unifying mechanism with multiple entries? *Genes Chromosomes Cancer*, 48(9), 816-827. <https://doi.org/10.1002/gcc.20686>
- Corrêa, S., Binato, R., Du Rocher, B., Castelo-Branco, M. T., Pizzatti, L., & Abdelhay, E. (2012). Wnt/ β -catenin pathway regulates ABCB1 transcription in chronic myeloid leukemia. *BMC Cancer*, 12, 303. <https://doi.org/10.1186/1471-2407-12-303>
- Crane, G. M., Jeffery, E., & Morrison, S. J. (2017). Adult haematopoietic stem cell niches. *Nat Rev Immunol*, 17(9), 573-590. <https://doi.org/10.1038/nri.2017.53>
- Cunningham, T. J., Palumbo, I., Grosso, M., Slater, N., & Miles, C. G. (2013). WT1 regulates murine hematopoiesis via maintenance of VEGF isoform ratio. *Blood*, 122(2), 188-192. <https://doi.org/10.1182/blood-2012-11-466086>
- D'Uva, G., Bertoni, S., Lauriola, M., De Carolis, S., Pacilli, A., D'Anello, L., Santini, D., Taffurelli, M., Ceccarelli, C., Yarden, Y., Montanaro, L., Bonafé, M., & Storci, G. (2013). Beta-catenin/HuR post-transcriptional machinery governs cancer stem cell features in response to hypoxia. *PLoS One*, 8(11), e80742. <https://doi.org/10.1371/journal.pone.0080742>
- Dandekar, S., Romanos-Sirakis, E., Pais, F., Bhatla, T., Jones, C., Bourgeois, W., Hunger, S. P., Raetz, E. A., Hermiston, M. L., Dasgupta, R., Morrison, D. J., & Carroll, W. L. (2014). Wnt inhibition leads to improved chemosensitivity in paediatric acute lymphoblastic leukaemia. *Br J Haematol*, 167(1), 87-99. <https://doi.org/10.1111/bjh.13011>
- Danek, P., Kardosova, M., Janeckova, L., Karkoulia, E., Vanickova, K., Fabisik, M., Lozano-Asencio, C., Benoukraf, T., Tirado-Magallanes, R., Zhou, Q., Burocchiova, M., Rahmatova, S., Pytlik, R., Brdicka, T., Tenen, D. G., Korinek, V., & Alberich-Jorda, M. (2020). beta-Catenin-TCF/LEF signaling promotes steady-state and emergency granulopoiesis via G-CSF receptor upregulation. *Blood*, 136(22), 2574-2587. <https://doi.org/10.1182/blood.2019004664>
- Dar, M. S., Singh, P., Singh, G., Jamwal, G., Hussain, S. S., Rana, A., Akhter, Y., Monga, S. P., & Dar, M. J. (2016). Terminal regions of β -catenin are critical for regulating its adhesion and transcription functions. *Biochim Biophys Acta*, 1863(9), 2345-2357. <https://doi.org/10.1016/j.bbamcr.2016.06.010>
- De Kouchkovsky, I., & Abdul-Hay, M. (2016). 'Acute myeloid leukemia: a comprehensive review and 2016 update'. *Blood Cancer J*, 6(7), e441. <https://doi.org/10.1038/bcj.2016.50>
- de Lau, W., Peng, W. C., Gros, P., & Clevers, H. (2014). The R-spondin/Lgr5/Rnf43 module: regulator of Wnt signal strength. *Genes Dev*, 28(4), 305-316. <https://doi.org/10.1101/gad.235473.113>
- Di Stasi, A., Jimenez, A. M., Minagawa, K., Al-Obaidi, M., & Rezvani, K. (2015). Review of the Results of WT1 Peptide Vaccination Strategies for Myelodysplastic Syndromes and Acute Myeloid Leukemia from Nine Different Studies. *Front Immunol*, 6, 36. <https://doi.org/10.3389/fimmu.2015.00036>
- Dietrich, P. A., Yang, C., Leung, H. H., Lynch, J. R., Gonzales, E., Liu, B., Haber, M., Norris, M. D., Wang, J., & Wang, J. Y. (2014). GPR84 sustains aberrant β -catenin signaling in leukemic stem cells for maintenance of MLL leukemogenesis. *Blood*, 124(22), 3284-3294. <https://doi.org/10.1182/blood-2013-10-532523>

- DiNardo, C. D., & Cortes, J. E. (2016). Mutations in AML: prognostic and therapeutic implications. *Hematology Am Soc Hematol Educ Program*, 2016(1), 348-355.
<https://doi.org/10.1182/asheducation-2016.1.348>
- Döhner, H., Wei, A. H., & Löwenberg, B. (2021). Towards precision medicine for AML. *Nat Rev Clin Oncol*, 18(9), 577-590. <https://doi.org/10.1038/s41571-021-00509-w>
- Dombret, H., Seymour, J. F., Butrym, A., Wierzbowska, A., Selleslag, D., Jang, J. H., Kumar, R., Cavenagh, J., Schuh, A. C., Candoni, A., Récher, C., Sandhu, I., Bernal del Castillo, T., Al-Ali, H. K., Martinelli, G., Falantes, J., Noppeney, R., Stone, R. M., Minden, M. D., . . . Döhner, H. (2015). International phase 3 study of azacitidine vs conventional care regimens in older patients with newly diagnosed AML with >30% blasts. *Blood*, 126(3), 291-299.
<https://doi.org/10.1182/blood-2015-01-621664>
- Edwards, T. A., Pyle, S. E., Wharton, R. P., & Aggarwal, A. K. (2001). Structure of Pumilio reveals similarity between RNA and peptide binding motifs. *Cell*, 105(2), 281-289.
[https://doi.org/10.1016/s0092-8674\(01\)00318-x](https://doi.org/10.1016/s0092-8674(01)00318-x)
- Ehyai, S., Miyake, T., Williams, D., Vinayak, J., Bayfield, M. A., & McDermott, J. C. (2018). FMRP recruitment of β -catenin to the translation pre-initiation complex represses translation. *EMBO Rep*, 19(12). <https://doi.org/10.15252/embr.201745536>
- Estey, E. H. (2014). Acute myeloid leukemia: 2014 update on risk-stratification and management. *Am J Hematol*, 89(11), 1063-1081. <https://doi.org/10.1002/ajh.23834>
- Fagerlund, R. D., Ooi, P. L., & Wilbanks, S. M. (2012). Soluble expression and purification of tumor suppressor WT1 and its zinc finger domain. *Protein Expr Purif*, 85(2), 165-172.
<https://doi.org/10.1016/j.pep.2012.08.002>
- Famili, F., Brugman, M. H., Taskesen, E., Naber, B. E. A., Fodde, R., & Staal, F. J. T. (2016). High Levels of Canonical Wnt Signaling Lead to Loss of Stemness and Increased Differentiation in Hematopoietic Stem Cells. *Stem Cell Reports*, 6(5), 652-659.
<https://doi.org/10.1016/j.stemcr.2016.04.009>
- Fernandez, A., Huggins, I. J., Perna, L., Brafman, D., Lu, D., Yao, S., Gaasterland, T., Carson, D. A., & Willert, K. (2014). The WNT receptor FZD7 is required for maintenance of the pluripotent state in human embryonic stem cells. *Proc Natl Acad Sci U S A*, 111(4), 1409-1414.
<https://doi.org/10.1073/pnas.1323697111>
- Fiskus, W., Sharma, S., Saha, S., Shah, B., Devaraj, S. G., Sun, B., Horrigan, S., Leveque, C., Zu, Y., Iyer, S., & Bhalla, K. N. (2015). Pre-clinical efficacy of combined therapy with novel β -catenin antagonist BC2059 and histone deacetylase inhibitor against AML cells. *Leukemia*, 29(6), 1267-1278. <https://doi.org/10.1038/leu.2014.340>
- Fleming, H. E., Janzen, V., Lo Celso, C., Guo, J., Leahy, K. M., Kronenberg, H. M., & Scadden, D. T. (2008). Wnt signaling in the niche enforces hematopoietic stem cell quiescence and is necessary to preserve self-renewal in vivo. *Cell Stem Cell*, 2(3), 274-283.
<https://doi.org/10.1016/j.stem.2008.01.003>
- Fong, C. Y., Gilan, O., Lam, E. Y., Rubin, A. F., Ftouni, S., Tyler, D., Stanley, K., Sinha, D., Yeh, P., Morison, J., Giotopoulos, G., Lugo, D., Jeffrey, P., Lee, S. C., Carpenter, C., Gregory, R., Ramsay, R. G., Lane, S. W., Abdel-Wahab, O., . . . Dawson, M. A. (2015). BET inhibitor resistance emerges from leukaemia stem cells. *Nature*, 525(7570), 538-542.
<https://doi.org/10.1038/nature14888>
- Friedman, A. D. (2007). Transcriptional control of granulocyte and monocyte development. *Oncogene*, 26(47), 6816-6828. <https://doi.org/10.1038/sj.onc.1210764>
- Fry, E. A., & Inoue, K. (2018). Aberrant expression of ETS1 and ETS2 proteins in cancer. *Cancer Rep Rev*, 2(3). <https://doi.org/10.15761/crr.1000151>
- Fukuzawa, R., Anaka, M. R., Weeks, R. J., Morison, I. M., & Reeve, A. E. (2009). Canonical WNT signalling determines lineage specificity in Wilms tumour. *Oncogene*, 28(8), 1063-1075.
<https://doi.org/10.1038/onc.2008.455>

- Fukuzawa, R., Heathcott, R. W., Sano, M., Morison, I. M., Yun, K., & Reeve, A. E. (2004). Myogenesis in Wilms' tumors is associated with mutations of the WT1 gene and activation of Bcl-2 and the Wnt signaling pathway. *Pediatr Dev Pathol*, 7(2), 125-137. <https://doi.org/10.1007/s10024-003-3023-8>
- Gaidzik, V. I., Schlenk, R. F., Moschny, S., Becker, A., Bullinger, L., Corbacioglu, A., Krauter, J., Schlegelberger, B., Ganser, A., Döhner, H., & Döhner, K. (2009). Prognostic impact of WT1 mutations in cytogenetically normal acute myeloid leukemia: a study of the German-Austrian AML Study Group. *Blood*, 113(19), 4505-4511. <https://doi.org/10.1182/blood-2008-10-183392>
- Galimberti, S., Canestraro, M., Khan, R., Buda, G., Orciuolo, E., Guerrini, F., Fazzi, R., Maffei, R., Marasca, R., & Petrini, M. (2008). Vorinostat and bortezomib significantly inhibit WT1 gene expression in MO7-e and P39 cell lines. *Leukemia*, 22(3), 628-631. <https://doi.org/10.1038/sj.leu.2404918>
- Gao, C., Xiao, G., & Hu, J. (2014). Regulation of Wnt/ β -catenin signaling by posttranslational modifications. *Cell Biosci*, 4(1), 13. <https://doi.org/10.1186/2045-3701-4-13>
- Ge, A., Gao, S., Liu, Y., Zhang, H., Wang, X., Zhang, L., Pang, D., & Zhao, Y. (2020). Methylation of WT1, CA10 in peripheral blood leukocyte is associated with breast cancer risk: a case-control study. *BMC Cancer*, 20(1), 713. <https://doi.org/10.1186/s12885-020-07183-8>
- Gebauer, F., Schwarzl, T., Valcárcel, J., & Hentze, M. W. (2021). RNA-binding proteins in human genetic disease. *Nat Rev Genet*, 22(3), 185-198. <https://doi.org/10.1038/s41576-020-00302-y>
- Griffiths, E. A., Golding, M. C., Srivastava, P., Povinelli, B. J., James, S. R., Ford, L. A., Wetzler, M., Wang, E. S., & Nemeth, M. J. (2015). Pharmacological targeting of β -catenin in normal karyotype acute myeloid leukemia blasts. *Haematologica*, 100(2), e49-52. <https://doi.org/10.3324/haematol.2014.113118>
- Grover, A., Sanjuan-Pla, A., Thongjuea, S., Carrelha, J., Giustacchini, A., Gambardella, A., Macaulay, I., Mancini, E., Luis, T. C., Mead, A., Jacobsen, S. E., & Nerlov, C. (2016). Single-cell RNA sequencing reveals molecular and functional platelet bias of aged haematopoietic stem cells. *Nat Commun*, 7, 11075. <https://doi.org/10.1038/ncomms11075>
- Gu, W., Hu, S., Chen, Z., Qiu, G., Cen, J., He, B., He, J., & Wu, W. (2010). High expression of WT1 gene in acute myeloid leukemias with more predominant WT1+17AA isoforms at relapse. *Leuk Res*, 34(1), 46-49. <https://doi.org/10.1016/j.leukres.2009.04.004>
- Gurzov, E. N., Bakiri, L., Alfaro, J. M., Wagner, E. F., & Izquierdo, M. (2008). Targeting c-Jun and JunB proteins as potential anticancer cell therapy. *Oncogene*, 27(5), 641-652. <https://doi.org/10.1038/sj.onc.1210690>
- Han, T., Yang, C. S., Chang, K. Y., Zhang, D., Imam, F. B., & Rana, T. M. (2016). Identification of novel genes and networks governing hematopoietic stem cell development. *EMBO Rep*, 17(12), 1814-1828. <https://doi.org/10.15252/embr.201642395>
- Han, Y., San-Marina, S., Liu, J., & Minden, M. D. (2004). Transcriptional activation of c-myc proto-oncogene by WT1 protein. *Oncogene*, 23(41), 6933-6941. <https://doi.org/10.1038/sj.onc.1207609>
- Han, Y., Ye, A., Zhang, Y., Cai, Z., Wang, W., Sun, L., Jiang, S., Wu, J., Yu, K., & Zhang, S. (2015). Musashi-2 Silencing Exerts Potent Activity against Acute Myeloid Leukemia and Enhances Chemosensitivity to Daunorubicin. *PLoS One*, 10(8), e0136484. <https://doi.org/10.1371/journal.pone.0136484>
- He, S., Lu, Y., Liu, X., Huang, X., Keller, E. T., Qian, C. N., & Zhang, J. (2015). Wnt3a: functions and implications in cancer. *Chin J Cancer*, 34(12), 554-562. <https://doi.org/10.1186/s40880-015-0052-4>
- He, T. C., Sparks, A. B., Rago, C., Hermeking, H., Zawel, L., da Costa, L. T., Morin, P. J., Vogelstein, B., & Kinzler, K. W. (1998). Identification of c-MYC as a target of the APC pathway. *Science*, 281(5382), 1509-1512. <https://doi.org/10.1126/science.281.5382.1509>

- Helsmoortel, H. H., De Moerloose, B., Pieters, T., Ghazavi, F., Bresolin, S., Cavé, H., de Vries, A., de Haas, V., Flotho, C., Labarque, V., Niemeyer, C., De Paepe, P., Van Roy, N., Stary, J., van den Heuvel-Eibrink, M. M., Benoit, Y., Schulte, J., Goossens, S., Berx, G., . . . Lammens, T. (2016). LIN28B is over-expressed in specific subtypes of pediatric leukemia and regulates lncRNA H19. *Haematologica*, 101(6), e240-244. <https://doi.org/10.3324/haematol.2016.143818>
- Ho, P. A., Zeng, R., Alonzo, T. A., Gerbing, R. B., Miller, K. L., Pollard, J. A., Stirewalt, D. L., Heerema, N. A., Raimondi, S. C., Hirsch, B., Franklin, J. L., Lange, B., & Meshinchi, S. (2010). Prevalence and prognostic implications of WT1 mutations in pediatric acute myeloid leukemia (AML): a report from the Children's Oncology Group. *Blood*, 116(5), 702-710. <https://doi.org/10.1182/blood-2010-02-268953>
- Hodson, D. J., Screen, M., & Turner, M. (2019). RNA-binding proteins in hematopoiesis and hematological malignancy. *Blood*, 133(22), 2365-2373. <https://doi.org/10.1182/blood-2018-10-839985>
- Hosen, N., Shirakata, T., Nishida, S., Yanagihara, M., Tsuboi, A., Kawakami, M., Oji, Y., Oka, Y., Okabe, M., Tan, B., Sugiyama, H., & Weissman, I. L. (2007). The Wilms' tumor gene WT1-GFP knock-in mouse reveals the dynamic regulation of WT1 expression in normal and leukemic hematopoiesis. *Leukemia*, 21(8), 1783-1791. <https://doi.org/10.1038/sj.leu.2404752>
- Hosen, N., Sonoda, Y., Oji, Y., Kimura, T., Minamiguchi, H., Tamaki, H., Kawakami, M., Asada, M., Kanato, K., Motomura, M., Murakami, M., Fujioka, T., Masuda, T., Kim, E. H., Tsuboi, A., Oka, Y., Soma, T., Ogawa, H., & Sugiyama, H. (2002). Very low frequencies of human normal CD34+ haematopoietic progenitor cells express the Wilms' tumour gene WT1 at levels similar to those in leukaemia cells. *Br J Haematol*, 116(2), 409-420. <https://doi.org/10.1046/j.1365-2141.2002.03261.x>
- Hou, H. A., Huang, T. C., Lin, L. I., Liu, C. Y., Chen, C. Y., Chou, W. C., Tang, J. L., Tseng, M. H., Huang, C. F., Chiang, Y. C., Lee, F. Y., Liu, M. C., Yao, M., Huang, S. Y., Ko, B. S., Hsu, S. C., Wu, S. J., Tsay, W., Chen, Y. C., & Tien, H. F. (2010). WT1 mutation in 470 adult patients with acute myeloid leukemia: stability during disease evolution and implication of its incorporation into a survival scoring system. *Blood*, 115(25), 5222-5231. <https://doi.org/10.1182/blood-2009-12-259390>
- Hovanes, K., Li, T. W., Munguia, J. E., Truong, T., Milovanovic, T., Lawrence Marsh, J., Holcombe, R. F., & Waterman, M. L. (2001). Beta-catenin-sensitive isoforms of lymphoid enhancer factor-1 are selectively expressed in colon cancer. *Nat Genet*, 28(1), 53-57. <https://doi.org/10.1038/ng0501-53>
- Huber, A. H., Nelson, W. J., & Weis, W. I. (1997). Three-dimensional structure of the armadillo repeat region of beta-catenin. *Cell*, 90(5), 871-882. [https://doi.org/10.1016/s0092-8674\(00\)80352-9](https://doi.org/10.1016/s0092-8674(00)80352-9)
- Hülsken, J., Birchmeier, W., & Behrens, J. (1994). E-cadherin and APC compete for the interaction with beta-catenin and the cytoskeleton. *J Cell Biol*, 127(6 Pt 2), 2061-2069. <https://doi.org/10.1083/jcb.127.6.2061>
- Hur, J., & Jeong, S. (2013). Multitasking β -catenin: from adhesion and transcription to RNA regulation. *Animal Cells and Systems*, 17(5), 299-305. <https://doi.org/10.1080/19768354.2013.853694>
- Hwang, S. Y., Deng, X., Byun, S., Lee, C., Lee, S. J., Suh, H., Zhang, J., Kang, Q., Zhang, T., Westover, K. D., Mandinova, A., & Lee, S. W. (2016). Direct Targeting of β -Catenin by a Small Molecule Stimulates Proteasomal Degradation and Suppresses Oncogenic Wnt/ β -Catenin Signaling. *Cell Rep*, 16(1), 28-36. <https://doi.org/10.1016/j.celrep.2016.05.071>
- Ianniello, Z., Paiardini, A., & Fatica, A. (2019). N(6)-Methyladenosine (m(6)A): A Promising New Molecular Target in Acute Myeloid Leukemia. *Front Oncol*, 9, 251. <https://doi.org/10.3389/fonc.2019.00251>
- Ito, K., Oji, Y., Tatsumi, N., Shimizu, S., Kanai, Y., Nakazawa, T., Asada, M., Jomgeow, T., Aoyagi, S., Nakano, Y., Tamaki, H., Sakaguchi, N., Shirakata, T., Nishida, S., Kawakami, M., Tsuboi, A., Oka, Y., Tsujimoto, Y., & Sugiyama, H. (2006). Antiapoptotic function of 17AA(+)WT1 (Wilms'

- tumor gene) isoforms on the intrinsic apoptosis pathway. *Oncogene*, 25(30), 4217-4229. <https://doi.org/10.1038/sj.onc.1209455>
- Jagannathan-Bogdan, M., & Zon, L. I. (2013). Hematopoiesis. *Development*, 140(12), 2463-2467. <https://doi.org/10.1242/dev.083147>
- Jiang, X., Mak, P. Y., Mu, H., Tao, W., Mak, D. H., Kornblau, S., Zhang, Q., Ruvolo, P., Burks, J. K., Zhang, W., McQueen, T., Pan, R., Zhou, H., Konopleva, M., Cortes, J., Liu, Q., Andreeff, M., & Carter, B. Z. (2018). Disruption of Wnt/ β -Catenin Exerts Antileukemia Activity and Synergizes with FLT3 Inhibition in FLT3-Mutant Acute Myeloid Leukemia. *Clin Cancer Res*, 24(10), 2417-2429. <https://doi.org/10.1158/1078-0432.Ccr-17-1556>
- Jing, Z., Wei-jie, Y., & Yi-Feng, Z. G. (2015). Down-regulation of Wt1 activates Wnt/ β -catenin signaling through modulating endocytic route of LRP6 in podocyte dysfunction in vitro. *Cell Signal*, 27(9), 1772-1780. <https://doi.org/10.1016/j.cellsig.2015.05.018>
- Joseph, R., Srivastava, O. P., & Pfister, R. R. (2014). Downregulation of β -actin and its regulatory gene HuR affect cell migration of human corneal fibroblasts. *Mol Vis*, 20, 593-605.
- Kabiri, Z., Numata, A., Kawasaki, A., Edison, Tenen, D. G., & Virshup, D. M. (2015). Wnts are dispensable for differentiation and self-renewal of adult murine hematopoietic stem cells. *Blood*, 126(9), 1086-1094. <https://doi.org/10.1182/blood-2014-09-598540>
- Kadekar, D., Kale, V., & Limaye, L. (2015). Differential ability of MSCs isolated from placenta and cord as feeders for supporting ex vivo expansion of umbilical cord blood derived CD34(+) cells. *Stem Cell Res Ther*, 6, 201. <https://doi.org/10.1186/s13287-015-0194-y>
- Kaleem, Z., Crawford, E., Pathan, M. H., Jasper, L., Covinsky, M. A., Johnson, L. R., & White, G. (2003). Flow cytometric analysis of acute leukemias. Diagnostic utility and critical analysis of data. *Arch Pathol Lab Med*, 127(1), 42-48. <https://doi.org/10.5858/2003-127-42-fcaoa>
- Kantarjian, H., Kadia, T., DiNardo, C., Daver, N., Borthakur, G., Jabbour, E., Garcia-Manero, G., Konopleva, M., & Ravandi, F. (2021). Acute myeloid leukemia: current progress and future directions. *Blood Cancer J*, 11(2), 41. <https://doi.org/10.1038/s41408-021-00425-3>
- Kaverina, N. V., Eng, D. G., Largent, A. D., Daehn, I., Chang, A., Gross, K. W., Pippin, J. W., Hohenstein, P., & Shankland, S. J. (2017). WT1 Is Necessary for the Proliferation and Migration of Cells of Renin Lineage Following Kidney Podocyte Depletion. *Stem Cell Reports*, 9(4), 1152-1166. <https://doi.org/10.1016/j.stemcr.2017.08.020>
- Kayser, S., & Levis, M. J. (2021). Updates on targeted therapies for acute myeloid leukaemia. *Br J Haematol*. <https://doi.org/10.1111/bjh.17746>
- Keilholz, U., Letsch, A., Busse, A., Asemissen, A. M., Bauer, S., Blau, I. W., Hofmann, W. K., Uharek, L., Thiel, E., & Scheibenbogen, C. (2009). A clinical and immunologic phase 2 trial of Wilms tumor gene product 1 (WT1) peptide vaccination in patients with AML and MDS. *Blood*, 113(26), 6541-6548. <https://doi.org/10.1182/blood-2009-02-202598>
- Kim, A. D., Stachura, D. L., & Traver, D. (2014). Cell signaling pathways involved in hematopoietic stem cell specification. *Exp Cell Res*, 329(2), 227-233. <https://doi.org/10.1016/j.yexcr.2014.10.011>
- Kim, I., Kwak, H., Lee, H. K., Hyun, S., & Jeong, S. (2012). β -Catenin recognizes a specific RNA motif in the cyclooxygenase-2 mRNA 3'-UTR and interacts with HuR in colon cancer cells. *Nucleic Acids Res*, 40(14), 6863-6872. <https://doi.org/10.1093/nar/gks331>
- Kim, M. K., McGarry, T. J., P, O. B., Flatow, J. M., Golden, A. A., & Licht, J. D. (2009). An integrated genome screen identifies the Wnt signaling pathway as a major target of WT1. *Proc Natl Acad Sci U S A*, 106(27), 11154-11159. <https://doi.org/10.1073/pnas.0901591106>
- Kim, M. S., Yoon, S. K., Bollig, F., Kitagaki, J., Hur, W., Whye, N. J., Wu, Y. P., Rivera, M. N., Park, J. Y., Kim, H. S., Malik, K., Bell, D. W., Englert, C., Perantoni, A. O., & Lee, S. B. (2010). A novel Wilms tumor 1 (WT1) target gene negatively regulates the WNT signaling pathway. *J Biol Chem*, 285(19), 14585-14593. <https://doi.org/10.1074/jbc.M109.094334>
- King-Underwood, L., Renshaw, J., & Pritchard-Jones, K. (1996). Mutations in the Wilms' tumor gene WT1 in leukemias. *Blood*, 87(6), 2171-2179.

- Koch, U., Wilson, A., Cobas, M., Kemler, R., Macdonald, H. R., & Radtke, F. (2008). Simultaneous loss of beta- and gamma-catenin does not perturb hematopoiesis or lymphopoiesis. *Blood*, 111(1), 160-164. <https://doi.org/10.1182/blood-2007-07-099754>
- Kode, A., Manavalan, J. S., Mosialou, I., Bhagat, G., Rathinam, C. V., Luo, N., Khiabani, H., Lee, A., Murty, V. V., Friedman, R., Brum, A., Park, D., Galili, N., Mukherjee, S., Teruya-Feldstein, J., Raza, A., Rabadan, R., Berman, E., & Kousteni, S. (2014). Leukaemogenesis induced by an activating β -catenin mutation in osteoblasts. *Nature*, 506(7487), 240-244. <https://doi.org/10.1038/nature12883>
- Krauth, M. T., Alpermann, T., Bacher, U., Eder, C., Dicker, F., Ulke, M., Kuznia, S., Nadarajah, N., Kern, W., Haferlach, C., Haferlach, T., & Schnittger, S. (2015). WT1 mutations are secondary events in AML, show varying frequencies and impact on prognosis between genetic subgroups. *Leukemia*, 29(3), 660-667. <https://doi.org/10.1038/leu.2014.243>
- Kumar, C. C. (2011). Genetic abnormalities and challenges in the treatment of acute myeloid leukemia. *Genes Cancer*, 2(2), 95-107. <https://doi.org/10.1177/1947601911408076>
- Lagunas-Rangel, F. A., Chávez-Valencia, V., Gómez-Guijosa, M., & Cortes-Penagos, C. (2017). Acute Myeloid Leukemia-Genetic Alterations and Their Clinical Prognosis. *Int J Hematol Oncol Stem Cell Res*, 11(4), 328-339.
- Lambert, M., Alioui, M., Jambon, S., Depauw, S., Van Seuningen, I., & David-Cordonnier, M. H. (2019). Direct and Indirect Targeting of HOXA9 Transcription Factor in Acute Myeloid Leukemia. *Cancers (Basel)*, 11(6). <https://doi.org/10.3390/cancers11060837>
- Lane, S. W., Sykes, S. M., Al-Shahrour, F., Shterental, S., Paktinat, M., Lo Celso, C., Jesneck, J. L., Ebert, B. L., Williams, D. A., & Gilliland, D. G. (2010). The Apc(min) mouse has altered hematopoietic stem cell function and provides a model for MPD/MDS. *Blood*, 115(17), 3489-3497. <https://doi.org/10.1182/blood-2009-11-251728>
- Lecarpentier, Y., Schussler, O., Hébert, J. L., & Vallée, A. (2019). Multiple Targets of the Canonical WNT/ β -Catenin Signaling in Cancers. *Front Oncol*, 9, 1248. <https://doi.org/10.3389/fonc.2019.01248>
- Lee, H. K., & Jeong, S. (2006). Beta-Catenin stabilizes cyclooxygenase-2 mRNA by interacting with AU-rich elements of 3'-UTR. *Nucleic Acids Res*, 34(19), 5705-5714. <https://doi.org/10.1093/nar/gkl698>
- Lee, H. K., Kwak, H. Y., Hur, J., Kim, I. A., Yang, J. S., Park, M. W., Yu, J., & Jeong, S. (2007). beta-catenin regulates multiple steps of RNA metabolism as revealed by the RNA aptamer in colon cancer cells. *Cancer Res*, 67(19), 9315-9321. <https://doi.org/10.1158/0008-5472.Can-07-1128>
- Li, J., & Wang, C. Y. (2008). TBL1-TBLR1 and beta-catenin recruit each other to Wnt target-gene promoter for transcription activation and oncogenesis. *Nat Cell Biol*, 10(2), 160-169. <https://doi.org/10.1038/ncb1684>
- Li, K., Hu, C., Mei, C., Ren, Z., Vera, J. C., Zhuang, Z., Jin, J., & Tong, H. (2014). Sequential combination of decitabine and idarubicin synergistically enhances anti-leukemia effect followed by demethylating Wnt pathway inhibitor promoters and downregulating Wnt pathway nuclear target. *J Transl Med*, 12, 167. <https://doi.org/10.1186/1479-5876-12-167>
- Li, L., Sheng, Y., Li, W., Hu, C., Mittal, N., Tohyama, K., Seba, A., Zhao, Y. Y., Ozer, H., Zhu, T., & Qian, Z. (2017). β -Catenin Is a Candidate Therapeutic Target for Myeloid Neoplasms with del(5q). *Cancer Res*, 77(15), 4116-4126. <https://doi.org/10.1158/0008-5472.Can-17-0202>
- Li, V. S., Ng, S. S., Boersema, P. J., Low, T. Y., Karthaus, W. R., Gerlach, J. P., Mohammed, S., Heck, A. J., Maurice, M. M., Mahmoudi, T., & Clevers, H. (2012). Wnt signaling through inhibition of β -catenin degradation in an intact Axin1 complex. *Cell*, 149(6), 1245-1256. <https://doi.org/10.1016/j.cell.2012.05.002>
- Li, Y., Wang, J., Li, X., Jia, Y., Huai, L., He, K., Yu, P., Wang, M., Xing, H., Rao, Q., Tian, Z., Tang, K., Wang, J., & Mi, Y. (2014). Role of the Wilms' tumor 1 gene in the aberrant biological

- behavior of leukemic cells and the related mechanisms. *Oncol Rep*, 32(6), 2680-2686. <https://doi.org/10.3892/or.2014.3529>
- Li, Z., Jin, H., Mao, G., Wu, L., & Guo, Q. (2017). Msi2 plays a carcinogenic role in esophageal squamous cell carcinoma via regulation of the Wnt/ β -catenin and Hedgehog signaling pathways. *Exp Cell Res*, 361(1), 170-177. <https://doi.org/10.1016/j.yexcr.2017.10.016>
- Liu, C., Zhang, A., Cheng, L., & Gao, Y. (2016). miR-410 regulates apoptosis by targeting Bak1 in human colorectal cancer cells. *Mol Med Rep*, 14(1), 467-473. <https://doi.org/10.3892/mmr.2016.5271>
- Logan, C. Y., & Nusse, R. (2004). The Wnt signaling pathway in development and disease. *Annu Rev Cell Dev Biol*, 20, 781-810. <https://doi.org/10.1146/annurev.cellbio.20.010403.113126>
- Luis, T. C., Ichii, M., Brugman, M. H., Kincade, P., & Staal, F. J. (2012). Wnt signaling strength regulates normal hematopoiesis and its deregulation is involved in leukemia development. *Leukemia*, 26(3), 414-421. <https://doi.org/10.1038/leu.2011.387>
- Luna, I., Such, E., Cervera, J., Barragán, E., Ibañez, M., Gómez-Seguí, I., López-Pavía, M., Llop, M., Fuster, O., Dolz, S., Oltra, S., Alonso, C., Vera, B., Lorenzo, I., Martínez-Cuadrón, D., Montesinos, P., Senent, M. L., Moscardó, F., Bolufer, P., & Sanz, M. A. (2013). WT1 isoform expression pattern in acute myeloid leukemia. *Leuk Res*, 37(12), 1744-1749. <https://doi.org/10.1016/j.leukres.2013.10.009>
- Lustig, B., Jerchow, B., Sachs, M., Weiler, S., Pietsch, T., Karsten, U., van de Wetering, M., Clevers, H., Schlag, P. M., Birchmeier, W., & Behrens, J. (2002). Negative feedback loop of Wnt signaling through upregulation of conductin/axin2 in colorectal and liver tumors. *Mol Cell Biol*, 22(4), 1184-1193. <https://doi.org/10.1128/mcb.22.4.1184-1193.2002>
- Ma, Z., Morris, S. W., Valentine, V., Li, M., Herbrick, J. A., Cui, X., Bouman, D., Li, Y., Mehta, P. K., Nizetic, D., Kaneko, Y., Chan, G. C., Chan, L. C., Squire, J., Scherer, S. W., & Hitzler, J. K. (2001). Fusion of two novel genes, RBM15 and MKL1, in the t(1;22)(p13;q13) of acute megakaryoblastic leukemia. *Nat Genet*, 28(3), 220-221. <https://doi.org/10.1038/90054>
- MacDonald, B. T., Tamai, K., & He, X. (2009). Wnt/beta-catenin signaling: components, mechanisms, and diseases. *Dev Cell*, 17(1), 9-26. <https://doi.org/10.1016/j.devcel.2009.06.016>
- Maiti, S., Alam, R., Amos, C. I., & Huff, V. (2000). Frequent association of beta-catenin and WT1 mutations in Wilms tumors. *Cancer Res*, 60(22), 6288-6292.
- Major, M. B., Camp, N. D., Berndt, J. D., Yi, X., Goldenberg, S. J., Hubbert, C., Biechele, T. L., Gingras, A. C., Zheng, N., Maccoss, M. J., Angers, S., & Moon, R. T. (2007). Wilms tumor suppressor WTX negatively regulates WNT/beta-catenin signaling. *Science*, 316(5827), 1043-1046. <https://doi.org/10.1126/science.1141515>
- Makki, M. S., Heinzl, T., & Englert, C. (2008). TSA downregulates Wilms tumor gene 1 (Wt1) expression at multiple levels. *Nucleic Acids Res*, 36(12), 4067-4078. <https://doi.org/10.1093/nar/gkn356>
- Maruyama, K., Uematsu, S., Kondo, T., Takeuchi, O., Martino, M. M., Kawasaki, T., & Akira, S. (2013). Strawberry notch homologue 2 regulates osteoclast fusion by enhancing the expression of DC-STAMP. *J Exp Med*, 210(10), 1947-1960. <https://doi.org/10.1084/jem.20130512>
- Maslak, P. G., Dao, T., Bernal, Y., Chanel, S. M., Zhang, R., Frattini, M., Rosenblat, T., Jurcic, J. G., Brentjens, R. J., Arcila, M. E., Rampal, R., Park, J. H., Douer, D., Katz, L., Sarlis, N., Tallman, M. S., & Scheinberg, D. A. (2018). Phase 2 trial of a multivalent WT1 peptide vaccine (galinpepimut-S) in acute myeloid leukemia. *Blood Adv*, 2(3), 224-234. <https://doi.org/10.1182/bloodadvances.2017014175>
- Mayer, H., Bertram, H., Lindenmaier, W., Korff, T., Weber, H., & Weich, H. (2005). Vascular endothelial growth factor (VEGF-A) expression in human mesenchymal stem cells: autocrine and paracrine role on osteoblastic and endothelial differentiation. *J Cell Biochem*, 95(4), 827-839. <https://doi.org/10.1002/jcb.20462>
- Meyers, J., Yu, Y., Kaye, J. A., & Davis, K. L. (2013). Medicare fee-for-service enrollees with primary acute myeloid leukemia: an analysis of treatment patterns, survival, and healthcare resource

- utilization and costs. *Appl Health Econ Health Policy*, 11(3), 275-286.
<https://doi.org/10.1007/s40258-013-0032-2>
- Minke, K. S., Staib, P., Puetter, A., Gehrke, I., Gandhirajan, R. K., Schlösser, A., Schmitt, E. K., Hallek, M., & Kreuzer, K. A. (2009). Small molecule inhibitors of WNT signaling effectively induce apoptosis in acute myeloid leukemia cells. *Eur J Haematol*, 82(3), 165-175.
<https://doi.org/10.1111/j.1600-0609.2008.01188.x>
- Moore, M. J. (2005). From birth to death: the complex lives of eukaryotic mRNAs. *Science*, 309(5740), 1514-1518. <https://doi.org/10.1126/science.1111443>
- Moore, S., Järvelin, A. I., Davis, I., Bond, G. L., & Castello, A. (2018). Expanding horizons: new roles for non-canonical RNA-binding proteins in cancer. *Curr Opin Genet Dev*, 48, 112-120.
<https://doi.org/10.1016/j.gde.2017.11.006>
- Morgan, R. G., Liddiard, K., Pearn, L., Pumford, S. L., Burnett, A. K., Darley, R. L., & Tonks, A. (2013). gamma-Catenin is expressed throughout normal human hematopoietic development and is required for normal PU.1-dependent monocyte differentiation. *Leukemia*, 27(10), 2096-2100. <https://doi.org/10.1038/leu.2013.96>
- Morgan, R. G., Ridsdale, J., Payne, M., Heesom, K. J., Wilson, M. C., Davidson, A., Greenhough, A., Davies, S., Williams, A. C., Blair, A., Waterman, M. L., Tonks, A., & Darley, R. L. (2019). LEF-1 drives aberrant β -catenin nuclear localization in myeloid leukemia cells. *Haematologica*, 104(7), 1365-1377. <https://doi.org/10.3324/haematol.2018.202846>
- Morgan, R. G., Ridsdale, J., Tonks, A., & Darley, R. L. (2014). Factors affecting the nuclear localization of β -catenin in normal and malignant tissue. *J Cell Biochem*, 115(8), 1351-1361.
<https://doi.org/10.1002/jcb.24803>
- Morrison, A. A., Venables, J. P., Dellaire, G., & Lodomery, M. R. (2006). The Wilms tumour suppressor protein WT1 (+KTS isoform) binds alpha-actinin 1 mRNA via its zinc-finger domain. *Biochem Cell Biol*, 84(5), 789-798. <https://doi.org/10.1139/o06-065>
- Morrison, A. A., Viney, R. L., Saleem, M. A., & Lodomery, M. R. (2008). New insights into the function of the Wilms tumor suppressor gene WT1 in podocytes. *Am J Physiol Renal Physiol*, 295(1), F12-17. <https://doi.org/10.1152/ajprenal.00597.2007>
- Müller-Tidow, C., Steffen, B., Cauvet, T., Tickenbrock, L., Ji, P., Diederichs, S., Sargin, B., Köhler, G., Stelljes, M., Puccetti, E., Ruthardt, M., deVos, S., Hiebert, S. W., Koeffler, H. P., Berdel, W. E., & Serve, H. (2004). Translocation products in acute myeloid leukemia activate the Wnt signaling pathway in hematopoietic cells. *Mol Cell Biol*, 24(7), 2890-2904.
<https://doi.org/10.1128/mcb.24.7.2890-2904.2004>
- Mundlos, S., Pelletier, J., Darveau, A., Bachmann, M., Winterpacht, A., & Zabel, B. (1993). Nuclear localization of the protein encoded by the Wilms' tumor gene WT1 in embryonic and adult tissues. *Development*, 119(4), 1329-1341.
- Naudin, C., Hattabi, A., Michelet, F., Miri-Nezhad, A., Benyoucef, A., Pflumio, F., Guillonnet, F., Fichelson, S., Vigon, I., Dusanter-Fourt, I., & Lauret, E. (2017). PUMILIO/FOXP1 signaling drives expansion of hematopoietic stem/progenitor and leukemia cells. *Blood*, 129(18), 2493-2506. <https://doi.org/10.1182/blood-2016-10-747436>
- Nemeth, M. J., Mak, K. K., Yang, Y., & Bodine, D. M. (2009). beta-Catenin expression in the bone marrow microenvironment is required for long-term maintenance of primitive hematopoietic cells. *Stem Cells*, 27(5), 1109-1119. <https://doi.org/10.1002/stem.32>
- Niktoreh, N., Leri, B., Zimmermann, M., Gruhn, B., Escherich, G., Bourquin, J. P., Dworzak, M., Sramkova, L., Rossig, C., Creutzig, U., Reinhardt, D., & Rasche, M. (2019). Gemtuzumab ozogamicin in children with relapsed or refractory acute myeloid leukemia: a report by Berlin-Frankfurt-Münster study group. *Haematologica*, 104(1), 120-127.
<https://doi.org/10.3324/haematol.2018.191841>
- Nishida, S., Hosen, N., Shirakata, T., Kanato, K., Yanagihara, M., Nakatsuka, S., Hoshida, Y., Nakazawa, T., Harada, Y., Tatsumi, N., Tsuboi, A., Kawakami, M., Oka, Y., Oji, Y., Aozasa, K., Kawase, I., & Sugiyama, H. (2006). AML1-ETO rapidly induces acute myeloblastic leukemia in cooperation

- with the Wilms tumor gene, WT1. *Blood*, 107(8), 3303-3312. <https://doi.org/10.1182/blood-2005-04-1656>
- Nusse, R., & Clevers, H. (2017). Wnt/ β -Catenin Signaling, Disease, and Emerging Therapeutic Modalities. *Cell*, 169(6), 985-999. <https://doi.org/10.1016/j.cell.2017.05.016>
- Oka, Y., Tsuboi, A., Nakata, J., Nishida, S., Hosen, N., Kumanogoh, A., Oji, Y., & Sugiyama, H. (2017). Wilms' Tumor Gene 1 (WT1) Peptide Vaccine Therapy for Hematological Malignancies: From CTL Epitope Identification to Recent Progress in Clinical Studies Including a Cure-Oriented Strategy. *Oncol Res Treat*, 40(11), 682-690. <https://doi.org/10.1159/000481353>
- Paluszczak, J., Sarbak, J., Kostrzewska-Poczekaj, M., Kiwerska, K., Jarmuż-Szymczak, M., Grenman, R., Mielcarek-Kuchta, D., & Baer-Dubowska, W. (2015). The negative regulators of Wnt pathway-DACH1, DKK1, and WIF1 are methylated in oral and oropharyngeal cancer and WIF1 methylation predicts shorter survival. *Tumour Biol*, 36(4), 2855-2861. <https://doi.org/10.1007/s13277-014-2913-x>
- Papaemmanuil, E., Gerstung, M., Bullinger, L., Gaidzik, V. I., Paschka, P., Roberts, N. D., Potter, N. E., Heuser, M., Thol, F., Bolli, N., Gundem, G., Van Loo, P., Martincorena, I., Ganly, P., Mudie, L., McLaren, S., O'Meara, S., Raine, K., Jones, D. R., . . . Campbell, P. J. (2016). Genomic Classification and Prognosis in Acute Myeloid Leukemia. *N Engl J Med*, 374(23), 2209-2221. <https://doi.org/10.1056/NEJMoa1516192>
- Paris, N. D., Coles, G. L., & Ackerman, K. G. (2015). Wt1 and β -catenin cooperatively regulate diaphragm development in the mouse. *Dev Biol*, 407(1), 40-56. <https://doi.org/10.1016/j.ydbio.2015.08.009>
- Park, S. M., Cho, H., Thornton, A. M., Barlowe, T. S., Chou, T., Chhangawala, S., Fairchild, L., Taggart, J., Chow, A., Schurer, A., Gruet, A., Witkin, M. D., Kim, J. H., Shevach, E. M., Krivtsov, A., Armstrong, S. A., Leslie, C., & Kharas, M. G. (2019). IKZF2 Drives Leukemia Stem Cell Self-Renewal and Inhibits Myeloid Differentiation. *Cell Stem Cell*, 24(1), 153-165.e157. <https://doi.org/10.1016/j.stem.2018.10.016>
- Paschka, P., & Döhner, K. (2013). Core-binding factor acute myeloid leukemia: can we improve on HiDAC consolidation? *Hematology Am Soc Hematol Educ Program*, 2013, 209-219. <https://doi.org/10.1182/asheducation-2013.1.209>
- Patel, J. P., Gönen, M., Figueroa, M. E., Fernandez, H., Sun, Z., Racevskis, J., Van Vlierberghe, P., Dolgalev, I., Thomas, S., Aminova, O., Huberman, K., Cheng, J., Viale, A., Socci, N. D., Heguy, A., Cherry, A., Vance, G., Higgins, R. R., Ketterling, R. P., . . . Levine, R. L. (2012). Prognostic relevance of integrated genetic profiling in acute myeloid leukemia. *N Engl J Med*, 366(12), 1079-1089. <https://doi.org/10.1056/NEJMoa1112304>
- Pehlivan, M., Çalışkan, C., Yüce, Z., & Sercan, H. O. (2018). Secreted Wnt antagonists in leukemia: A road yet to be paved. *Leuk Res*, 69, 24-30. <https://doi.org/10.1016/j.leukres.2018.03.011>
- Pelliccia, F., Ubertini, V., & Bosco, N. (2012). The importance of molecular cytogenetic analysis prior to using cell lines in research: The case of the KG-1a leukemia cell line. *Oncol Lett*, 4(2), 237-240. <https://doi.org/10.3892/ol.2012.709>
- Pepe, F., Bill, M., Papaioannou, D., Karunasiri, M., Walker, A., Naumann, E., Snyder, K., Ranganathan, P., Dorrance, A., & Garzon, R. (2022). Targeting Wnt signaling in acute myeloid leukemia stem cells. *Haematologica*, 107(1), 307-311. <https://doi.org/10.3324/haematol.2020.266155>
- Perissi, V., Aggarwal, A., Glass, C. K., Rose, D. W., & Rosenfeld, M. G. (2004). A corepressor/coactivator exchange complex required for transcriptional activation by nuclear receptors and other regulated transcription factors. *Cell*, 116(4), 511-526. [https://doi.org/10.1016/s0092-8674\(04\)00133-3](https://doi.org/10.1016/s0092-8674(04)00133-3)
- Perry, J. M., Tao, F., Roy, A., Lin, T., He, X. C., Chen, S., Lu, X., Nemecek, J., Ruan, L., Yu, X., Dukes, D., Moran, A., Pace, J., Schroeder, K., Zhao, M., Venkatraman, A., Qian, P., Li, Z., Hembree, M., . . . Li, L. (2020). Overcoming Wnt- β -catenin dependent anticancer therapy resistance in leukaemia stem cells. *Nat Cell Biol*, 22(6), 689-700. <https://doi.org/10.1038/s41556-020-0507-y>

- Pievani, A., Biondi, M., Tomasoni, C., Biondi, A., & Serafini, M. (2020). Location First: Targeting Acute Myeloid Leukemia Within Its Niche. *J Clin Med*, 9(5). <https://doi.org/10.3390/jcm9051513>
- Pospíšek, M., & Valášek, L. (2013). Polysome profile analysis--yeast. *Methods Enzymol*, 530, 173-181. <https://doi.org/10.1016/b978-0-12-420037-1.00009-9>
- Potluri, S., Assi, S. A., Chin, P. S., Coleman, D. J. L., Pickin, A., Moriya, S., Seki, N., Heidenreich, O., Cockerill, P. N., & Bonifer, C. (2021). Isoform-specific and signaling-dependent propagation of acute myeloid leukemia by Wilms tumor 1. *Cell Rep*, 35(3), 109010. <https://doi.org/10.1016/j.celrep.2021.109010>
- Pradella, D., Naro, C., Sette, C., & Ghigna, C. (2017). EMT and stemness: flexible processes tuned by alternative splicing in development and cancer progression. *Mol Cancer*, 16(1), 8. <https://doi.org/10.1186/s12943-016-0579-2>
- Pundhir, S., Bratt Lauridsen, F. K., Schuster, M. B., Jakobsen, J. S., Ge, Y., Schoof, E. M., Rapin, N., Waage, J., Hasemann, M. S., & Porse, B. T. (2018). Enhancer and Transcription Factor Dynamics during Myeloid Differentiation Reveal an Early Differentiation Block in Cebpa null Progenitors. *Cell Rep*, 23(9), 2744-2757. <https://doi.org/10.1016/j.celrep.2018.05.012>
- Rampal, R., & Figueroa, M. E. (2016). Wilms tumor 1 mutations in the pathogenesis of acute myeloid leukemia. *Haematologica*, 101(6), 672-679. <https://doi.org/10.3324/haematol.2015.141796>
- Reddy, V. S., Valente, A. J., Delafontaine, P., & Chandrasekar, B. (2011). Interleukin-18/WNT1-inducible signaling pathway protein-1 signaling mediates human saphenous vein smooth muscle cell proliferation. *J Cell Physiol*, 126(12), 3303-3315. <https://doi.org/10.1002/jcp.22676>
- Renneville, A., Boissel, N., Zurawski, V., Llopis, L., Biggio, V., Nibourel, O., Philippe, N., Thomas, X., Dombret, H., & Preudhomme, C. (2009). Wilms tumor 1 gene mutations are associated with a higher risk of recurrence in young adults with acute myeloid leukemia: a study from the Acute Leukemia French Association. *Cancer*, 115(16), 3719-3727. <https://doi.org/10.1002/cncr.24442>
- Rennoll, S., & Yochum, G. (2015). Regulation of MYC gene expression by aberrant Wnt/ β -catenin signaling in colorectal cancer. *World J Biol Chem*, 6(4), 290-300. <https://doi.org/10.4331/wjbc.v6.i4.290>
- Reya, T., Duncan, A. W., Ailles, L., Domen, J., Scherer, D. C., Willert, K., Hintz, L., Nusse, R., & Weissman, I. L. (2003). A role for Wnt signalling in self-renewal of haematopoietic stem cells. *Nature*, 423(6938), 409-414. <https://doi.org/10.1038/nature01593>
- Rieger, M. A., & Schroeder, T. (2012). Hematopoiesis. *Cold Spring Harb Perspect Biol*, 4(12). <https://doi.org/10.1101/cshperspect.a008250>
- Riether, C., Schürch, C. M., Bühner, E. D., Hinterbrandner, M., Huguenin, A. L., Hoepner, S., Zlobec, I., Pabst, T., Radpour, R., & Ochsenbein, A. F. (2017). CD70/CD27 signaling promotes blast stemness and is a viable therapeutic target in acute myeloid leukemia. *J Exp Med*, 214(2), 359-380. <https://doi.org/10.1084/jem.20152008>
- Riether, C., Schürch, C. M., & Ochsenbein, A. F. (2015). Regulation of hematopoietic and leukemic stem cells by the immune system. *Cell Death Differ*, 22(2), 187-198. <https://doi.org/10.1038/cdd.2014.89>
- Rivera, M. N., Kim, W. J., Wells, J., Stone, A., Burger, A., Coffman, E. J., Zhang, J., & Haber, D. A. (2009). The tumor suppressor WTX shuttles to the nucleus and modulates WT1 activity. *Proc Natl Acad Sci U S A*, 106(20), 8338-8343. <https://doi.org/10.1073/pnas.0811349106>
- Saenz, D. T., Fiskus, W., Manshouri, T., Mill, C. P., Qian, Y., Raina, K., Rajapakshe, K., Coarfa, C., Soldi, R., Bose, P., Borthakur, G., Kadia, T. M., Khoury, J. D., Masarova, L., Nowak, A. J., Sun, B., Saenz, D. N., Kornblau, S. M., Horrigian, S., . . . Bhalla, K. N. (2019). Targeting nuclear β -catenin as therapy for post-myeloproliferative neoplasm secondary AML. *Leukemia*, 33(6), 1373-1386. <https://doi.org/10.1038/s41375-018-0334-3>
- Salik, B., Yi, H., Hassan, N., Santiappillai, N., Vick, B., Connerty, P., Duly, A., Trahair, T., Woo, A. J., Beck, D., Liu, T., Spiekermann, K., Jeremias, I., Wang, J., Kavallaris, M., Haber, M., Norris, M.

- D., Liebermann, D. A., D'Andrea, R. J., . . . Wang, J. Y. (2020). Targeting RSPO3-LGR4 Signaling for Leukemia Stem Cell Eradication in Acute Myeloid Leukemia. *Cancer Cell*, 38(2), 263-278.e266. <https://doi.org/10.1016/j.ccell.2020.05.014>
- Sanjuan-Pla, A., Macaulay, I. C., Jensen, C. T., Woll, P. S., Luis, T. C., Mead, A., Moore, S., Carella, C., Matsuoka, S., Bouriez Jones, T., Chowdhury, O., Stenson, L., Lutteropp, M., Green, J. C., Facchini, R., Boukarabila, H., Grover, A., Gambardella, A., Thongjuea, S., . . . Jacobsen, S. E. (2013). Platelet-biased stem cells reside at the apex of the haematopoietic stem-cell hierarchy. *Nature*, 502(7470), 232-236. <https://doi.org/10.1038/nature12495>
- Santiago, L., Daniels, G., Wang, D., Deng, F. M., & Lee, P. (2017). Wnt signaling pathway protein LEF1 in cancer, as a biomarker for prognosis and a target for treatment. *Am J Cancer Res*, 7(6), 1389-1406.
- Sato, S., Idogawa, M., Honda, K., Fujii, G., Kawashima, H., Takekuma, K., Hoshika, A., Hirohashi, S., & Yamada, T. (2005). Beta-catenin interacts with the FUS proto-oncogene product and regulates pre-mRNA splicing. *Gastroenterology*, 129(4), 1225-1236. <https://doi.org/10.1053/j.gastro.2005.07.025>
- Sheng, Y., Ju, W., Huang, Y., Li, J., Ozer, H., Qiao, X., & Qian, Z. (2016). Activation of wnt/beta-catenin signaling blocks monocyte-macrophage differentiation through antagonizing PU.1-targeted gene transcription. *Leukemia*, 30(10), 2106-2109. <https://doi.org/10.1038/leu.2016.146>
- Shi, Y., Liu, C. H., Roberts, A. I., Das, J., Xu, G., Ren, G., Zhang, Y., Zhang, L., Yuan, Z. R., Tan, H. S., Das, G., & Devadas, S. (2006). Granulocyte-macrophage colony-stimulating factor (GM-CSF) and T-cell responses: what we do and don't know. *Cell Res*, 16(2), 126-133. <https://doi.org/10.1038/sj.cr.7310017>
- Shin, S. H., Lim, D. Y., Reddy, K., Malakhova, M., Liu, F., Wang, T., Song, M., Chen, H., Bae, K. B., Ryu, J., Liu, K., Lee, M. H., Bode, A. M., & Dong, Z. (2017). A Small Molecule Inhibitor of the β -Catenin-TCF4 Interaction Suppresses Colorectal Cancer Growth In Vitro and In Vivo. *EBioMedicine*, 25, 22-31. <https://doi.org/10.1016/j.ebiom.2017.09.029>
- Short, N. J., Rytting, M. E., & Cortes, J. E. (2018). Acute myeloid leukaemia. *Lancet*, 392(10147), 593-606. [https://doi.org/10.1016/s0140-6736\(18\)31041-9](https://doi.org/10.1016/s0140-6736(18)31041-9)
- Shtutman, M., Zhurinsky, J., Simcha, I., Albanese, C., D'Amico, M., Pestell, R., & Ben-Ze'ev, A. (1999). The cyclin D1 gene is a target of the beta-catenin/LEF-1 pathway. *Proc Natl Acad Sci U S A*, 96(10), 5522-5527. <https://doi.org/10.1073/pnas.96.10.5522>
- Sim, E. U., Smith, A., Szilagi, E., Rae, F., Ioannou, P., Lindsay, M. H., & Little, M. H. (2002). Wnt-4 regulation by the Wilms' tumour suppressor gene, WT1. *Oncogene*, 21(19), 2948-2960. <https://doi.org/10.1038/sj.onc.1205373>
- Simon, M., Grandage, V. L., Linch, D. C., & Khwaja, A. (2005). Constitutive activation of the Wnt/beta-catenin signalling pathway in acute myeloid leukaemia. *Oncogene*, 24(14), 2410-2420. <https://doi.org/10.1038/sj.onc.1208431>
- Siriboonpiputtana, T., Zeisig, B. B., Zarowiecki, M., Fung, T. K., Mallardo, M., Tsai, C. T., Lau, P. N. I., Hoang, Q. C., Veiga, P., Barnes, J., Lynn, C., Wilson, A., Lenhard, B., & So, C. W. E. (2017). Transcriptional memory of cells of origin overrides β -catenin requirement of MLL cancer stem cells. *Embo j*, 36(21), 3139-3155. <https://doi.org/10.15252/embj.201797994>
- Staal, F. J., Famili, F., Garcia Perez, L., & Pike-Overzet, K. (2016). Aberrant Wnt Signaling in Leukemia. *Cancers (Basel)*, 8(9). <https://doi.org/10.3390/cancers8090078>
- Stoddart, A., Wang, J., Hu, C., Fernald, A. A., Davis, E. M., Cheng, J. X., & Le Beau, M. M. (2017). Inhibition of WNT signaling in the bone marrow niche prevents the development of MDS in the Apc(del/+) MDS mouse model. *Blood*, 129(22), 2959-2970. <https://doi.org/10.1182/blood-2016-08-736454>
- Sun, X., Gao, H., Yang, Y., He, M., Wu, Y., Song, Y., Tong, Y., & Rao, Y. (2019). PROTACs: great opportunities for academia and industry. *Signal Transduct Target Ther*, 4, 64. <https://doi.org/10.1038/s41392-019-0101-6>

- Svedberg, H., Chylicki, K., & Gullberg, U. (1999). Downregulation of Wilms' tumor gene (WT1) is not a prerequisite for erythroid or megakaryocytic differentiation of the leukemic cell line K562. *Exp Hematol*, 27(6), 1057-1062. [https://doi.org/10.1016/s0301-472x\(99\)00038-7](https://doi.org/10.1016/s0301-472x(99)00038-7)
- Svedberg, H., Richter, J., & Gullberg, U. (2001). Forced expression of the Wilms tumor 1 (WT1) gene inhibits proliferation of human hematopoietic CD34(+) progenitor cells. *Leukemia*, 15(12), 1914-1922. <https://doi.org/10.1038/sj.leu.2402303>
- Svitkin, Y. V., Pause, A., Haghighat, A., Pyronnet, S., Witherell, G., Belsham, G. J., & Sonenberg, N. (2001). The requirement for eukaryotic initiation factor 4A (eIF4A) in translation is in direct proportion to the degree of mRNA 5' secondary structure. *Rna*, 7(3), 382-394. <https://doi.org/10.1017/s135583820100108x>
- Takam Kamga, P., Bazzoni, R., Dal Collo, G., Cassaro, A., Tanasi, I., Russignan, A., Tecchio, C., & Krampera, M. (2020). The Role of Notch and Wnt Signaling in MSC Communication in Normal and Leukemic Bone Marrow Niche. *Front Cell Dev Biol*, 8, 599276. <https://doi.org/10.3389/fcell.2020.599276>
- Tamaki, H., Ogawa, H., Ohyashiki, K., Ohyashiki, J. H., Iwama, H., Inoue, K., Soma, T., Oka, Y., Tatekawa, T., Oji, Y., Tsuboi, A., Kim, E. H., Kawakami, M., Fuchigami, K., Tomonaga, M., Toyama, K., Aozasa, K., Kishimoto, T., & Sugiyama, H. (1999). The Wilms' tumor gene WT1 is a good marker for diagnosis of disease progression of myelodysplastic syndromes. *Leukemia*, 13(3), 393-399. <https://doi.org/10.1038/sj.leu.2401341>
- Tan, H. Y., Wang, N., Li, S., Hong, M., Guo, W., Man, K., Cheng, C. S., Chen, Z., & Feng, Y. (2018). Repression of WT1-Mediated LEF1 Transcription by Mangiferin Governs β -Catenin-Independent Wnt Signalling Inactivation in Hepatocellular Carcinoma. *Cell Physiol Biochem*, 47(5), 1819-1834. <https://doi.org/10.1159/000491063>
- Tang, S., Zhao, Y., He, X., Zhu, J., Chen, S., Wen, J., & Deng, Y. (2020). Identification of NOVA family proteins as novel β -catenin RNA-binding proteins that promote epithelial-mesenchymal transition. *RNA Biol*, 17(6), 881-891. <https://doi.org/10.1080/15476286.2020.1734372>
- Tarafdar, A., Dobbin, E., Corrigan, P., Freeburn, R., & Wheadon, H. (2013). Canonical Wnt signaling promotes early hematopoietic progenitor formation and erythroid specification during embryonic stem cell differentiation. *PLoS One*, 8(11), e81030. <https://doi.org/10.1371/journal.pone.0081030>
- Thoma, C., Fraterman, S., Gentzel, M., Wilm, M., & Hentze, M. W. (2008). Translation initiation by the c-myc mRNA internal ribosome entry sequence and the poly(A) tail. *Rna*, 14(8), 1579-1589. <https://doi.org/10.1261/rna.1043908>
- Toska, E., & Roberts, S. G. (2014). Mechanisms of transcriptional regulation by WT1 (Wilms' tumour 1). *Biochem J*, 461(1), 15-32. <https://doi.org/10.1042/bj20131587>
- Ullmark, T., Järnstråt, L., Sandén, C., Montano, G., Jernmark-Nilsson, H., Lilljebjörn, H., Lennartsson, A., Fioretos, T., Drott, K., Vidovic, K., Nilsson, B., & Gullberg, U. (2017). Distinct global binding patterns of the Wilms tumor gene 1 (WT1) -KTS and +KTS isoforms in leukemic cells. *Haematologica*, 102(2), 336-345. <https://doi.org/10.3324/haematol.2016.149815>
- Uzan, B., Poglio, S., Gerby, B., Wu, C. L., Gross, J., Armstrong, F., Calvo, J., Cahu, X., Deswarte, C., Dumont, F., Passaro, D., Besnard-Guérin, C., Leblanc, T., Baruchel, A., Landman-Parker, J., Ballerini, P., Baud, V., Ghysdael, J., Baleyrier, F., . . . Pflumio, F. (2014). Interleukin-18 produced by bone marrow-derived stromal cells supports T-cell acute leukaemia progression. *EMBO Mol Med*, 6(6), 821-834. <https://doi.org/10.1002/emmm.201303286>
- Valenta, T., Hausmann, G., & Basler, K. (2012). The many faces and functions of β -catenin. *Embo j*, 31(12), 2714-2736. <https://doi.org/10.1038/emboj.2012.150>
- Velten, L., Haas, S. F., Raffel, S., Blaszkiewicz, S., Islam, S., Hennig, B. P., Hirche, C., Lutz, C., Buss, E. C., Nowak, D., Boch, T., Hofmann, W. K., Ho, A. D., Huber, W., Trump, A., Essers, M. A., & Steinmetz, L. M. (2017). Human haematopoietic stem cell lineage commitment is a continuous process. *Nat Cell Biol*, 19(4), 271-281. <https://doi.org/10.1038/ncb3493>

- Vergara, D., Stanca, E., Guerra, F., Priore, P., Gaballo, A., Franck, J., Simeone, P., Trerotola, M., De Domenico, S., Fournier, I., Bucci, C., Salzet, M., Giudetti, A. M., & Maffia, M. (2017). β -Catenin Knockdown Affects Mitochondrial Biogenesis and Lipid Metabolism in Breast Cancer Cells. *Front Physiol*, 8, 544. <https://doi.org/10.3389/fphys.2017.00544>
- von Gise, A., Zhou, B., Honor, L. B., Ma, Q., Petryk, A., & Pu, W. T. (2011). WT1 regulates epicardial epithelial to mesenchymal transition through β -catenin and retinoic acid signaling pathways. *Dev Biol*, 356(2), 421-431. <https://doi.org/10.1016/j.ydbio.2011.05.668>
- Wang, W., Lee, S. B., Palmer, R., Ellisen, L. W., & Haber, D. A. (2001). A functional interaction with CBP contributes to transcriptional activation by the Wilms tumor suppressor WT1. *J Biol Chem*, 276(20), 16810-16816. <https://doi.org/10.1074/jbc.M009687200>
- Wang, Y., Krivtsov, A. V., Sinha, A. U., North, T. E., Goessling, W., Feng, Z., Zon, L. I., & Armstrong, S. A. (2010). The Wnt/ β -catenin pathway is required for the development of leukemia stem cells in AML. *Science*, 327(5973), 1650-1653. <https://doi.org/10.1126/science.1186624>
- Wang, Y., Xiao, M., Chen, X., Chen, L., Xu, Y., Lv, L., Wang, P., Yang, H., Ma, S., Lin, H., Jiao, B., Ren, R., Ye, D., Guan, K. L., & Xiong, Y. (2015). WT1 recruits TET2 to regulate its target gene expression and suppress leukemia cell proliferation. *Mol Cell*, 57(4), 662-673. <https://doi.org/10.1016/j.molcel.2014.12.023>
- Watts, J., & Nimer, S. (2018). Recent advances in the understanding and treatment of acute myeloid leukemia. *F1000Res*, 7. <https://doi.org/10.12688/f1000research.14116.1>
- Weidenaar, A. C., ter Elst, A., Koopmans-Klein, G., Rosati, S., den Dunnen, W. F., Meeuwse-de Boer, T., Kamps, W. A., Vellenga, E., & de Bont, E. S. (2011). High acute myeloid leukemia derived VEGFA levels are associated with a specific vascular morphology in the leukemic bone marrow. *Cell Oncol (Dordr)*, 34(4), 289-296. <https://doi.org/10.1007/s13402-011-0017-9>
- Weisberg, E., Halilovic, E., Cooke, V. G., Nonami, A., Ren, T., Sanda, T., Simkin, I., Yuan, J., Antonakos, B., Barys, L., Ito, M., Stone, R., Galinsky, I., Cowens, K., Nelson, E., Sattler, M., Jeay, S., Wuerthner, J. U., McDonough, S. M., . . . Griffin, J. D. (2015). Inhibition of Wild-Type p53-Expressing AML by the Novel Small Molecule HDM2 Inhibitor CGM097. *Mol Cancer Ther*, 14(10), 2249-2259. <https://doi.org/10.1158/1535-7163.Mct-15-0429>
- Wu, C., Zhang, H. F., Gupta, N., Alshareef, A., Wang, Q., Huang, Y. H., Lewis, J. T., Douglas, D. N., Kneteman, N. M., & Lai, R. (2016). A positive feedback loop involving the Wnt/ β -catenin/MYC/Sox2 axis defines a highly tumorigenic cell subpopulation in ALK-positive anaplastic large cell lymphoma. *J Hematol Oncol*, 9(1), 120. <https://doi.org/10.1186/s13045-016-0349-z>
- Xing, Y., Takemaru, K., Liu, J., Berndt, J. D., Zheng, J. J., Moon, R. T., & Xu, W. (2008). Crystal structure of a full-length β -catenin. *Structure*, 16(3), 478-487. <https://doi.org/10.1016/j.str.2007.12.021>
- Xu, C., Wu, C., Xia, Y., Zhong, Z., Liu, X., Xu, J., Cui, F., Chen, B., Røe, O. D., Li, A., & Chen, Y. (2013). WT1 promotes cell proliferation in non-small cell lung cancer cell lines through up-regulating cyclin D1 and p-pRb in vitro and in vivo. *PLoS One*, 8(8), e68837. <https://doi.org/10.1371/journal.pone.0068837>
- Yamagami, T., Sugiyama, H., Inoue, K., Ogawa, H., Tatekawa, T., Hirata, M., Kudoh, T., Akiyama, T., Murakami, A., & Maekawa, T. (1996). Growth inhibition of human leukemic cells by WT1 (Wilms tumor gene) antisense oligodeoxynucleotides: implications for the involvement of WT1 in leukemogenesis. *Blood*, 87(7), 2878-2884.
- Yang, L., Han, Y., Suarez Saiz, F., & Minden, M. D. (2007). A tumor suppressor and oncogene: the WT1 story. *Leukemia*, 21(5), 868-876. <https://doi.org/10.1038/sj.leu.2404624>
- Yasukawa, M., Fujiwara, H., Ochi, T., Suemori, K., Narumi, H., Azuma, T., & Kuzushima, K. (2009). Clinical efficacy of WT1 peptide vaccination in patients with acute myelogenous leukemia and myelodysplastic syndrome. *Am J Hematol*, 84(5), 314-315. <https://doi.org/10.1002/ajh.21387>

- Yeung, J., Esposito, M. T., Gandillet, A., Zeisig, B. B., Griessinger, E., Bonnet, D., & So, C. W. (2010). β -Catenin mediates the establishment and drug resistance of MLL leukemic stem cells. *Cancer Cell*, 18(6), 606-618. <https://doi.org/10.1016/j.ccr.2010.10.032>
- Yoon, J. H., Kim, H. J., Kwak, D. H., Park, S. S., Jeon, Y. W., Lee, S. E., Cho, B. S., Eom, K. S., Kim, Y. J., Lee, S., Min, C. K., Cho, S. G., Kim, D. W., Lee, J. W., & Min, W. S. (2017). High WT1 expression is an early predictor for relapse in patients with acute promyelocytic leukemia in first remission with negative PML-RAR α after anthracycline-based chemotherapy: a single-center cohort study. *J Hematol Oncol*, 10(1), 30. <https://doi.org/10.1186/s13045-017-0404-4>
- Ysebaert, L., Chicanne, G., Demur, C., De Toni, F., Prade-Houdellier, N., Ruidavets, J. B., Mansat-De Mas, V., Rigal-Huguet, F., Laurent, G., Payrastre, B., Manenti, S., & Racaud-Sultan, C. (2006). Expression of beta-catenin by acute myeloid leukemia cells predicts enhanced clonogenic capacities and poor prognosis. *Leukemia*, 20(7), 1211-1216. <https://doi.org/10.1038/sj.leu.2404239>
- Zhang, L., Yan, R., Zhang, Q., Wang, H., Kang, X., Li, J., Yang, S., Zhang, J., Liu, Z., & Yang, X. (2013). Survivin, a key component of the Wnt/ β -catenin signaling pathway, contributes to traumatic brain injury-induced adult neurogenesis in the mouse dentate gyrus. *Int J Mol Med*, 32(4), 867-875. <https://doi.org/10.3892/ijmm.2013.1456>
- Zhang, T., Otevrel, T., Gao, Z., Gao, Z., Ehrlich, S. M., Fields, J. Z., & Boman, B. M. (2001). Evidence that APC regulates survivin expression: a possible mechanism contributing to the stem cell origin of colon cancer. *Cancer Res*, 61(24), 8664-8667.
- Zhang, Y., & Wang, X. (2020). Targeting the Wnt/ β -catenin signaling pathway in cancer. *J Hematol Oncol*, 13(1), 165. <https://doi.org/10.1186/s13045-020-00990-3>
- Zhao, C., Blum, J., Chen, A., Kwon, H. Y., Jung, S. H., Cook, J. M., Lagoo, A., & Reya, T. (2007). Loss of beta-catenin impairs the renewal of normal and CML stem cells in vivo. *Cancer Cell*, 12(6), 528-541. <https://doi.org/10.1016/j.ccr.2007.11.003>
- Zhao, X., Shao, P., Gai, K., Li, F., Shan, Q., & Xue, H. H. (2020). β -catenin and γ -catenin are dispensable for T lymphocytes and AML leukemic stem cells. *Elife*, 9. <https://doi.org/10.7554/eLife.55360>
- Zhou, B., Jin, X., Jin, W., Huang, X., Wu, Y., Li, H., Zhu, W., Qin, X., Ye, H., & Gao, S. (2020). WT1 facilitates the self-renewal of leukemia-initiating cells through the upregulation of BCL2L2: WT1-BCL2L2 axis as a new acute myeloid leukemia therapy target. *J Transl Med*, 18(1), 254. <https://doi.org/10.1186/s12967-020-02384-y>
- Zhou, C., Martinez, E., Di Marcantonio, D., Solanki-Patel, N., Aghayev, T., Peri, S., Ferraro, F., Skorski, T., Scholl, C., Fröhling, S., Balachandran, S., Wiest, D. L., & Sykes, S. M. (2017). JUN is a key transcriptional regulator of the unfolded protein response in acute myeloid leukemia. *Leukemia*, 31(5), 1196-1205. <https://doi.org/10.1038/leu.2016.329>
- Zhou, J., Bi, C., Ching, Y. Q., Chooi, J. Y., Lu, X., Quah, J. Y., Toh, S. H., Chan, Z. L., Tan, T. Z., Chong, P. S., & Chng, W. J. (2017). Inhibition of LIN28B impairs leukemia cell growth and metabolism in acute myeloid leukemia. *J Hematol Oncol*, 10(1), 138. <https://doi.org/10.1186/s13045-017-0507-y>
- Zhou, J., Chan, Z. L., Bi, C., Lu, X., Chong, P. S., Chooi, J. Y., Cheong, L. L., Liu, S. C., Ching, Y. Q., Zhou, Y., Osato, M., Tan, T. Z., Ng, C. H., Ng, S. B., Wang, S., Zeng, Q., & Chng, W. J. (2017). LIN28B Activation by PRL-3 Promotes Leukemogenesis and a Stem Cell-like Transcriptional Program in AML. *Mol Cancer Res*, 15(3), 294-303. <https://doi.org/10.1158/1541-7786.Mcr-16-0275-t>
- Zhou, J., Toh, S. H., Chan, Z. L., Quah, J. Y., Chooi, J. Y., Tan, T. Z., Chong, P. S. Y., Zeng, Q., & Chng, W. J. (2018). A loss-of-function genetic screening reveals synergistic targeting of AKT/mTOR and WTN/ β -catenin pathways for treatment of AML with high PRL-3 phosphatase. *J Hematol Oncol*, 11(1), 36. <https://doi.org/10.1186/s13045-018-0581-9>
- Zhou, L., Li, Y., He, W., Zhou, D., Tan, R. J., Nie, J., Hou, F. F., & Liu, Y. (2015). Mutual antagonism of Wilms' tumor 1 and β -catenin dictates podocyte health and disease. *J Am Soc Nephrol*, 26(3), 677-691. <https://doi.org/10.1681/asn.2013101067>

Appendix

Appendix Table 1: Clinical characteristics of AML/MDS patient diagnostic/relapse samples used in this study.

Patient no.	Age (at diagnosis)	Sex	WBC count (x10 ⁹ /L)	Sample type	Secondary disease (Y/N)	Genetic information	Other clinical information
1 DS397	76	F	389	LP	N	Normal karyotype, NPM1 ⁺ , FLT3 ⁺	n/a
2 FJ080	4	M	n/a	BM	n/a	n/a	n/a
3 KA122	10	F	n/a	BM	n/a	n/a	Deceased
4 MD064	n/a	n/a	>200	PB	Y	n/a	Post-allogeneic transplant. M0/1 (previously diagnosed with M3 10 years previous)
5 JC110	n/a	n/a	n/a	n/a	n/a	n/a	n/a
6 SW104	17	M	n/a	BM	Y	n/a	Post-BMT for AML following 2 relapses. Deceased
7 HD209	6	M	70.7	n/a	Y	n/a	Secondary to Ewings Sarcoma. Myelomonocytic morphology. Deceased.
8 CG336	14	F	7.6	BM	N	MLL rearrangement. Karyotype: 46,XX,ins(10;11)(q11.2;q23.1q23.3).ish ins(10;11)?inv(11)(q23.3)(5'MLL+)(q23.1)(3'MLL+)	BMT for high-risk AML. CD33+, MPO+, CD34-, CD117+, TdT+, CD64+, CD11c+, CD15+, CD11b+, NG2+
9 1977	24	M	256	BM	N	46,XY,inv(16)(p13q22)[16].ish inv(16)(p13)[MYH11+,CBFB+](q22)(CBFB+,MYH11+)[5]	M4, relapsed, deceased.
10 1410	17	M	294	BM	N	46,XY[20]	Alive, complete remission.
11 KM429	64	F	13.3	BM	N	Normal karyotype	AML with underlying MDS like changes
12 TSD416	13	F	91.9	BM	Y	High Risk	Relapsed AML secondary to Rhabdoid tumour. Mixed cellular infiltrate consisting of predominantly monocyte/macrophages (CD14+, CD11c+, CD64+, CD34-, CD117-). Deceased
13 ET406	4	F	2.6	BM	N	Normal karyotype, NPM1 ⁺ (exon 12), FLT3 ⁺	MRD neg. CD13+, CD33+, CD34+, CD117+, MPO+
14 YM415	15	F	6.5	BM	N	MLL (KMT2A) rearrangement, t(10;11)(p11-p14,q23), MLL-MLLT10	MRD detected post treatment course 1

15 OM401	4	M	3.2	BM	N	t(10;11)(p11.2;q23) KMT2A-MLLT10. Cytogenetically cryptic. KMT2A ex8-MLLT10 ex9 or KMT2A ex9-MLLT10 ex10 fusion detected. NPM1-FLT3 ⁺	CD13-, CD33+, CD34-, CD117+/-, CD11c+, CD64+, CD14-, NG2+. High risk cytogenetics. BMT. MRD neg post course 1+2.
16 RD279	14	F	14.7	PB	N	t(8;21)(q22;q22) RUNX-RUNX1T1. 46,XX,der(8)?del(8)(q11.2q21.3)?dup(8)(q24.3q21.3)?ins(8;21)(q22;q22.12q22.3),der(21)?ins(8;21)(q22;q22.12q22.3)[10]	CD13+, CD33+, CD34+, CD117+, DR+, MPO+, CD19+. MRD negative post treatment course 1, 2 and EOT
17 RT161	5	M	1.6	BM	N	n/a	M5. Deceased.
18 AB312	14	F	2.1	BM	N	45,XX,-7,add(11)(p11.2)[9]/46,XX[1]	22% Myeloid blasts (CD117+, CD34+/-, CD33+, CD13+, MPO-)+ 10% immunophenotypically mature monocytes (CD11c+, CD64+, CD117+) BMT
19 NT026	8	F	n/a	BM	N	n/a	M4/5. Deceased.
20 KU250	7	F	34.4	BM	Y	MLL rearrangement t(9;11)	M5a morphology. BMT following relapse. Deceased
21 MS332	16	F	20.6	BM	N	Normal karyotype 46,XX[20]	CD33+, MPO+, CD34+, CD117+, CD13+, CD14-, CD7+, CD45 weak, CD11c+, TdT-
22 HG352	7	M	3.5	BM	N	t(8;21)(q22;q22) RUNX-RUNX1T1 45,X,-Y,t(8;21)(q22;q22)[9]/46,XY[1]	8% myeloid blasts present (CD13+, CD33+, CD34+, CD117+, MPO+)
23 JC125	11	M	n/a	BM	N	n/a	BMT for MDS. Deceased.
24 RD296	13	F	14.7	BM	N	Karyotype: 46,XX,der(8)?del(8)(q11.2q21.3)?dup(8)(q24.3q21.3)?ins(8;21)(q22;q22.12q22.3),der(21)?ins(8;21)(q22;q22.12q22.3)[10] CD13+, CD33+, CD34+, CD117+, DR+, MPO+, CD19+; AML	Only 2 megakaryocytes seen. Erythropoiesis reduced. Prominent eosinophils and eosinophil precursors - c. 12%. No significant monocytoid population. Densely infiltrated with myeloid blasts. Analysis showed an abnormal female clone with a derivative chromosome 8 from a variant 8;21 rearrangement. This abnormality is consistent with a diagnosis of AML (WHO 2008 subtype: AML with

							RUNX1T1) and is reported in association with a favourable prognosis[1,3].
25 OD368	2	M	2.4	BM	N	t(9;11)(p22;q23), t(11;21)(q23;q8)	Alive, and in complete remission.
26 WW061	4mo	M	5.1	BM	N	t(9;11)	n/a
27 BD002	7	F	n/a	BM	N	MPAL, 46XX, del5q, abnormal 21	BMT
28 AH509	7mo	F	168.6	BM	N	Karyotype: 47,XX,+21[5]/46,XX[5] nuc ish(CBFA2T3, GLIS2)X3(CBFA2T3 con GLIS2x2)[92/150] FISH showed no evidence of CBFB or RUNX1-RUNX1T1 rearrangement however, an additional copy of RUNX1 was found. 33+, CD34+, CD117+, MPO+, DR-, CD13+	n/a
29 KM464	5	F	29.5	BM	N	Karyotype: 45,X,-X,t(8;21)(q22;q22.1)[8]/46,XX[2] Analysis showed an abnormal female clone including an 8;21 translocation. This abnormality is consistent with a diagnosis of AML (WHO 2016[1] subtype: AML with t(8;21)(q22;q22.1);RUNX1-RUNX1T1) and is reported in association with a favourable prognosis[2]. 7% myeloid blasts (CD13+, CD33+, CD34+, CD117+, MPO+	BMT 24/12/20 due to high risk genetics. Alive, in remission. Chromosome and FISH analysis showed an inv(16)(p13.3q24.3) [CBFA2T3-GLIS2] rearrangement and trisomy for chromosome 21. This is consistent with a diagnosis of AML and the CBFA2T3-GLIS2 rearrangement is a poor risk finding according to the MyeChild 01 protocol (received Gemtuzumab as part of Myechild trial treatment.)
30 JO432	76	F		BM		D45X Polycythaemia vera. M99503, transformation in to MDS.	Alive, in complete remission. Treated on Myechild trial - 2 doses of Mylotarg received as part of Myechild trial treatment

BM = Bone marrow

PB = Peripheral blood

LP = Leukapheresis

MRD = Minimal residual disease

BMT = Bone marrow transplant

AML= Acute myeloid leukemia

MDS= Myelodysplastic syndrome

MPAL= Mixed phenotype acute leukemia

MLL = *Mixed-lineage leukemia*

NPM1 = *Nucleophosmin*

FLT3 = *Fms-like tyrosine kinase 3*

RUNX1 = *Runt-related transcription factor 1*

GATA2 = *GATA Binding Protein 2*

WHO = World Health Organisation

n/a = not available